Ca^{2+}_i and the Pancreatic α Cell – Intrinsic Regulation and Dysfunction in Type 2 Diabetes

Joely Kellard

The Queen's College

A thesis submitted for the Degree of Doctor of Philosophy at the University of Oxford



OXION-Wellcome Trust DPhil Programme

Oxford Centre for Diabetes, Endocrinology and Metabolism

University of Oxford

Michaelmas Term 2019

Statement of Authorship

RNAseq analysis was carried out by Dr Martijn van der Bunt. Figure 7.2 was generated by Dr Martijn van der Bunt.

All perfusion surgeries were carried out by Dr Nils Rorsman, Dr Thomas Hill, and Dr Jakob Knudsen.

Somatostatin measurements were carried out by myself and Dr Thomas Hill.

Dr Andrei Tarasov generated the script for analysis of widefield recordings, the analysis itself was carried out entirely by myself.

Animal work, particularly tolerance tests with measurements of plasma hormone concentrations were carried out with the assistance of either Dr Linford Briant, Dr Jakob Knudsen, or Dr Julie Adam. The ITT based on lean mass was carried out by Linford Briant, I designed the experiment.

Acknowledgements

Linford and Jakob, this thesis represents your continued effort and support more than anything. Thank you for all your help, input, direction and guidance. I have enjoyed doing experiments together and arguing about what they all meant.

Thank you Patrik for having me in the group. Thank you to the Rorsman Lab; all of you have helped me immensely, but in particular Julie Adam who supervised me during my first-year rotation and taught me many of the animal techniques I continued to use throughout my PhD.

Mum and dad, thank you for your support and encouragement throughout everything I have done and for keeping me positive. I would not be submitting this thesis if it were not for this from you.

Paul, thank you for giving me perspective, for bringing me chocolate, and for all the kitchen dancing to keep me smiling. My friends; particularly Luke (thanks for doing all that digging), Irina, Kathryn, and my brother Chris. Thank you for your companionship and support.

Before coming to Oxford, Dr Chris Mason instilled in me a sense of self belief that permitted to pursue a PhD. This was the most valuable thing you could have taught me, so thank you.

I would like to acknowledge everyone who made these experiments possible; those who have answered my questions, spared their hands, their time, and their expertise. It goes without saying that none of this would have been done alone.

Contents

Ca^{2+}_i and the Pancreatic α Cell – Intrinsic Regulation and Dysfunction in Type 2 Diabetes 1
Statement of Authorship 2
Acknowledgements 3
Abstract 13
Chapter 1 15
1 Introduction 15
1.1 Basic glucose homeostasis 15
1.2 Systemic actions of glucagon 18
1.3 T2D 20
1.3.1 Clinical features of T2D 20
1.3.2 The α cell in T2D 21
1.4 Pancreatic anatomy and the islet of Langerhans 26
1.4.1 α, β and δ cells 26
1.4.2 Human *vs.* rodent islets 26
1.5 The α cell, glucagon secretion and action 27
1.5.1 $[Ca^{2+}]_i$ signalling in α cells 27
1.5.2 Regulation of α cell function 31
1.5.3 Functional identification of α cells for $[Ca^{2+}]_i$ imaging 39
1.5.4 Glucagon synthesis from pre-proglucagon 39
1.6 Aims of thesis 41

1.6.1 Generate and validate GCaMP3 model 41

1.6.2 *In vivo* - Carry out extensive metabolic phenotyping 41

1.6.3 *Ex vivo* - Interrogate functional alterations in α cell activity following HFD 41

1.6.4 Interrogation of the role of fat metabolism in glucagon secretion from α cells 42

1.6.5 Investigate changes in α cell gene expression following HFD 42

Chapter 2 43

2.1 Animal husbandry 43

2.1.1 Ethical approval 43

2.1.2 Generation of GcgRFP/GCaMP3 mouse line 43

2.1.3 Generation of αCPT1a-KO mouse line 44

2.2 Genotyping 45

2.2.1 DNA isolation 45

2.2.2 PCR 45

2.3 Metabolic phenotyping 47

2.3.1 Glucose tolerance tests 47

2.3.2 Insulin tolerance tests 47

2.3.3 EchoMRI 48

2.3.4 Plasma hormone measurements 48

2.4 Islet Isolation 48

2.5 Dissociation of islets into single cells 49

2.5.1 Fluorescent activated cell-sorting of dispersed whole islets..... 50

2.6 RNA..... 53

2.6.1 RNA extraction, RNA-cDNA, qPCR of fluorescence-activated cell sorted cell fractions 53

2.6.2 Fluorescence-activated cell sorting of α and non-α cell fractions for RNAseq 53

2.7 Immunohistochemistry 54

2.7.1 Fixing and embedding of whole pancreases 54

2.7.2 Staining of whole pancreases 54

2.7.3 Fixing and staining of whole islets 55

2.8 $[Ca^{2+}]_i$ Imaging 57

2.8.1 $[Ca^{2+}]_i$ Imaging using the Zoom microscope 57

2.8.1a Amino acid mixes for acute exposure and widefield (Zoom) imaging 58

2.8.1b High Fat Incubation 58

2.8.2 $[Ca^{2+}]_i$ imaging using the confocal microscope 58

2.9 Measurements of hormone secretion 62

2.9.1 Secretion 62

2.9.2 MSD measurement of secretory output..... 62

2.9.3 Perfusion experiments 62

2.10 High fat diet 64

2.11 Statistical analysis 64

2.12 A note on selection of an appropriate HFD - Methodological considerations 65

2.12.1 Ob/bo, db/db 65

2.12.2 NOD 66

2.12.3 STZ 66

2.12.4 High fat diet 67

2.13 RNAseq - a note on protocol optimisation 69

2.13.1 Isolation of high quality RNA 69

2.13.2 Preparation of cell lysate and sample submission 70

Chapter 3 71

3. Development and characterisation of GcgCreGCaMP3 model 71

3.1 Introduction 71

3.1.1 α cell responses to known substrates 72

3.2 Methods 74

3.2.1 Wide field Ca^{2+}_i imaging 75

3.3 Results 75

3.3.1 In vivo experiments on glucose metabolism in GcgGCaMP3 model 75

3.3.2 GCaMP3 and RFP are well co-localised to α cells at the protein and RNA level 76

3.3.3 GcgGCaMP3 $[Ca^{2+}]_i$ imaging demonstrates intrinsic α cell glucose sensitivity 77

3.3.4 Confocal imaging reveals strong frequency modulation of $[Ca^{2+}]_i$ in α cells in response to glucose 78

3.4 Discussion 81

3.4.1 GCaMP/RFP are expressed specifically in α cells 81

3.4.2 Confocal imaging is most appropriate for Ca^{2+}_i imaging of α cells 82

3.4.3 α cell Ca^{2+}_I signalling is frequency, not amplitude modulated in response to glucose 86

3.4.4 Preprandial amino acids are able to stimulate α cell $[Ca^{2+}]_i$ 88

3.4.5 Ca^{2+}_i signalling in a diabetogenic model 88

Chapter 4 97

4. High fat experiments (*in vivo*) 97

4.1 Introduction 97

4.1.2 Experimental justification 98

4.2 Results 100

4.2.1 Week 6 phenotyping 100

4.2.2 Week 12 phenotyping 100

4.2.3 Expression of Fluorescent marker does not influence the HFD phenotype 104

4.3 Discussion 105

4.3.1 Summary of results 105

4.3.2 HFD provokes a pre-diabetic state in mice 105

4.3.3 Hyperglucagonaemia in prediabetes 107

4.3.4 Intrinsic changes in the α cell and contribution to the diabetic state 108

Chapter 5 122
5. High fat feeding (*ex vivo* experiments) 122

5.1 Introduction 122

5.2 Results 125

5.2.1 HFD feeding increases α cell glucagon output in response to glucose 125

5.2.2 $[Ca^{2+}]_i$ responses 126

5.2.3 Causes of increased $[Ca^{2+}]_i$ activity 127

5.3 Discussion 129

5.3.1 Summary of results 129

5.3.2 α cell function is altered intrinsically 129

5.3.3 Paracrine changes may drive altered α cell function 132

5.3.4 Altered metabolism as a driver for changed α cell function 134

Chapter 6 143
6. High fat feeding in α-CPT1α-KO mice 143

6.1 Introduction 143

6.2 Results 146

6.2.1 αCPT1a-KO mouse 146

6.2.2 Isolated islets 147

6.3 Discussion 148

6.3.1 Summary of results 148

6.3.2 α cell independent mechanisms of αCPT1a-KO 148

6.3.3 Counterregulation of αCPT1a-KO 149

6.3.4 Etomoxir in the study of α cell $[Ca^{2+}]_i$ dynamics 150

6.3.5 Lipotoxicity in CPT1a KO 151

6.3.6 Time sensitivity of αCPT1a-KO protection 152

6.3.7 Future considerations 153

Chapter 7 157

7. RNAseq in FACS sorted α and non-α cells 157

7.1 Introduction 157

7.1.1 Justification of RNAseq 157

7.2 Results 159

7.3 Discussion 161

7.3.1 Sorting separates α and non α cells 161

7.3.2 RNAseq in HFD islets 162

7.3.3 β cell gene expression is more sensitive to HFD than α cell expression 162

7.3.4 Future considerations 165

7.3.4a Sample size and power 165

7.3.4b FACS sorting of cells for RNAseq 165

7.3.4c RNAseq approach 166

7.3.5 Conclusions 168

Chapter 8 173

8. Discussion 173

8.1 Summary 173

8.2 Key findings 173

8.3 Regulation of glucagon secretion by glucose 174

8.3.1 α cell $[Ca^{2+}]_i$ oscillations are frequency modulated in response to glucose 174

8.3.2 How may frequency modulation of $[Ca^{2+}]_i$ oscillations be achieved in α cells 176

8.3.3 $[Ca^{2+}]_i$ independent control of glucagon secretion 179

8.4 Impact of HFD on pancreatic islet and α cell function 180

8.4.1 Summary of HFD observations 180

8.4.2 Mechanisms of altered SST signalling 180

8.4.3 HFD and α cell function 182

8.5 Reflections on the whole thesis 185

8.5.1 The magnitude of secretory response 185

8.5.2 The importance of SST sensitivity 185

8.6 Implications for understanding and treatment of T2D 186

8.6.1 Relevance to human disease 186

8.7 Summary, thesis aims 188

1. Generate and validate GCaMP3 model 188

2. *In vivo* - Carry out extensive metabolic phenotyping 188

3. *Ex vivo* - Interrogate functional alterations in α cell activity following HFD 188

4. Interrogation of the role of fat metabolism in glucagon secretion from α cells 188

5. Investigate changes in α cell gene expression following HFD 189

8.8 Conclusions 189

Abstract

In type 2 diabetes (T2D), elevated plasma glucagon concentration (hyperglucagonaemia) exacerbates hyperglycaemia due to inappropriate insulin secretion. Despite this, very little is known about why glucagon secreting α cells become dysfunctional.

In α cells, intracellular Ca^{2+} ($[Ca^{2+}]_i$) oscillations drive glucagon secretion but much of their regulation remains obscure. Here we investigate how $[Ca^{2+}]_i$ oscillations are regulated, and whether α cell $[Ca^{2+}]_i$ dynamics change when mice are fed a high fat diet (to induce a T2D-like state).

Mice expressing the genetically encoded calcium sensor GCaMP3 specifically in α cells were fed a control (10% calories from fat; CTL) or high fat (60% calories from fat; HFD) diet. After 12 weeks, glucose tolerance was impaired in HFD fed mice and plasma glucagon levels were elevated. Plasma glucagon was elevated in HFD mice *in vivo* during insulin-induced hypoglycaemia and in the perfused pancreas *in situ*. Glucagon secretion from HFD islets was elevated *ex vivo* suggesting that intra-islet (intrinsic) effects are involved. While the $[Ca^{2+}]_i$ oscillation frequency in α cells was reduced by high (6-15 mM) glucose in both CTL and HFD islets, the frequency was higher in HFD fed mice. Following HFD, α cell $[Ca^{2+}]_i$ oscillations and glucagon secretion were also less sensitive to inhibition by somatostatin (SST), an effect that correlated with reduced SST secretion from δ cells in mice fed the HFD.

Collectively, these data indicate that altered α cell activity underlies hyperglucagonaemia in HFD. These data provide evidence that α cell dysfunction and altered intra-islet signalling manifests early in T2D. Correcting the glucagon secretion

defects may provide therapeutic advantages, highlighting the potential of the α cell as a potential pharmacological target.

Chapter 1

1 Introduction

1.1 Basic glucose homeostasis

Homeostatic control of the concentration of glucose in the blood is essential for life. Under normal conditions, pancreatic hormones are secreted to stop blood glucose concentrations straying too far above, or below, a safe physiological range. Plasma glucose concentration naturally fluctuates as a result of factors including food consumption, exercise, and prolonged fasting.

The homeostatic range for glucose in human plasma is ~4-6 mM (Gerich 1993). When blood glucose concentration becomes elevated, increased glucose metabolism in pancreatic β cells results in insulin secretion into the blood. Insulin signalling in peripheral tissues (including the liver, skeletal muscle and fat cells) induces translocation of the glucose transporter 4 (GLUT4) to the plasma membrane of muscle, liver and adipose cells. Movement of glucose out of the circulation into cells via GLUT4 causes a decrease in plasma glucose concentration, returning to the homeostatic set point (Herman et al. 2006).

If the blood glucose concentration becomes too low (hypoglycaemia), pancreatic α cells, which are inhibited at normal and high glucose concentrations, become active and secrete glucagon. Glucagon's main physiological role is to stimulate hepatic glycogenolysis. Hepatic glucose production results in an increase in plasma glucose (

Figure 1.1, (Koenig et al. 2012)).

Hypoglycaemia is particularly dangerous for the brain, where glucose is the primary fuel. Prolonged hypoglycaemia can lead to syncope, coma, and even death (Boron et al. 2009). Conversely, elevations in blood glucose above the normal range are not without consequence; high blood glucose (hyperglycaemia) can lead to nerve damage, cardiac arrhythmias and increased risk of infection (Butler et al. 2005, Figueroa-Romero et al. 2008, Tran et al. 2018).

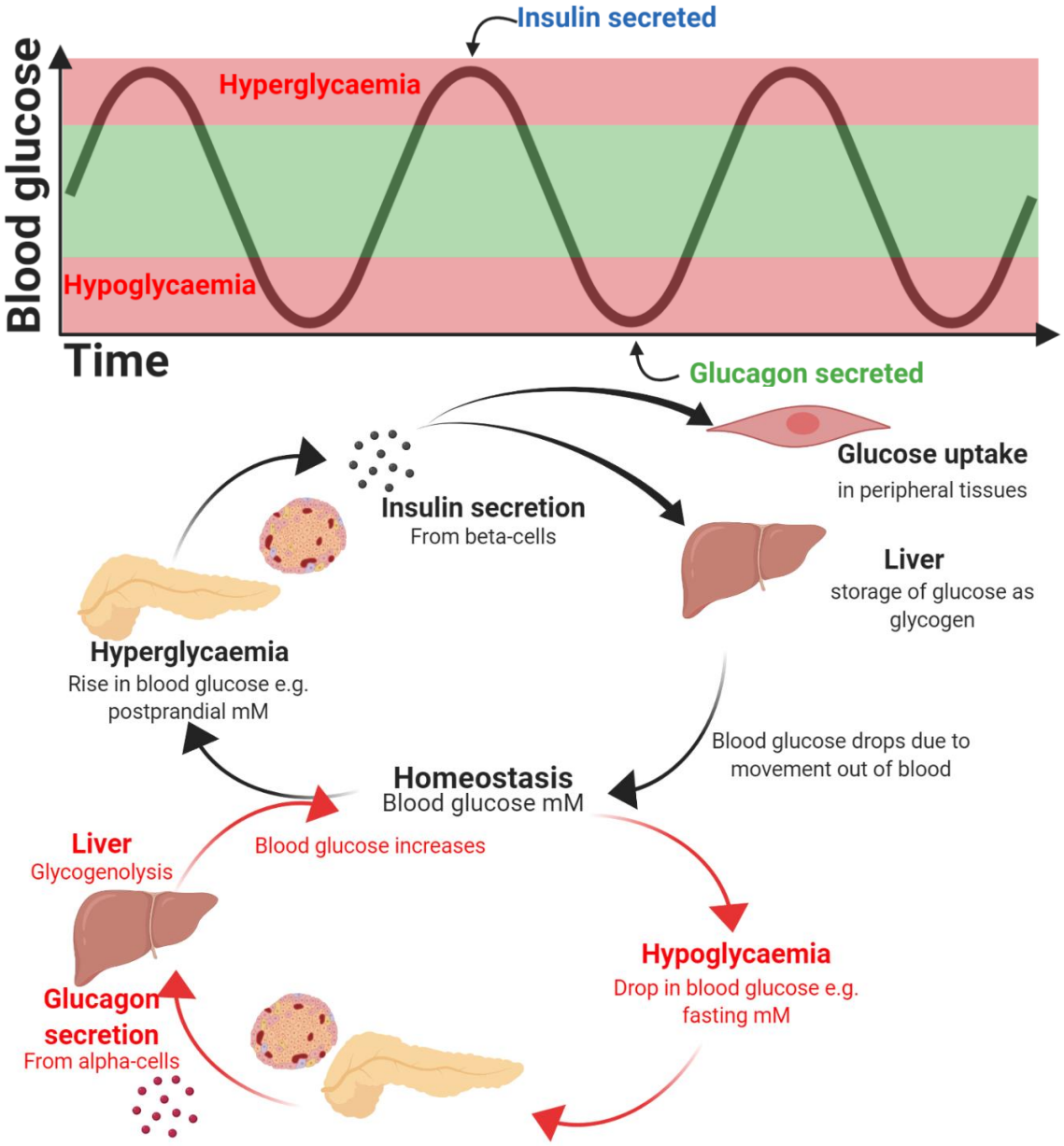

Figure 1.1 *Mechanism of glucose homeostasis including insulin secretion in response to hyperglycaemia and glucose lowering actions via increased glucose uptake into peripheral tissues. In response to hypoglycaemia, glucagon secretion from α cells acts via increased hepatic gluconeogenesis and glycogenolysis to increase serum glucose and return to the homeostatic set point.*

1.2 Systemic actions of glucagon

The systemic actions of glucagon are mediated through activation of the glucagon receptor (GCGR). The GCGR is widely expressed throughout the body with binding identified in the kidney, intestinal smooth muscle, adipose tissue, central nervous system (CNS), heart and β cells. GCGR expression is most enriched in the liver (Ouhilal et al. 2012, Uhlen et al. 2015). Indeed, it is via its actions in the liver that glucagon exerts most of its glucose elevating effects. GCGR is a $G_{s/q}$-coupled Class-B GPCR (Zhang et al. 2018). GCGR stimulation results in activation of adenylate cyclase, increased cAMP and increased $[Ca^{2+}]_i$. In the liver, increased intracellular cAMP activates cAMP-dependent protein kinase (PKA). Subsequent phosphorylation of glycogen phosphorylase b activates the conversion of glycogen to glucose (glycogenolysis) and thereby (following downhill transport of glucose by GLUT2 across the hepatocyte membrane into the blood) restores normoglycaemia (**Figure 1.2** (Berg et al. 2002)). In the longer term, glucagon signalling in the liver affects expression of gluconeogenic genes through activation of the cAMP response-element binding protein (CREB) and CREB-related transcription co-activator (Herzig et al. 2001, Koo et al. 2005). Glucagon-responsive genes include many involved in hepatic anatomy and zonation; close to one quarter of plasma glucagon is removed by movement through the hepatic circulation, with 17% removed by the kidneys (Dobbins et al. 1995, Cheng et al. 2018). Glucagon signalling is a dynamic and complex process that is influenced by metabolic and disease states (including hepatic steatosis).

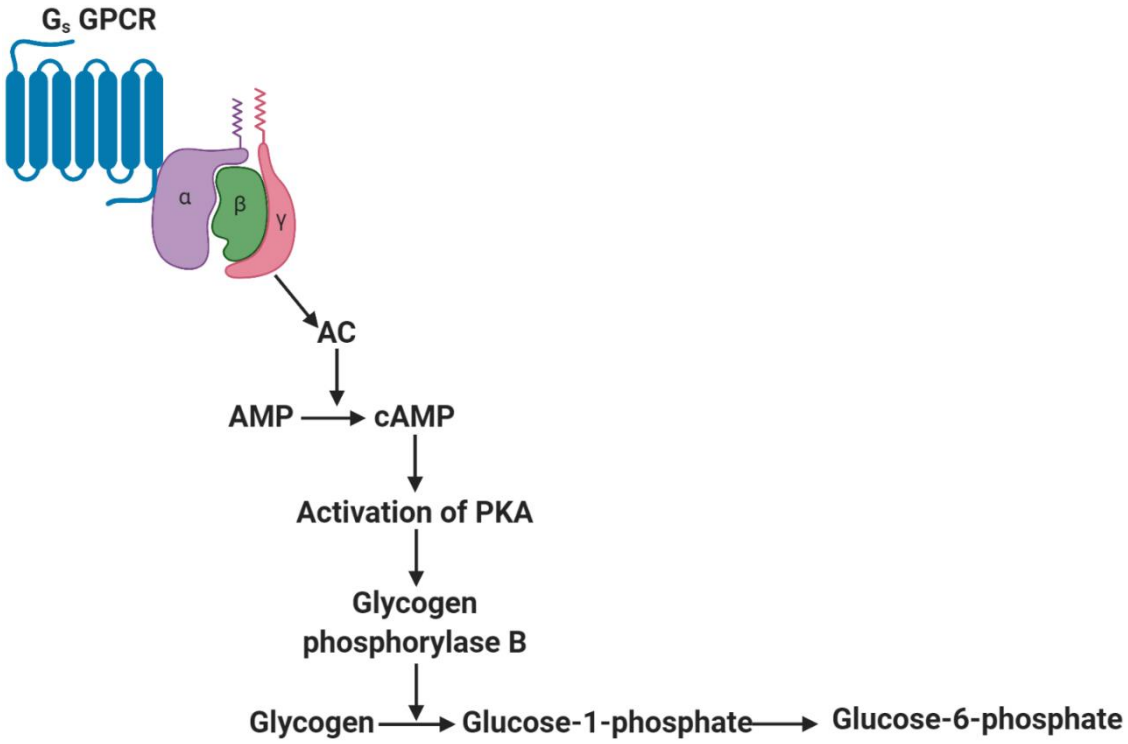

Figure 1.2 *Hepatic activation of glycogenolysis by glucagon.*

1.3 T2D

1.3.1 Clinical features of T2D

4.7 million people in the UK have diabetes with type 2 diabetes (T2D) accounting for 90% of diabetes diagnoses (Diabetes UK 2019). Currently, 10% of the entire NHS budget is spent on the treatment of diabetes and its complications (Hex et al. 2012). In diabetes, effective homeostasis of plasma glucose concentration fails. In type 1 diabetes (T1D), hyperglycaemia occurs due to immune destruction of pancreatic β cells and a lack of insulin. Features of T2D include hyperglycaemia, insulin resistance, and inappropriate glucagon secretion. T2D is associated with increased prevalence of cardiovascular disease (Stearne et al., 1998), kidney disease (Health, 2007), retinopathy (Stratton et al., 2000), amputation (Williams & Pickup, 2004), nerve damage (Stratton et al., 2000) and depression (Katon et al., 2004). A complex combination of risk factors contribute to an individual's likelihood of developing T2D with major factors including genetic susceptibility, obesity, and level of physical exercise (**Figure 1.3**, (Wu et al. 2014)).

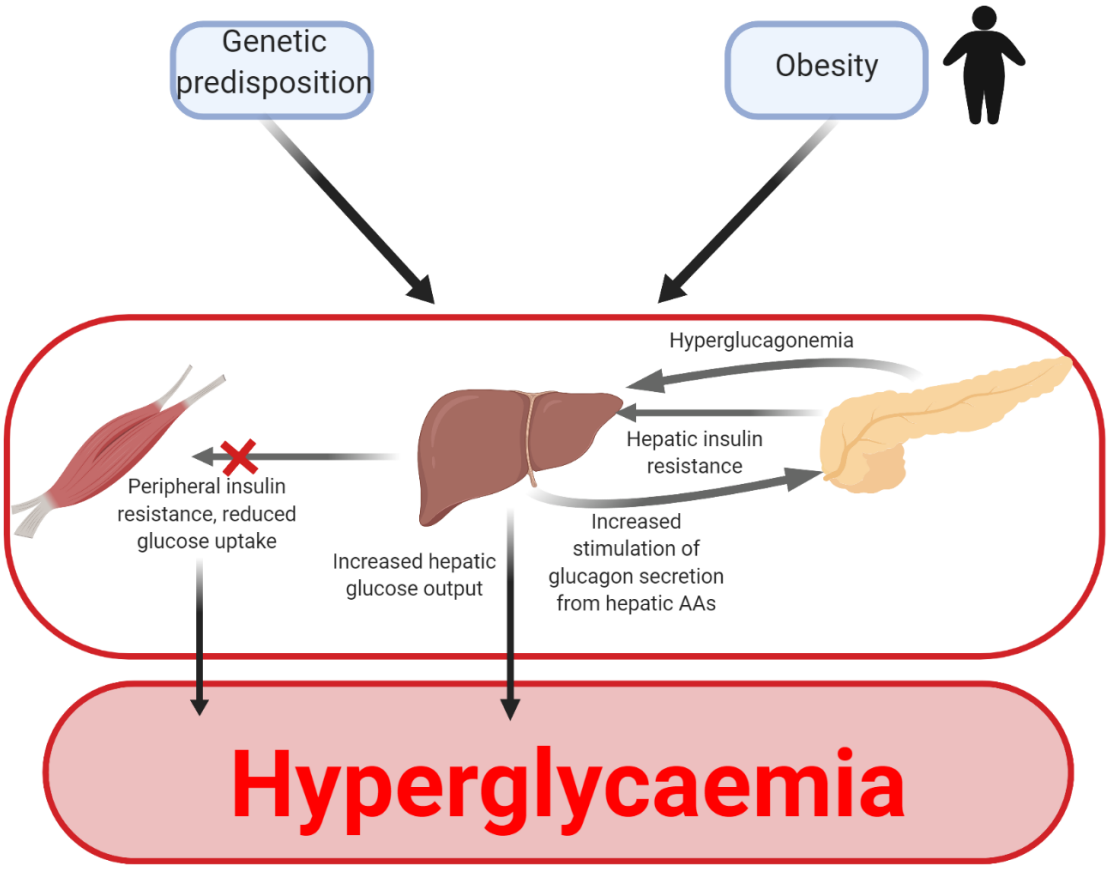

Figure 1.3 *Contributing factors to the development of hyperglycaemia, prediabetes, and T2D. Genetic predisposition, combined with lifestyle factors including obesity and lack of physical exercise influence an individual's disease risk. Hepatic insulin resistance, increased plasma amino acids, and hyperglucagonaemia increase glycaemia. Peripheral insulin resistance and increased hepatic glucose output further exacerbate defective glucose homeostasis.*

1.3.2 The α cell in T2D

Following the identification of insulin and its role in diabetes in the 1920s, an "insulinocentric" view of diabetic abnormalities has persisted. In 1975, Unger and Orci suggested a bihormonal model of the diabetic aetiology. In the bihormonal model, defective insulin secretion decreases glucose utilisation by peripheral tissues, causing glucose to remain in the circulation.

Experimentally, characterising plasma glucagon concentrations in obesity and diabetes is challenging as glucagon levels depend on the state of feeding. Plasma glucagon is lower obese individuals compared to lean controls following infusion with arginine (Schade et al. 1974), and in HFD fed mice compared to controls following prolonged fasting (Merino et al. 2015, Stern et al. 2019). However, under hyperglycaemic conditions (for example during a GTT) humans with obesity and T2D, and HFD fed mice have elevated plasma glucagon compared to lean controls (Merino et al. 2015, Manell et al. 2016). Despite the difficulty characterising plasma glucagon concentration, it is relatively well accepted that glucagon (particularly when considered relative to glycemia) is elevated in obesity and T2D (Starke et al. 1984, Anoop et al. 2017). Elevated glucagon, which drives hepatic glucose output, exacerbates hyperglycaemia due to the lack of insulin (Unger et al. 1970, Unger et al. 1975).

The role of α cell dysfunction as a contributing factor in T2D is widely accepted but our understanding of α cell physiology is still limited. A number of studies have indicated that glucagon not only contributes to, but that it is essential for the development of hyperglycaemia (Dobbs et al. 1975, Lee et al. 2011). Plasma glucagon is elevated in obesity (Starke et al. 1984), pre-diabetes (Faerch et al. 2016) and T2D (Dunning et al. 2007), especially when you consider the suppression of glucagon secretion that would normally occur with such high plasma glucose concentrations.

1.3.2a Glucagon signalling is essential for the development of hyperglycaemia

A dramatic illustration of the role of glucagon as a contributor to hyperglycaemia comes from studies on mice that lack the glucagon receptor (*Gcgr*$^{-/-}$ mice). These mice exhibit reduced plasma glucose concentrations at rest and during an intraperitoneal glucose tolerance test (IPGTT) (Gelling et al. 2003). G*cgr*$^{-/-}$ mice are resistant to many of the physiological effects of HFD: they gain less weight than WT littermate controls and have improved plasma glucose during an oral glucose tolerance test (OGTT) (Conarello et al. 2007).

When *Gcgr*$^{-/-}$ mice are treated with streptozotocin (STZ), which selectively kills β cells (thereby inducing a T1D-like state), they do not develop hyperglycaemia despite the complete absence of insulin (Conarello et al. 2007). Levels of P-CREB, a downstream effector of glucagon signalling in the liver, were undetectable in *Ggcr*$^{-/-}$ mice indicating effective ablation of receptor signalling (Lee et al. 2011). Restoration of glucagon receptor cDNA to the liver in STZ treated *Gcgr*$^{-/-}$ causes severe hyperglycaemia to develop (Lee et al. 2012).

Ideally, GCGR knockout studies will be extended into mice with inducible knockout of receptor expression. As the lines studied here are germline knock outs, loss of GCGR signalling during development may result in altered physiology and activation of compensatory mechanisms for glucose homeostasis. Indeed, *GCGR*$^{-/-}$ mice have α cell hyperplasia and elevated plasma glucagon levels (Lee et al. 2011). Tamoxifen induced loss of GCGR signalling specifically in α cells using the Gcg-CreER mouse line

(Ackermann et al. 2017) could be used to investigate compensatory changes that occur within α cells upon loss of GCGR signalling.

In humans, a number of individuals with glucagon receptor (*GCGR*) mutations have been identified. They exhibit hyperglucagonaemia and α cell hyperplasia but do not exhibit hypoglycaemia, liver failure or dislipidaemia (Zhou et al. 2009, Miller et al. 2015, Larger et al. 2016). Conversely, 70% of patients with hyperglucagonaemia (caused by glucagonoma) develop diabetes, indicating that glucagon alone is capable of inducing diabetes (Wei et al. 2018).

Collectively, observations in mice and humans, indicate that even in the absence of fully functioning insulin signalling, hyperglycaemia does not develop unless glucagon signalling is intact. For these reasons there has been an increasing focus on the possible contribution of glucagon to the development of T2D. Indeed, GCGR antagonism has been investigated as a therapeutic target in the treatment of T2D (Brand et al. 1994, Pearson et al. 2016). However, fundamental understanding about the mechanisms by which α cell dysfunction develops in T2D remains limited. We do not understand which elements of the T2D phenotype are particularly deleterious to α cell function and it is not clear whether α cell dysfunction contributes to, or results from, diabetes. Improved understanding of α cell behaviours in obese, pre-diabetic, and T2D contexts will prove valuable in understanding the onset and progression of impaired glucose tolerance, and the development of overt T2D.

1.3.2b Impaired glucose counter regulation in T2D

Whereas elevated glucagon secretion at high glucose concentrations may exacerbate hyperglycaemia, T2D is often (especially in insulin-treated individuals) also associated with reduced glucagon secretion at low glucose, leaving individuals at risk of hypoglycaemia (Zhang et al. 2013, Bokhari et al. 2014).

Although widely believed to mainly affect patients with T1D, hypoglycaemia also occurs in patients with T2D (Bonds et al. 2010). On average, 62% of T2D patients will have a hypoglycaemic episode in a year, with an average of each person having 30 mild or moderate hypoglycaemic episodes per year (compared to 83% of T1D patients having a hypoglycaemic event each year, with 58 hypoglycaemic events per person per year) (Ratzki-Leewing et al. 2018). Hypoglycaemic episodes are associated with increased risk of cardiovascular events, hospitalisation, and mortality (Hsu et al. 2013).

The underlying mechanisms remain unknown but it is not because glucagon is not produced or cannot be released by the α cells (Gerich et al. 1973). Whether loss of glucagon secretion at low glucose is intrinsic, or a result of glucose-lowering therapies also remains unclear (Heller et al. 1987, Gerich 1993, Landstedt-Hallin et al. 1999). Clearly, the elucidation of the underlying causes remains an important step in developing effective disease treatments and interventions that specifically target α cell dysfunction.

1.4 Pancreatic anatomy and the islet of Langerhans

1.4.1 α, β and δ cells

Located within the endocrine pancreas, the islets of Langerhans contain the hormone secreting α and β cells essential in homeostatic control of blood glucose concentration. Human pancreatic islets consist of roughly 35% glucagon secreting α cells, 55% insulin secreting β cells, 10% SST secreting δ cells, <5% pancreatic polypeptide secreting PP cells and <1% ghrelin secreting Ɛ cells (Brissova et al. 2005, Andralojc et al. 2009). SST is an important paracrine regulator of α and β cell secretion (Hauge-Evans et al. 2009). α, β, and δ cells are all electrically active with action potential firing producing $[Ca^{2+}]_i$ oscillations which in turn drive hormone secretion.

1.4.2 Human *vs.* rodent islets

Human islets consist of α and β cells roughly evenly dispersed throughout individual islets. However, mouse islets consist of a β cell "core" surrounded by α cells on the outside (Kim et al. 2009). Clearly, this may influence the nature and extent of paracrine interactions between individual cell types and overall islet physiology. Mouse islets consist of 75% β, 19% α, 6% δ cells (Brissova et al. 2005), rather different from the composition of human islets. Nevertheless, mouse islets are often used as a model for studying human disease. They provide readily available access to tissue and can be genetically manipulated. However, these anatomical and physiological differences must not be overlooked. Notably, the homeostatic set-point for plasma glucose concentration is much higher in mice (Gerich 1993) resulting in different thresholds for islet cell activation (Rorsman et al. 2018).

1.5 The α cell, glucagon secretion and action

In secretory cells including α cells, fusion of hormone containing vesicles for secretion is a stepwise process involving membrane bound fusion proteins. The soluble NSF attachment proteins (SNAP) Receptor (SNARE) model provides a unifying model for membrane fusion for many different cell-types. Briefly, secretory vesicles are equipped with synaptobrevin II (V-SNARE; "V" for vesicle) on the cystolic side of the vesicle membrane (Sollner et al. 1993). When vesicles approach the plasma membrane, synaptobrevin interacts with syntaxin and SNAP-25 (T-SNAREs; "T" for target) on the cystolic side of the plasma membrane to form a SNARE complex (Bennett et al. 1992, Sollner et al. 1993). In the absence of $[Ca^{2+}]_i$, the protein complexin inhibits 'zippering' of SNARE complexes and they are locked in a hemifused state ("hemifusion block"). α cells express synaptotagmins (including synaptotagmin 7 at the protein level (Gustavsson et al. 2009)) which act as $[Ca^{2+}]_i$ binding proteins. When $[Ca^{2+}]_i$ becomes elevated, synaptotagmins interact with complexin (possibly inducing a conformational change) which releases the hemifusion block, permitting completion of zippering and vesicle fusion (Schaub et al. 2006, Lee et al. 2010, Lai et al. 2014). Therefore, $[Ca^{2+}]_i$ signalling within α cells is important in determining vesicle fusion, and hormone secretion. How $[Ca^{2+}]_i$ signalling is controlled in α cells and its modulation by different stimuli/inhibitors of glucagon secretion remains a focus of α cell research.

1.5.1 $[Ca^{2+}]_i$ signalling in α cells

The elevation of $[Ca^{2+}]_i$ that drives vesicle fusion and glucagon exocytosis may result from influx of extracellular Ca^{2+} or mobilization of Ca^{2+} from intracellular stores.

Ca^{2+} entry into α cells through voltage-gated Ca^{2+} (Ca_v) channels is well characterised and occurs principally via L and P/Q-type Ca^{2+} channels (Ramracheya et al. 2010, Zhang et al. 2013). In both human and mouse α cells, P/Q-type Ca_v channels are particularly important for glucagon secretion in response to hypoglycaemia (Ramracheya et al. 2010, Rorsman et al. 2012). The L-type Ca^{2+} channels become more important when glucagon secretion is stimulated by β adrenergic agonists and other agents that increase $[cAMP]_i$ (De Marinis et al., 2010) via mechanisms that involve a complex crosstalk between intracellular and plasmalemmal Ca^{2+} channels (Hamilton et al. (2018), see below).

Ca_v channels open as a result of membrane depolarisation, with L-type channels contributing the largest proportion of Ca^{2+} entry. However, when L-type channels are blocked (with isradipine or nifedipine) glucagon secretion is maintained at low glucose (Barg et al. 2000, MacDonald et al. 2007). This may be due to voltage-gated Na^+ channels (Na_v), activated by electrical activity, providing enough inward current to initiate action potential firing and activate the P/Q-type Ca_v channels.

$[Ca^{2+}]_i$ is not only dependent on membrane potential (V_m). As mentioned above, adrenaline stimulates glucagon secretion via increased $[Ca^{2+}]_i$ mobilisation from the intracellular stores. α cells express G_s-coupled β-adrenoceptor, which increases $[cAMP]_i$ when stimulated. In addition to protein kinase A, increased $[cAMP]_i$ also activates the exchange protein directly activated by cAMP 2 (Epac2). Epac2 was originally proposed to increase recruitment of granules to L-type Ca_v channels to promote secretion upon local increases in $[Ca^{2+}]_i$ (Gromada et al. 1997). However,

more recent observations suggest that Epac2 instead acts by promoting calcium-induced calcium release (CICR) by activation of two pore segment channel 2 (TPC2) channels in the lysosomal membrane. When open, Ca^{2+} can move out of acidic stores into the cystol which in turn provides $[Ca^{2+}]_i$ for activation of CICR via activation of ryanodine receptors (RYR) on the ER membrane. The resulting increase in $[Ca^{2+}]_i$ can cause all release-competent granules close to the plasma membrane to undergo exocytosis regardless of their proximity to the Ca_v channels (Rorsman et al. 2012, Hamilton et al. 2018).

This suggests that in α cells, $Ca^{2+}{}_i$ released from intracellular stores, or entering the cell via Ca_v channels in the plasma membrane is capable of stimulating RYR receptors and inducing CICR. ER $Ca^{2+}{}_i$ release may be essential for driving fusion of large numbers of secretion-competent vesicles under conditions where secretary output is highly stimulated, however capacitance recordings demonstrate that vesicle fusion occurs mainly during the upstroke of an action potential in α cells (and fusion decreases after the initial phase of the action potential, during which CICR is triggered (Zhang et al. 2013)). This suggests that local changes in $[Ca^{2+}]_l$, occurring in the vicinity of secretory vesicles and as a result of membrane depolarisation, may be essential in driving fusion of the ready-releasable pool of glucagon containing vesicles particularly under basal conditions.

Adrenaline can induce a $Ca^{2+}{}_i$ response in α cells even during hyperpolarisation using diazoxide and when extracellular calcium is chelated using ethylene glycol-bis(β-aminoethyl ether)-N,N,N',N'-tetraacetic acid (EGTA) (Hamilton et al. 2018). This

illustrates that intracellular Ca^{2+} stores are sufficient to elevate $[Ca^{2+}]_i$ even in the absence of membrane depolarisation. However, the $Ca^{2+}{}_i$ response under these conditions is shorter than normal suggesting that prolonged $Ca^{2+}{}_i$ oscillatory activity is dependent on the ability to depolarise and allow $Ca^{2+}{}_i$ into cells through Ca_v channels (Liu et al. 2004).

1.5.2 Regulation of α cell function

1.5.2a Intrinsic α cell regulation

Due to the activation of Ca_v channels by membrane depolarisation, electrical activity and $[Ca^{2+}]_i$ are intrinsically linked and control glucagon secretion. α cells secrete glucagon at low, but not high glucose concentrations. How exactly α cells respond to different plasma glucose concentrations with changes in electrical activity, $[Ca^{2+}]_i$, and hormone secretion remains poorly understood. It appears that α cell action potential firing is not suppressed at glucose concentrations that inhibit glucagon secretion (Gromada et al. 2004, Zhang et al. 2013). α cell activity (electrical activity and $[Ca^{2+}]_i$ signalling) can be influenced by paracrine regulation from neighbouring β and δ cells. However, glucagon secretion is inhibited at glucose concentrations below which SST or insulin secretion are stimulated (MacDonald et al. 2007, Vieira et al. 2007, Walker et al. 2011, Gylfe 2016). Therefore, glucose-induced inhibition of glucagon secretion can clearly be controlled by processes that do not involve paracrine input and α cells must have some intrinsic mechanisms for responding to changing glucose.

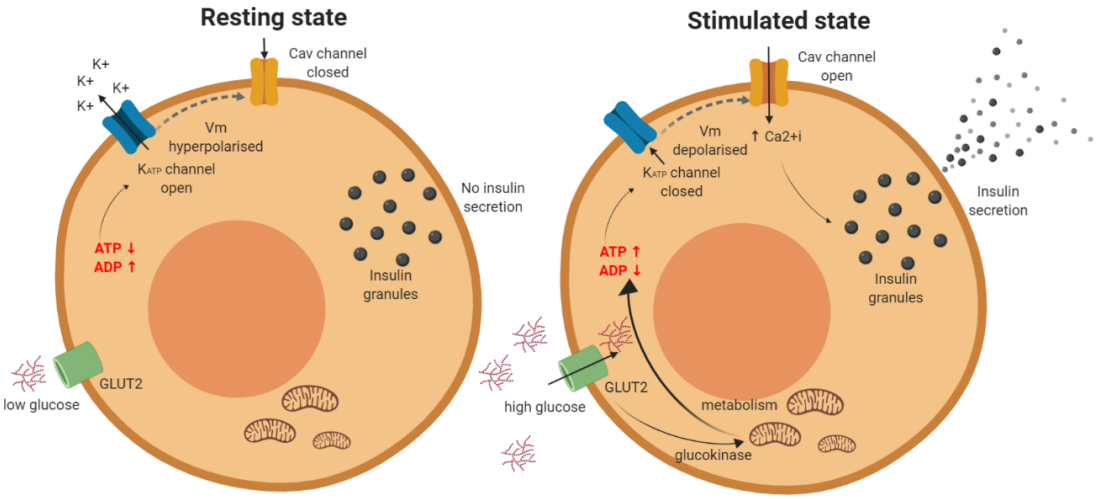

Figure 1.4 *β cell model for glucose-induced insulin secretion; under resting conditions, the K_{ATP} channel is open, High K^+ permeability through K_{ATP} maintains V_m in a hyperpolarised state. Voltage gated Ca_v channels are closed, and insulin secretion does not take place. As plasma glucose rises, glucose enters the β cell via GLUT2. Glucose metabolism (glycolytic and mitochondrial metabolism) leads to increased ATP:ADP ratio. This, in turn causes closure of the K_{ATP} channel. When K_{ATP} channels close, the membrane is depolarised, leading to activation of Ca_v channels. The resultant increase in $[Ca^{2+}]_i$ triggers vesicle fusion at the plasma membrane and insulin secretion.*

In β cells, an increase in glucose concentration results in increased glucose oxidation and an increase in intracellular ATP concentration ($[ATP]_i$). ATP-sensitive potassium channels (K_{ATP}) close in response to the increased $[ATP]_i$ resulting in V_m depolarisation, activation of Ca_v channels increasing $[Ca^{2+}]_i$ and stimulating vesicle fusion and insulin secretion (**Figure 1.4**, (Ashcroft et al. 1990, Koster et al. 2005, Lai et al. 2018).

Unlike β cells, α cells are most active when the extracellular glucose concentration is low. This raises the question as to the mechanism by which glucose inhibits α cells. There are two consensus mechanisms for how this occurs: the 'K_{ATP}' and the 'store-operated conductance' (SOC) models. According to the two models, an increase in glucose will affect $[Ca^{2+}]_i$ differentially (increase/no change and decrease, respectively).

The K_{ATP} model posits that high glucose influences the α and β cells similarly. Like β cells, α cells express K_{ATP} channels and glucokinase and in both cell types high glucose increases $[ATP]_i$ (Ravier et al. 2005). Importantly, the whole-cell K_{ATP} channel conductance at low glucose is much lower in α cells than in β cells and this results in slight membrane depolarisation of the α cells and action potential firing under hypoglycaemic conditions (Zhang et al. 2013). Whereas β cells express principally $Na_v1.7$ channels, α cells express primarily $Na_v1.3$. The two channels have different inactivation properties and this is part of the reason why half-maximal Na_v current inactivation ($V_{0.5}$) occurs at -100 mV in β cells but at -50 mV in α cells (Zhang et al. 2014). In β cells, Na_v currents are therefore largely redundant (because they are permanently inactivated at physiological membrane potentials) and Ca_v currents underlie action potential firing. However, in α cells Na_v currents play an essential role in permitting electrical activity. When glucose is increased and the K_{ATP} conductance diminishes, the associated membrane depolarisation will result in (partial) inactivation of the Na_v channels. A consequential reduction of action potential height leads to reduced voltage-dependent activation of the P/Q-type Ca_v channels and suppression of glucagon secretion. The model is supported by the finding that $[Ca^{2+}]_i$ oscillations and action potential firing persist at high glucose, although the height of action potentials is reduced (Gopel et al. 2000, Le Marchand et al. 2010, Ramracheya et al. 2010, Zhang et al. 2013, Zhang et al. 2014).

According to the SOC model, an increase in glucose leads to increased ATP production and this promotes Ca^{2+} uptake into sarco/endoplasmic reticulum (SER) by activation of the SER Ca^{2+}-ATPase (SERCA) pump. The resulting lowering of $[Ca^{2+}]_i$ in itself

inhibits glucagon secretion and may also decrease electrical activity by switching off the store-operated Ca^{2+} channel Orai1, whose activity is regulated STIM1 (STIM1 senses SER Ca^{2+} filling). When Ca^{2+} stores are full, Orai1 channels close and this was speculated to result in membrane repolarization, reduced action potential firing and suppression of glucagon secretion. Conversely, emptying of Ca^{2+} stores at low glucose concentrations activates Orai1 channels, which provides a depolarising inward current for activation of Ca_V channels and therefore secretion (Johansson et al. 1987, Liu et al. 2004, Vieira et al. 2007, Watts et al. 2014).

Modelling reveals that either of these models can account for the inhibition of glucagon secretion with increasing glucose concentration. However, both models must be combined to recreate the slight increase in glucagon secretion seen at high glucose concentrations that has been described in some studies (Watts et al. 2014). This indicates that the two models may not be mutually exclusive, and rather may both contribute to control of α cell activity.

The elucidation of how glucose regulates glucagon secretion remains a great hurdle in our understanding of the α cell. Indeed, the models described rely mainly on the role of glucose metabolism in determining α cell function but its regulation is much more complex than this. Electrical activity and hormone secretion are highly energy-dependent processes. Somewhat paradoxically, α cells are most active at low glucose concentrations when glucose-derived ATP is low. This has led to the proposal that the α cells metabolise fat in the absence of glucose and that this provides the metabolic energy to sustain electrical activity and hormone secretion at low glucose

concentrations (Briant et al. 2018). A cocktail of amino acids have long been recognised as a powerful stimulus of glucagon secretion (Unger et al. 1969, Rocha et al. 1972), an observation that probably explains the transient stimulation of glucagon secretion that occurs following ingestion of a mixed meal despite the increase in plasma glucose (Alsalim et al. 2016).

1.5.2b Extrinsic regulation

As discussed, α cells have intrinsic mechanisms for responding to changing glucose concentration. However, when islets are dispersed into single cells, α cell behaviour changes markedly (Le Marchand et al. 2010). This indicates that intact islet architecture and paracrine signalling are essential for normal α cell function.

Within islets, cells interact extensively through paracrine signalling to regulate secretory output (**Figure 1.5**). Insulin inhibits glucagon secretion, either via the insulin receptor (InsR) or by alteration of α cell glucose utilisation (Ostenson 1979). γ-aminobutyric acid (GABA), known to inhibit α cells via activation of $GABA_A$ Cl^- channels, is secreted from β cells (Rorsman et al. 1989, Reetz et al. 1991, Braun et al. 2004, Wendt et al. 2004, Braun et al. 2007, Braun et al. 2010, Menegaz et al. 2019). α cells express $GABA_A$ and antagonism of the $GABA_A$ receptor with SR95531 reverses inhibition of glucagon secretion by high glucose (Bailey et al. 2007).

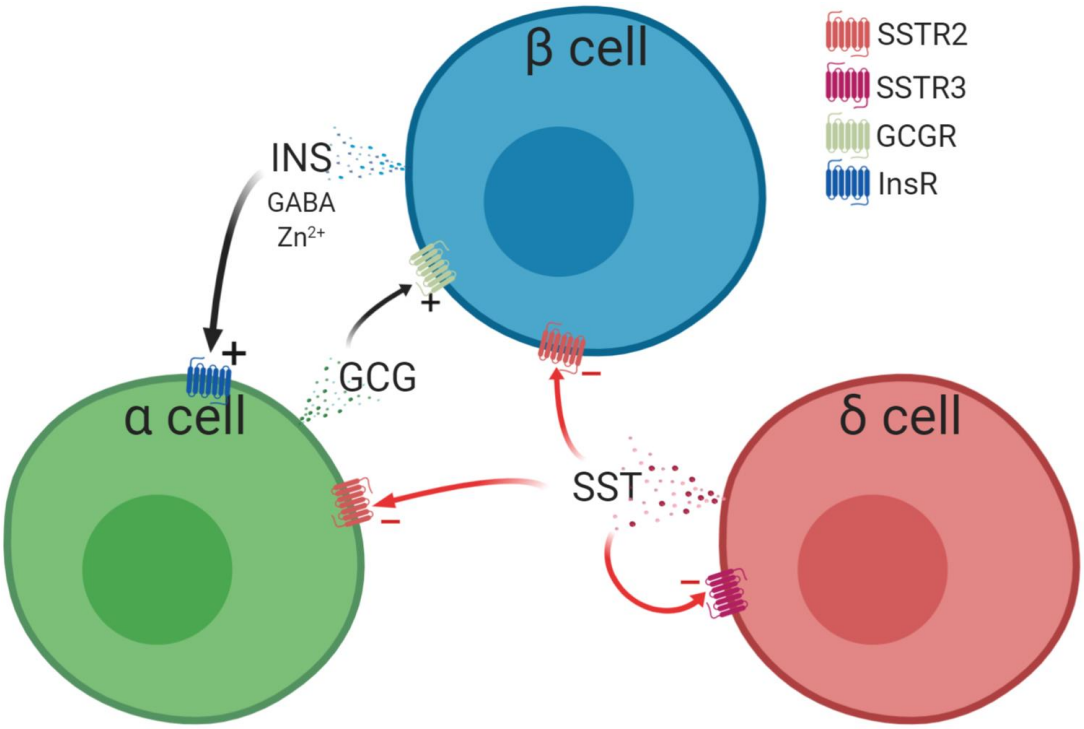

Figure 1.5 *Paracrine signalling between α, β, and δ cells of the endocrine pancreas. SST secreted from δ cells is a major paracrine regulator – inhibiting activity in neighbouring α and β cells through paracrine signalling at the SSTR2. SST also acts on the δ cell in an autocrine manner via SSTR3. Insulin, secreted from the β cell, and glucagon, secreted from the α cell, each stimulate each other's activity via the InsR and GCGR respectively.*

There is much debate around the role of Zn^{2+}, co-released with insulin, in regulating α cell activity (Raskin et al. 1975, Ishihara et al. 2003). Mice lacking the Zn^{2+} transporter Znt8 specifically in α cells have elevated glucagon secretion. ZnT8 KO α cells displayed normal $[Ca^{2+}]_i$ oscillation frequency and amplitude, suggesting that Zn^{2+} alters glucagon secretion via a $[Ca^{2+}]_i$ independent mechanism (Solomou et al. 2015). Overexpression of ZnT8 in α cells reduces glucagon secretion (Solomou et al. 2016). During *in vivo* perfusions, Zn^{2+} can inhibit glucagon secretion in the absence of insulin, however insulin cannot inhibit glucagon in the absence of Zn^{2+} (Zhou et al. 2007) or in the absence of δ cell InsR (Vergari et al. 2019).

Zn^{2+} may be important in tonic inhibition of α cells as the effect of inhibition/overexpression of ZnT8 in α cells on glucagon secretion is greatest at low

glucose concentrations (Solomou et al. 2015, Solomou et al. 2016). However, under normal conditions the glucose concentrations at which insulin and glucagon secretion are altered in response to glucose do not overlap (Salehi et al. 2006). Therefore, regardless of the ability of insulin and/or Zn^{2+} to inhibit glucagon secretion, it may not have physiological relevance as Zn^{2+}/insulin are never present when glucagon secretion is occurring. It is worth noting that in these experiments, the relationship between glucagon and paracrine regulation has been investigated in the context of different glucose concentrations. In reality, changing fatty acid and amino acid concentrations may alter the secretory ranges of insulin and glucagon such that they do overlap allowing Zn^{2+} and GABA to play important roles in paracrine regulation.

SST inhibits α cell activity and glucagon secretion via the somatostatin receptor-2 (SSTR2). The SST-secreting δ cells are most active at high glucose concentrations and have been proposed to protect against insulin over-secretion (Hauge-Evans et al. 2009). The relationship between α and δ cells is complex; Glucagon secretion from *Sst*$^{-/-}$ islets is unaffected at low (0-7 mM), but increased at high (15-30 mM) glucose (Hauge-Evans et al. 2009). This indicates that SST is of varying importance to α cell function depending on glucose concentration. These data also demonstrate a huge challenge in interpreting data from intact pancreatic islets. It has been proposed that glucose regulation of glucagon secretion reflects a mosaic of different mechanisms, the contribution of which is difficult to disentangle (Briant et al. 2016). Separating the effect of something on an individual cell/cell type from indirect effects on other cell types is particularly difficult and experiments must be done in a considered manner.

α cells are also thought to act on themselves in an autocrine manner. Glucagon increases α cell exocytosis (Ma et al. 2005) and *Gcg* gene expression (Leibiger et al. 2012). Furthermore, glutamate, co-released with glucagon, stimulates α cell electrical activity via activation of α-amino-3-hydroxy-5-methyl-4-isoxazolepropionic acid (AMPA) receptors (Cabrera et al. 2008, Cho et al. 2010).

Finally, a number of endocrine regulators of α cell function are known. Leptin, released from adipocytes at a level proportional to fat mass, reduces α cell $[Ca^{2+}]_i$ and glucagon secretion when applied acutely to intact islets (Tuduri et al. 2009). GLP-1, released by intestinal L-cells, inhibits glucagon secretion (De Marinis et al. 2010, Ramracheya et al. 2018). Therapeutically, the inhibition of glucagon secretion in T2D patients at high glucose concentrations is particularly relevant as (as discussed above) hyperglycaemia caused by hypoinsulinaemia/insulin resistance in T2D is exacerbated by hypersecretion of glucagon (Nauck et al. 2002, Menge et al. 2011, Zhang et al. 2019). The mechanism of action of GLP-1 on α cells is highly controversial as the presence of the GLP-1 receptor (GLP-1R) in α cells has ranged from totally absent (Moens et al. 1996, Tornehave et al. 2008) to present in 20% of α cells (rat (Heller et al. 1997)) to functionally present in 100% of cells (Ding et al. 1997). More recently, fluorescent staining of GLP-1R using LUXendin has confirmed that GLP-1R is present in ~5% of α cells (Ast et al. 2020). GLP-1 has been proposed to inhibit glucagon secretion by a direct effect on α cells via closure of Ca_V channels (De Marinis et al. 2010) or via a paracrine effect mediated by δ cell SST secretion (at elevated glucose concentrations) to reduce glucagon secretion (Orgaard et al. 2017).

1.5.3 Functional identification of α cells for $[Ca^{2+}]_i$ imaging

As outlined above, α cells make up 35% of the cells in human but only 19% of the cells in mouse islets. Different islet cell types are morphologically indistinguishable so when imaging whole islets for $[Ca^{2+}]_i$, α cells have traditionally been identified using functional methods including the presence of $[Ca^{2+}]_i$ signalling at low glucose, stimulation by glutamate, and stimulation by adrenaline at high glucose (Santos-Silva et al. 2015, Hamilton et al. 2018). These identification techniques have not been fully validated, high resolution imaging requires islets to remain stable for the whole duration of a recording so each cell can be tracked (although this is less of an issue at low resolution) and pharmacological tools may influence cell behaviour if applied at the beginning of recordings. For these reasons, a mouse with a genetically encoded $[Ca^{2+}]_i$ indicator expressed specifically in the α cell was used in this work. This model is superior as it facilitates reliable identification of α cells and direct measurement of $[Ca^{2+}]_i$. Chapter 3 describes the generation of GcgGCaMP3 mice and the characterisation of α cell $[Ca^{2+}]_i$ dynamics in response to glucose. These mice were also used in Chapters 5 and 6 to study how α cell $[Ca^{2+}]_i$ dynamics are altered as a result of HFD.

1.5.4 Glucagon synthesis from pre-proglucagon

Glucagon is a 29-amino acid peptide encoded by the proglucagon (*GCG)* gene which (in humans) is located on chromosome 2 (Bataille 1996). The *GCG* gene is expressed in numerous locations throughout the body including in pancreatic α cells, intestinal L-cells and the hypothalamus in the CNS (Drucker et al. 1988, Albrechtsen et al. 2016). Differential expression of prohormone convertase (PC) enzymes allows for tissue-

specific expression of proglucagon gene products. This explains why the pancreatic α cells (that express PC2) produce glucagon whereas the gut and the brain, that express PC1 and PC3, release glicentin, GLP-1, GLP-2, GRPP, and oxyntomodulin amongst other peptides. Due to the similarity of peptide products from the proglucagon gene, antibody detection of glucagon must be carried out with antibody binding at both the C- and N-termini, as indicated in **Figure 1.6** (Albrechtsen et al. 2016).

Although it is traditionally thought that the pancreas provides much of the glucagon in the circulation, it is important to consider the contribution of glucagon from the gut (Ravazzola et al. 1981). In fully pancreatectomised individuals, some remaining glucagon can be measured (Lund et al. 2016, Lund et al. 2019). Therefore, plasma glucagon could be elevated even in the absence of α cell dysfunction due to increased intestinal output. However, the relative contribution of these two sources to circulating glucagon is unknown and pancreatectomy could result in a compensatory increase in output from the gut relative to non-pancreatectomised individuals.

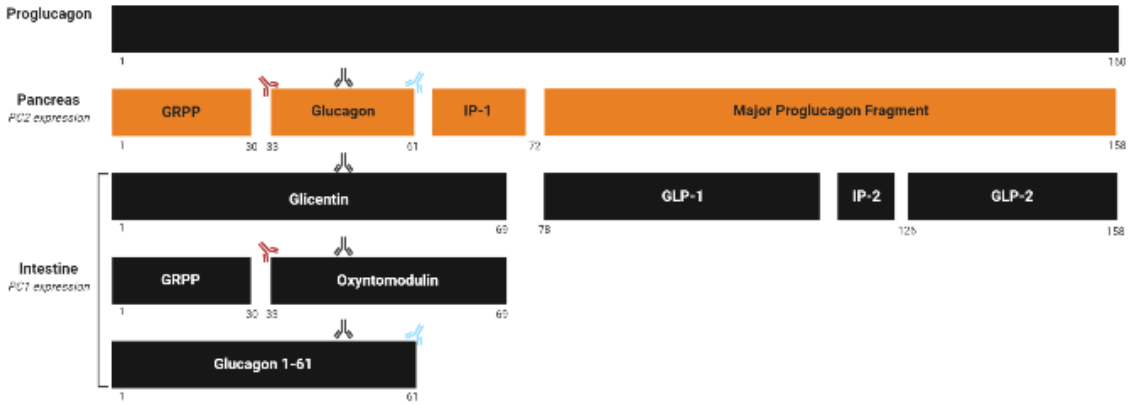

Figure 1.6 *Generation of tissue specific products from the Proglucagon gene through tissue specific expression of prohormone convertase. Albrechtsen et al. (2016) used for reference.*

1.6 Aims of thesis

1.6.1 Generate and validate GCaMP3 model

As discussed, reliable identification of α cells remains a limiting factor to progression in understanding of the fundamental physiology of these cells. The first aim of this thesis was therefore to establish a mouse line expressing the genetically encoded fluorescent proteins GCaMP3 and/or RFP under the control of the glucagon promotor. This tool will allow for reliable identification of α cells and interrogation of $[Ca^{2+}]_i$ dynamics. The aim is to generate the mouse line, validate specificity of marker expression, and carry out initial characterisation of the $[Ca^{2+}]_i$ dynamics in α cells in response to known stimulants.

1.6.2 *In vivo* - Carry out extensive metabolic phenotyping

In order to assess α cell dysfunction under diabetogenic conditions, mice generated under the first aim will be placed on a high fat diet (HFD). Thorough characterisation of metabolic and endocrine changes in the mice will be used to assess how and when dysfunctional glucagon secretion develops, and the extent to which this contributes to the disease phenotype.

1.6.3 *Ex vivo* - Interrogate functional alterations in α cell activity following HFD

Following metabolic characterisation, islets isolated from HFD mice will be interrogated to identify ways in which their function is altered. Secretion from the perfused pancreas and isolated islets, and $[Ca^{2+}]_i$ imaging will be used to characterised changes in glucose sensitivity of α cells following HFD.

1.6.4 Interrogation of the role of fat metabolism in glucagon secretion from α cells

In order to investigate the importance of fat metabolism in α cell dysfunction following HFD we will place mice lacking the enzyme involved in fatty acid oxidation carnitine palmitoyltransferase I specifically in their α cells (αCTP1a) on a HFD and will investigate whether these mice are protected from the development of hyperglucagonaemia. We will also use pharmacological tools to inhibit islet cell fatty acid oxidation to identify the relative importance of this to islets from mice fed control and high fat diets.

1.6.5 Investigate changes in α cell gene expression following HFD

Finally, in order to understand the changes at the gene level which underlie altered α cell function, we will carry out RNAseq on α and non α cells from HFD fed mice. This will be used to assess whether functional changes observed can be explained by changes in mRNA expression and to identify targets for onward investigation.

Chapter 2

2.1 Animal husbandry

2.1.1 Ethical approval

All animal work was performed in accordance with the UK Scientific Procedures Act (1986) and University of Oxford ethical guidelines, and were approved by the local Ethical Committee.2.1.2 Generation of GcgRFP/GCaMP3 mouse line

Our aim was to generate mice expressing RFP and/or GCaMP under the control of the glucagon promoter "GcgRFP" and "GcgGCaMP" respectively.

To generate GcgRFP mice, we took mice heterozygous for a proglucagon driven iCre recombinase (*Tg(Gcg-icre)*^{12Fmgb}) (GcgCRE$^{+/-}$) and crossed them with mice heterozygous for tdRFP reporter insert in the ROSA26 gene (*Gt(ROSA)26Sor*^{tm1Hjf}) (GcgRFP$^{+/-}$), as described in Parker (2012).

To generate GcgGCaMP3 mice we crossed GcgCRE$^{+/-}$ mice with mice heterozygous for an insert in the ROSA26 locus containing a CAG promoter followed by a floxed stop codon and the genetic sequence for the *Gcamp3* allele (*Gt(ROSA)26Sor*$^{tm38(CAG-GCaMP3)Hze}$), Jackson Laboratory No. 014538, (Zariwala et al. 2012)) (GcgGcamp$^{+/-}$). Alleles were passed, were possible, through the paternal line to generate offspring heterozygous for any allele Gcg RFP$^{+/-}$ or GCaMP$^{+/-}$ in combination with GcgCRE$^{+/-}$. C57BL/6j females WT for all alleles were used for breeding to ensure regular back-crossing of the line and maintenance of heterozygosity.

In mice carrying both the *Cre* and *GCamp3/RFP* alleles, expression of Cre recombinase (under the control of the glucagon promoter) would result in excision

of the stop codon and expression of the GCaMP3/RFP proteins. We acknowledge that GCaMP will also be expressed outside the islet due to the expression of the proglucagon gene in numerous specific locations throughout the body (including the brain, and the gut (Parker et al. 2012)) but this is unlikely to affect the function of these cells.

Table 2-1 *Table outlining allele information for mice of various genotypes*

Mouse model	**Alleles**
GCGRFPGCaMP3	*Tg(Gcg-icre)*^{12Fmgb} *Gt(ROSA)26Sor*^{tm1Hjf} *Gt(ROSA)26Sor*$^{tm38(CAG-GCaMP3)Hze}$/J
GcgRFP	*Tg(Gcg-icre)*^{12Fmgb} *Gt(ROSA)26Sor*^{tm1Hjf}
GcgGCaMP3	*Tg(Gcg-icre)*^{12Fmgb} *Gt(ROSA)26Sor*$^{tm38(CAG-GCaMP3)Hze}$/J

2.1.3 Generation of αCPT1a-KO mouse line

Mice carrying a loxP insert flanking exons 11 and 12 of the *Cpt1a* gene (*Cpt1a*$^{lox/lox}$) (Schoors et al. 2015) were crossed with GcgCre mice described earlier (Parker et al. 2012) to generate mice lacking CPT1a protein expression specifically in glucagon expressing cells (Briant et al. 2018). Littermates mice lacking either the *GcgCre* allele and/or the *Cpt1a* loxP insert were used as controls "CON" (Briant et al. 2018).

2.2 Genotyping

2.2.1 DNA isolation

Mice were ear-clipped (minimum age 10 days) and genomic DNA (gDNA) was isolated from earclips using ChargeSwitch^{TM} gDNA Micro Tissue Kits (Thermo Fisher #CS11203) according to manufacturer's instructions.

2.2.2 PCR

Polymerase chain reaction (PCR) was performed using BioMixRed (Bioline #Bio-25006) ready to use PCR reaction mix. BioMixRed contains 5 mM $MgCl_2$, dNTPs and Taq DNA polymerase. The ready to use reaction mix is diluted in water and added directly to isolated DNA (**Table 2-4**). Dimethyl sulphoxide (DMSO) may be added to improve reaction efficiency as outlined in **Table 2-2**. Reaction protocol is outlined in **Table 2-3**.

Table 2-2 Primer mixes and concentrations for genotyping of Cre, Rfp and Gcamp3 genes

Cre PCR mix (25 µl)	volume
BioMixRed 2x	12.5
Primer Mix Stock 10 µM Cre Primers 2-5 µM Housekeeper	1 µl
diH_2O	9.5 µl
DMSO	1 µl
DNA	1 µl

RFP/GCaMP3 PCR mix (25 µl)	volume
BioMixRed 2x	12.5
Primer Mix Stock 10 µM RFP or GCaMP3 Primers 2-5 µM Housekeeper	1.25 µl
diH_2O	10.25 µl
DNA	1 µl

Table 2-3 PCR reaction protocol for Cre, RFP and GCaMP3 PCR reactions

Step		**Temp**	**Duration**
Denaturation		95°C	1 min
Amplification			
Repeat for 39 cycles	Denaturation	95°C	15 sec
	Annealing	58°C	30 sec
	Extension	72°C	45 sec
Final extension		72°C	5 min
Holding		8°C	Until end

Table 2-4 Primer information for mouse genotyping

Gene	**Sequence**	**Fragment size**
β catenin		220 bp
Rm41	AAGGTAGAGTGATGAAAGTTGTT	
Rm42	CACCATGTCCTCTGTCTATTC	
Cre		537 bp
iCre002	GACAGGCAGGCCTTCTCTGAA	
iCre003	CTTCTCCACACCAGCTGTGGA	
Gcamp3		500 bp
ME38	CTTCAAGATCCGCCACAACATCG	
ME39	TTGAAGAAGATGGTGCGCTCCTG	

After PCR, reaction product was run on a 1.5% agarose gel (Sigma #A9539) made up in 1x Tris-Acetate-EDTA (TAE) buffer (sigma #1060231000). Gels were visualised using a ChemiDoc™ XRS+ Machine running Image Lab software (BioRad, Hurcules, CA, USA).

2.3 Metabolic phenotyping

2.3.1 Glucose tolerance tests

Mice aged 10-15 weeks were used for IPGTTs. Prior to the experiment, mice were weighed and blood glucose measured. They were fasted for five hours prior to an intraperitoneal (IP) injection of 2 g/kg glucose. Blood glucose was measured from a cut to the tail using the Bayer Contour Next Blood Glucose Monitoring System and Bayer Contour Next test strips (Bayer #7308). Blood glucose measurements were taken before fasting and at 0, 15, 30, 60 and 120 min after IP injection of glucose.

2.3.2 Insulin tolerance tests

Mice aged 10-15 weeks were used for intraperitoneal insulin tolerance tests (IPITTs). Prior to the experiment mice were weighed and blood glucose measured as described above. They were fasted for five hours prior to an IP injection of 0.75 U/kg insulin (Humalog, Ely Lilly). Blood glucose was measured at 0, 15, 30, 60 and 120 min after IP injection of insulin.

CTL mice had 69.5% lean mass, whereas HFD fed mice had 59.5% lean mass. For the lean mass-based ITT, CTL mice received 0.75 U/kg total weight, whereas HFD fed mice received 0.64U/kg thereby giving the mice the same dose of insulin per gram lean mass.

2.3.3 EchoMRI

Mice underwent EchoMRI measurement of lean, fat and water mass using an EchoMRI^{TM} machine following 6 weeks altered diet and again following 12 weeks of diet. Free water is measured twice in EchoMRI analysis – once as free water and once as a constituent part of the lean mass. This explains why the sum of mean lean mass, water and fat in grams equals more than the mean total body weight.

2.3.4 Plasma hormone measurements

At 0 and 30 min of GTT and ITT protocols, as well as at several time points during the day, 25 µl whole blood was collected into Vitrex Ethylenediaminetetraacetic acid (EDTA) coated capillary tubes and blood expelled directly into Sarstedt Microvette EDTA coated tubes (300 µl) prefilled with 5 µl Aprotinin per 25 µl whole blood (1:5, 4 trypsin inhibitor unit (TIU)/ml; Sigma-Aldrich, UK). Blood was spun at 2000 g for 10 min at 4 ^{o}C and plasma collected and stored immediately on dry ice. Glucagon measurements were performed using the 10 µl Glucagon enzyme-linked immunosorbent assay (ELISA) kit (Mercodia, Sweden), insulin measured using Mouse Insulin ELISA (Mercodia), and GLP-1 using a Northern Lights Total GLP-1 ELISA (Mercodia).

2.4 Islet Isolation

Mice were killed by Schedule 1 cervical dislocation as approved by the home office. Mouse pancreatic islets were isolated by Liberase™ TL (Roche #05401020001) injection into the common bile duct and enzymatic digestion of exocrine tissue by

incubation for 13 min at 37°C. Islets were hand-picked from exocrine tissue and used for onward experiments, culturing for a maximum of 36 hours following isolation. Islets were kept in RPMI medium (Gibco 11879-020) with 11 mM glucose (Sigma), 10% foetal bovine serum (FBS, Sigma), 1% Penicillin-Streptomycin (Pen-Strep, Gibco) at 37°C 5% CO_2.

2.5 Dissociation of islets into single cells

Isolated pancreatic islets from GgcRFP mice were disassociated into single cells following washing in Phosphate Buffered Saline (PBS) by 5 min incubation in 1 ml trypsin (TrypLE, Gibco). 9 ml RPMI 1640 medium (10% serum, 1% Pen-Strep, 11 mM glucose) was used to stop digestion and islets were pipetted up and down twice using a 10 ml pipette. The cell suspension was spun at 400 g for 5 min at room temperature. Medium was removed from the dispersed cell pellet. 500 µl RPMI 1640 (2% serum, 1% Pen-Strep) was added to re-suspend pelleted cells prior to mechanical disassociation (60 times pipetting up and down using 1 ml pipette). Dispersed cells were filtered using a 30 µm filter prior to fluorescence-activated cell sorting (FACS).

Samples for RNAseq were dispersed differently to allow the addition of a live dead stain step (LIVE/DEAD™ Fixable Far Red Dead Cell Stain, Invitrogen #L10120). Islets were first washed in PBS and then digested for 5 min at 37 °C in TrypLE. After 5 min, trypsin was removed and replaced with 1 ml PBS (11 mM glucose). Islets were allowed to settle and the PBS removed and replaced with 500 µl PBS to wash the islets. Whole islets were triturated 60 times to disperse into single cells. Cell death was evaluated using 1 µl/ml live/dead stain as described above which was added to

cells for 30 min to stain (as per the manufacturer's instructions). After 30 min cells were spun at 700 g for 10 min and supernatant removed and discarded. Cells were resuspended in 500µl PBS + 2% FCS (1 mM glucose) until sorting within 1 h)

2.5.1 Fluorescent activated cell-sorting of dispersed whole islets

Dispersed cells underwent FACS by Andrew Worth at the Jenner Institute for Vaccine Research, Old Road Campus, Oxford using a MoFlo Legacy FAC-Sorter from Beckman Coulter. **Figure 2.1** outlines the process of FACS.

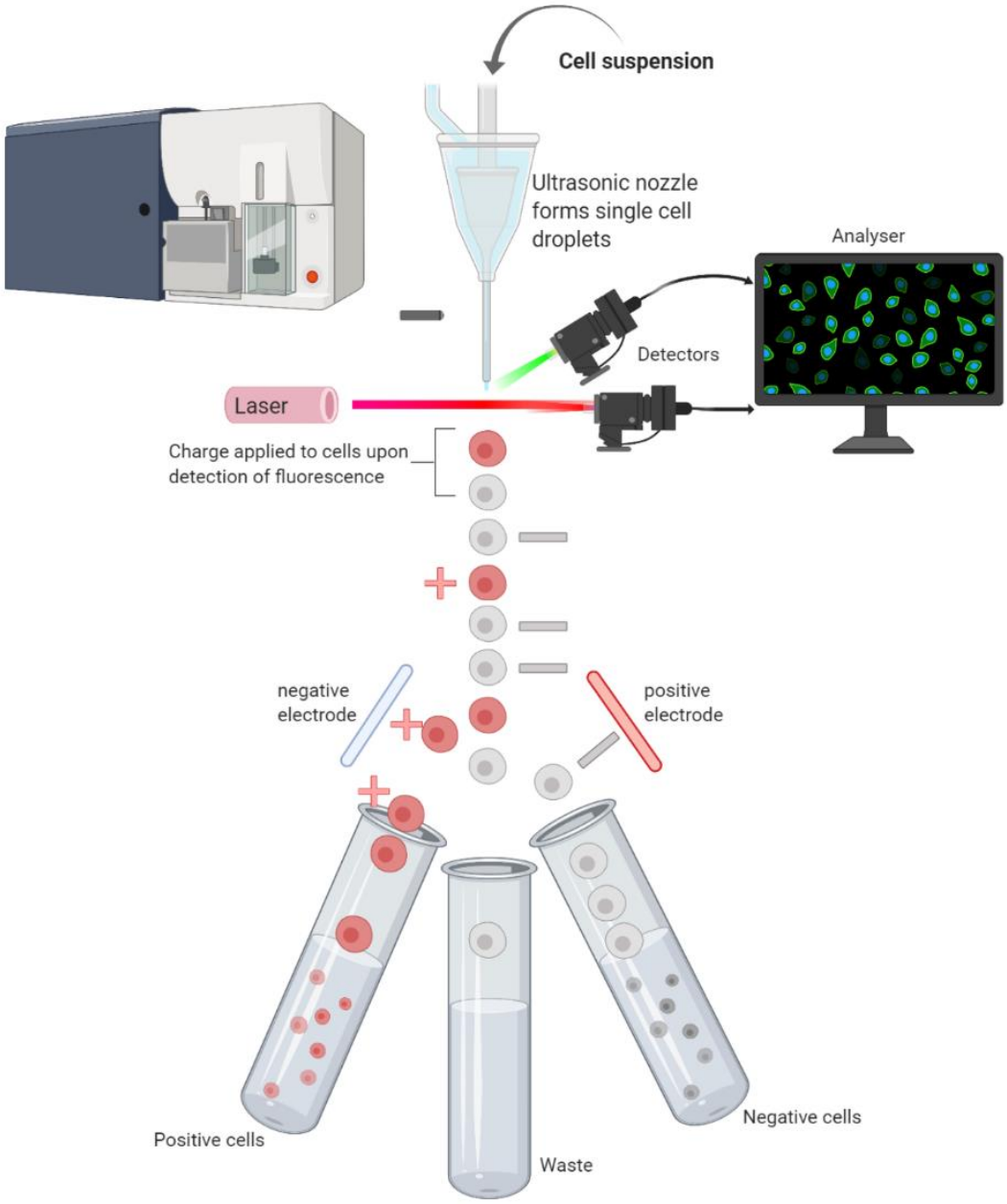

Figure 2.1 *Schematic of the FACS process of sorting cells based on the presence of a fluorescent marker.*

As displayed in **Figure 2.2,** forward and side scatter were used to exclude cell debris (R5) and exclude very small/very large cells (R1). Doublets/triplets and larger cell debris were excluded from the positive fraction by gating based on pulse width (R2). RFP was used to identify α cells by excitation at 488 nm and emission at 565-595 nm (580/30 bandpass filter) (R4), $RFP^{-/-}$ cells were identified by lack of fluorescence (R3).

Cells exhibiting far-red fluorescence were excluded (R7). The live dead stain works by binding covalently to intracellular amines. Therefore broken cells/fragments fluoresce and can be excluded. One mouse was used per sample; i.e. islets/cells from different mice were not pooled prior to sorting.

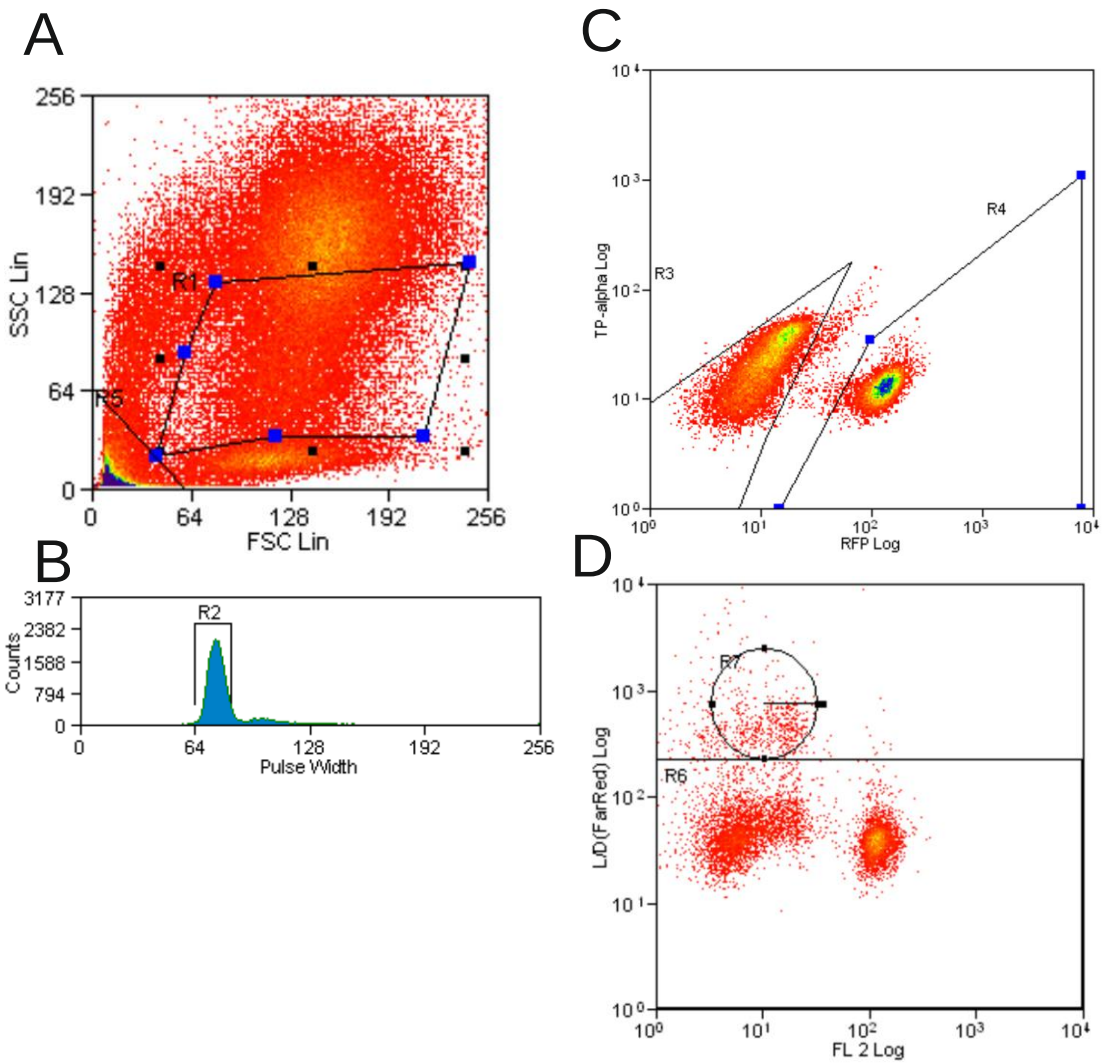

Figure 2.2 *Gating profiles for FAC-Sorting of pancreatic islets. R1 gate was used to select cells of appropriate size, and R5 was used to exclude small cell fragments (A). R2 to select singlet cells rather than ineffectively dispersed doublet or triplets (B). R3 was used to collect RFP$^-$ cells and R4 RFP$^+$ cells (C). Finally, R6 was used to select live cells, and R7 to exclude dead cells (D).*

2.6 RNA

2.6.1 RNA extraction, RNA-cDNA, qPCR of fluorescence-activated cell sorted cell fractions

RNA from cells was extracted following FACS using the RNeasy Micro Kit (Qiagen) using the standard protocol. RNA concentration following extraction was, on average, approximately 1 ng/µl for the RFP^+ cells and 10 ng/µl for the RFP^- cells. cDNA was synthesised using the High Capacity RNA-to-cDNA kit from Applied Biosystems using approximately 10 ng purified RNA per reaction. Quantitative reverse transcription polymerase chain reaction (RT-qPCR) was carried out using the QuantiFast SYBR Green PCR kit (Qiagen) and ABI 7900 Sequence Detection System PCR machine (Applied Biosystems). Details of primers used for qPCR are outlined in **Table 2-5**.

Table 2-5 *details of qPCR primers*

Gene name	**Gene**	**Primer ID**
Beta-actin	*Actb*	QT00095242
Glyceraldehyde 3-phosphate dehydrogenase	*Gapdh*	QT01658692
Insulin	*Ins2*	QT00114289
Glucagon	*Gcg*	QT00124033
SST	*Sst*	QT00239295

Samples were run in triplicate and RNA quantified using the 2^ΔCT method (2^sample cycle quantification (CT) value - housekeeper CT value; Schmittgen and Livak (2008)).

2.6.2 Fluorescence-activated cell sorting of α and non-α cell fractions for RNAseq

During FACS, 550 α and 550 β cells were sorted directly into 2.3 µl lysis buffer (0.8% Triton-X 100 with 2U/µl RNase inhibitor, cell volume approx. 1.8 ul). Following lysis,

cells were promptly loaded into a 96 well plate and frozen on dry ice for onward processing. Library Prep and RNAseq was carried out by the core facility at the Wellcome Trust Centre for Human Genomics (Oxford) using the SmartSeq-2 approach with HiSeq4000 sequencing (≥2 million reads/sample).

Analysis of the RNAseq data was carried out by Martijn van de Bunt (Novo Nordisk, Denmark). Salmon v0.8.1 software (Patro et al. 2017) was used to quantify expression of protein-coding transcripts from Ensembl v89 based on the mouse reference genome (GRCm38). Expression was corrected for GC bias and calculated at the gene level. *Voom* (Law et al. 2014) was used to normalise pseudocounts and differential expression analysis (α *vs.* non-α, CTL *vs.* HFD) was performed in R using a paired design in *limma* (Ritchie et al. 2015).

2.7 Immunohistochemistry

2.7.1 Fixing and embedding of whole pancreases

Whole pancreases were harvested and placed in 4% PFA for up to 24 hours before placing into 70% EtOH until wax embedding. Whole pancreases were dehydrated and embedded into wax using a Leica TP 1020 wax embedding machine. Samples were passed through (for 1 h each) formalin, 50% IMS, 70% IMS, 90% IMS, 100% IMS x 3, xylene x 2 and paraffin x 2. Pancreases were then embedded in a wax block for sectioning.

2.7.2 Staining of whole pancreases

Whole pancreases were sectioned at approximately 7 µm thick using a Leica RM 2235 and placed onto Frost Free tissue slides prior to staining of slices.

Slices were first dewaxed in xylene for 5 min x2 and slices were then passed through descending concentrations of EtOH (3- 5 min each) 100% x2, 95%, 70%, water was then run over slides for 5 min. Slides were heated for 5 min in a microwave to reveal antigens. Slides were washed 3x 5 min in Tris saline. Samples were blocked with swine serum for 20 min before overnight application of primary antibody (1° Ig) diluted in TRIS buffer. After binding of 1° Ig, slides were washed 3x 5 min in TBS. secondary antibody (2° Ig) was then applied for 30 min binding (in the dark). Stained slides were washed in TBS x 3 (5 min each) before application and securing of cover slips. Antibodies outlined in **Table 2-6**. Pancreas slices were imaged using a BioRad Radiance 2100 Scanning Laser Confocal Microscope with a 60x 1.0 NA water emersion objective. The three channels were acquired consecutively using LaserSharp 2000 software (Zeiss).

2.7.3 Fixing and staining of whole islets

Whole islets were fixed in 4% paraformaldehyde for at least 30 min. Individual whole islets were permeablised in 0.1% Triton and blocked in 5% goat serum. Islets were incubated in antibodies, as described above (1 h in each antibody). Islets were imaged using the Zeiss LSM 510 Laser scanning microscope.

Primary Ig	**Dilution**	**Supplier**		
Chicken anti GFP	1:500	Life Tech		
Mouse anti glucagon	1:500	Sigma		
Guinea pig anti insulin	1:500	Sigma		
Rabbit anti somatostatin	1:500	Sigma		
Goat anti somatostatin	1:500	Internal		
Secondary Ig	**Dilution**	**Supplier**	**Excitation wavelength**	**Laser (nm)**
Goat anti Chicken	1:500	Invitrogen	488 nm	488
Goat anti mouse	1:500	Invitrogen	568 nm	568
Goat anti mouse	1:500	Invitrogen	488 nm	488
Goat anti guinea pig	1:500	Invitrogen	633 nm	637
Donkey anti goat	1:500	Invitrogen	549 nm	568

Table 2-6 Summary of staining antibodies and imaging wavelengths

2.8 $[Ca^{2+}]_i$ Imaging

2.8.1 $[Ca^{2+}]_i$ Imaging using the Zoom microscope

Widefield imaging was performed using the Zeiss AxioZoom.V16 microscope (16x zoom, NA of 0.25). Islets were perfused with a modified KRB solution, (mM – 140 NaCl, 5 KCl, 1.2 $MgCl_2$, 2.6 $CaCl_2$, 1 NaH_2PO_4, 5 $NaHCO_3$, 10 HEPES, pH 7.4, 200 mg/ml (0.2%) BSA) with glucose at the indicated concentrations. All solutions were corrected for osmotic differences with mannitol.

Islets were immobilised using a mesh system to minimize islet movement. Images were acquired approximately every 5 s with an exposure time of approximately 70 ms at approximately 100x zoom.

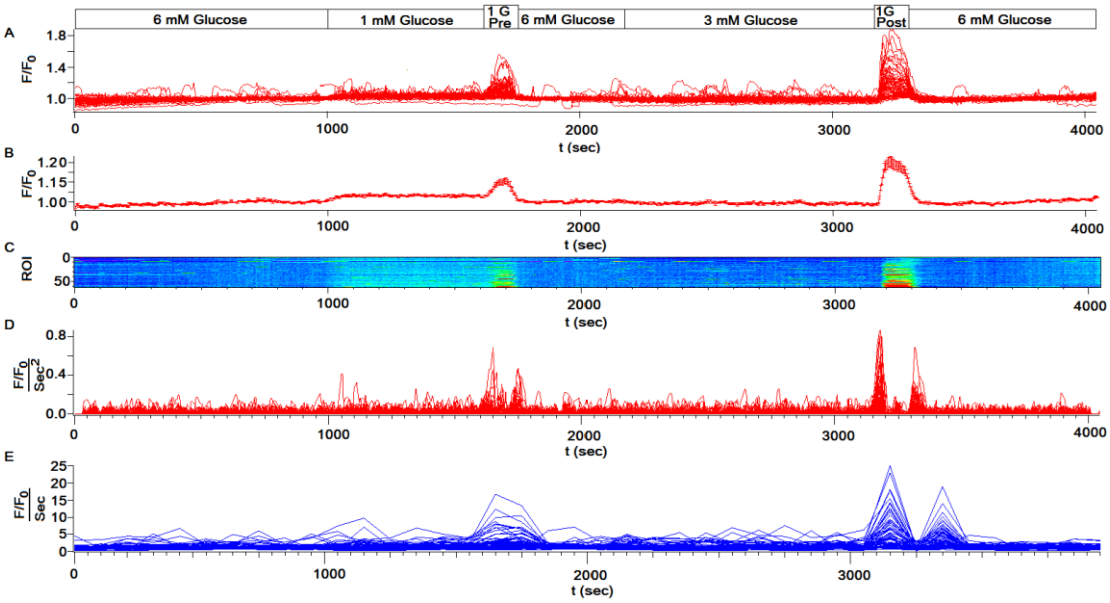

Figure 2.3 *Example trace showing analysis of $[Ca^{2+}]_i$ data from zoom imaging.*

Widefield (AxioZoom) recordings were analysed using FIJI (http://fiji.sc/Fiji) to measure fluorescence in individual cells or "regions of interest" (ROI) over time. Data was analysed using a combination of IgorPro and MatLab (**Figure 2.3**):

A - Raw data following baseline subtraction (IgorPro). Fluorescence intensity in each ROI over time represented by an individual line.

B - Mean of data in A

C - Data in A shown as a raster plot where each row represents a ROI over time and a change in colour from blue to red indicates increased fluorescence.

D - Following baseline subtraction a Mexican hat filter is applied to each trace (MatLab) to account for noise and slow changes in baseline.

E - Area under the curve (AUC) over 100 second periods (20 data points) is calculated from filtered data (D). Mean AUC during different conditions is used for onward analysis/figures.

2.8.1a Amino acid mixes for acute exposure and widefield (Zoom) imaging

AAMa (preprandial 2 mM); mM 0.15 L-threonine, 0.15 L-leucine, 0.2 L-lysine, 0.1 L-serine, 0.25 L-glycine, 0.4 L-alanine, 0.5 L-glutamine, 0.25 L-valine.

AAMb (postprandial 6 mM); mM 2 L-alanine, 2 L-glutamine, 2 L-arginine.

2.8.1b High Fat Incubation

For FA incubation experiments islets were kept in RPMI (as above) with 11 mM glucose, 1% Pen-Strep, 1.34% FA free BSA, and with or without 357.2 µM FA mix (23.5% palmitate, 51% oleate, 25.5% linoleic acid) for 24h prior to imaging.

2.8.2 $[Ca^{2+}]_i$ imaging using the confocal microscope

For confocal imaging, islets were placed in a chamber with a cover slip as the bottom and immobilised using a piece of mesh held in place with a small weight (**Figure 2.1**).

Time-lapse imaging of the intracellular GCaMP3 was performed on the inverted Zeiss AxioVert 200 microscope, equipped with the Zeiss LSM 510-META laser confocal scanning system, using a 40x/1.3 NA water immersion objective. Islets were continuously perfused with KRB solution (as described in Zoom $[Ca^{2+}]_i$ experiments section 2.8) at a rate of 200 µl/min. All solutions were corrected for osmotic differences with mannitol. GCaMP3 was excited at 488 nm and fluorescence emission collected at 530 nm. Frames of 256x256 pixels were taken at a frequency of 1.3 Hz (1 frame per 782 msec). The pinhole diameter was kept to a section thickness of 10±1µm.

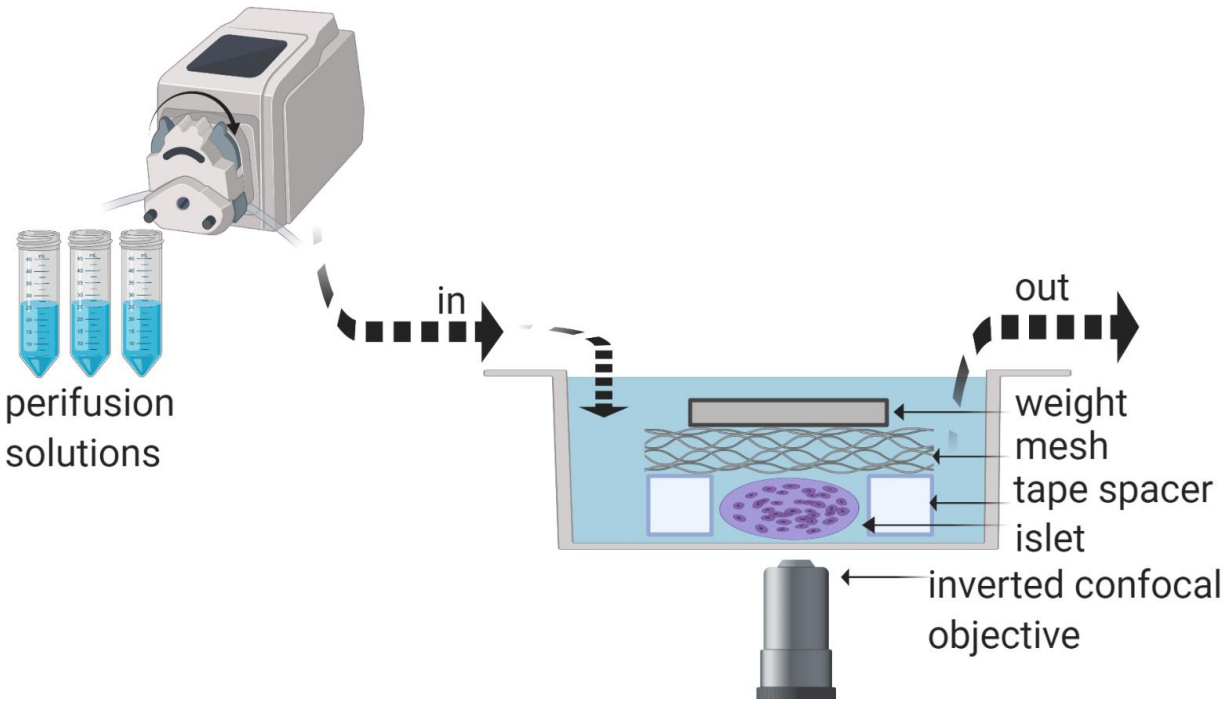

Figure 2.4 *Schematic demonstrating chamber setup for inverted confocal imaging of live islets. Islets are immobilised under a mesh held down with a small weight. A tape spacer ensures islets are not destroyed by the weight. A peristaltic pump perifuses islets with various solutions for imaging. Islets are imaged from below through the glass-bottomed chamber using an inverted confocal setup.*

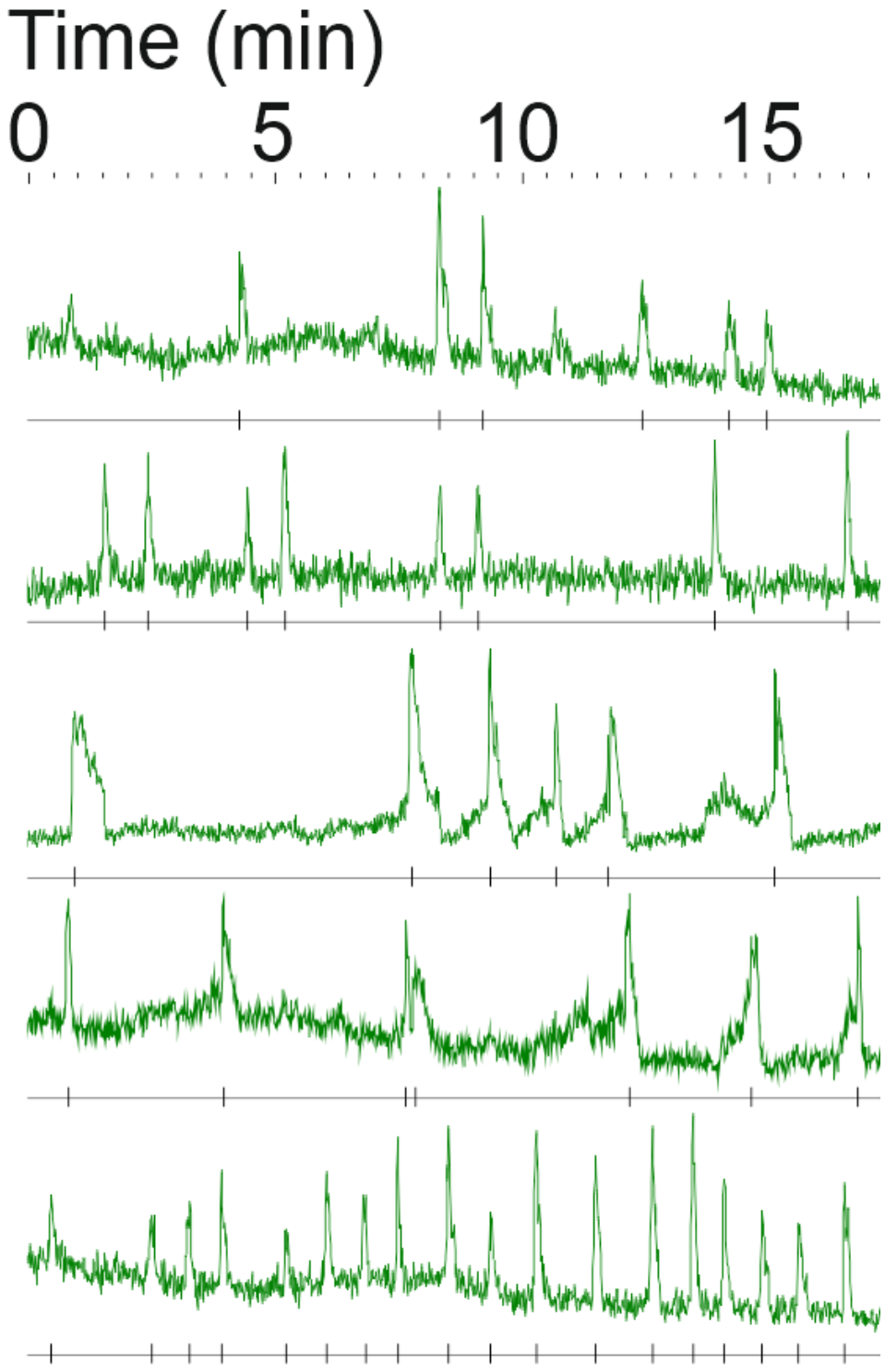

Figure 2.5 *Example trace showing analysis of $[Ca^{2+}]_i$ data from confocal imaging. All at 1 mM glucose. Green trace shows calcium fluorescence, black bar shows identification of spikes from above trace.*

Images were analysed using FIJI (http://fiji.sc/Fiji) to measure ROI intensity over time. Data was analysed using Spike2 (http://ced.co.uk/products/spkovin). $[Ca^{2+}]_i$ transients were identified from each individual $[Ca^{2+}]_i$ trace as shown (**Figure 2.5**)

Average amplitude of identified $[Ca^{2+}]_i$ spikes was calculated as shown (**Figure 2.6**). Normalised fluorescence was taken ± 10s of a spike occurrence and an average of all the spikes during a set time period (during a particular condition) was generated from which changes in peak amplitude were measured.

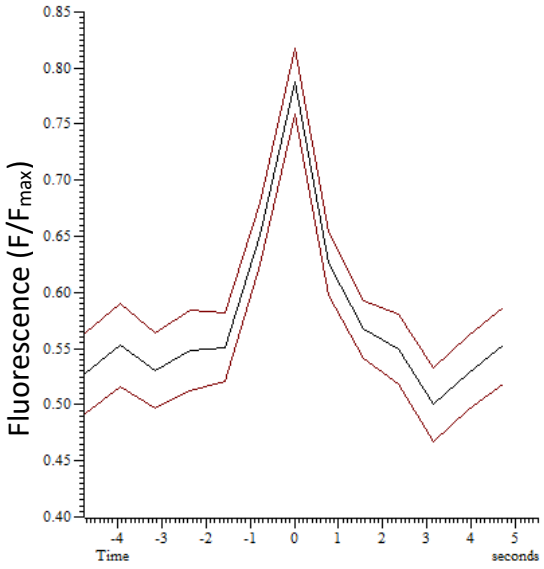

Figure 2.6 *Calculation of spike amplitude, average of all spikes within an individual cell at 1 mM glucose (black) with SEM of spike average in red*

2.9 Measurements of hormone secretion

2.9.1 Secretion

Unless treated with FA, islets were incubated following isolation for 1-2 h prior to secretion. For each condition, ~20 size-matched islets were washed in RPMI 1640 containing 0 mM glucose. Islets were then pre-incubated in 200 µl KRB (mM 120 NaCl, 4.7 KCl, 2.5 $CaCl_2$, 25 $NaHCO_3$ 1.2 KH_2PO_4, 10 HEPES, 0.1 % BSA, pH 7.4) containing 3 mM glucose for 1h. This supernatant was then removed and discarded and KRB containing the relevant glucose/experimental condition applied and islets incubated for another 1 h. The supernatant was then removed and snap frozen on dry ice in 100 µl acid ethanol (Acid:EtOH 1:15) applied to the islets prior to freezing. Supernatant and islets were stored at -80°C until measurement of secretion.

2.9.2 MSD measurement of secretory output

Insulin/glucagon content in solutions was measured using a M/R Insulin, glucagon Kit (K15145C-1, MESOSCALE DIAGNOSTICS) and read using a Meso QuickPlex reader. Lysed islets were diluted 1:400 per islet in RIA buffer (HBSS with 0.08% sodium Azide and 0.025% BSA) for measurements of content. Secretory output is shown as raw values and as a% of total hormone content. SST from both perfusate and islet secretion was measured using EuroDiagnostica SST EURIA kit (RB306RUO). Lysed islets were diluted 1:25 per islet in RIA buffer.

2.9.3 Perfusion experiments

The perfused mouse pancreas was used to measure glucagon secretion *in situ*. These experiments were conducted by Nils J. G. Rosman and Thomas G. Hill; I designed the

experiments, was present during the experiments and assayed and analysed all the perfusate data, but did not do the surgery.

The protocol for the surgery is as follows (performed on Harvard Apparatus heated rodent operating table, Hollison MA, USA.). Mice are killed by cervical dislocation, the aorta was cannulated by ligating above the coeliac artery and below the superior mesenteric artery and was then perfused at 37°C (Warner Instruments temperature control unit TC-32 4B in conjunction with an in-line heater P/N 64-0102, Reglo Digital MS2/8peristaltic pump). The portal vein was used to collect perfusate effluent at 1 min intervals using a Teledynd ISCO Foxy R1 reaction collector. Samples were collected into a 96 well plate on ice containing aprotinin and subsequently stored at -80°C.

KRB containing varying concentrations of glucose and SST as indicated in the figures was used to perfuse the pancreas. Mice have 0.0008 g pancreas per g of total body weight (Bock et al. 2005). To ensure that alterations in hormone secretion collected in the perfusate where not due to differences in pancreas weight (i.e. greater dilution of perfusate in smaller mice due to smaller pancreas mass), the perfusion speed was adjusted to account for differences in pancreas weight and was performed at a rate of 1.34 ul/min/mg pancreas weight (to match required flow (Carlsson et al. 1996)).

At the start of the protocol, the pancreas was perfused for 10 min with 6 mM glucose to equilibrate and establish a basal level of secretion (“run in” period) after which the experimental protocol begun. Glucagon concentrations in the perfusate were

measured using the Human U-plex Glucagon ELISA (Mesoscale Discovery). RIA for measurement of SST was performed as described above.

2.10 High fat diet

The following HFD feeding protocol was ultimately decided upon. Immediately post weaning (mean age 4.6 weeks ± 0.2, n=114 mice, with GcgGCaMP, GcgRFP or littermates with no fluorescent marker) were fed a high fat (% kcal protein 18.3, carbohydrate 21.4, fat 60.3, TD.06414, Envigo) or a control diet (% kcal protein 20.5, carbohydrate 69.1, fat 10.5, TD.08806, Envigo). Mice were maintained on the diet for 14 weeks (13.8 ±0.2, 144 mice), following *in vivo* metabolic phenotyping and for experimental protocols (following Schedule 1 killing). Mean age at death was 18.5±0.3 weeks (n=144 mice). Mice were weighed regularly and food consumption recorded when cage feed was refilled.

2.11 Statistical analysis

Unless reported otherwise, data is displayed as mean±SEM and n refers to the number of mice. A p-value <0.05 was considered statistically significant. All statistical tests were carried out using GraphPad Prism 8 (GraphPad Software, San Diego, CA, USA). Where two groups were being compared, a parametric t-tests (paired or non-paired) was used. Where more than two groups were being compared a (repeated-measures where appropriate) one-way ANOVA was used with Sidak's multiple comparisons test. If data were separated by more than two factors, a two-way ANOVA, with a mixed-models ANOVA used with Tukey's multiple comparison's test, with the recommend Geisser-Greenhouse correction for repeated-measures data.

For multiple comparisons following a two-way ANOVA, a Bonferonni correction was conducted.

2.12 A note on selection of an appropriate HFD - Methodological considerations

In order to investigate α cell function in a disease relevant context, a number of animal models of obesity/pre-diabetes/diabetes were considered. Selection of the most appropriate animal model is critical to the question being asked in order not to confound conclusions. A number of the models considered are discussed below:

2.12.1 Ob/bo, db/db

A result of autosomal recessive mutations in either the leptin gene or the leptin receptor gene, the ob/ob mouse lacks leptin and db/db mouse lacks leptin receptor signalling (Wang et al. 2014). Leptin, secreted from mature adipocytes, is an important satiety hormone. Without leptin signalling, mice develop obesity within 4 weeks of age with both mouse models exhibiting hyperinsulinaemia (Hummel et al. 1972, Tassava et al. 1992). Islet morphology is markedly changed in ob/ob mice where the proportion of β cells is markedly increased to account for 92% of the islet (Kim et al. 2009).

Although these models are useful tools for generating obese mice with features reminiscent of human T2D, these mice exhibit altered islet cell ratios and islet structure. Furthermore, leptin is important in signalling to the α cell influencing control of secretory output (Tuduri et al. 2009). These changes in ob/ob and db/db

mice confound the use of these models in studying α cell dysfunction in obesity/T2D.

2.12.2 NOD

In the non-obese diabetic (NOD) mouse line, genetic predisposition leads to spontaneous hyperglycaemia which occurs in 50% of mice within 20 weeks of age (female mice) (McDuffie et al. 2008). The NOD mouse model is a spontaneous model of autoimmune T1DM. α cells are preserved in T1DM and the loss of β cell signalling is thought to contribute to elevated glucagon secretion during hyperglycaemia. Although this would allow study of the effect of hyperglycaemia on α cell function, this islet-centric model is not appropriate as it does not recapitulate the wider physiological features of obesity that contribute to T2D (Hughes et al. 2014).

2.12.3 STZ

STZ induced diabetes involves administration of the STZ toxin to mice by injection. The toxin enters pancreatic β cells through the glucose transporter GLUT2 (Schnedl et al. 1994) transporter. Once inside, STZ causes DNA damage and cell death. Within the pancreas, GLUT2 is expressed more in β cells than α or δ cells (DiGruccio et al. 2016) and as a result α and δ cells survive STZ-treatment (as do PP cells) (Zhang et al. 2012). Following injection of a high dose of STZ, mice become hyperglycaemic within a few days, with >90% of mice being diabetic after 5 days (Deeds et al. 2011). STZ-induced hyperglycaemia is a useful tool for studying the systematic effects of hypoinsulinaemia, and hyperglycaemia.

STZ is often used at lower concentrations with multiple doses in conjunction with a high fat diet to recapitulate the combination of an obesogenic phenotype and β cell dysfunction seen in T2D (Srinivasan et al. 2005). However, this is used more commonly, and therefore better characterised, in rats. Ideally we would use a mouse model as the GcgCreGCaMP3 tool we have is in mice. As we are interested in α cell function preceding and during T2D, we took the view that maintaining intact islet morphology, and β cell function, was important. Specifically, changes in β cell function may contribute to α cell dysfunction (and vice-versa) and an STZ-induced model will not effectively recapitulate these conditions.

2.12.4 High fat diet

High fat, high fat high sucrose

In order to study the nature, and contribution, of α cell dysfunction to the development of T2D, we reason that an altered diet model of obesity is the most appropriate for our experimental questions. Diet-induced obesity (DIO) recapitulates systemic changes thought to contribute to islet dysfunction in T2D. Specifically, elevated circulating free fatty acids, altered plasma amino acid composition, altered plasma hormone levels and sensitivity (including insulin resistance), which are all factors that may contribute to the development of prediabetes and T2D in obesity (Felig et al. 1969, Reaven et al. 1988, Nakamura et al. 2014). There are many iterations of diet combinations and durations however there were two main options for the purpose of this work; the high fat diet (HFD), or the high fat high sucrose diet. We are specifically interested in the contribution

of α cell fat metabolism to the development of α cell dysfunction. Therefore we selected a HFD in order to investigate the contribution of fat to α cell dysfunction.

C57Bl6J mice fed a high fat (60% dietary calories from fat) diet for 14 weeks gain significantly more weight and fat mass than littermate controls fed a 10% fat control diet. Mice exhibit elevated blood glucose concentration during a GTT and at some time points during an ITT (Nicholson et al. 2010). Although insulin sensitivity is preserved, insulin-induced glucose uptake in muscle has been shown to be reduced following 6-weeks HFD (Fisher-Wellman et al. 2016). HFD fed mice developed elevated plasma glucose and insulin concentrations, hallmarks of the T2D phenotype (Montgomery et al. 2013). Many features of the HFD fed C57Bl6j mouse mimic relevant T2D and pre-diabetic features including obesity, hyperglycaemia and dysregulated insulin function (Winzell et al. 2004).

Duration

Merino, Alonso-Magdalena et al. (2015) described the effect of 12 and 24 weeks of HFD on islet function. By 24 weeks, mice exhibited normalisation of α cell morphology and plasma glucagon levels. The authors concluded that α cell changes induced by 12 weeks HFD were transitory and lost with longer exposure. As the aim of this work was to investigate α cell dysfunction and the contribution of this to the development of aberrant glucose regulation in the early stages of T2D development, we will feed the mice a HFD for 12 weeks. The control diet selected was matched to the HFD in terms of % kcal from protein, was less calorie dense than the HFD and made up most of its calories from carbohydrate.

2.13 RNAseq - a note on protocol optimisation

2.13.1 Isolation of high quality RNA

A large amount of time was spend developing a successful protocol of preparation of cells/RNA for RNAseq experiments. The steps involved/options investigated are outlined below.

RNAseq requires a large amount (10ng) of high-quality RNA (optical density (OD) 260/280 and 260/230 of ~2, RIN of >8). Although the RNeasy micro kit for RNA extraction is adequate for qPCR of highly expressed genes, initial analysis showed that the material obtained from the kit was not of high enough quality (mean values; conc of 9.2 ng/ul, 260/280 (ideally ~2 for RNA) of 2.1, 260/230 (ideally >2) of 0.5, RIN (RNA Integrity Number, 28S to 18S RNA rRNA ratio) 2.5). RNA isolation using Trizol was also investigated (*Trizol extraction involves lysis of cells using 1 ml Trizol, addition of 200µl chloroform induces phase separation of lysate components – RNA separates into a clear top layer and is carefully pipetted off. RNA is then precipitated by addition of in 500 µl isopropanol for 1-16h. 3 µl of 20 mg/ml glycogen is added and the precipitate spun 1200 xg for 30 minutes at 4°C. Isopropanol is removed and the RNA pellet is washed by addition of 75% EtOH and then 70% EtOH. EtOH is removed and the RNA pellet left to dry for 25 minutes before resuspension in H_2O*). RNA quality was measured using a Bioanalyzer 2100 instrument with Agilent RNA 600 pico chips for high sensitivity analysis of total mRNA. Following optimisation, the mean RNA concentration obtained from 10000 cells only reached 12.8 ng/µl (RIN undetectable, mean 260/280 of 1.81, 260/230 of 0.17). Therefore, despite investigating this alternative approach of using trizol RNA

extraction, the material following RNA extraction from such a small amount of material remained far too low quality for RNAseq.

Next, the possibility of submitting cell lysate, rather than RNA, was investigated. Two groups in Oxford provided services for RNAseq library prep – One option was to submit samples in 100 cell batches for sequencing. As α cells are known to be heterogeneous in their expression profiles, it was ultimately decided that too many individual samples (at great expense) would be needed for this approach to provide enough data for analysis.

2.13.2 Preparation of cell lysate and sample submission

The option to sequence up to 2.3 µl of lysed cells using SmartSeq2 amplification (Picelli et al. 2014) via the Oxford Genomic Centre was pursued. When cells are sorted, each cell is sorted in a droplet of 4nl. Therefore, we could theoretically contain ~575 cells within the 2.3µl lysate volume. This is an achievable cell number based on previous sorts and submission of cell lysate substantially improves the reproducibility of the sample preparations as they are not subject to RNA-extraction batch effects.

Ultimately, RNAseq using Nextera XT cDNA sample preparation and Smart-seq2 library prep (HiSeq4000) was selected as the most appropriate protocol. This protocol is optimised for RNAseq of single cells therefore it is sensitive enough to sequence cell lysate from a far smaller number of cells than required with traditional bulk sequencing techniques. The analysis was carried out by Dr Martijn van de Bunt (Novo Nordisk).

Chapter 3

3. Development and characterisation of GcgCreGCaMP3 model

3.1 Introduction

Reliable identification of pancreatic α cells remains one of the major limiting factors to progression of understanding of α cell behaviour. As α cells comprise only 15-25% of the mouse islet and have heterogeneous patterns of activity, activity at low glucose, positive $[Ca^{2+}]_i$ response to glutamate, and positive response to adrenaline have all been used as tools for identification (Santos-Silva et al. 2015, Hamilton et al. 2018). However, functional identification techniques are poorly validated, and may confound experimental results where pharmacological agents are applied early during functional recordings. Alternatively, dispersal into single cells allows imaging of a single layer of cells (overcoming a technical challenge of imaging a spherical islet; see Quoix *et al.* (2007)). However, disassociation of cells from their paracrine and extracellular environment changes cell function and glucose sensitivity of glucagon secretion (Le Marchand et al. 2010). More recently, viral vectors have been used to transduce cell-type-specific promoter-driven expression of fluorescent proteins for cell identification (Shuai et al. 2016). This allows for robust identification of cell type, however islets from different experimental groups may be differently sensitive to viral infection, and this approach still requires the use of loadable dyes.

For the purposes of our work, the GcgCre mouse (Parker et al. 2012) was crossed with GCaMP3 (Zariwala et al. 2012) for specific expression of the calcium-sensitive fluorescent indicator GCaMP3 within the α cell. GcgCre mice were also crossed with

mice carrying the *RFP* allele. Therefore, mice carrying the *Cre* allele and *RFP* and/or *GCaMP3* can be used for identification, or identification and direct $[Ca^{2+}]_i$ imaging in α cells.

3.1.1 α cell responses to known substrates

3.3.1a Glucose

By carrying out $[Ca^{2+}]_i$ imaging and then staining cells to determine their identity, the following patterns of glucose-sensitive $[Ca^{2+}]_i$ signalling have been established; α cells are defined as being active at low (0.5-3 mM) glucose with some (but not all) cells becoming less active/silent at high (11 mM) glucose. β cells have the opposite pattern and are inactive at low (<3 mM) glucose and active at high (>11 mM) glucose. δ cells are less well characterised but described as mostly (80%) inactive at 1 mM glucose, active at 3 mM glucose, with altered pattern of activity at high glucose (Asada et al. 1998, Nadal et al. 1999, Quesada et al. 1999, Quesada et al. 2006, Kenty et al. 2015, Vergari et al. 2019). Observations using functional identification have been broadly confirmed using combinations of genetically encoded indicators and $[Ca^{2+}]_i$ dyes (Le Marchand et al. 2012, Li et al. 2015), and more recently, $[Ca^{2+}]_i$-sensitive dyes expressed specifically in one cell type (Chen et al. 2016, Denwood et al. 2019). However, many of the existing studies into α cell $[Ca^{2+}]_i$ responses, due to their low throughput nature, have low n-numbers, or provide only broad information about $[Ca^{2+}]_i$ (e.g. overall change in concentration or AUC, rather than detailed interrogation of oscillation characteristics under different conditions). The use of GcgGCaMP3 will

allow for definitive identification of α cells, far higher throughput of data collection, and generation of data for in-depth characterisation of α cell signalling.

3.3.1b Glutamate

Glutamate stimulates glucagon secretion in the perfused rat pancreas (Eisenstein et al. 1978), and a positive $[Ca^{2+}]_i$ response to glutamate has been used in $[Ca^{2+}]_i$ imaging as a tool for α cell identification (Menge et al. 2011, Hamilton et al. 2018). For these reasons, we will test what proportion of GCaMP3$^+$ cells respond to glutamate.

3.3.1c Adrenaline

Catecholamines, including adrenaline, act on α cells via the G_q-coupled α1 and Gs-coupled β2 adrenoceptors, activation of which increases intracellular cAMP, intracellular $[Ca^{2+}]_i$ signalling, and glucagon secretion (Gromada et al. 1997, De Marinis et al. 2010, Hamilton et al. 2018). α adrenergic stimulation increases glucagon secretion (by activation of α1 receptors), but inhibits secretion of insulin and SST (by activation of α2 receptors) (in the presence of β-adrenergic blockade see Samols and Weir (1979)). Adrenaline can therefore be used as a positive indicator of α cell identity when imaging $[Ca^{2+}]_i$ (Hamilton et al. 2018). Similar to glutamate, a positive $[Ca^{2+}]_i$ response to adrenaline (5-10 μM) was used, during confocal microscopy, as an additional method for testing the identity of cells imaged.

3.3.1d Amino acids

α cells are known to respond to certain amino acids with an increase in glucagon secretion (Unger et al. 1969, Rocha et al. 1972). We were therefore interested in the

effect of α cell stimulation by amino acids on $[Ca^{2+}]_{i.}$ Following ingestion of a meal, the concentration of plasma amino acids increases, and the composition of amino acids in the plasma changes. Zhang *et al.* (2013) tested pre- and post-prandial amino acid mixes and found that only postprandial amino acid mix stimulated glucagon secretion. How amino acids stimulate glucagon secretion (via stimulation of membrane receptors, by providing a substrate for metabolism, or by depolarising V_m by electrogenic and/or Na^+-dependent uptake) remains poorly understood. We will use the GcgGCaMP3 model to interrogate α cell calcium in response to pre- and post-prandial amino acids.

3.3.1e High fat incubations

α cell function is disturbed in obesity, prediabetes, and diabetes. We therefore wanted to study α cell $[Ca^{2+}]_i$ signalling in a diabetogenic condition. Glucagon secretion is increased following incubation in elevated free fatty acids (FAs) (Olofsson et al. 2004). In order to understand the mechanism of α cell dysfunction following incubation in elevated FA, we investigated changes in $[Ca^{2+}]_i$ do identify whether, in conditions of altered secretion, $[Ca^{2+}]_i$ is perturbed.

This chapter describes the generation of this mouse line, *in vivo* phenotyping, and *ex vivo* $[Ca^{2+}]_i$ imaging experiments with development of analysis protocols.

3.2 Methods

$[Ca^{2+}]_i$ imaging methods are outlined in Chapter 2 section **2.8**.

3.2.1 Wide field Ca^{2+}_i imaging

In the $[Ca^{2+}]_i$ imaging data presented, a number of selection criteria were used for identifying α cells. As demonstrated in the results section, 86% of GCaMP3 cells co-stained positive for glucagon, however 6% of GCaMP3$^+$ cells are insulin positive, and the identity of the remaining cells is unknown. Although use of the GluGCaMP3 line facilitates identification of large numbers of α cells, this nonspecific expression could confound results if it assumed that all GCaMP3$^+$ cells are α cells. Therefore, we used known methods to identify α cells to provide a "belt and braces" approach to cell type identification. The selection criteria included 1) $[Ca^{2+}]_i$ signalling at low glucose and 2) positive $[Ca^{2+}]_i$ response to adrenaline/glutamate. In case of any non-specific expression of GCaMP3 in non-α cells, this approach will help to further enrich the α cell population within the analysed dataset.

3.3 Results

3.3.1 In vivo experiments on glucose metabolism in GcgGCaMP3 model

Expression of fluorescent markers can exert cytotoxic effects on cells and activate the immune system (Liu et al. 1999, Stripecke et al. 1999). To assess whether expression of GCaMP3 in the α cells affects glycaemic control, plasma glucose concentrations during IPGTT were measured and compared in GcgGCaMP3/GcgRFP/GcgGCaMP3RFP and control mice. There was no difference in blood glucose at any time point (**Figure 3.2a**) nor was there an overall effect of marker expression or a difference in mean AUC between controls and GcgGCaMP3 mice (**Figure 3.2b**).

Given that the markers are expressed in α cells, and plasma glucagon normally increases in response to an ITT, we assessed whether the blood glucose response was different between the groups following an insulin bolus to establish whether glucagon secretion was altered during insulin induced hypoglycaemia. There was no significant difference in blood glucose concentration at any time point (**Figure 3.2c**), nor was there a difference in mean AUC between controls and GcgGCaMP3 mice (**Figure 3.2d**).

Body weight was measured in mice with and without fluorescent marker expression. Within sexes, there were no significant differences between the mean weights of mice with or without fluorescent marker expression, nor was there an overall effect of marker expression when analysed using an ordinary one-way ANOVA (**Figure 3.2e**).

3.3.2 GCaMP3 and RFP are well co-localised to α cells at the protein and RNA level

Wax embedded whole pancreases from GcgGCaMP3 mice were sectioned and stained for GCaMP3, glucagon, and insulin to determine specificity of expression (**Figure 3.3**). 86% of GCaMP+ cells co-stained for glucagon, with 6% of cells co-staining for insulin (**Figure 3.4a**).

In order to investigate the specificity of RFP expression to α cells, qPCR was carried out on cells isolated by FACS on the basis of RFP expression. Glucagon expression was 23 times higher in RFP+ cells (**Figure 3.4c**), insulin expression was 37 times higher in RFP- cells (**Figure 3.4b**), and SST expression was two-fold higher in the RFP- cells (**Figure 3.4d**).

3.3.3 GcgGCaMP3 $[Ca^{2+}]_i$ imaging demonstrates intrinsic α cell glucose sensitivity

3.3.3a Zoom imaging; Glucose responses

Once validated, islets isolated from these mice were imaged using a widefield system (Zeiss AxioZoom.V16) to investigate $[Ca^{2+}]_i$ signal intensity and dynamics in response to glucose, glutamate, AA and prolonged FA incubation (24h). **Figure 3.5.1-3** demonstrates analysis of an example Zoom recording from GcgGCaMP islets. As further validation of GcgGCaMP3 expression, the response to glutamate (a known α cell activator) was tested. Glutamate activated 83% of $GCaMP^+$ cells (**Figure 3.5.1**).

Glucagon secretion is a glucose regulated, $[Ca^{2+}]_i$-dependent process. Thus, it may be speculated that elevation of glucose should be associated with reduced $[Ca^{2+}]_i$ but the reported data are conflicting (MacDonald et al. 2007, Le Marchand et al. 2010, Li et al. 2015). Here, the nature of α cell $[Ca^{2+}]_i$ dynamics in intact GcgGCaMP3 islets was investigated (**Figure 3.6a**). $[Ca^{2+}]_i$ AUC was moderately but significantly (-15% GCaMP3 fluorescence) reduced at 6 mM glucose compared to 1 mM. Surprisingly, $[Ca^{2+}]_i$ AUC increased at 15 mM glucose compared to 3 mM and 6 mM.

3.3.3b Amino acid responses

$[Ca^{2+}]_i$ in GcgGCaMP3 islets was recorded during acute exposure to the pre- and post-prandial AA mixtures used by Zhang et al., (2013) to stimulate glucagon secretion (AA1, 2 mM and AA2, 6 mM). Both AA mixes induced a significant increase in $[Ca^{2}]_i$ (AU) at both 3 and 6 mM glucose relative to AA free conditions (**Figure 3.6b**).

3.3.3c High fat incubations

α cell physiology, specifically changes to $[Ca^{2+}]_i$ in the context of diabetogenic conditions, remains poorly understood. Long-term exposure to FAs is known to change glucagon secretion in response to glucose, mirroring changes seen in T2D human islets (Olofsson et al. 2004). To study the influence of FA on $[Ca^{2+}]_i$ signalling, islets were incubated in high (0.72 mM), low (0.36 mM) or in the complete absence of FAs (a mix of oleate, palmitate, and linoleic acid was used, see methods Chapter 2) at 11 mM glucose for 24h. Concentrations used were based on historical measurements of plasma NEFA in HFD fed mice (Pinnick, unpublished)). $[Ca^{2+}]_i$ responses were measured in GcgGCaMP3 islets following 24h incubation with or without FA (**Figure 3.6c**). In FA-free conditions, $[Ca^{2+}]_i$ (AU) was maximal at 1 mM glucose and reduced at both 3 mM and 6 mM. In the presence of 0.36 mM FA, however, $[Ca^{2+}]_i$ was at its lowest at 1 mM glucose and was increased by both 3 mM and 6 mM. $[Ca^{2+}]_i$ was higher in islets exposed to 0.36 mM FA compared to FA-free islets at both 3 and 6 mM glucose. In the presence of 0.72 mM FA, $[Ca^{2+}]_i$ became glucose insensitive.

3.3.4 Confocal imaging reveals strong frequency modulation of $[Ca^{2+}]_i$ in α cells in response to glucose

Widefield microscopy is unable to capture the fast nature of $[Ca^{2+}]_i$ signals at the cellular level. For this reason, confocal microscopy was used to further interrogate the dependence of α cell $[Ca^{2+}]_i$ on glucose. In the first instance, a binary observation as to whether cells were active or not in a particular condition was made. The largest

proportion of cells exhibited oscillatory behaviour at 1 mM glucose (82%, **Figure 3.7c**). A significant proportion of cells were silenced at 6 mM (decreased to 55% active) glucose but not 15 mM glucose (70% active cells).

$Ca^{2+}{}_i$ oscillation frequency was maximal at 1 mM glucose (0.87 spikes per min) and was significantly reduced by roughly two thirds at 6 and 15 mM glucose (0.30 and 0.33 spikes per min, **Figure 3.7e**). If recording averages were calculated, the significance of these observations does not change (**Figure 3.7b**). The order of conditions for each experiment was randomised in order to avoid the issue of photo-bleaching during experiments confounding results.

Change in AUC in $[Ca^{2+}]_i$ is often used as a metric in $[Ca^{2+}]_i$ imaging of islets (Dadi et al. 2015, Hamilton et al. 2018). The contribution of a change in the amplitude or area to the change in AUC was investigated here. There was no relationship between spike amplitude or area and glucose concentration in α cells (**Figure 3.7.c and d**). For each cell, fluorescence was measured relative to maximum (which was normally achieved on application of adrenaline). Therefore, each $[Ca^{2+}]_i$ spike has an amplitude between 0 and 1. When spike amplitude was calculated, there was no significant change regardless of whether a baseline subtraction was applied or not.

The presence of $[Ca^{2+}]_i$ oscillations at 1 mM glucose was considered a selection criteria for identification of α cells as well as expression of GCaMP3 and positive response to adrenaline at 15 mM glucose (if an adrenaline condition was included in the recording). However, in order to analyse changes in spike amplitude using a repeated measures analysis, spike amplitude can only be analysed from cells that

showed oscillatory activity at all glucose concentrations. This raised a question as to whether, if spike frequency was measured only in cells that are active at all glucose concentrations, does frequency fundamentally differ (**Figure 3.7e-j**). Even amongst the cells that are active at all glucose concentrations, frequency modulation occurs. Likewise, if all cells are included (regardless of whether they are silent at any particular condition), the same trend in frequency modulation can be observed.

3.4 Discussion

This chapter has described the initial $[Ca^{2+}]_i$ imaging experiments carried out on GcgGCaMP3 islets and the development of the experimental and analytical approaches to generate meaningful measurements from the recordings.

3.4.1 GCaMP/RFP are expressed specifically in α cells

The staining and qPCR experiments further validate expression of GCaMP3 and RFP under control of the glucagon promoter (Parker et al. 2012, Dadi et al. 2015). For staining, 86% co-staining of GCaMP3 cells is higher than 59% previously reported (Parker et al. 2012) and will provide significant enrichment of α cells, as demonstrated with RFP in the qPCR experiments. 80% recombination of Cre in glucagon positive cells in this GluCre line has been reported previously (Soedling et al. 2015). However, the authors found a 20% recombination rate in insulin positive β cells. This is much higher than the 6% expression of GCaMP3 in insulin positive cells that we observed. In order to validate the specificity of the anti GFP antibody used, experiments with GCaMP3 negative islets are needed. The antibody could be further validated using MIN6-GCaMP6 cells as positive controls.

GCaMP3 expression under the control of the glucagon promoter, as used here, has been previously published (Dadi et al. 2015). The $[Ca^{2+}]_i$ response to glutamate demonstrates that the majority of GCaMP3-expressing cells (82%) do indeed respond to this α-cell-specific stimulus (Menge et al. 2011, Hamilton et al. 2018). Although a

response to ~5 µM adrenaline was used as a selection criteria for α cells, the number of GCaMP3 cells that did not respond to adrenaline was not analysed.

In vivo phenotyping results do not indicate a difference in metabolic parameters between mice with and without expression of a fluorescent protein in their α cells, indicating that GCaMP3/RFP expression does not impair α cell function.

3.4.2 Confocal imaging is most appropriate for $Ca^{2+}{}_i$ imaging of α cells

Using the wide field imaging set up, a number of interesting observations about α cells were able to be made; in the light of the observation that α cell $[Ca^{2+}]_i$ is clearly glucose-sensitive, we wanted to carry out more detailed analysis of α cell $[Ca^{2+}]_i$ dynamics. The widefield microscope offers many advantages in imaging – many individual islets, and different groups of islets (e.g. from different treatment groups) can be simultaneously imaged (allowing for a direct comparison between treatments without the added experimental variation of separate experiments). Furthermore in widefield imaging, there is no lag that occurs with laser scanning imaging (the whole imaged area is captured at the same point in time), and complementary metal-oxide semiconductor or electron multiplier charge-coupled device (CMOS/EM-CCD) image sensors typically have a larger dynamic range compared to photomultiplier tube (PMT) image sensors used for confocal imaging. The relatively small dynamic range of PMT image sensors limits the ability to detect the whole dynamic range of indicators such as GCaMP3. If the sensor saturates below the intensity at which GCamP3 saturates, signal amplitude is cropped.

Ultimately, we decided that a confocal setup was most appropriate for onward experiments. The reasons for which are outlined below.

- A confocal set up allows for resolution in the z-axis (i.e. because of the presence of the pinhole, a "slice" of defined depth within an islet can be imaged. This allows for individual cells sitting above or below one-another to be imaged separately. This will allow true measurements of $[Ca^{2+}]_i$ in well separated, individual cells.
- Identification of individual cells from the widefield setup is technically challenging. Although one can identify a large number of individual cells, the reduced resolution makes reliable separation of ROIs a challenge, and the individual islets can be prone to movement. With the confocal setup, islets can be more easily immobilised and with the increased resolution, individual cells within an islet can be easily identified.
- The confocal microscope allows for a much faster image acquisition frequency. Ultimately, in the experiments performed, the acquisition frequency used was 1 image/786 msec on the confocal setup but only 1 image every 5 seconds on the widefield. With improved temporal resolution, individual $[Ca^{2+}]_i$ spikes in individual cells could be identified. Therefore, rather than measuring just AUC, confocal imaging gives the resolution to measure spike frequency, allowing the dynamics of $[Ca^{2+}]_i$ signalling in α cells to be broken down more thoroughly. This is important as for secretion to occur, it is not the total $[Ca^{2+}]_i$ concentration, but $[Ca^{2+}]_i$ oscillations or the

concentration just below the plasma membrane at the release sites, that are thought to drive vesicle fusion and secretory output.

For these reasons, $[Ca^{2+}]_i$ imaging experiments were performed from this point onwards using confocal imaging. Following initial tweaking of the microscope setup, a temporal resolution of 1 frame every 786 msec was achieved (1.3 Hz). Acquisition of detailed $[Ca^{2+}]_i$ oscillation frequency data is a major advantage of using a laser scanning confocal microscope for imaging. A frequency of acquisition of 1.3 Hz approaches the maximal time resolution of the microscope (without reducing field of view/pixel dwell significantly) as well as the maximal time resolution of GCaMP3 (GCaMP3 rise half life ($t_{1/2}$) = 80±2 ms and decay $t_{1/2}$=610±3 ms (Tian et al. 2009)). 1.3 Hz was found to be the fastest imaging frequency that could be used without reducing image quality due to reduced pixel dwell and increased scanning speed time.

The presence of very fast Ca^{2+}_i transients has never been investigated in α cells, therefore Ca^{2+}_i signals could be missed when imaging at a frequency of 1.3 Hz. GCaMP3 is a relatively slow Ca^{2+}_i indicator compared to the fast variants of GCaMP6f (with a rise $t_{1/2}$ of 26 msec and decay $t_{1/2}$ of 140 msec (Dana et al. 2019)). Subcellular Ca^{2+}_i signals as fast as <10 msec have been detected in hippocampal neurons using Fluo-4 loadable dye (Basnayake et al. 2019). In the future, Fluo-4 or other fast indicators may be appropriate tools for investigating and characterising faster Ca^{2+}_i transients in α cells.

With data gathered from these traces, ROIs were manually identified and fluorescence measurements made at each time point. Each individual trace could then be analysed to identify where $[Ca^{2+}]_i$ spikes occur. From this, spike (oscillation) frequency can robustly be calculated, as can spike amplitude, spike duration, and therefore area. This represents a preferable analysis approach than seen previously as it allows individual features of $[Ca^{2+}]_i$ signalling to be "picked apart" – rather than having one AUC measurement, changes in frequency, duration, number of cells active can all be determined separately.

In the confocal work presented, $[Ca^{2+}]_i$ imaging results come from 221 cells, 12 islets, 9 mice. This number of cells is markedly higher than any existing work where α cell number in published. n numbers in work on whole islets has been as little as 18-22 cells from 6-7 islets (Le Marchand et al. 2010, Le Marchand et al. 2012), 61 cells from 10 islets (Quesada et al. 2006), 63 cells from 15 islets (MacDonald et al. 2007) and 153 cells (Hamilton et al. 2018).

In work by Shuai et al. (2016) TIRF microscopy is used to image sub-plasma membrane $[Ca^{2+}]_i$ oscillations. This is a very high-resolution imaging approach, however it is limited with regards to the number of cells that can be imaged (18 cells from 5 islets). Although our data is highly powered with regards to cell number and demonstrates the importance of cell number in characterising α cell activity, the number of islets and animals could be improved, as could the resolution in order to interrogate subcellular Ca^{2+}_i signalling.

3.4.3 α cell Ca^{2+}_i signalling is frequency, not amplitude modulated in response to glucose

α cell $[Ca^{2+}]_i$ oscillation frequency is mediated by ***both*** cells being silenced by glucose (**Figure 3.7a**) ***and*** by a reduction in $[Ca^{2+}]_i$ oscillation frequency in those cells that remain active (**Figure 3.7g**) but ***not*** by a change in spike amplitude/area (**Figure 3.7c/d**) i.e. there is not a set oscillation frequency, with average frequency determined by the number of cells active, but rather α cells respond to changing glucose with a spectrum of frequencies more like a "dimmer switch".

The benefits of analysing more cells are many. This number of analysed cells provides the statistical power to make new observations about α cell physiology. In particular, we were able to identify the moderate decrease in the proportion of cells active at 6 mM glucose compared to 1 mM (i.e. glucose does not *silence* cells) which has never previously been described, in addition to the decrease in the amount of $[Ca^{2+}]_i$ signalling (oscillation frequency) in those cells remaining active. The observation that α cells remain active as glucose concentration increases fits with electrophysiological data. As glucose concentration increases, the α cells depolarise and the Na_v channels cannot be reactivated. As a result, α cells remain "electrically active" but cannot depolarise enough (due to the lack of Na^+ current) to activate Ca_v channels and drive secretion (Zhang et al. 2013).

An oscillation frequency of approximately 0.9 spikes per min at 1 mM glucose is roughly consistent with existing published data; 0.7 spikes/min at 3 mM glucose (human islets, cells identified by staining (Quesada et al. 2006)) and in perfect

agreement with 0.9 spikes per min at 1 mM glucose (mouse islets, α cells identified by RFP staining (Le Marchand et al. 2010)), and 1 spike per min at 1 mM glucose (αTC1-9 cells infected with ratiometric pericam-encoding adenovirus (Ravier et al. 2005)).

The nature of the relationship between $[Ca^{2+}]_i$ and secretion is inevitably cell-specific. However, in numerous neuroendocrine cell types, secretion is thought to be most strongly driven by the frequency of $[Ca^{2+}]_i$ spikes, with the amplitude being of less relevance due to the maximal number of vesicles being released prior to $[Ca^{2+}]_i$ reaching its peak (Charles et al. 1999).

There are limitations to using GCaMP3 fluorescence as an indicator of $[Ca^{2+}]_i$ concentration. Firstly, GCaMP3 fluorescence has not been calibrated against any known standard and the relationship between protein expression and fluorescence is unknown. For this reason, normalised measurements e.g. F/F_0 or F/F_{Max} are used for relative comparisons of $[Ca^{2+}]_i$ concentrations. The GCaMP3 transgene is located in the ROSA26 locus, and expression is driven by the CAG promoter. Although this is said to induce "robust and ubiquitous expression" (Zariwala et al. 2012), strength of expression may still vary between cells and treatment groups. If GCaMP3 expression is fundamentally different between experimental groups (e.g. as a result of incubation in FAs) the level of fluorescence may differ, despite no change in $[Ca^{2+}]_i$. This must be considered when normalising recordings and relating changes in amplitude to $[Ca^{2+}]_i$ concentration changes.

The relationship of $[Ca^{2+}]_i$ concentration and fluorescence is known to differ *in vitro* and *in vivo*, and within different cell types depending on their internal structure (e.g. presence of organelles) (Whitaker 2010). Therefore, there are limitations as to how meaningful the extent of a change in fluorescence relates to a difference in $[Ca^{2+}]_i$ between two separate cells or treatment groups that may have different GCaMP3 expression profiles (Cho et al. 2017). Nonetheless, normalisation of F/F_{max} provides some standardisation of the signal. Alternative quantitative methods include the use of ratiometric dyes. However, these can often only be imaged at a relatively shallow tissue depth, their excitation by UV or near UV wavelengths cause rapid damage to cells (Cho et al. 2017), and the two components of the dye can bleach at different rates (Broder et al. 2007).

3.4.4 Preprandial amino acids are able to stimulate α cell $[Ca^{2+}]_i$

Although Zhang *et al.* (2013) did not see a stimulation of glucagon secretion by the preprandial AA1 mix, we saw a clear increased in α cell $[Ca^{2+}]_i$. This indicates that there may be a threshold between increases in $[Ca^{2+}]_i$ and increases in secretion. Indeed, in rat type II alveolar cells, % increases in $[Ca^{2+}]_i$ are greater than % increases in surfactant secretion (Pian et al. 1988). The same may be true in α cells whereby the relationship between $[Ca^{2+}]_i$ and secretion is not linear.

3.4.5 $Ca^{2+}{}_i$ signalling in a diabetogenic model

The results gathered from islets incubated in high fat conditions show a clear change in α cell function. The increase in α cell $[Ca^{2+}]_i$ AUC following high fat incubation is

consistent with the stimulation of glucagon secretion by FAs previously reported (Olofsson et al. 2004).

α cell dysfunction in diabetogenic conditions is the question of interest here. Next, the optimised $[Ca^{2+}]_i$ imaging protocol is used to asses α cell function in the more physiological high fat diet fed mouse model of obesity. The next two chapters describe the *in vivo* and *ex vivo* elements of this work.

Figure 3.1

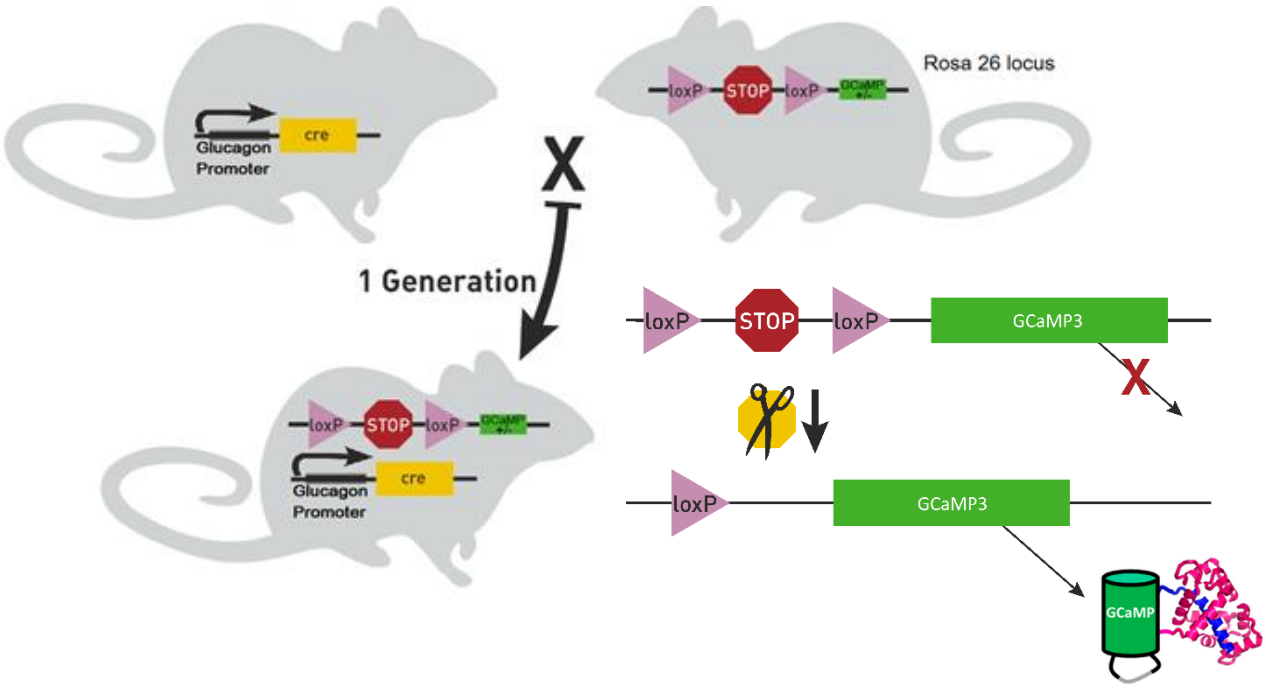

Figure 3.1 *Generation of GcgGCaMP3 mouse line.*

Figure 3.2

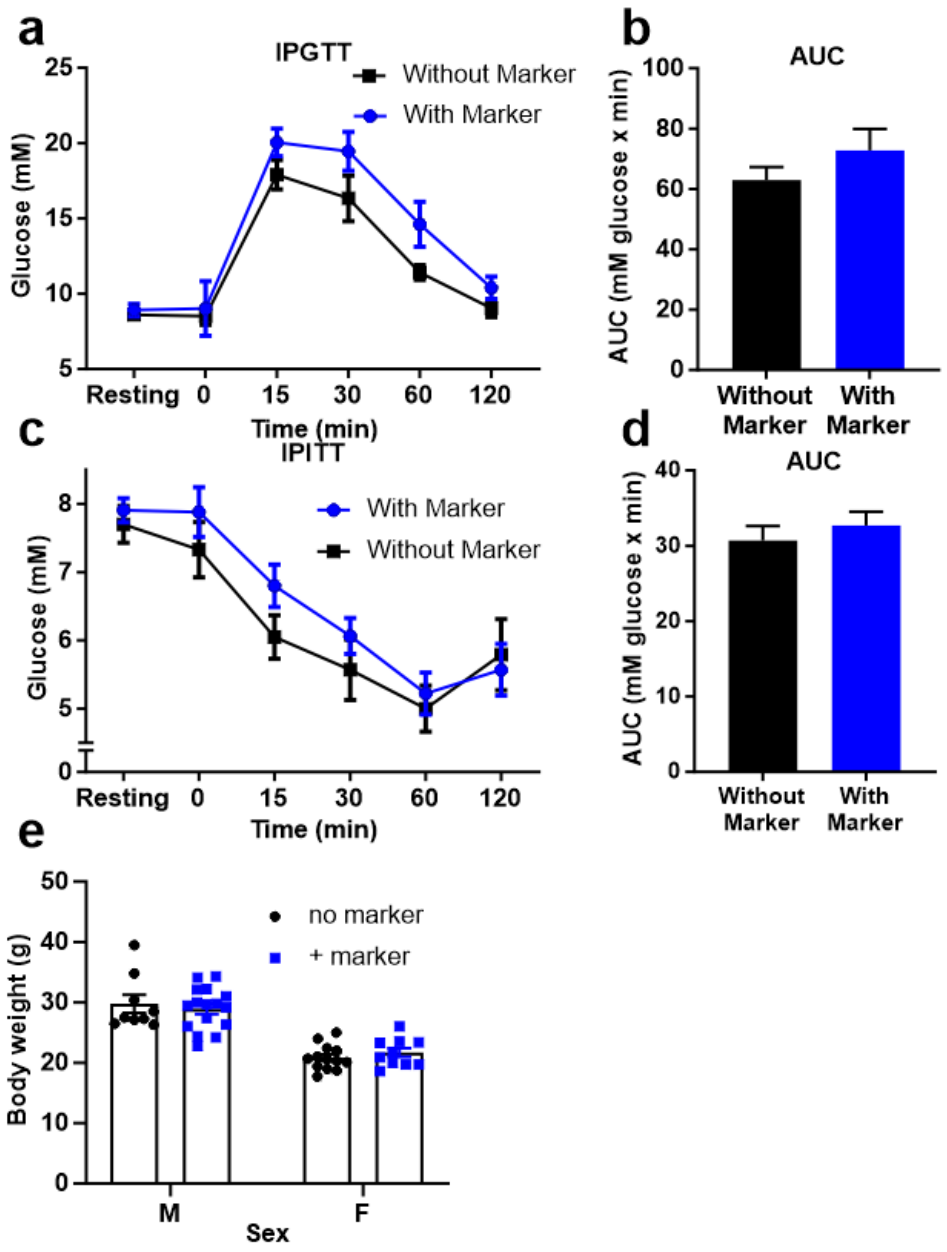

Figure 3.2 *Phenotyping of mice with (blue) or without (black) expression of a fluorescent marker in α cells.* ***a,*** *Plasma glucose concentration during IPGTT (2 mg/kg). There was no difference in blood glucose at any time point (p=0.7, 2-way ANOVA).* ***b****, Average AUC for blood glucose during IPGTT. Mean AUC was not significantly different between groups (p=0.18, n=12 with marker and n=9 without).* ***c,*** *plasma glucose concentration during IPITT (0.75U/kg). There was no difference in blood glucose at any time point (p=0.3376). 2-way ANOVA****.* ***d,*** *Average AUC for blood glucose during IPITT. Mean AUC was not significantly different between groups (p=0.471, n= 14 with marker, n=10 without). e, Mean bodyweight in mice with or without fluorescent marker expression (n=9-16 mice per group).*

Figure 3.3

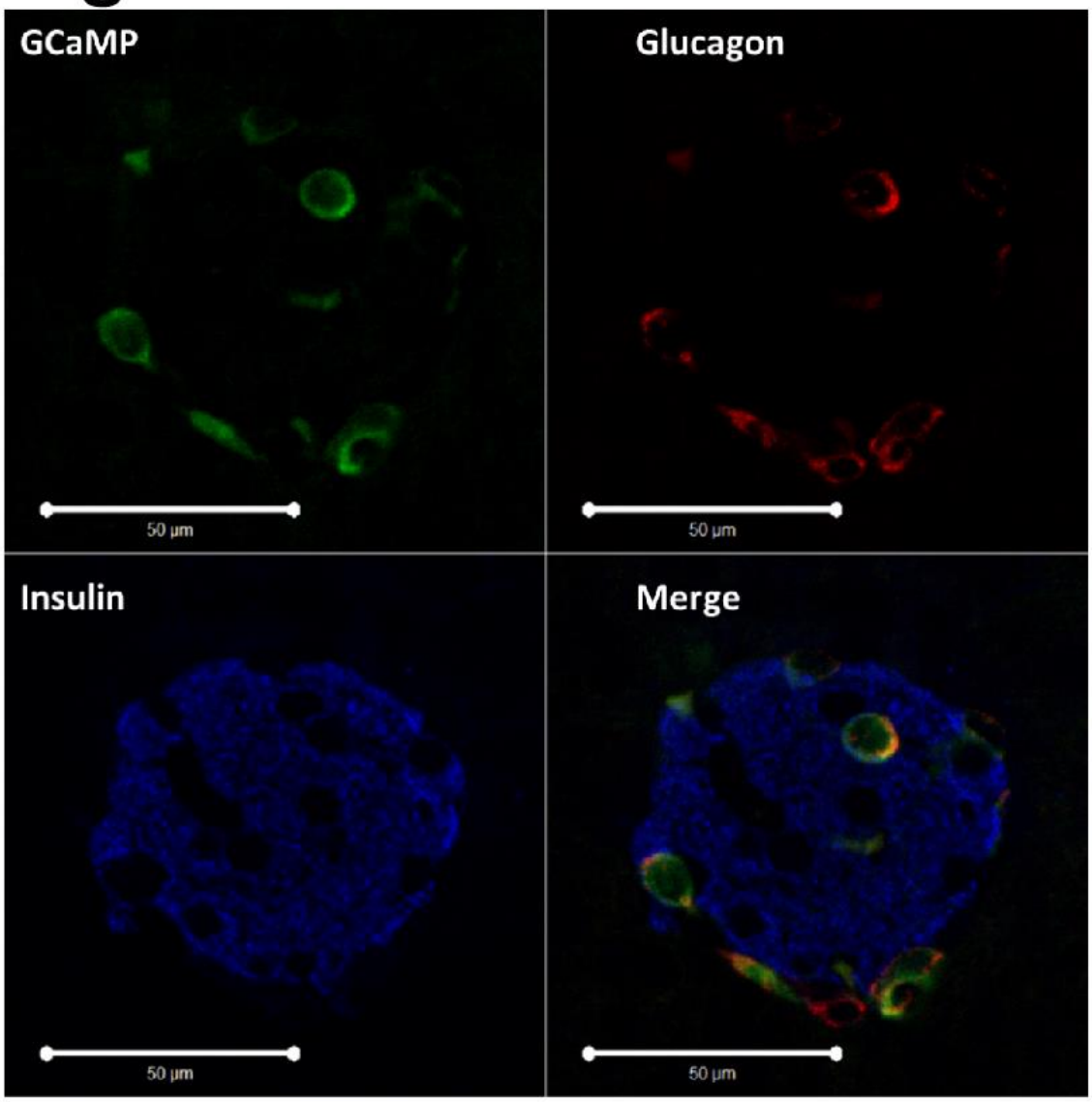

Figure 3.3 *Staining of GcgGCaMP3 islets to verify specificity of GCaMP3 expression. GCaMP3 staining (green - top left), glucagon staining (red - top right), Insulin staining (blue - bottom left), overlay of all three channels (bottom right).*

Figure 3.4

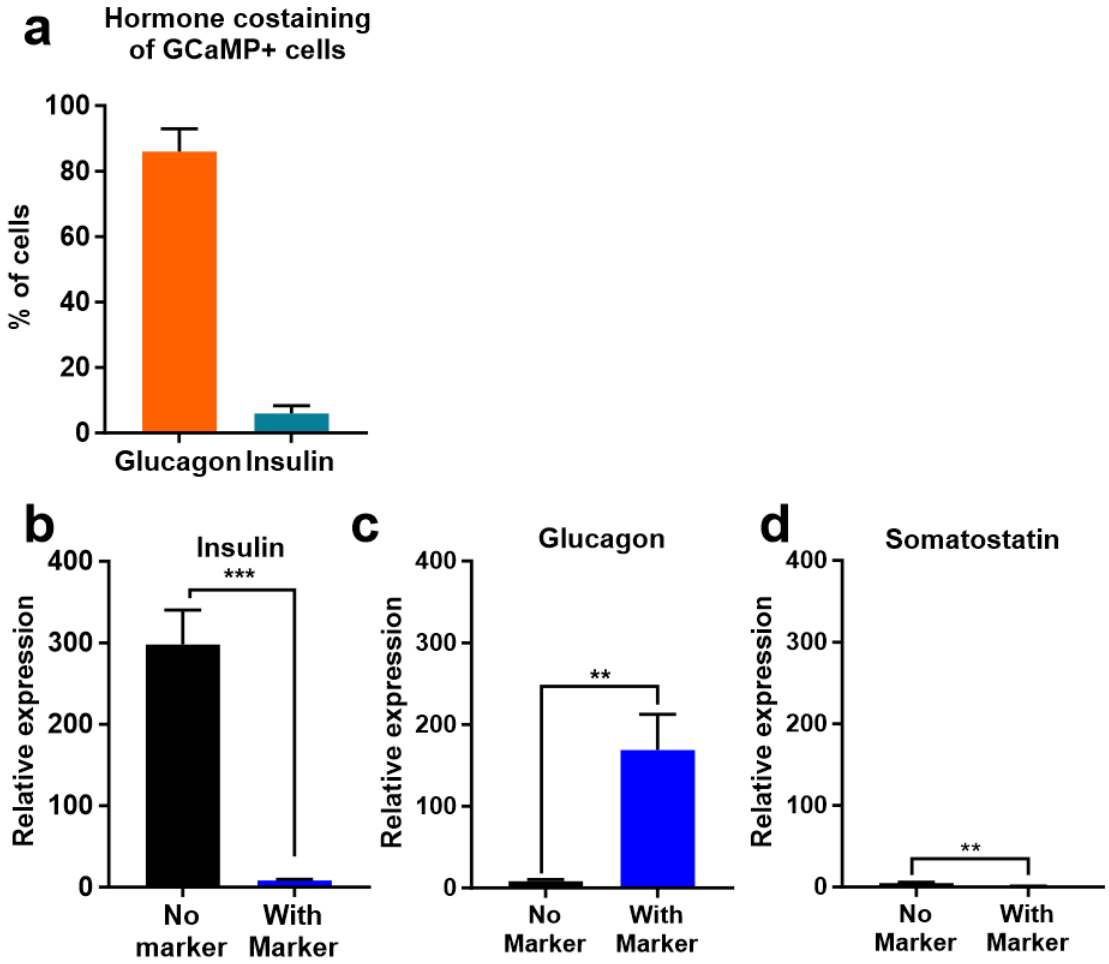

***Figure 3.4 a**, Quantification of number of GCaMP3 cells positive for glucagon (orange) and insulin (blue, n=65 cells from 3 mice, average 3 islets per mouse). **b**, Relative mRNA expression of insulin (left), **c,** glucagon (middle) and **d,** somatostatin (right) represented as a fold change relative to GAPDH in GcgRFP+ cells. n=FACS sorted islets from 9 mice.*

Figure 3.5

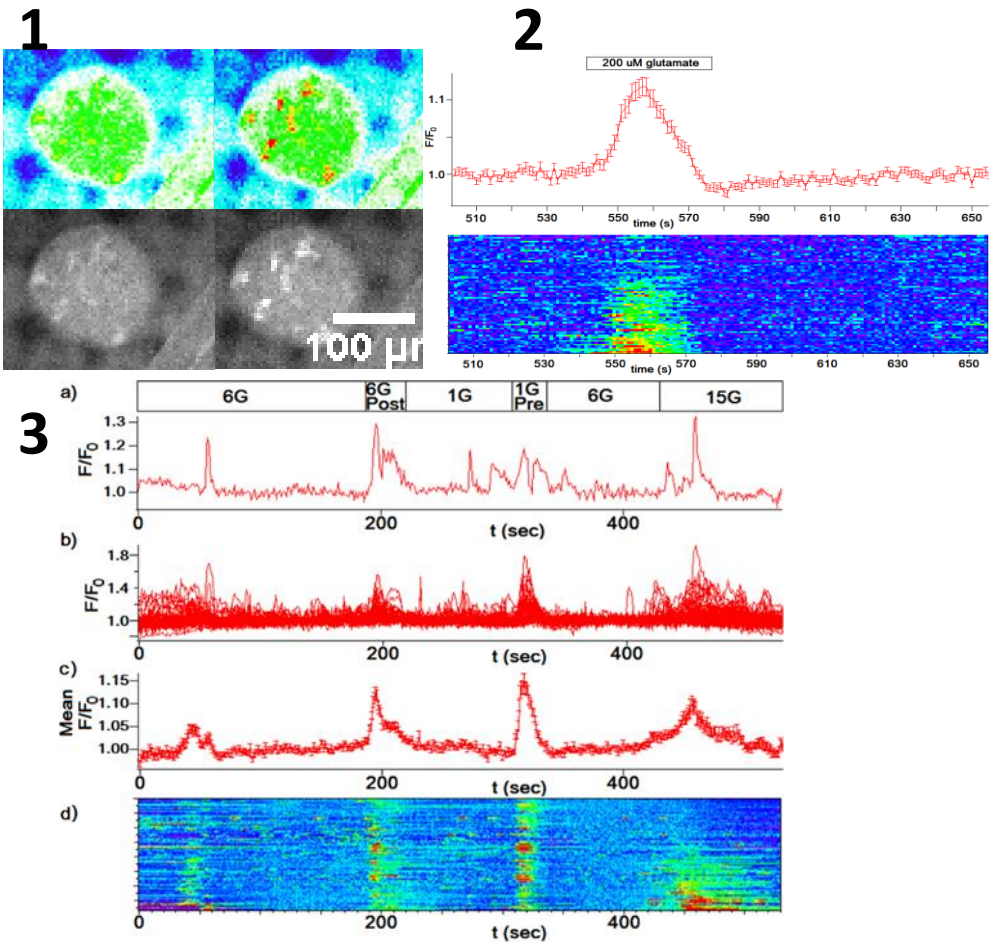

Figure 3.5 1, *Fluorescence of one GcgGCaMP3 islet before (left panels) and after (right panels) application of 200 µM glutamate. Top panels, image in LUT. Bottom panels, images in greyscale.* ***2,*** *Mean fluorescence population response represented as an XY trace and, below, as a heat map where each line represents a cell and a change in colour from blue, through green, to res indicative of an increase in fluorescence.* ***3,*** *Example $[Ca^{2+}]_i$ data showing* ***a)*** *$[Ca^{2+}]_i$ in one cell over time for one cell,* ***b)*** *$[Ca^{2+}]_i$ of all ROIs in the recording,* ***c)*** *mean of data in b,* ***d)*** *$[Ca^{2+}]_i$ shown in a raster plot where each line represents a ROI over time and a change in colour from dark blue through green to red an increase in fluorescence intensity. "6G post" refers to postprandial AA2 mix and "1G pre" to preprandial AA2 amino acid mix.*

Figure 3.6

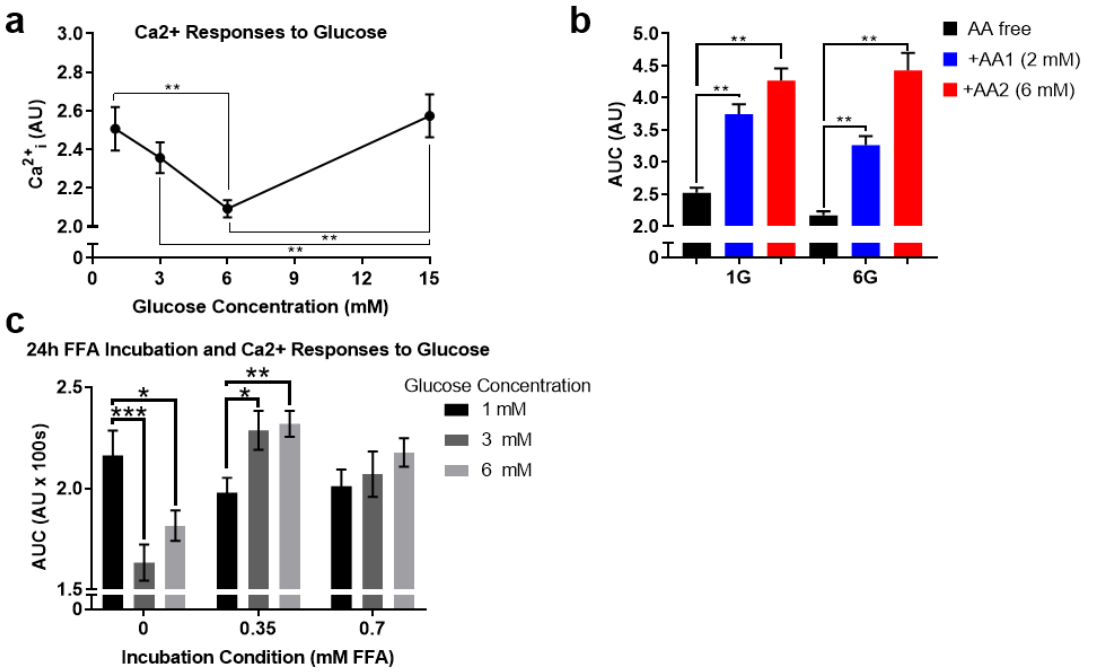

Figure 3.6 a, *Average $[Ca^{2+}]_i$ responses in GcgGCaMP⁺ islets during application of glucose (one-way ANOVA; ** = P<0.01. n=3 recordings from 3 mice (1 per mouse), 259-539 ROIs per recording).* ***b,*** *average $[Ca^{2+}]_i$ in GcgGCaMP3 islets during application of extracellular solution containing glucose and AA. Glucose was present at 1 or 6 mM glucose as indicted (* = p<0.01, one-way ANOVA, data from 3 mice, 250-280 ROIs per recording).* ***c,*** *Increasing glucose from 1 mM to 3 or 6 mM significantly decreased $[Ca^{2+}]_i$ in islets incubated in 0 mM FA but elevated [Ca2+]i in islets incubated in 0.35 mM FA and had no effect in islets incubated in 0.7 mM FA (Tukey's multiple comparisons test, *p<0.05, **p<0.01, ***p<0.001, n=102 – 285 from 3 recordings, 3 mice).*

Figure 3.7

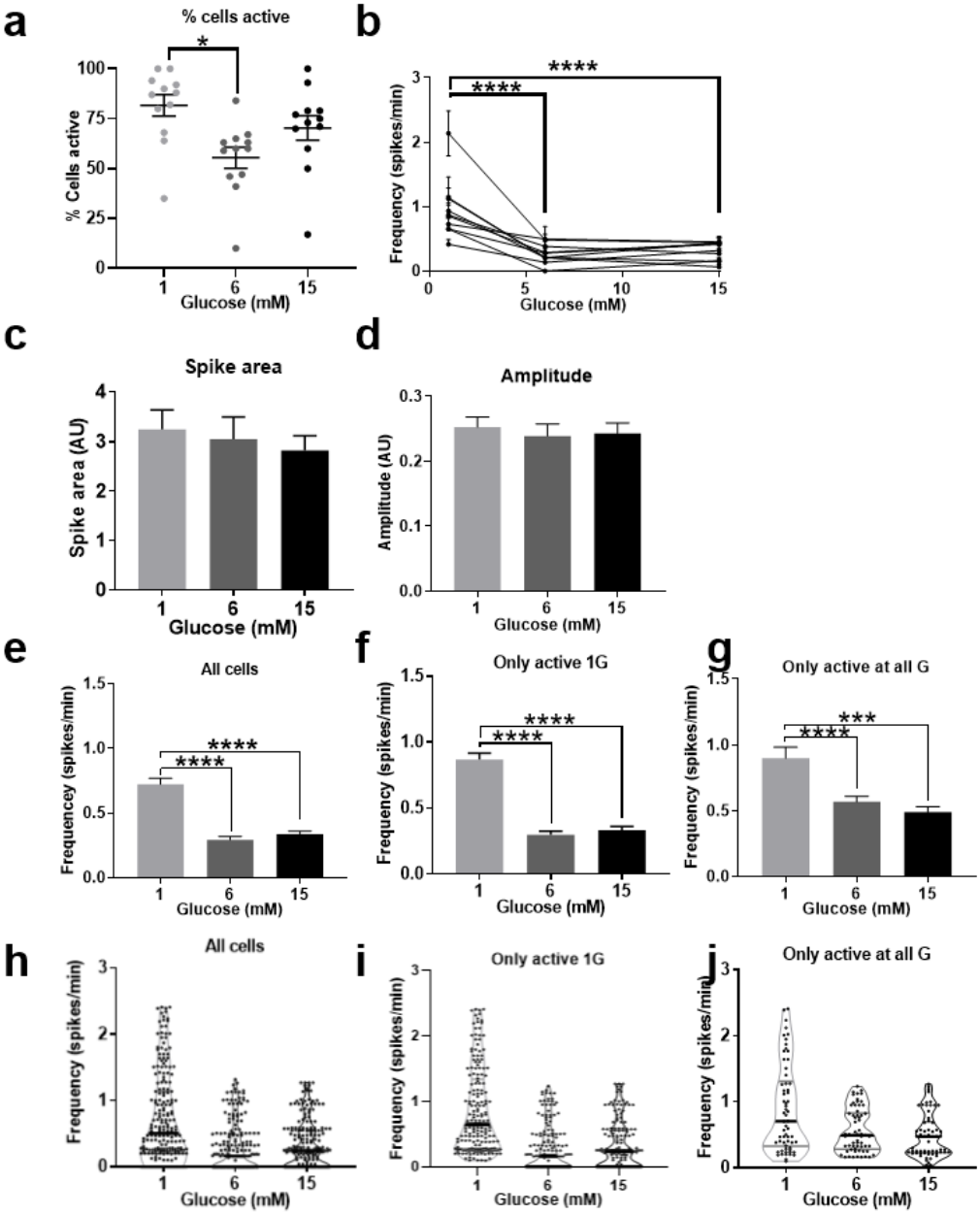

Figure 3.7 a, *% of cells active at different glucose concentrations (n=12 recordings, p=0.0133 for 1 vs. 6 mM glucose, one-way ANOVA).* ***b,*** *Animal averages of frequency (n=201-221 cells from 12 islets, 9 mice. p<0.0001, one-way ANOVA).* ***c*** *$[Ca^{2+}]_i$ oscillation area and* ***d****, amplitude in response to glucose (n=144 cells from 9 islets).* ***e****, oscillation frequency at 6 and 15 mM glucose relative to that at 1 mM. Breakdown of frequency analysis depending on cell inclusion criteria; Inclusion of all cells (**e,h**), Inclusion of cells only if they exhibited activity at 1 mM glucose (**f,i**). Inclusion of cells only if they exhibited activity at all glucose concentrations (**g,j**). mean values (**e-g**), violin plots (**h-j**, solid lines; black – median, grey – confidence interval, ***p<0.001, ****p<0.0001)*

Chapter 4

4. High fat experiments (*in vivo*)

4.1 Introduction

The aim of this project is to understand the deterioration in α cell function that occurs in pre-diabetes and T2D with the intention to understand a) what α cell dysfunction looks like and b) how this contributes to the development of a disease phenotype.

There are numerous models of hyperglycaemia/T2D that could be used to approach these experimental questions; however great care must be taken to the mechanisms by which they work to avoid making confounding conclusions about α cell behaviour.

Chapter 2 (section 2.12) discusses the different animal models available and their relevance for our experimental questions. Ultimately, we reasoned that the 12 –week 60% HFD model was most appropriate due to its effects on glucose homeostasis (as discussed in the Methods Chapter).

The previous chapter describes characterisation of the GgcGCaMP3 mouse line. High fat incubation resulted in a reduction in $[Ca^{2+}]_i$ AUC at 1 mM glucose, and an increase at 6 and 15 mM glucose. Investigation of α cell function in high fat conditions has been expanded upon in this chapter using an *in vivo* model of high fat diet. Mice from the GcgGCaMP3 line were placed on a 12 week control or high fat diet (HFD - 60% of calories from fat, CTL - 10% calories from fat). This chapter describes the results of *in vivo* metabolic phenotyping experiments.

4.1.2 Experimental justification

In people, plasma glucagon is elevated in obesity (Starke et al. 1984), pre-diabetes (Faerch et al. 2016), in patients with fasting hyperglycaemia (Faerch et al. 2008), and in T2D (Dunning et al. 2007). In HFD fed mice, plasma glucagon has been variously reported to be normal (Ahren et al. 1997, Winzell et al. 2007), increased (Ellingsgaard et al. 2008, Stern et al. 2019) and decreased (Conarello et al. 2007). Therefore, although it is commonly agreed that α cell function is perturbed in the prediabetic/diabetic state, the nature of the changes in α cell function, how they occur, and how they contribute to the disease phenotype is poorly understood.

In mice, HFD causes hyperglycaemia (Nicholson et al. 2010), altered insulin sensitivity (Fisher-Wellman et al. 2016) and hyperinsulinaemia (Montgomery et al. 2013). Plasma glucagon was also shown to be decreased following 12 weeks on HFD, glucagon secretion was decreased at low glucose but increased at elevated glucose, and immunofluorescence staining revealed elevated apoptosis and reduced proliferation in α cells (Merino et al. 2015).

Current literature therefore presents an unclear picture of how α cell function changes in obesity. We are interested in establishing the manifestations of HFD-induced diabetes on α cell function, how this may contribute to the disease phenotype, and in identifying the mechanisms causing altered α cell function. In order to address these questions, we have carried out metabolic phenotyping in HFD mice to characterise the *in vivo* changes in α cell function, including plasma hormone concentrations at rest, inhibition of glucagon secretion at elevated plasma glucose

concentrations, and stimulation of secretion during hypoglycaemia. These observations should help us address questions regarding the conditions under which α cell function becomes perturbed following HFD, and whether this may contribute to any hyperglycaemic phenotype.

4.2 Results

4.2.1 Week 6 phenotyping

Following initiation of the HFD after weaning, we carried out metabolic phenotyping of the mice at 6 weeks to investigate the short-term effects of the diet. Weight was significantly elevated by approximately 10% in HFD female mice (**Table 4.1**) although there were no statistically significant differences between HFD and CTL in either lean or fat mass. Male body weight was more sensitive to HFD and was 40% higher than CTL mice at 6 weeks. Much of this increase could be accounted for by increased fat mass, which was three times higher in HFD (**Table 4.3**).

We carried out a preliminary GTT at 6 weeks measuring plasma glucose at 0 and 30 min following injection of a glucose bolus (due to technical limitations and to avoid taking too much blood from the mice). Both female and male HFD mice were glucose intolerant compared to CTL mice during the GTT (**Figure 4.2c, Figure 4.3c**)

4.2.2 Week 12 phenotyping

4.2.2a Weight gain

After 12 weeks of high fat feeding, both males and females had gained visibly more weight on the HFD compared to mice on chow (**Figure 4.1**, **Figure 4.2a, Figure 4.3a**). HFD resulted in higher fat mass in both female and male mice (**Figure 4.2b**, **Figure 4.3b**) with increases in fat mass accounting for most of the increase in bodyweight (**Table 4.2**, **Table 4.4**). Due to the higher calorie content of the HFD feed, HFD mice continued to consume more calories even when food intake was not changed or reduced in terms of grams eaten (**Figure 4.2d,e, Figure 4.3d,e**).

4.2.2b Week 12 GTTs

Inhibition of plasma glucagon by hyperglycaemia following HFD was then investigated. Elevated plasma glucose during a GTT was maintained at 12 weeks (**Figure 4.4a, Figure 4.5a**). In female CTL mice, glucose returned to baseline within 60 min but in HFD mice it took 120 min, indicating altered kinetics of the GTT (a higher peak, and a delayed return to normoglycaemia). HFD fed male mice also exhibit a delayed return to normoglycaemia following injection of glucose bolus, with plasma glucose returning to baseline levels within 120 min in CTL but not in HFD animals.

AUC during the GTT was elevated in HFD male and female mice compared to CTLs. The difference in glucose concentration between 0 and 30 min (Δ[Glucose]) was significantly higher in HFD fed compared to CTL animals (**Figure 4.4d, Figure 4.5d**). The fold change in glucose concentration between 0 and 30 min was also greater in HFD animals (**Figure 4.4f, Figure 4.5f**). These results indicate that HFD fed mice struggle to respond appropriately to hyperglycaemic challenge resulting in greater changes in blood glucose concentration and delayed GTT kinetics.

Plasma glucagon measured at 0 and 30 min following glucose injection, was not different between CTL and HFD mice at either time (**Figure 4.4b, Figure 4.5b**). However, in female mice plasma glucagon was significantly decreased in response to the glucose bolus in both CTL and HFD animals. Linear regression showed a difference in the relationship between plasma glucose and glucagon with a significantly steeper slope in CTL mice due to lower plasma glucose during the bolus (**Figure 4.4c**), y-intercept was not different between the groups. R^2 values were 0.43 and 0.32 for CTL

and HFD mice respectively, the pM change in glucagon following the glucose bolus was normally distributed for both CTL and HFD mice (Shapiro-Wilk test, W=0.96 and 0.94 respectively, P>0.05 in both cases). This suggests that the CTL and HFD groups do not have subcategories of responders and non-responders (although this may be underpowered as n=11 mice). Linear regression analysis revealed no relationship between glucose and glucagon concentration in either CTL or HFD male mice following injection of the glucose bolus (**Figure 4.5i**).

4.2.2c Week 12 ITTs

Mice were next subjected to insulin tolerance tests (ITTs) to determine whether insulin sensitivity was altered in response to HFD feeding and whether HFD mice remain able to respond to hypoglycaemia/insulin with increased secretion of glucagon. HFD fed male mice exhibited elevated plasma glucose concentrations during the ITT (**Figure 4.5g**) although AUC was not different. Both groups maintained insulin sensitivity and the change in blood glucose in response to insulin was not different between the groups (**Figure 4.5j**). In female mice, there was no difference in plasma glucose or AUC during the ITT but the change in plasma glucose in response to insulin was greater in HFD compared to CTL mice, indicating an increased insulin sensitivity **Figure 4.4j**).

There was no diet-dependent difference in insulin-stimulated glucagon secretion in either male (**Figure 4.5h**) or female (**Figure 4.4h**) mice. Linear regression analysis showed no difference in the gradient of the slope or in the y-intercept for female mice (**Figure 4.4i**). In male mice, linear regression analysis revealed a decrease in the

slope gradient following HFD (**Figure 4.5i**). This indicates that glucagon secretion is elevated relative to the glucose concentration in HFD mice.

When the ITT was repeated with dosing calculated based on lean mass (insulin dose adjusted for the reduced lean mass in HFD fed mice, Methods section 2.3.2), rather than overall weight, HFD and CTL mice showed the same level of insulin sensitivity, and stimulation of glucagon secretion was greater in HFD mice at 30 min (**Figure 4.4m** and **n**).

4.2.2d Basal glycaemia

In order to investigate whether there were differences in plasma glucose and glucagon levels in mice at rest, plasma glucose in unfasted female mice was measured at three time points throughout the day (**Figure 4.6** and **Figure 4.7**) – 0900 am, 1300 pm and 1700 pm (Zeitgeber time (ZT) 1, 5 and 9 respectively. Lights on 08.00 am – 20.00 pm). There were no differences in blood glucose concentration between the diet groups at any time point, nor was there an overall difference when assessed using a mixed effects analysis. However, whereas blood glucose was static throughout the day in female HFD mice, in CTL mice, plasma glucose was lowest at 0900 am (ZT 1) and increased at 1300 pm (ZT 5) and 1700 pm (ZT 9, **Figure 4.6a**). Insulin was significantly elevated at 1300 pm (ZT 5) in HFD mice compared to CTL (**Figure 4.6**). Plasma glucagon concentration was significantly higher in HFD mice at 0900 am (ZT 1, **Figure 4.6c**). The glucagon:glucose ratio (pM/mM) is 33% higher in HFD compared to CTL female mice indicating that at a given glucose concentration, glucagon secretion is elevated in HFD animals compared to CTLs (**Figure 4.6d**). The

insulin:glucose ratio was not different between HFD and CTL female mice (**Figure 4.6f**). No differences in resting fed glycaemia or hormone concentrations were seen in male mice (**Figure 4.7**).

4.2.3 Expression of Fluorescent marker does not influence the HFD phenotype

The effect of fluorescent protein expression (RFP and/or GCaMP3) in α cells on glycaemia has been previously investigated (Section 3.3.1) and no significant difference between groups was found. However, we wanted to investigate whether "stressing" the transgenic mice with the HFD might reveal differences in glucose homeostasis as a result of expressing the fluorescent proteins within α cells. In mice fed a HFD for 12 weeks, mean glycaemia during the GTT was not different between mice with and mice without a fluorescent marker (**Figure 4.8**).

4.3 Discussion

4.3.1 Summary of results

These experiments demonstrate that 12 weeks HFD feeding increased calorie intake and was sufficient to induce significant weight gain and increased fat mass. Mice exhibited elevated plasma glucose during a GTT after 6 weeks of HFD, maintained at 12 weeks. HFD female mice exhibited hyperglucagonaemia and elevated insulin at rest, had an elevated glucose:glucagon ratio, and had elevated plasma glucose during both GTTs and ITTs. Male mice also exhibited elevated plasma glucose during both GTTs and ITTs however no differences were found in glycaemia or plasma hormone concentrations at rest.

4.3.2 HFD provokes a pre-diabetic state in mice

Many of the changes identified through metabolic phenotyping indicate a pre-diabetic or diabetic state (impaired glucose tolerance, elevated fasting glucose, and hyperglucagonaemia). The American Diabetes Association defines a non-fasting plasma glucose of >11 mM as indicative of diabetes (7 mM when fasted). Plasma glucose concentration in a mouse tends to be higher than in humans and a recommended criteria for identifying diabetic mice puts non-fasting plasma glucose at >14 mM (Leiter 2009). In light of this, elevated plasma glucose during GTT and ITTs indicate, despite normoglycaemia at rest, development of a pre-diabetic state.

We might expect these mice to display insulin resistance (Conarello et al. 2007). Although HFD mice had elevated plasma glucose during the GTT, during the ITT HFD mice displayed greater mM change in response to insulin compared to CTL mice. The

volumes of insulin/glucose injected for ITT's/GTT's were calculated as a dose per gram of body weight. However, it is the lean mass that is the target for insulin during ITTs and HFD mice have increased fat, but not lean, mass. Therefore, per g of lean mass, HFD mice actually receive a larger insulin dose. As a result, lean-mass based dosing has been recommended (McGuinness et al. 2009, Pacini et al. 2013, Alquier et al. 2018). Starting glucose concentration is relevant when measuring insulin sensitivity - where baseline glucose is elevated, insulin sensitivity may *appear* blunted. However, the change in plasma glucose response to insulin – i.e. the gradient between blood glucose at 0 and 30 min (Δ[Glucose]), is the most useful indicator of insulin sensitivity. When the dose of insulin was given based on lean mass, rather than total weight, there was no difference in insulin sensitivity between the two groups. This may indicate that the unadjusted dose of 0.75 U/kg whole body weight was high enough to overcome any insulin resistance in HFD fed mice. We see a difference in stimulation of glucagon secretion following the insulin bolus. However, we cannot separate the effect of insulin from the effect of hypoglycaemia on the α cell in this context. The same weight-based caveat is relevant for GTTs. Although lean-mass or standardised dosing has been recommended, it does not appear to affect the main observations/conclusions drawn from GTT experiments in HFD mice (Jorgensen et al. 2017). Mice showed hyperglycaemia during the GTT, and elevated plasma glucose, glucagon, and insulin at rest. In conclusion, HFD induces many of the changes in whole body physiology associated with a pre-diabetic state.

4.3.3 Hyperglucagonaemia in prediabetes

Plasma glucagon was elevated relative to glucose in resting unfasted mice. This is clear at 0900 am (ZT 1) and is time-dependent. Circadian rhythms of plasma glucagon concentration is an understudied area. In fed rats, plasma glucose drops during the dark cycle. However, there is no clear diurnal rhythm in plasma glucagon. Fasting rats for 13-18h increases plasma glucagon (Ruiter et al. 2003). In fed humans, plasma glucose increases at midnight (VanCauter et al. 1997). Due to the nocturnal nature of mice, any measurements carried out during daylight hours are effectively occurring during the inactive phase of their 24h cycle. Furthermore, separating the effect of time of day from time since last feed is challenging in mice where, despite ad libitum access to food, feeding will not be continuous throughout a 24h period. Whereas humans eat 3-4 meals during the day, mice eat throughout the 24-hour cycle with more frequent visits to the hopper during the night (the active phase for mice) (Bechtold et al. 2008). Mealtime is a strong entrainment cue for circadian rhythm (Stokkan et al. 2001) and caloric restriction with time-limited access to feed can be used to entrain mice (Froy et al. 2010). Feeding behaviours must be carefully considered, and if possible accounted for, when assessing circadian changes in plasma hormone concentrations and comparing between humans and mice.

The increase in plasma glucagon at 0900 am (ZT 1) could be a stress response to the lights coming on an hour before. HFD fed rats show hypersensitivity of the hypothalamic-pituitary-axis (HPA) and elevated cortisol levels compared to chow fed controls (Liu et al. 2017). This hypersensitivity may make HFD mice more susceptible to stress induced elevations in plasma glucose and glucagon concentrations. Shifting

the time of measurements (e.g. starting at 1000 am (ZT 2)) and taking more frequent measurements to resolve trends over time more clearly would be useful in the future to identify the influence of daily stressors on measurements.

We show here that HFD mice have elevated glucagon:glucose ratio at rest. Merino *et al.* (2015) observed that HFD mice maintained insulin sensitivity, and remained able to stimulate glucagon secretion in both HFD and CTL mice. In line with this, we found that plasma glucose was higher in HFD fed mice 30 min after the glucose bolus during a GTT. However, rather than stimulating glucagon release (Merino et al. 2015), in our experiments the glucose bolus inhibited glucagon release (**Figure 4.4b**). Therefore, although plasma glucagon is elevated relative to glucose concentration, the ability of α cells to respond to hyperglycaemia with reduced glucagon secretion is maintained. This may indicate that a shift in the homeostatic set-point or baseline for control of glucagon secretion to a more hyperglycaemic value may occur in obesity. In summary, we show that HFD mice are hyperglycaemic and also exhibit hyperglucagonaemia which may contribute to their metabolic phenotype.

4.3.4 Intrinsic changes in the α cell and contribution to the diabetic state

In these studies, we have demonstrated that HFD fed mice exhibit hallmarks of prediabetes. We have also seen disturbances in plasma glucose homeostasis and glucagon concentrations. Specifically, an elevated glucagon:glucose ratio indicates that per unit of glucose, HFD fed mice have more plasma glucagon. Although the reduction of plasma glucagon during a GTT indicates that α cells do still respond to

hyperglycaemia, the elevation in glucagon:glucose ratio may contribute to the hyperglycaemic, prediabetic state.

It is well established that α cell function is changed in T2D human islets with insufficient glucagon secretion at low glucose concentrations and increased glucagon secretion at high glucose (Zhang et al. 2013, Briant et al. 2018). α cells also change in HFD with altered glucagon secretion, reduced membrane capacitance, reduced α cell mass and cell size, and increased α cell apoptosis (Merino et al. 2015). These observations indicate that changes intrinsic to the α cell/islet, and independent of the rest of the body, may drive altered activity and glucagon secretion. We are therefore interested whether, in the HFD fed pre-diabetic model, changes in intrinsic α cell function can already be observed, and whether they might be driving the metabolic phenotype. How α cells change functionally to maintain hyperglucagonaemia remains unanswered. To answer these islet-centric questions in the next chapter, we will carry out a number of *ex vivo* experiments using tissue from HFD and CTL fed mice. These experiments will be used to study whether changes in α cell calcium signalling, secretion, and perfusion occur, and whether any changes mirror those seen *in vivo,* explaining why α cells become dysfunctional.

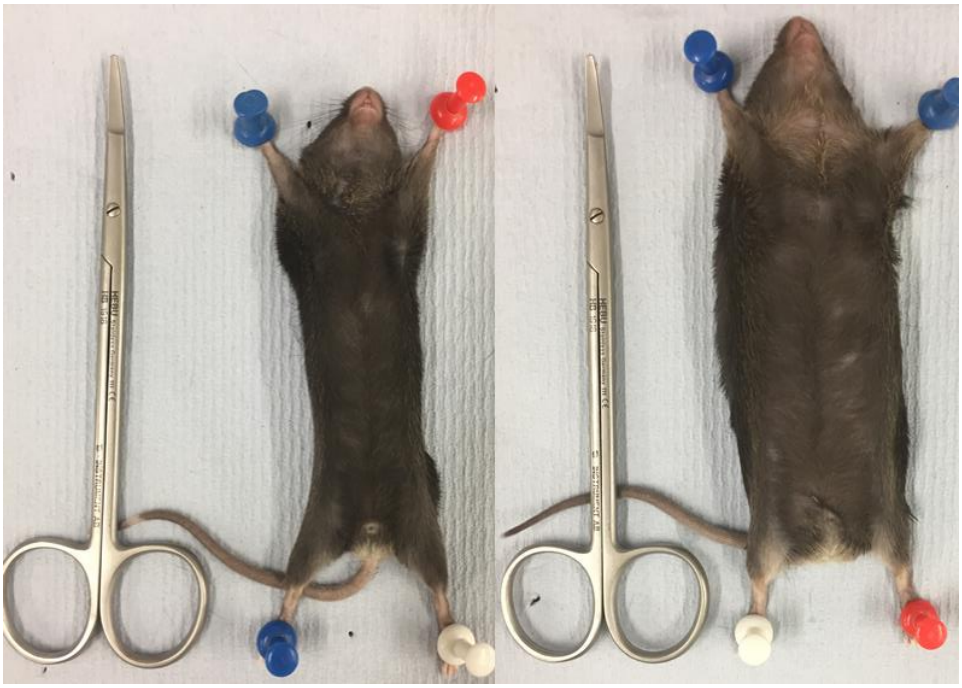

Figure 4.1 *Left; mouse following 12 weeks CTL diet, right; mouse following 12 weeks HFD diet*

Table 4.1 *6-week EchoMRI of female HFD and CTL fed mice, n=6 mice.*

Female 6 week	**Control**	**HFD**	**Unpaired t-test p=**
Weight (g)	19.70	21.69	0.0267
Fat %	20.36	25.36	0.1623
Lean mass %	67.86	67.44	0.8931
Total water %	54.78	56.69	0.5902
Fat (g)	4.00	5.61	0.0879
Lean mass (g)	13.38	14.63	0.1888
Total water (g)	10.80	12.26	0.0904

Table 4.2 *12 week EchoMRI of female HFD and CTL fed mice, n=6 mice.*

Female 12 week	**Control**	**HFD**	**Unpaired t-test p=**
Weight (g)	20.77	26.25	0.0035
Fat %	20.33	32.88	0.0273
Lean mass %	69.50	59.50	0.0268
Total water %	57.16	48.63	0.0151
Fat (g)	4.21	8.90	0.0183
Lean mass (g)	14.44	15.41	0.2464
Total water (g)	11.88	12.62	0.3054

Table 4.3 *6-week EchoMRI of male HFD and CTL fed mice, n=4-5 mice.*

Male 6 week	**Control**	**HFD**	**Unpaired t-test p=**
Weight (g)	20.0	28.06	<0.0001
Fat %	13.03	28.05	0.0002
Lean mass %	72.98	64.71	0.0163
Total water %	60.15	51.91	0.0063
Fat (g)	2.605	7.87	<0.0001
Lean mass (g)	14.60	18.16	0.0043
Total water (g)	12.04	14.57	0.0065

Table 4.4 *12 week EchoMRI of male HFD and CTL fed mice, n=4-5 mice.*

Male 12 week	**Control**	**HFD**	**Unpaired t-test p=**
Weight (g)	22.38	34.68	<0.0001
Fat %	12.26	36.59	<0.0001
Lean mass %	76.94	54.57	<0.0001
Total water %	65.19	44.30	<0.0001
Fat (g)	2.75	12.74	<0.0001
Lean mass (g)	17.21	18.89	0.0420
Total water (g)	14.58	15.37	0.3833

Figure 4.2

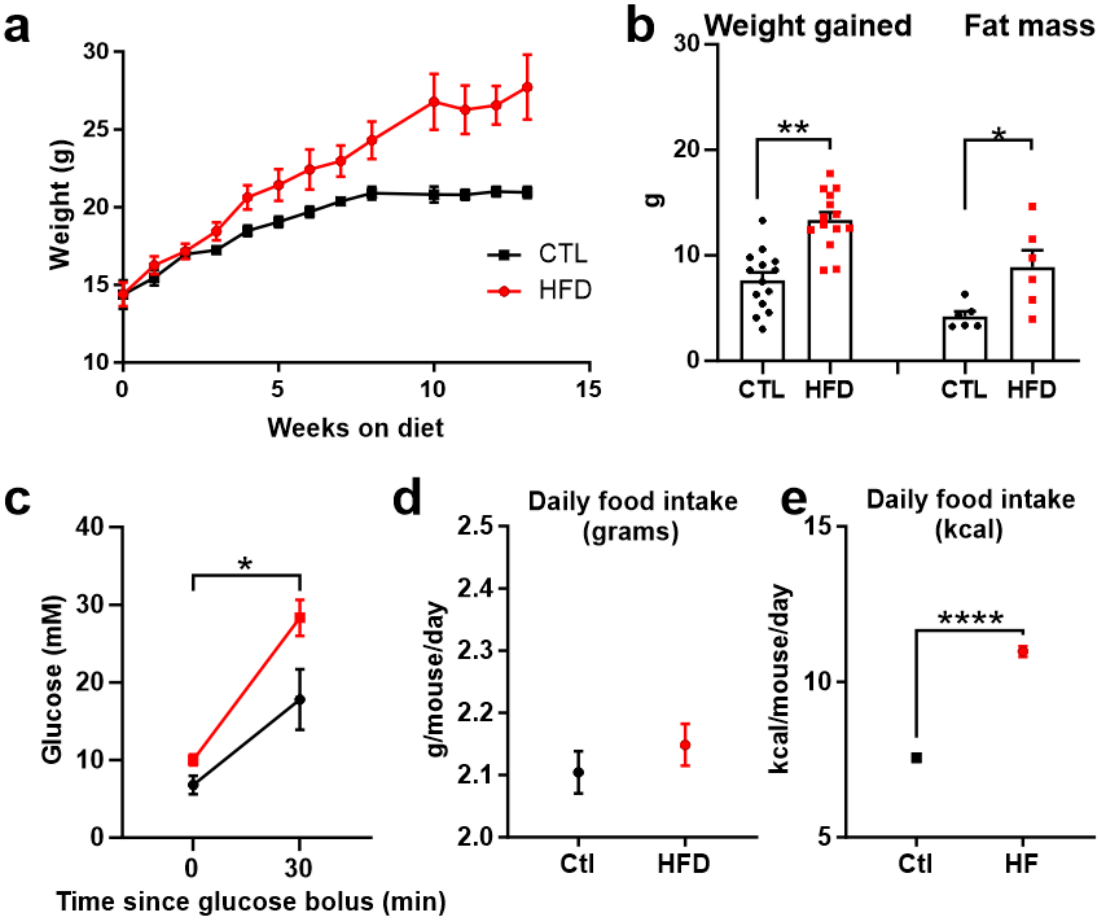

Figure 4.2 *Female phenotyping; Control - black, HFD fed - red.* ***a,*** *Weight (g) over 12 weeks of feeding (n=24 mice).* ***b,*** *Weight gain at 12 weeks was significantly higher in HFD vs. CTL mice (n=14 mice). Body fat was significantly higher in HFD* vs. *CTL mice (n=6 mice, unpaired t-tests).* ***c,*** *Mean blood glucose concentration (mM) following injection of a glucose bolus at 6 weeks, IPGTT increased glucose in both CTL and HFD fed mice 30 min after bolus, (n=4 mice, p=0.0393 for the overall column effect between HFD and CTL mice, two way ANOVA followed by Sidak's multiple comparisons test).* ***d,*** *Mean daily food intake per mouse shown as grams or e, kcal (n=food measured on a total of 55 occasions from 3 cages, mean 18 measurements per cage, t-test). *=p<0.05, **=p<0.01, ***=p<0.001, ****=p<0.0001*

Figure 4.3

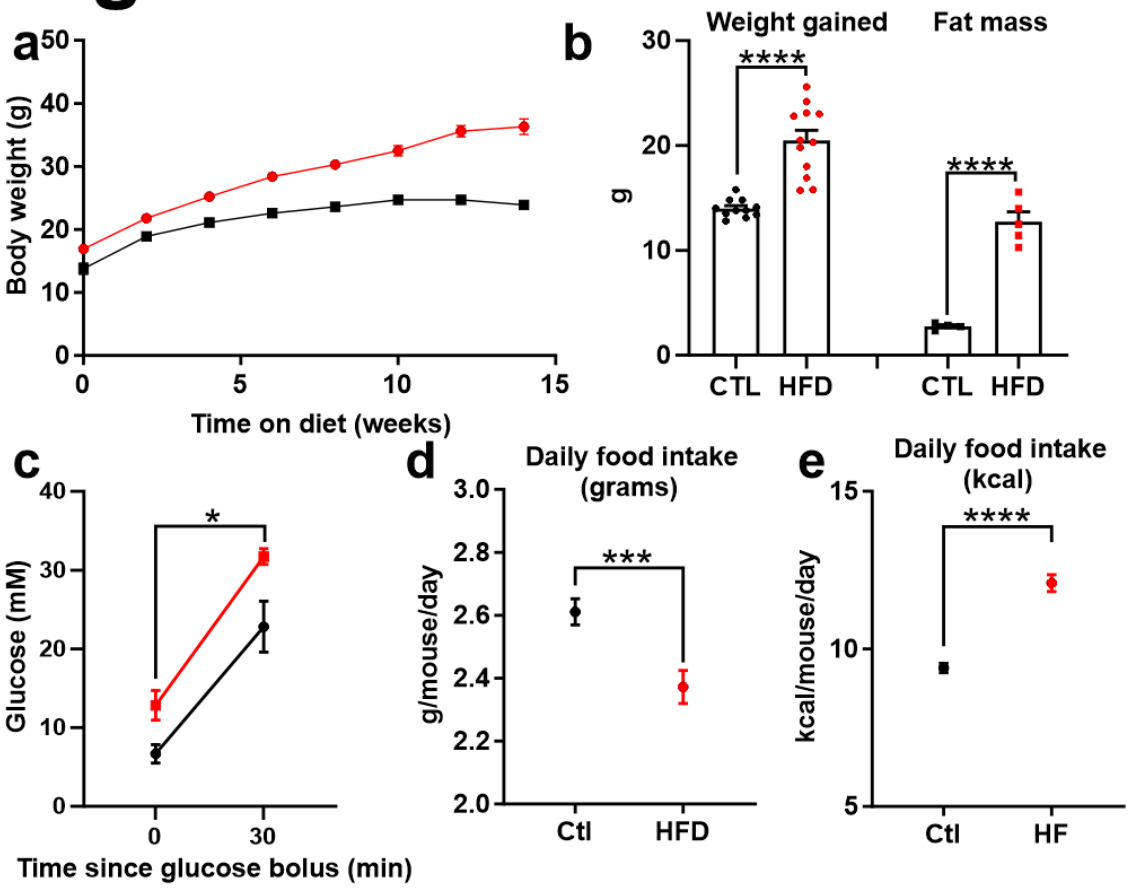

Figure 4.3 *Male phenotyping; Control - black, HFD fed - red.* ***a,*** *Weight gain (g) over 12 weeks of altered diet (n=24 mice).* ***b****, Body weight gained following 12 weeks altered diet was significantly higher in HFD* vs. *CTL mice (n=11-13 mice, p<0.0001, unpaired t-test). Body fat was significantly higher in HFD mice (n=4-5 mice, *p<0.0001, unpaired t-test).* ***c,*** *Mean blood glucose concentration (mM) following injection of a glucose bolus at 6 weeks (0 and 30 min, n=4 mice, p=0.0133 for the difference between HFD and CTL, p<0.0001 for effect of glucose).* ***d,*** *Mean daily food intake per mouse shown as grams (2.61 vs. 2.37g p=0.0004, n=107-108) or e, kcal in mice (9.40 vs. 12.1 kcal, p<0.0001, n=106-110, n=food measured on a total of 55 occasions from 3 cages, mean 18 measurements per cage). *=p<0.05, **=p<0.01, ***=p<0.001, ****=p<0.0001*

Figure 4.4

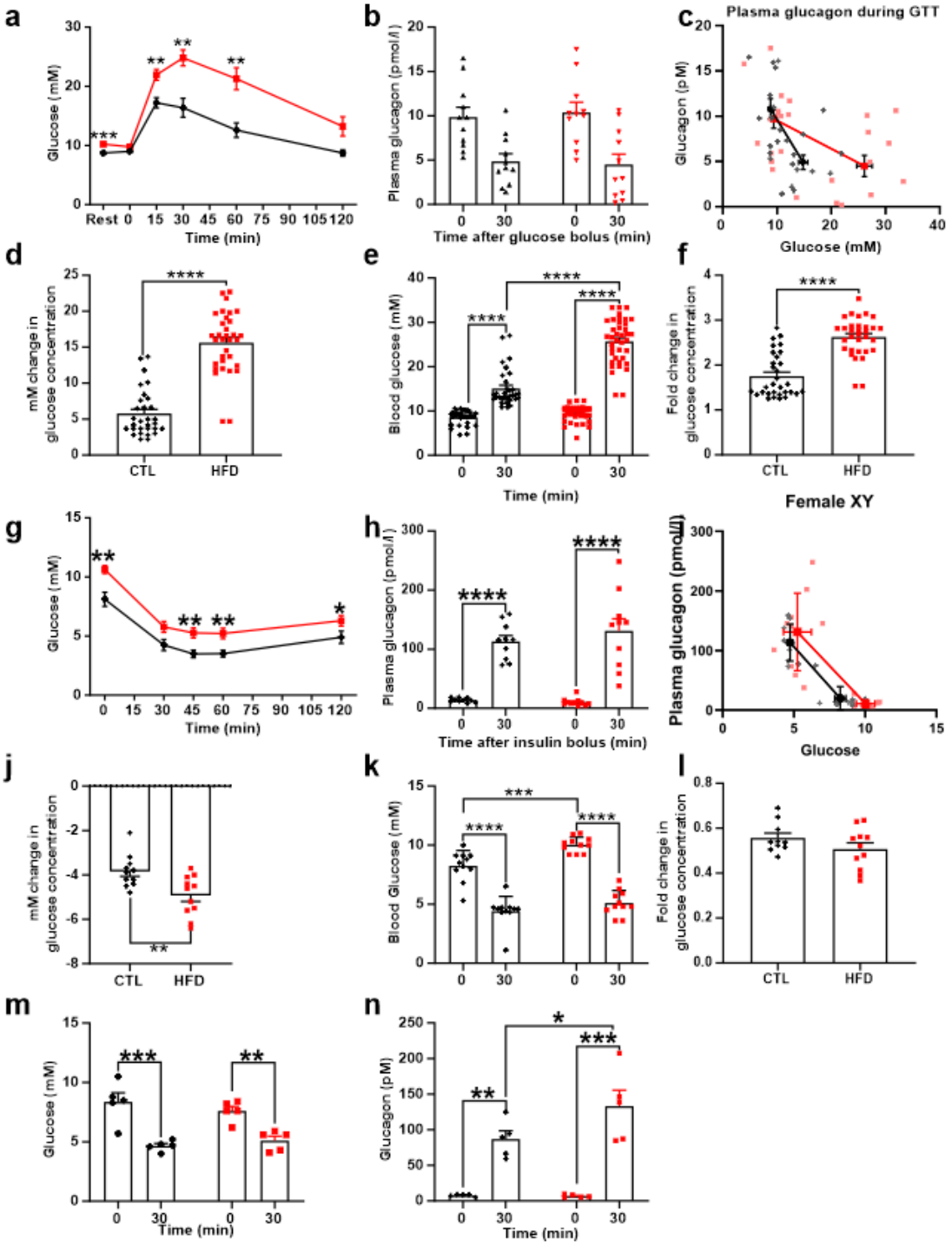

Figure 4.4 *Female phenotyping; Control - black, HFD fed - red.* ***a,*** *Plasma glucose concentration (mM) during IPGTT (n=12 CTL and 13 HFD mice, **p<0.01, ***p<0.001, one-way ANOVA followed by Sidak's multiple comparisons test).* ***b,*** *Plasma glucagon concentration (pM) during IPGTT (n=11 CTL and HFD mice, p>0.05 at both 0 and 30 min, mixed-effects analysis followed by Sidak's multiple comparisons test).* ***c,*** *Linear regression of glucose/glucagon concentration at 0 and 30 min of GTT. The gradient of the slope was reduced in HFD fed mice (p=0.0179), however the y-intercept was not different (p=0.0584, n=11-14 mice, unpaired t-tests).* ***d,*** *mM, changes in plasma glucose at 0 and 30 min after*

injection of 2 mg/kg glucose bolus (n=31-32 female mice, unpaired t-test). ***e,*** *Plasma glucose concentrations at 0 and 30 min following 2mg/kg glucose bolus. Pooled data from GTT and plasma glucagon measurements. Plasma glucose concentration was increased by the glucose bolus in both CTL and HFD mice. Plasma glucose was not different between the diets at 0 min but was lower in CTL compared to HFD animals at 30 min (two-way ANOVA with multiple comparisons, n=32 CTL and 39 HFD fed female mice).* ***f,*** *Fold changes in plasma glucose at 0 and 30 min after injection of 2 mg/kg glucose bolus (n=31-32 mice, unpaired t-test).* ***g,*** *Plasma glucose concentration (mM) during IPITT (n=5 CTL and 5 HFD mice, mixed-effects analysis followed by Sidak's multiple comparisons test).* ***h,*** *Plasma glucagon concentration (pM) during IPITT (p>0.05 between HFD and CTL at both 0 and 30 min, n=32 CTL and 39 HFD fed mice, mixed-effects analysis followed by Sidak's multiple comparisons test).* ***i,*** *Linear regression of glucose/glucagon concentration at 0 and 30 min of ITT. Gradient of slope was not different between HFD and CTL mice (p=0.5534), nor was y-intercept (p=0.9335, n=10 mice, unpaired t-tests).* ***j,*** *mM changes in plasma glucose at 0 and 30 min after injection of an insulin bolus (n=11 mice, unpaired t-test).* ***k****, Plasma glucose concentrations at 0 and 30 min following insulin bolus. CTL and HFD fed female mice. Plasma glucose concentration was reduced by the insulin bolus in both CTL and HFD mice. Plasma glucose was elevated in HFD fed mice at 0 min but not different at 30 min (two-way ANOVA with multiple comparisons).* ***l,*** *Fold changes in plasma glucose at 0 and 30 min after injection of an insulin bolus (n=11 mice, unpaired t-tests).* ***m,*** *Plasma glucose during an ITT dose based on lean mass (n=5 mice, two-way ANOVA with Sidak's multiple comparisons).* ***n,*** *Plasma glucagon during an ITT dosed based on lean mass (n=5 mice, two-way ANOVA with Sidak's multiple comparisons). *=p<0.05, **=p<0.01, ***=p<0.001, ****=p<0.0001*

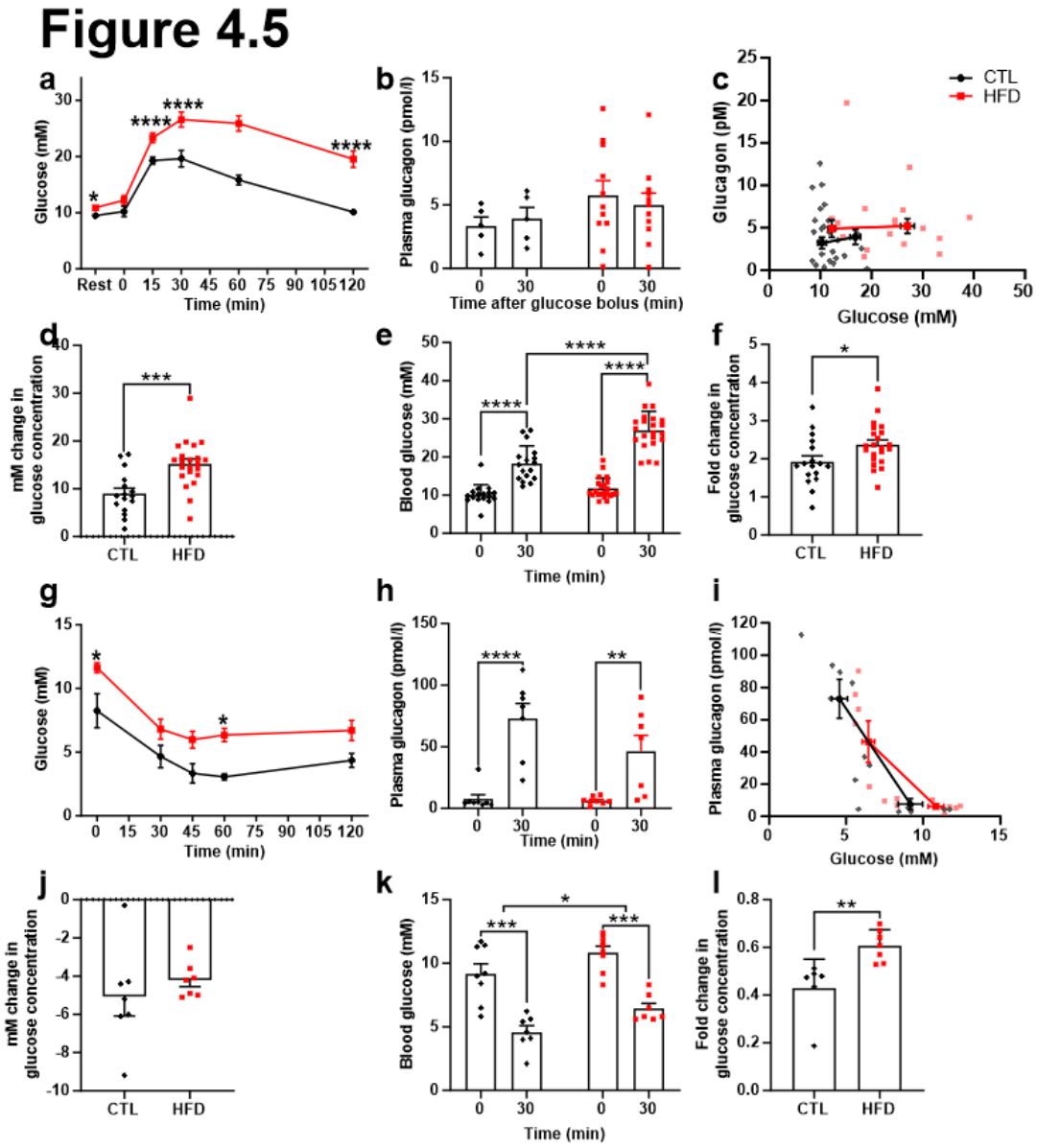

Figure 4.5 *Male phenotyping; Control - black, HFD fed - red.* ***a,*** *Plasma glucose concentration (mM) during IPGTT (n=11 CTL and 12 HFD mice, two-way ANOVA followed by Sidak's multiple comparisons test).* ***b,*** *Plasma glucagon concentration (pM) during IPGTT (n=6 CTL and 12 HFD mice, p>0.05 at both 0 and 30 min, two-way ANOVA with Sidak's multiple comparisons test).* ***c,*** *Linear regression of glucose/glucagon concentration at 0 and 30 min of GTT. The gradient of the slope was not different between HFD and CTL mice, nor was y-intercept (n=17-28 mice, p>0.05 unpaired t-tests).* ***d,*** *mM, changes in plasma glucose at 0 and 30 min after injection of 2 mg/kg glucose bolus. (n=16-22 mice, unpaired t-test).* ***e,*** *Plasma glucose concentrations at 0 and 30 min following 2mg/kg glucose bolus. Plasma glucose concentration was increased by the glucose bolus in both CTL and HFD mice. Plasma glucose was not different between the diets at 0 min but was lower in CTL compared to HFD animals at 30 min (n=17 CTL and 22 HFD mice, two-way ANOVA with Sidak's multiple comparisons).* ***f,*** *Fold changes in plasma glucose at 0 and 30 min after injection of 2 mg/kg glucose bolus (n=16-22 mice, unpaired t-tests).* ***g,*** *Plasma glucose concentration during IPITT (n=4 CTL and 4 HFD mice, mixed-effects analysis followed by Sidak's multiple comparisons test).* ***h,*** *Plasma glucagon concentration (pM) during IPITT (n=8 CTL and 8 HFD mice, two-way ANOVA followed by Sidak's multiple comparisons test).* ***I,*** *Linear regression of glucose/glucagon*

concentration at 0 and 30 min of GTT. The gradient of the slope was reduced in HFD fed mice (p=0.01), however the y-intercept was not (p=0.3057, n=11-14 mice, unpaired t-tests). ***j,*** *mM changes in plasma glucose at 0 and 30 min after injection of an insulin bolus (n=7 mice, unpaired t-tests).* ***k,*** *Plasma glucose concentrations at 0 and 30 min following insulin bolus. Plasma glucose concentration was reduced by the insulin bolus in both CTL and fed mice. Plasma glucose was not different between CTL and HFD mice at 0 or 30 min (n=8 CTL and 7 HFD mice, two-way ANOVA with multiple comparisons).* ***l,*** *Fold changes in plasma glucose at 0 and 30 min after injection of an insulin bolus (n=7 mice, unpaired t-test). *=p<0.05, **=p<0.01, ***=p<0.001, ****=p<0.0001*

Figure 4.6

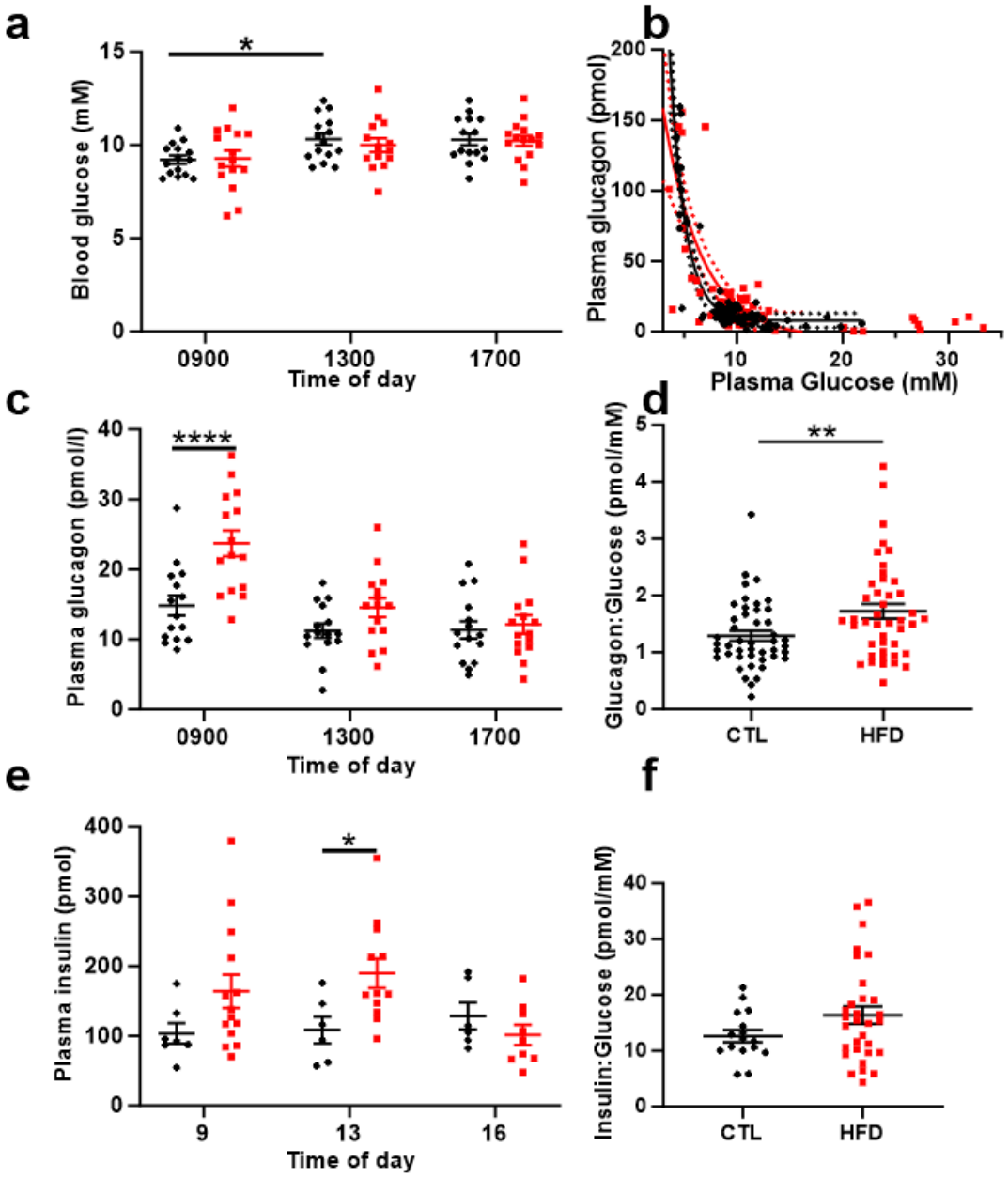

Figure 4.6 *Plasma hormone levels in female mice; Control - black, HFD fed - red.* ***a,*** *Plasma glucose concentration (mM) in unfasted CTL and HFD mice (n=14-15, p>0.05 at all time points except 0900 vs. 1300 in CTL mice, t-test).* ***b,*** *Nonlinear best fit curve for all glucose:glucagon measurement made (including at rest, during GTT and during ITT), R^2= 0.83 for CTL and = 0.41 for HFD fed mice. Half life = 1.0 for CTL and 2.4 for HFD (n=91 CTL and 90 HFD mice).* ***c,*** *Plasma glucagon concentration (pM, n=15 CTL and HFD mice, p=0.0081 for overall effect of diet – two-way ANOVA followed by Sidak's multiple comparisons test).* ***d,*** *Glucagon:glucose ratio, pM/mM (n=45 CTL and 43 HFD mice, unpaired t-test).* ***e,*** *Plasma insulin concentration (pM) (n=4-12 mice, p=0.0444 at 1300 pm, two-way ANOVA followed by Sidak's multiple comparison's tests).* ***f,*** *Insulin:glucose ratio, pM/mM (n=16 CTL and 31 HFD mice, t-test). 0900 am (ZT 1), 1300 pm (ZT 5), 1700 pm (ZT 9). *=p<0.05, **=p<0.01, ***=p<0.001, ****=p<0.0001*

Figure 4.7

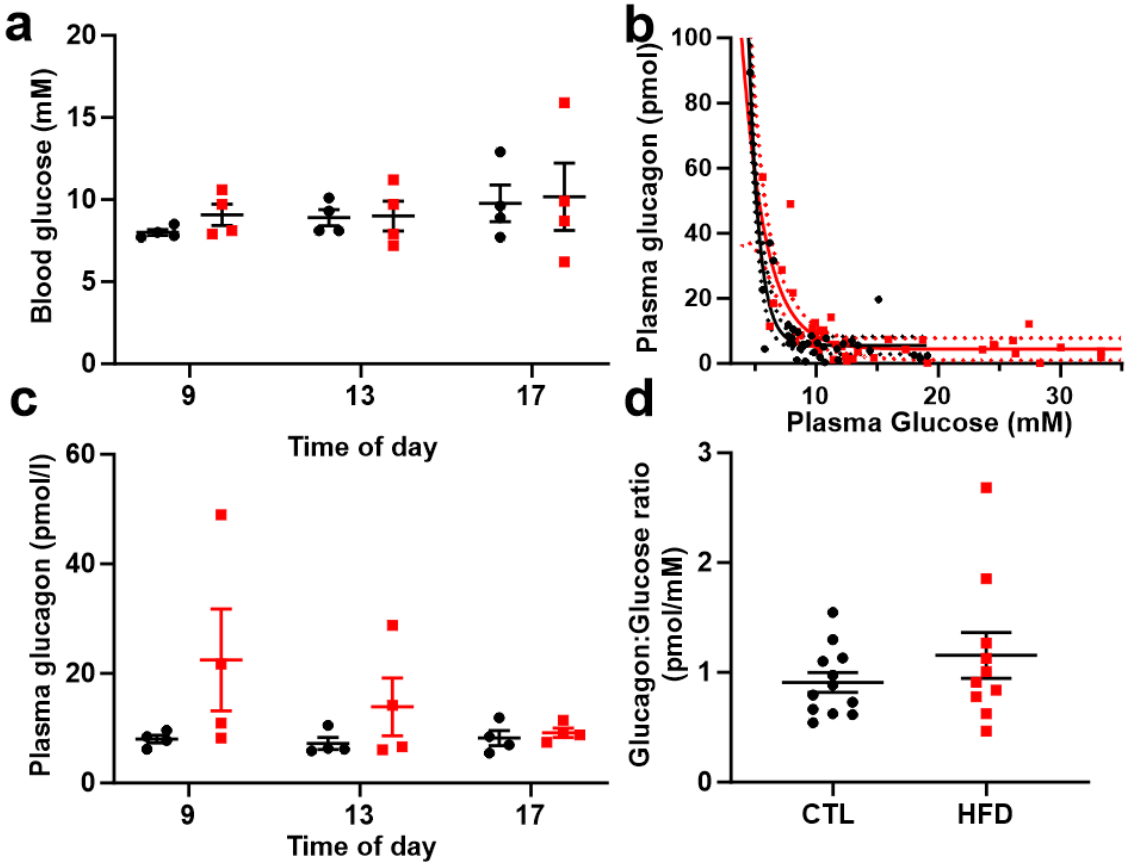

Figure 4.7*a, Plasma hormone levels in male mice; Control - black, HFD fed - red.* ***a,*** *Plasma glucose concentration (mM) in unfasted mice (n=4, p>0.05 at all time points, no overall column effect).* ***b,*** *Nonlinear best fit curve for all glucose:glucagon measurement made (including at rest, during GTT and during ITT), R^2= 0.82 for CTL and = 0.55 for HFD fed mice. Half life = 0.58 for CTL and 1.33 for HFD (n=37 CTL and 45 HFD mice).* ***c,*** *Plasma glucagon concentration (pM) in unfasted mice (n=4, no overall effect of diet p=0.1863).* ***d****. Glucagon:glucose ratio, pM/mM (unpaired t-test).*

Figure 4.8

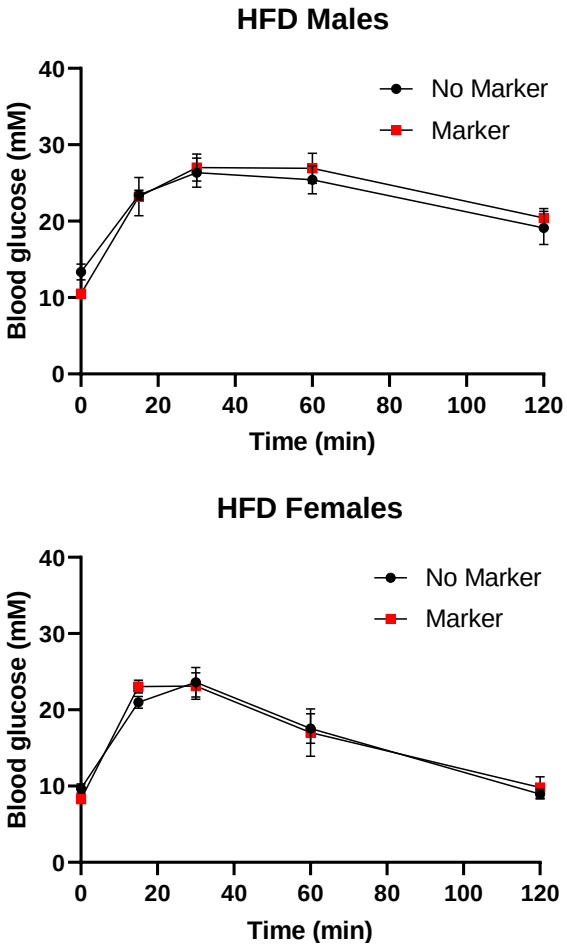

Figure 4.8 *Effect of expression of fluorescent marker expression on plasma glycaemia under conditions of high fat feeding. Mice with no fluorescent marker expression (black) or with marker expression (red) fed a HFD for 12 weeks underwent GTTs (n=4-8 mice per group, p>0.05, two-way ANOVA with Sidak's multiple comparisons test).*

Chapter 5

5. High fat feeding (*ex vivo* experiments)

5.1 Introduction

Mice fed a high fat diet for 12 weeks gain significant fat mass, have elevated plasma glucose during GTTs and ITTs and exhibit elevated plasma glucagon concentration in the fed state. Considering these changes in whole body glucose homeostasis and the elevation of plasma glucagon concentrations, it is therefore important to establish if these changes are due to changes in α cell function.

β cell proliferation is elevated within 4 days of HFD feeding beginning, and β cell mass is increased at 7 days. This is associated with increased expression of proliferative mRNA and develops before insulin resistance can be detected (Stamateris et al. 2013). Increased β cell mass and proliferation following HFD is maintained at 8 weeks (Peyot et al. 2010) and is associated with increased insulin mRNA levels and hormone secretion from isolated islets (Ahren et al. 1997). Mechanistic details are understood about the nature of β cell dysfunction including altered dispersion of $[Ca^{2+}]_i$ signalling contributing to reduced vesicle fusion (Collins et al. 2010), increased oxidative stress (Zhang 2006), β cell dedifferentiation (Guo et al. 2013), altered gap junction signalling and reduced β cell coordination (Carvalho et al. 2012), decreased GLP-1R function and loss of incretin mediated amplification of insulin secretion (Hodson et al. 2013, Rajan et al. 2015) and increased β cell apoptosis (Jurgens et al. 2011).

In contrast to our understanding of the β cell, less is known about α cell function/dysfunction in pre-diabetes and diabetes. There is evidence to suggest that

changes intrinsic to the α cell drive hyperglucagonaemia in T2D and prediabetes (Zhang et al. 2013). When islets are isolated from HFD or obese mice (and therefore independent of external influences), glucagon secretion is increased at elevated glucose concentrations relative to controls (Santos-Silva et al. 2015, Dusaulcy et al. 2016). Changes that may be driving altered α cell function include morphological changes (α cell hypertrophy, increased apoptosis and decreased proliferation), insulin resistance, and changes in $[Ca^{2+}]_i$ signalling (Olofsson et al. 2004, Zhang et al. 2013, Merino et al. 2015, Dusaulcy et al. 2016).

The earlier studies provide valuable clues to the nature of α cell dysfunction in HFD and prediabetes. However, each only partially address changes in α cell physiology. Zhang *et al.* (2013) used human islets from non-diabetic and T2D donors to study secretion but due to the limited availability of human islets from T2D donors, the sample size was low (10 donors) and the effects variable, with some islet preparations being essentially normal but with 50% of the preparations showing an inverted response to high glucose (stimulation rather than inhibition of glucagon secretion). Dusaulcy *et al.* (2016) looked exclusively at gene expression in HFD fed mouse islet cells, and did not conduct any functional characterisation of α cells. Olofsson *et al.* (2004) used *ex vivo* high fat incubations of mouse islets at supraphysiological conncentrations (0.5-1 mM oleate or palmitate); although this is a useful tool for investigating changes in α cell function, it fails to recapitulate the dynamic whole-body physiological changes that will occur as a result of obesity. Furthermore, palmitate is toxic at mM concentrations (Moffitt et al. 2005). The most extensive of the above studies (Merino et al. 2015) functionally characterised α cells following

HFD with secretion studies and patch clamp electrophysiology. However, due to the low-throughput nature of patch clamp membrane capacitance measurements (that reflect exocytosis), the authors only achieved an n number of 6-7 cells and were unable to assess exocytosis in different glucose conditions. As a result, there are fundamental gaps in our understanding of α cell function in pre-diabetes. For example, are changes intrinsic to the islet contributing to diabetic hyperglucagonaemia, and how do changes in islet/α cell physiology relate to whole-body hormonal control of plasma glucose concentration?

This chapter describes an interrogation of α cell function *ex vivo* following HFD with the aim to understand whether perturbations in glucagon physiology seen *in vivo* are observed *ex vivo* and the mechanistic cause(s) of these changes.

5.2 Results

5.2.1 HFD feeding increases α cell glucagon output in response to glucose

First, islet area and relative hormonal staining was investigated (**Figure 5.1**). Islet area (μm^2) was not affected by HFD feeding (**Figure 5.1b**). However, although islets from CTL mice were normally distributed in terms of their size (Shapiro-Wilk test, W=0.95, p=0.25), islets from HFD fed mice were not normally distributed (W=0.84, p=0.0024, Figure **Figure 5.1**c). Despite this, the distributions are not different by Chi-squared (p=0.86). Median islet size was 47.5 and 50.5 μm^2 for CTL and HFD islets respectively.

The fraction (%) insulin-positive β cells, glucagon-positive α cells and somatostatin-positive δ cells was not different between HFD and CTL islets (**Figure 5.1a**).

Next, secretory output from isolated islets was assessed. HFD islets showed 3.2 times more glucagon secretion (pg/islet/h) compared to CTL islets at 6 mM glucose (**Figure 5.2**a). Glucagon secretion relative to glucagon content was elevated in HFD mice at 6 mM but this did not reach significance (**Figure 5.2c**). Glucagon content was not different between the groups (**Figure 5.2b, e**). If the individual replicates were considered, rather than the animal averages, glucagon secretion was elevated at 6 mM glucose when represented as pg/islet/h and as % content (**Figure 5.2d** and **f**) but decreased at 15 mM glucose (when represented as % of content, **Figure 5.2f**).

Insulin secretion (pg/islet/h) was elevated in HFD islets at 15 mM glucose (individual replicates, **Figure 5.3d**), as was content. When calculated as a % of content, insulin secretion was reduced in HFD islets compared to CTL at 1 mM glucose (individual

replicates, **Figure 5.2f**). Insulin secretion at 6 mM glucose was not significantly different between HFD and CTL.

Glucagon secretion in the perfused pancreas was increased 100% in HFD mice at 1 mM glucose but was not different at 6 mM (**Figure 5.4**).

5.2.2 $[Ca^{2+}]_i$ responses

In order to understand the driving factors behind the increased α cell output observed, $[Ca^{2+}]_i$ in isolated islets was monitored (**Figure 5.5**). The % of active α cells was higher in HFD mice (main effect), and the effect was statistically significant at 15 mM glucose (10% more cells active in HFD, **Figure 5.5a**).

In HFD fed mice α cells, the $[Ca^{2+}]_i$ oscillation frequency was significantly higher than that found in CTL cells at 6 and 15 but not 1 mM glucose (**Figure 5.5d**). In both HFD and CTL mice, $[Ca^{2+}]_i$ oscillation frequency was maximal at 1 mM glucose and was significantly reduced at 6 and 15 mM glucose (**Figure 5.5d**). The frequency of $[Ca^{2+}]_i$ oscillations was also elevated at 6 mM and 15 mM glucose as a result of HFD when the recording average (rather than the individual cell) was considered as a statistical unit (**Figure 5.5f**).

Mean spike amplitude at 6 and 15 mM glucose (relative to amplitude at 1 mM glucose for each cell) was elevated as an overall result of the diet (main effect) but not significantly at any given glucose concentration (**Figure 5.5e**). Spike amplitude was not changed in either CTL or HFD mice in response to any glucose concentration. **Figure 5.5g** demonstrates waveform average (at 6 mM glucose relative to that at 1 mM) in a selection of CTL and HFD recordings.

5.2.3 Causes of increased $[Ca^{2+}]_i$ activity

α cells are under strong paracrine regulation from neighbouring β cells (Ostenson 1979) and δ cells (Starke et al. 1987, Strowski et al. 2000). In light of altered glucagon output and $[Ca^{2+}]_i$ activity *ex vivo*, the possibility that a change in paracrine signalling could be driving increased α cell activity and output was investigated. Exogenous insulin (100 nM) did not affect oscillation frequency in either HFD or CTL mice at 1 mM glucose (**Figure 5.6a**). Likewise, $[Ca^{2+}]_i$ activity was unaffected in either group by inhibiting insulin signalling using S961, an antagonist of the insulin receptor (**Figure 5.6b**). In rat L6-hIR cells which overexpress the IR, S961 has a narrow range of specificity. S961 is antagonistic of insulin above 10 nM, but agonistic in the 1-10 nM range (Knudsen et al. 2012). The 10 uM concentration used is well within the antagonistic range of s961, and together with insulin secretion data (**Figure 5.3**), this establishes that α cell dysfunction in HFD is unlikely to be due to aberrant insulin signalling.

Next, the role of SST was assessed. CYN-154806 (100 nM), an antagonist of the SSTR2 receptor, increased α cell oscillation frequency by roughly 50% in CTL but not HFD islets (**Figure 5.6c,d**). In order to establish whether this was due to reduced SST secretion and/or reduced sensitivity to SST, SST sensitivity was investigated (**Figure 5.7**). Oscillation frequency was significantly inhibited by SST in both CTL and HFD fed mice (**Figure 5.7a**). However, CTL α cells were significantly more sensitive to SST than HFD; application of 1 nM SST reduced frequency by 0.67 spikes/min in CTL islets, but had no effect in HFD islets. Overall, inhibition was significantly greater in CTL

compared to HFD islets, achieving 88% inhibition by 10 nM SST compared to 57% in HFD islets (**Figure 5.7a**).

At 1 mM glucose, glucagon secretion was significantly reduced by 25 pM SST in CTL and HFD islets (**Figure 5.7b**). In the perfused pancreas, the IC_{50} for inhibition of glucagon secretion at 1 mM glucose by SST was 21 pM in WT chow fed mice (**Figure 5.7d**). This concentration was used to investigate SST sensitivity in the perfused pancreas of HFD and CTL fed mice. Although 25 pM SST inhibited glucagon secretion in CTL mice, it had no effect in HFD (**Figure 5.7e**). SST concentration from pancreas perfusate was measured and although no significant differences were seen, preliminary results suggest that SST secretion may be lower in HFD fed mice (n=5 CTL and 4 HFD animals, **Figure 5.7f**).

Finally, the secretion of SST from HFD islets was also quantified in isolated islets. SST release was reduced by >65% in HFD islets at 1 mM glucose (**Figure 5.8a-b**), content was not different between the groups (**Figure 5.8c**).

5.3 Discussion

5.3.1 Summary of results

The results of this chapter demonstrate clear perturbations in α cell function following HFD. Glucagon secretion was increased from both the *in situ* perfused pancreas and isolated islets. This indicates that α cell dysfunction is maintained even when islets are isolated and are therefore free from any extrinsic changes in whole body physiology that may result from the HFD. $[Ca^{2+}]_i$ imaging demonstrated that increased glucagon secretion may occur as a result of increased α cell $[Ca^{2+}]_i$ oscillation frequency following HFD.

In investigating the underlying causes for perturbed α cell function, we identified severe alterations in SST signalling. Using a combination of *in situ* perfused pancreas, secretion and $[Ca^{2+}]_i$ imaging, alterations in both SST secretion and sensitivity in the α cell were identified. Here, we discuss why, and the mechanisms by which, these changes may be occurring.

5.3.2 α cell function is altered intrinsically

Even after isolation, α cell activity remains altered with increased $[Ca^{2+}]_i$ oscillation frequency. This indicates that independent of wider physiological changes, intrinsic changes to the islet are (at least in part) responsible for increased α cell activity. Altered feedback from the liver-α-cell axis has been proposed to explain the increased output of glucagon in obesity. According to this concept, impaired liver function and hepatic insulin resistance in HFD result in elevated plasma amino acid levels. Plasma amino acids stimulate α cells therefore resulting in increased plasma

glucagon concentration (Albrechtsen et al. 2018, Albrechtsen et al. 2019). Although this could explain the changes in glucagon output seen *in vivo*, we demonstrate through $[Ca^{2+}]_i$ and secretion experiments in isolated islets that α cell dysfunction is maintained *ex vivo*, and in the absence of any effect of plasma amino acids. These intrinsic changes, observed in isolated islets, appear to be independent of any systemic factors that could alter α cell function; candidates include FAs and glucocorticoids. 11β-hydroxysteroid dehydrogenase type 1 (11BHSD1), the hormone responsible for converting cortisone to cortisol, is upregulated in adipose tissue (particularly in obesity (Paulsen et al. 2007)). Glucocorticoids have been implicated in both α and β cell function (Wise et al. 1973, Beaudry et al. 2013, Oh et al. 2018).

Elevated insulin secretion is a well established feature of HFD (Collins et al. 2010, Gonzalez et al. 2013). However, we did not see consistent differences in insulin secretion across the glucose conditions tested, including at high glucose where oxidative phosphorylation takes place and hyperinsulinemia in is most well described. More glucose concentrations, in particular 3 mM glucose, could be used to investigate whether insulin secretion is altered under basal conditions – above the maximal inhibition achieved at 1 mM glucose, but below concentrations were substantial oxidative phosphorylation begins to occur.

Importantly, although $[Ca^{2+}]_i$ oscillation frequency *and* glucagon secretion are elevated at 6 mM glucose, insulin secretion is not decreased under this condition. Previously, 15-week HFD has been shown to have no effect on insulin secretion at 5 mM glucose (Collins et al. 2010). This, together with the observation that

hyperglucagonaemia occurs *in vivo* in the absence of hypoinsulinaemia (**Figure 4.6**), indicates that hyperglucagonaemia does not occur as a result of reduced paracrine inhibition from β cells. As we did not see any changes in islet size or relative protein staining, the increase in α cell output must relate to a change in *function* rather than simply an increased number of α cells.

In diabetic mice, morphological changes in islet architecture that result from hyperglycaemia can be normalised by 4 weeks of insulin treatment (Brereton et al. 2014). This suggests that islet cells are able to recover although there may be a delay in this recovery. Here, measurements were made from isolated islets within 36h. Extended incubation could, potentially, return α cell function to normal. Therefore, although α cell changes appear intrinsic, they may rely on a sustained peripheral stimulus to be maintained.

Increased $[Ca^{2+}]_i$ oscillation frequency in α cells has been observed in the ob/ob model of obesity (α cells identified by activity at low glucose; see Santos-Silva *et al.* (2015)). Associating features of α cell function with HFD induced changes remains a challenge, particularly when comparing data across individual studies because the methods for assessing α cell function differ considerably.

Throughout these experiments, we consistently demonstrate that α cell activity and glucagon secretion are elevated following HFD. However, although the secretion experiments demonstrate the greatest difference between CTL and HFD islets at 6 mM glucose, in the prefusion data we see the greatest difference at 1 mM glucose. Isolated islets differ from the perfused pancreas in that they have disrupted

vasculature, and loss of directionality of blood flow – secretion of SST cannot flow directly downstream to adjacent α cells as it would in the perfused pancreas, therefore the strength of inhibition may be lost. On the converse, secretory products may build up in the secretion solution during experiments with isolated islets, this could lead to receptor inactivation. The isolation process is likely to be damaging to α cells located on the periphery of mouse islets, limiting secretory capacity at low glucose. Ultimately, isolated islets serve here to verify Ca^{2+}_i imaging data used as an indicator of α cell activity. The secretion data maps well to the differences in $[Ca^{2+}]_i$ oscillation frequency seen between HFD and CTL islets. This suggests that $[Ca^{2+}]_i$ oscillation frequency is a suitable proxy for glucagon secretion in response to glucose in isolated islets.

5.3.3 Paracrine changes may drive altered α cell function

In light of the observed islet-centric changes, we investigated paracrine signalling in HFD. Antagonizing SST inhibition of α cells using the SSTR2 antagonist CYN-154806 had less of an effect in HFD islets compared to CTL. We reasoned that two main changes to SST signalling could underlie this observation; first, reduced amount of local SST to antagonise (due to reduced δ cell function/SST secretion); second, reduced SSTR2 function in the α cell (due to reduced receptor expression, increased receptor internalisation, the presence of inactivating posttranslational modifications, or absence of downstream SSTR2 signalling pathways).

In order to understand why CYN-154806 sensitivity might be reduced we looked directly at SST sensitivity which was decreased in HFD. In human diabetic islets, α cells

have been shown to be insensitive to SST inhibition of exocytosis compared to islets from nondiabetic donors (Hmeadi et al. 2019). Although islets from HFD mice demonstrated a clear reduction in SST sensitivity, the authors also found that the secretory capacity of α cells was reduced in T2D due to reduced granule priming. Merino *et al.* (2015) observed reduced membrane capacitance (reflecting reduced exocytosis) in HFD α cells indicating that HFD does intrinsically change α cell function. The increase in $[Ca^{2+}]_i$ we observed (also reported by Santos-Silva *et al.* (2015)) following HFD could be a compensatory mechanism to overcome reduced granule docking and secretory output.

Function of the SSTR2 receptor can be regulated via numerous mechanisms. In pituitary adenomas, expression of the β-arrestin 1 scaffold protein influences SSTR2 desensitisation and internalisation. Following endocytosis of SSTR2, rate of recycling to the membrane can be increased by SST14 analogues (Nagel et al. 2010). Analogously, a change in the rate of receptor endocytosis and recycling in α cells could be affecting SSTR2 function.

In addition to a clear reduction in SST sensitivity, alterations in δ cell physiology in prediabetes have recently been described (Drigo et al. 2019). Islets from HFD fed mice display reduced $[Ca^{2+}]_i$ oscillation amplitude, increased proportion of unresponsive cells and increased proportion of cells spiking “slowly”.

Very little is known about what may be causing δ cell dysfunction in HFD but 72h exposure to FAs, albeit at supraphysiological concentrations (0.5 mM oleate or palmitate) at 15 mM glucose reduces SST secretion (Collins et al. 2008). Likewise,

glucose stimulated SST secretion is reduced during perfused pancreas experiments in Goto-Kakizaki non-obese-hyperglycaemic rats compared to normoglycaemic controls (Abdelhalim et al. 1993). Reduction of SST secretion in the presence of FA may be a result of δ cell inhibition by the NEFA-responsive G-protein FFAR4 (GPR120) agonists, which inhibit glucose induced SST secretion (Stone et al. 2014).

These data indicate that both α and δ cells are intrinsically altered as a result of HFD with δ cell function being sensitive to both high fat and hyperglycaemia. Reduced δ cell output in addition to decreased α cell sensitivity to SST may lead to hyperactivation of α cells, and this (by mechanisms that remain to be elucidated) culminates in the α cell dysfunction observed in prediabetes.

5.3.4 Altered metabolism as a driver for changed α cell function

We have clearly identified that altered SST signalling contributes to α cell dysfunction in HFD. However, we are also interested in whether changes in α cell metabolism contribute to dysfunction in T2D. At low glucose concentrations, metabolism of fat in α cells provides a large proportion of the energy for glucagon secretion (Briant et al. 2018). Considering that HFD increases total serum FA (Liu et al. 2013), and FAs stimulate glucagon secretion (Olofsson et al. 2004), we are interested in whether increased metabolism of fat could explain some of the observed changes in α cell function. In the next chapter, we use a combination of pharmacological tools and genetic models to alter fat metabolism, and we investigate how this influences α cell function in HFD conditions.

Figure 5.1

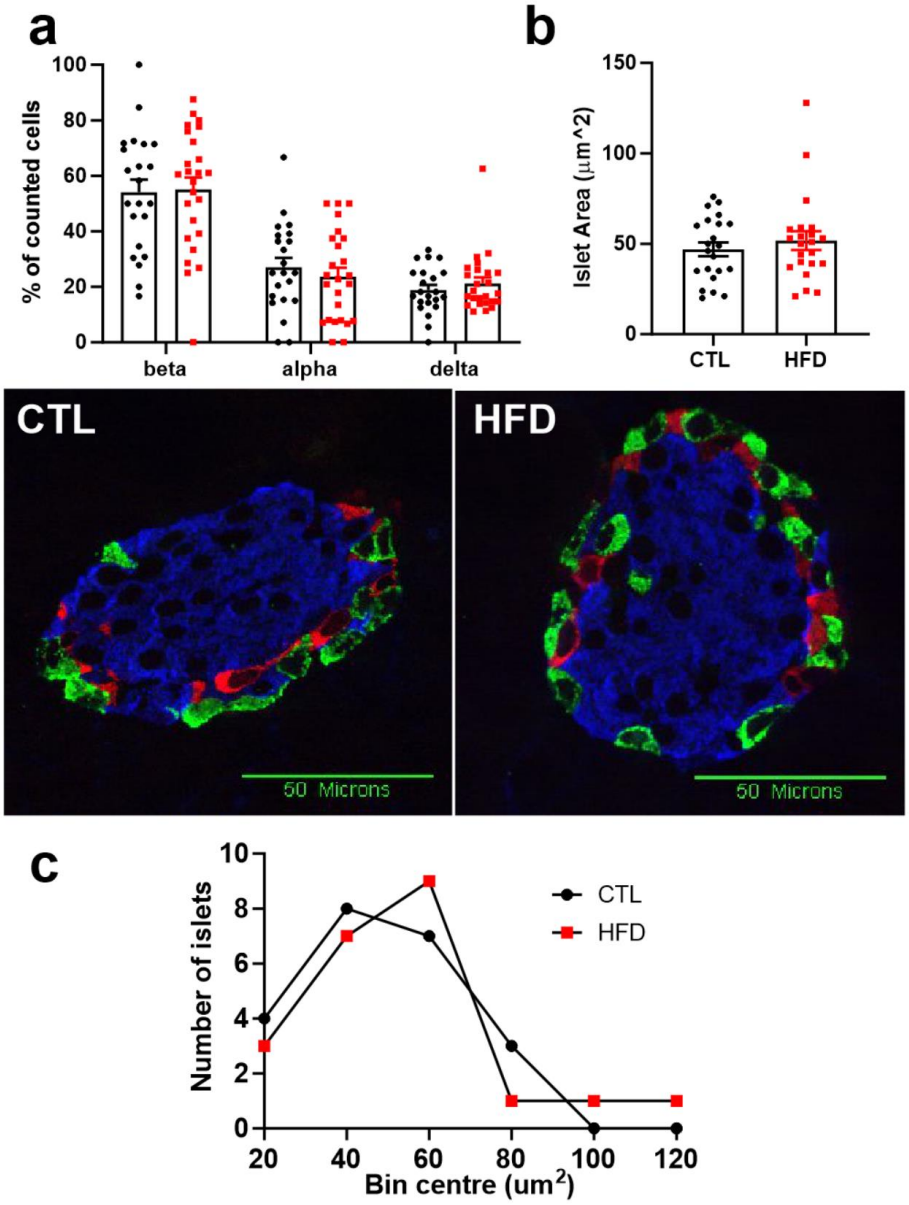

Figure 5.1 *Morphology in islets from CTL (black) vs. HFD (red) mice.* ***a,*** *insulin (beta), glucagon (alpha), and somatostatin (delta) staining (% of counted cells, p>0.05, two-way ANOVA column effect).* ***b,*** *islet area (AU, n=22 islets from 3 mice each, t-test). Middle, example CTL and HFD images (GCG – green, SST – red, INS – blue).* ***c****, Size distribution of islets pooled into bins of 20 µm², n=22 islets from both groups.*

Figure 5.2

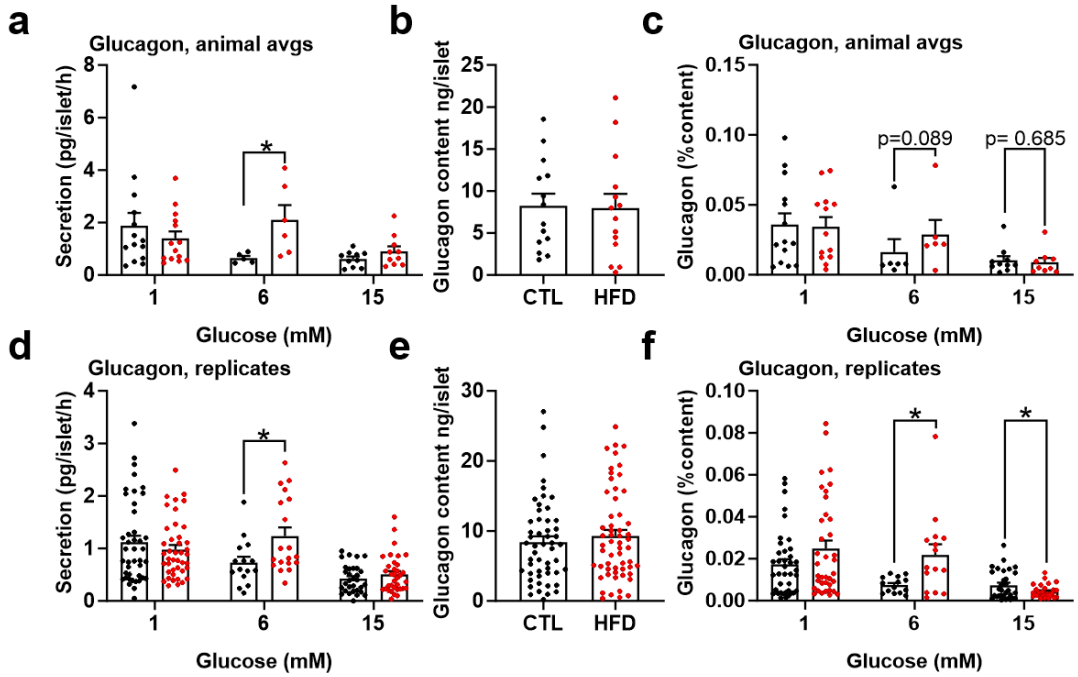

Figure 5.2 *Hormone secretion from CTL (black) and HFD (red) islets.* ***a****, Animal averages of glucagon secretion (pg/islet/h, n=6-14 mice, multiple t-tests).* ***b,*** *Animal averages of glucagon content (n=14 mice, t-test).* ***c,*** *Animal averages of glucagon secretion as a % of content (n= 6-14 mice, multiple t-tests).* ***d,*** *Individual measurement values for glucagon secretion (pg/islet/h, n=52-57 mice, multiple t-tests).* ***e,*** *Individual measurements of glucagon content (n=52-57 measurements from 14 mice).* ***f,*** *Individual measurements of glucagon secretion as a % of content (n= 14-39 measurements from 14 mice, multiple t-tests). *=p<0.05*

Figure 5.3

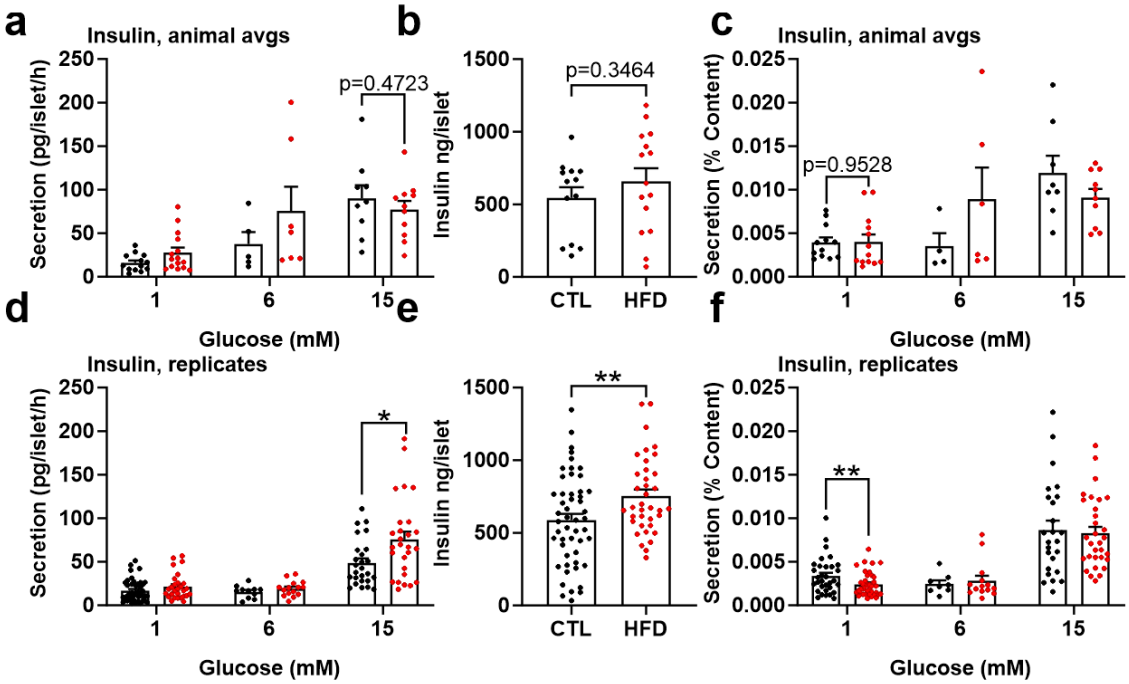

Figure 5.3a, *Animal averages of insulin secretion (pg/islet/h, n=5-15 mice, multiple t-tests).* ***b****, Animal averages of insulin content (pg/islet, n= 13-15 mice, t-test).* ***c,*** *Individual insulin secretion (% content) measurements (n=8-14 measurements from 4-6 mice, multiple t-tests).* ***d,*** *Individual measurement values for insulin secretion (pg/islet/h, n=13-51 measurements from 5-15 mice, multiple t-tests).* ***e,*** *Individual insulin content measurements (n=37-51 measurements from 13-15 mice, t-test).* ***f,*** *Individual insulin secretion (% content) measurements (n=8-14 measurements from 4-6 mice, multiple t-tests). *=p<0.05, **=p<0.01*

Figure 5.4

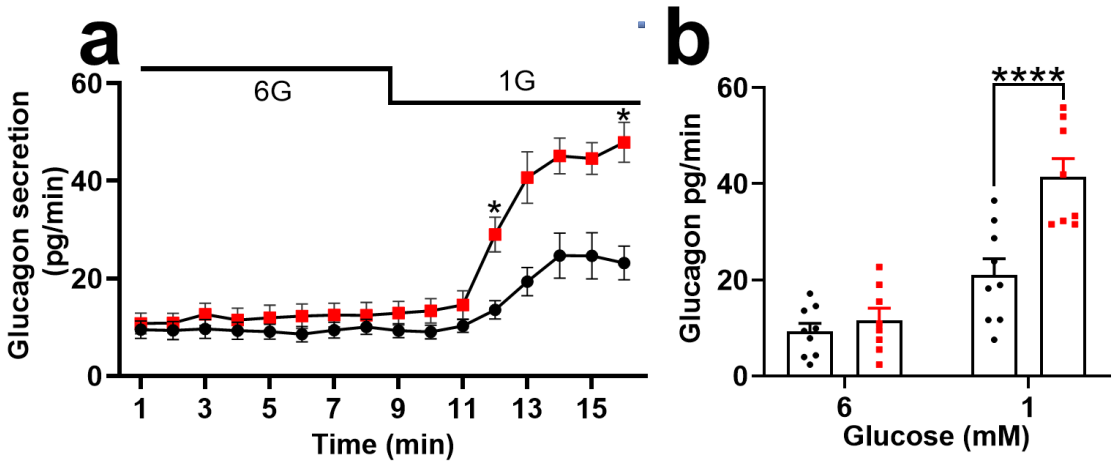

Figure 5.4 *All results described CTL vs. HFD (black and red respectively).* ***a****, Glucagon secretion from in situ perfused pancreas experiments (mixed effects analysis with Sidak's multiple comparisons test).* ***b,*** *Average glucagon secretion from perfused pancreas. The effect of glucose was significant in both HFD and CTL mice (average from first and last 5 time points, two-way ANOVA followed by Sidak's multiple comparison's test). n=9 CTL and 8 HFD mice, *p<0.05, ****=p<0.0001*

Figure 5.5

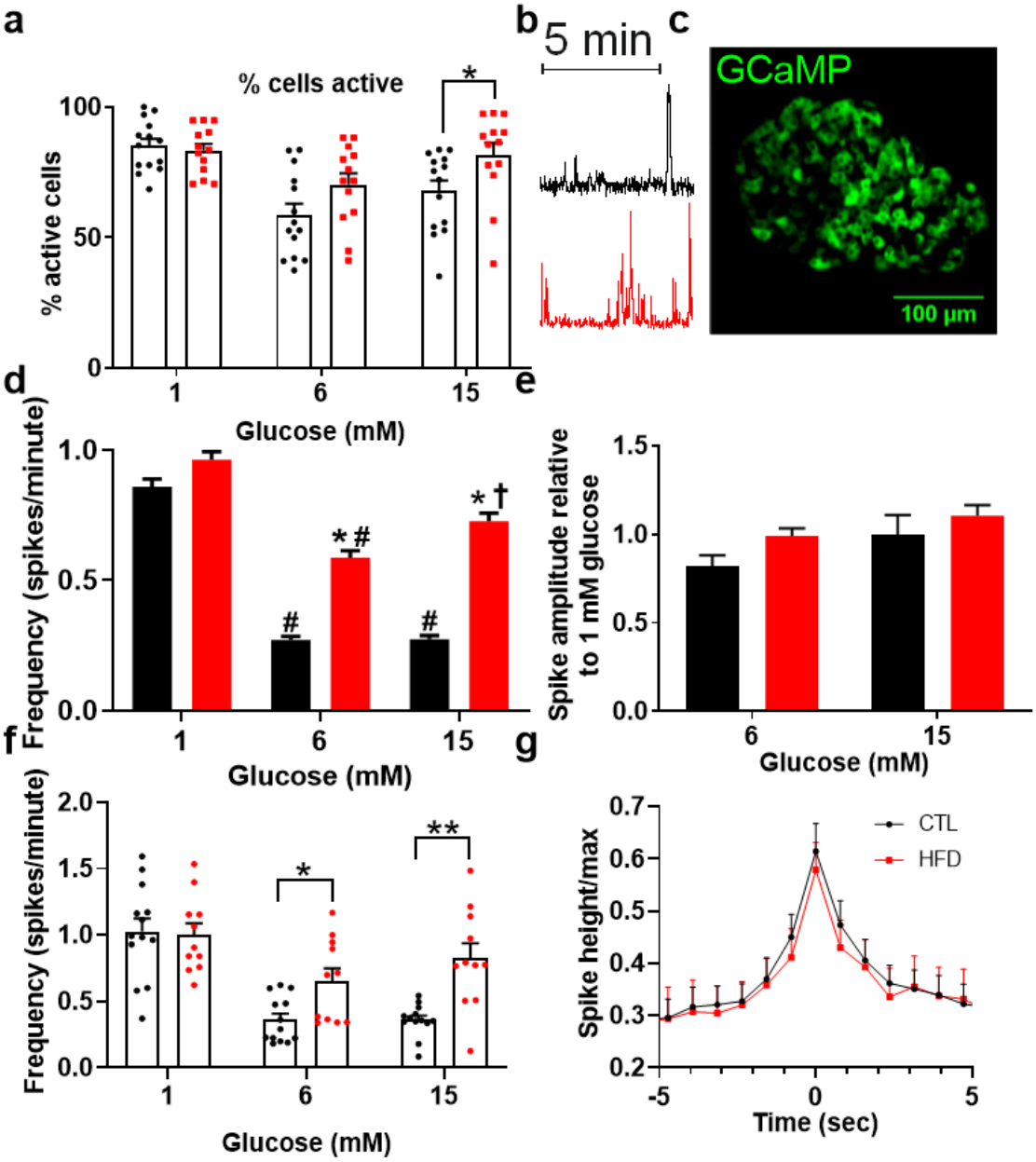

Figure 5.5 *Ca^{2+}_i activity in whole islets isolated from CTL (black) and HFD (red) mice.* ***a****, % cells active at 1, 6, and 15 mM glucose (n=14 recordings from 6-7 mice, *p<0.05, two-way ANOVA with Sidak's multiple comparisons test).* ***b****, Example imaging trace at 6 mM glucose.* ***c,*** *example islet image.* ***d,*** *Mean oscillation frequency at 1, 6 and 15 mM glucose in islets from CTL and HFD mice (n=508-561 cells from 13, recordings, 6-7 mice. * refers to p<0.0001 HFD* vs. *CTL, # refers to p<0.0001 within diet relative to 1 mM glucose, † refers to p<0.0001 within diet relative to 6 mM glucose, two-way ANOVA with Tukey's multiple comparisons test).* ***e,*** *Mean spike amplitude relative to amplitude at 1 mM glucose (n=31-71 cells, p>0.05, two-way ANOVA with Tukey's multiple comparisons test).* ***f****, Recording averages of Ca^{2+}_i oscillation frequency (n=13 recordings from 6-7 mice, *p<0.05, **p<0.01, two-way ANOVA with Sidak's multiple comparisons test).* ***g****, Waveform average at 6 mM glucose (n=average of 13 recordings, two-way ANOVA).*

Figure 5.6

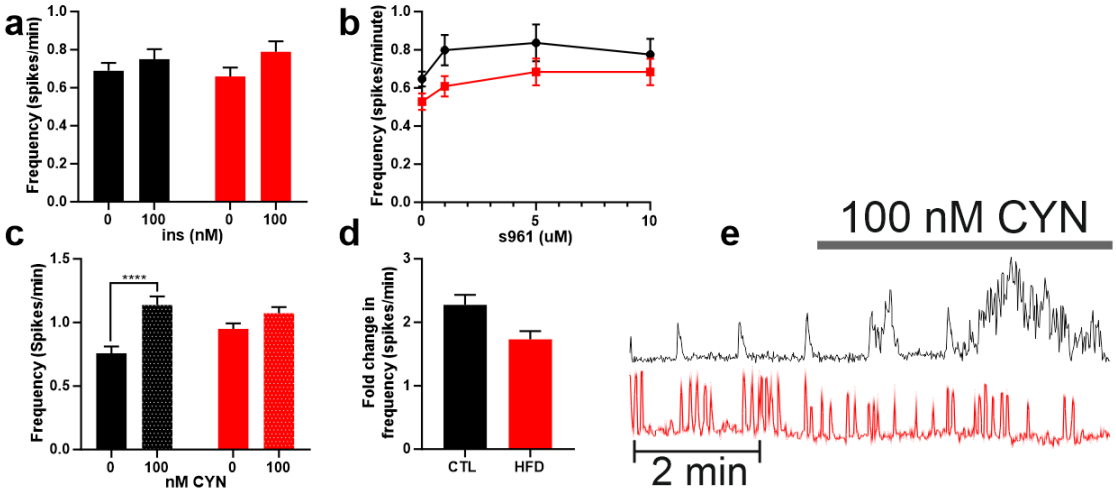

Figure 5.6 *Interrogation of paracrine signalling in HFD (red) and CTL (black) islets.* ***a****, $[Ca^{2+}]_i$ oscillation frequency upon application of 100 nM insulin at 1 mM glucose (n=100-105 cells, 5 recordings, 3 mice, two-way ANOVA with Sidak's multiple comparisons test).* ***b****, $[Ca^{2+}]_i$ oscillation frequency during application of s961 1, 5, 10 µM (n=88-125 cells, 4-5 recordings from 2 mice, two-way ANOVA with Sidak's multiple comparisons test).* ***c,*** *$[Ca^{2+}]_i$ oscillation frequency during application of 100 nM CYN at 6 mM glucose (n=220-224 cells, 9-10 recordings from 4-5 mice, ****p<0.0001, two-way ANOVA with Sidak's multiple comparisons test).* ***d,*** *Example trace showing calcium activity upon application of CYN-154806 at 6 mM glucose in CTL (black) and HFD (red) α cells.*

Figure 5.7

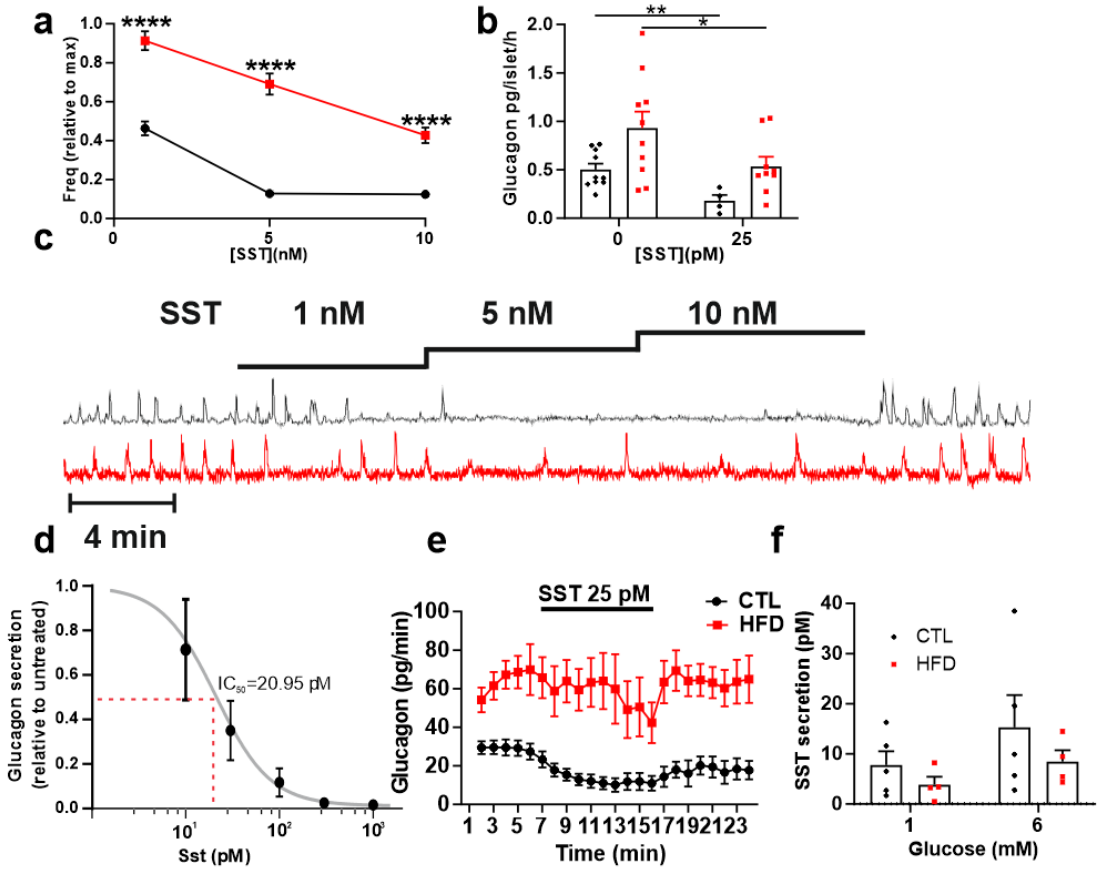

Figure 5.7 *Interrogation of SST signalling in HFD (red) and CTL (black) islets.* ***a****, Oscillation frequency at 1 mM glucose showing α cell response to inhibition by application of SST at 1, 5 and 10 nM (n= 192-233 cells, 10 recordings, 3-5 mice, two-way ANOVA with Sidak's multiple comparisons test).* ***b****, Glucagon secretion in the presence of 25 pM SST (pg/islet/h, n=4-10 individual measurements from 3 CTL and 3 HFD mice, individual t-tests).* ***c,*** *Example trace showing* $[Ca^{2+}]_i$ *oscillation frequency during application of SST.* ***d,*** *Concentration response of glucagon secretion in the perfused pancreas upon inhibition by SST (n=4-5 mice).* ***e****, Glucagon secretion from the perfused pancreas at 1 mM glucose and during application of 25 pM SST. glucagon secretion was significantly inhibited by SST in CTL (p=0.0155) but not HFD mice (n= 5 CTL and 5 HFD mice).* ***f****, Average of SST secretion during perfusion (n=4-5 mice, p>0.05 for both the effect of glucose and HFD vs. CTL, two-way ANOVA with Sidak's multiple comparisons test). *p<0.05, **p<0.01,****p<0.0001*

Figure 5.8

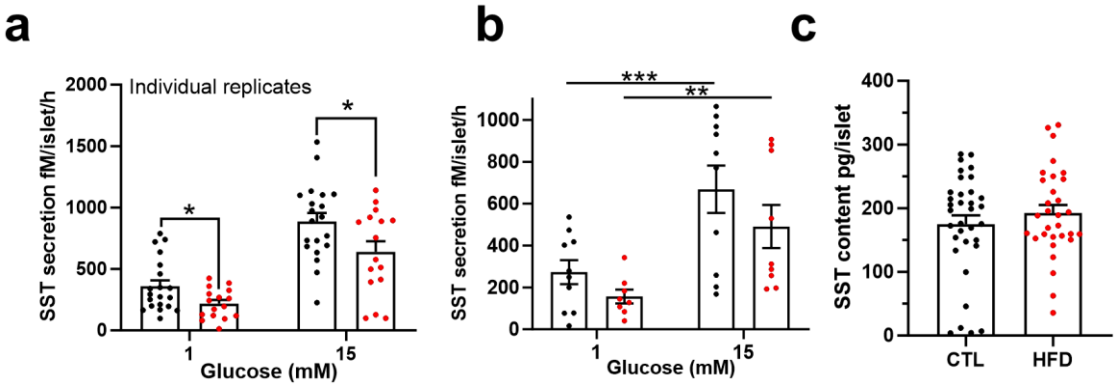

Figure 5.8 *SST secretion from CTL (black) and HFD (red) islets.* ***a****, Secretion of SST from isolated islets (fM/islet/h) in response to 1 and 15 mM glucose (n=20 individual replicates from 10 mice, p<0.0001 for effect of glucose in both HFD and CTL mice, p<0.05 for difference between HFD and CTL at 1 and 15 mM glucose, two-way ANOVA with Sidak's multiple comparisons test).* ***b****, SST secretion (fM/islet/h) animal averages (lines indicate effect of glucose within diet **p<0.01, ***p<0.001, SST secretion was not different between groups at either glucose concentration, two-way ANOVA with Sidak's multiple comparisons test).* ***c****, Islet SST content (pg/islet, n=31-14 measurements from 10 mice, t-test).*

Chapter 6

6. High fat feeding in α-CPT1α-KO mice

6.1 Introduction

At low glucose concentrations, paracrine input from neighbouring β or δ cells is absent due to their inactivity. Therefore, under these conditions control, of α cell function is regarded as intrinsic (Vieira et al. 2007, Zhang et al. 2013). Although α cells sense and respond to extracellular glucose levels, they also express proteins involved in fatty acid metabolism such as Carnitine palmitoyltransferase-1a (CPT1a) (DiGruccio et al. 2016, Briant et al. 2018). At low glucose concentrations α cells rely on energy production from alternate substrates such as fatty acids to drive glucagon secretion (Briant et al. 2018). It is clear that high levels of fatty acids can stimulate glucagon secretion (Bollheimer et al. 2004, Olofsson et al. 2004, Collins et al. 2008) possibly via GPCR signalling (Kristinsson et al. 2017) and increased β-oxidation (Hong et al. 2007, Briant et al. 2018).

CPT1a is a key regulator of fatty acid oxidation. The enzyme converts activated long-chain fatty acids (Acyl –CoAs) to Acyl-carnitines allowing long chain fatty acids to be transported in to the mitochondria for use in β-oxidation (Kim et al. 2000, Stephens et al. 2007). In α cells, loss of CPT1a causes a 40% reduction in glucagon secretion at 1 mM glucose, suggesting that β-oxidation is important in α cell function (**Figure 6.1**) (Briant et al. 2018). Importantly, plasma NEFA are elevated during prolonged fasting (Owen et al. 1990), a condition where secretion of glucagon at low blood glucose is essential in maintaining normoglycaemia. Fatty acid metabolism may

therefore represent an essential energy source under prolonged conditions of low glucose.

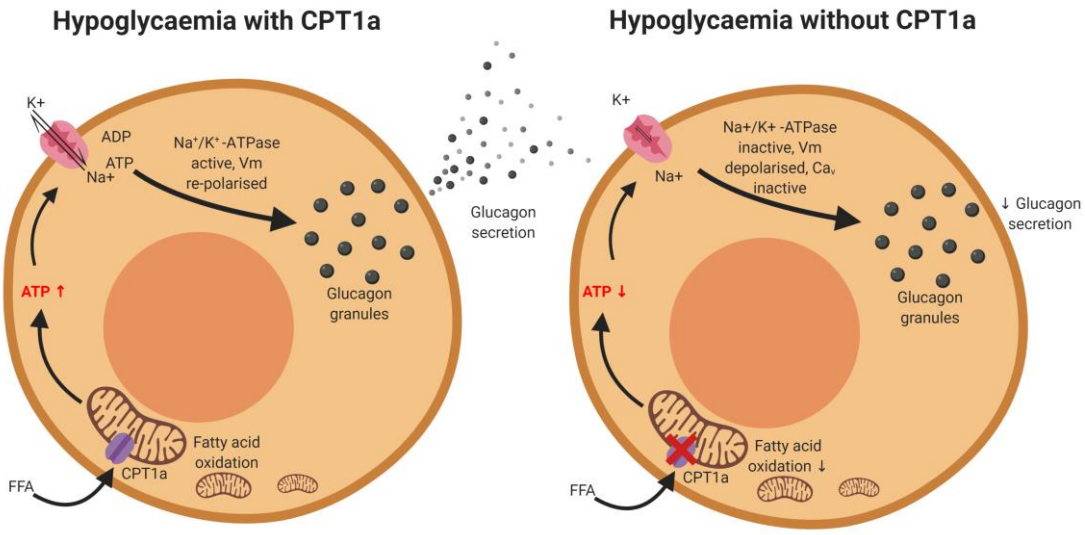

Figure 6.1 *Schematic demonstrating the role of CPT1a in fat metabolism in the α cell for glucagon secretion at low glucose concentrations and the effect of inhibition of this (either by application of etomoxir or genetic ablation) on glucagon secretion.*

In previous chapters, we have demonstrated that α cells have increased $[Ca^{2+}]_i$ oscillation frequency and glucagon secretion as a result of HFD feeding. While these effects may in part be due to changes in SST secretion and/or sensitivity, it is unclear what leads to these changes in sensitivity, and it is possible that other mechanisms contribute to α cell dysfunction.

In obese rats, circulating NEFA are elevated during the fed state (Liu et al. 2013), a phenomenon also observed in humans subjects whereby a modest increase in circulating NEFA is associated with higher fat mass in obesity (Karpe et al. 2011) and T2D (Reaven et al. 1988). Under normal conditions, insulin inhibits lipolysis causing a reduction in plasma NEFA levels when glucose concentrations are high (Carpentier

et al. 2005). However, insulin resistance in T2D causes a loss of this inhibition (Groop et al. 1989), which may contribute to elevated plasma NEFA.

Given the important role of fatty acid oxidation in α cells, it could be suggested that HFD induced obesity may result in elevated NEFA. Elevated NEFA may increase fatty acid oxidation, contributing to the increased α cell activity. To investigate this, we used a combination of genetic models (Briant et al. 2018) and pharmacological inhibition of fatty acid oxidation to interrogate whether increased CPT1a activity contributes to altered α cell function in the HFD fed animals.

6.2 Results

6.2.1 αCPT1a-KO mouse

In order to investigate whether increased β-oxidation contributes to α cell function and increased glucagon secretion in obesity, we fed female mice lacking CPT1a specifically in α cells "αCPT1a-KO" and littermate control mice "CON" a HFD to induce α cell dysfunction.

Both αCPT1a-KO and CON mice gained significant body weight (**Figure 6.2a**) after 12 and 20 weeks on the diet. There was no difference in weight between the cohorts at any time point.

At 12 weeks, there was no difference in fed resting plasma glucose, glucagon, or insulin concentration at 0900 am, 1300 pm or 1700 pm (**Figure 6.2h-j**). CON mice had significantly elevated plasma glucose during the 12 week GTT compared to αCPT1a-KO mice at the 30 min time point (p= 0.0105, **Figure 6.2b**). Both groups showed a significant decrease in plasma glucagon in response to the glucose bolus and there was no significant difference in plasma glucagon during the GTT between αCPT1a-KO and CON mice (**Figure 6.2c**). We carried out linear regression analysis of the relationship between glucose and glucagon at 0 and 30 minutes of the GTT. The gradient of this slope was greater in CTL mice (p=0.0208 **Figure 6.2d**). This indicates that at a given glucose concentration, αCPT1a-KO mice have a reduced plasma glucagon concentration relative to CONs.

As the αCPT1a-KO occurs in all proglucagon expressing cells including GLP-1 secreting enteroendocrine L-cells and cells within the hypothalamus, any whole

body effects may be mediated by altered function in these non α cells. Any difference in GLP-1 levels between αCPT1a-KO and CON mice would affect insulin and therefore glycaemia via the incretin effect. We wanted to establish whether increased GLP-1 secretion (as a result of loss of CPT1a function in the intestinal L-cells) was responsible for the protective effect seen in αCPT1a-KO mice during the 12 week GTT. Therefore the IPGTT protocol was repeated (by which time mice had been on the diet for 20 weeks), and plasma glucose, GLP-1 and insulin concentrations measured at 0 and 30 minutes after the glucose bolus. By 20 weeks, the effect of genotype on blood glucose during the GTT was lost (**Figure 6.2e**). Neither insulin nor GLP-1 were different between the genotypes at either 0 or 30 min, or as a result of the glucose bolus.

6.2.2 Isolated islets

Etomoxir was used to assess fat metabolism in α cells from GCaMP3 HFD and CTL fed mice. Etomoxir acts by binding irreversibly to the catalytic site of CPT1a (Rufer et al. 2009) therefore inhibiting fatty acid oxidation. If increased fatty acid oxidation (and downstream β-oxidation) in HFD fed animals is driving hyperglucagonaemia, application of etomoxir and inhibition of fatty acid oxidation would help to normalise α cell activity. α cell activity following application of (50 μM) etomoxir was measured (**Figure 6.3**). Etomoxir did not have a significant effect on $[Ca^{2+}]_i$ oscillation frequency at any glucose concentration in either CTL or HFD fed mice (**Figure 6.3a-c**). Oscillation amplitude at 6 mM glucose was not different between the groups (**Figure 6.3d**).

6.3 Discussion

6.3.1 Summary of results

αCPT1a-KO protects mice from the glucose intolerance seen in CON mice at 12 weeks. At 12 weeks, this did not appear to be due to a protective effect of αCPT1a-KO in reducing plasma glucagon levels. By 20 weeks of HFD feeding, αCPT1a-KO mice exhibit the same level of glucose intolerance as seen in CON mice, and they show no difference in glucagon, GLP-1 or insulin. Due to the inconsistency of the phenotype over time, we cannot confirm whether αCPT1a-KO exerts a protective effect against α cell dysfunction following 20 week HFD.

6.3.2 α cell independent mechanisms of αCPT1a-KO

We were surprised to observe a protection from glucose intolerance in αCPT1a-KO mice in the absence of a reduction in plasma glucagon level. This indicates that the protective effect seen in αCPT1a-KO may not be mediated by α cells but rather via other proglucagon expressing cells (including L-cells) that will also exhibit a potentially protective effect on αCPT1a-KO. Although no differences were seen in either GLP-1 or insulin at 20 weeks, the protective effect of αCPT1a-KO on glucose tolerance had also been lost by this time point.

In patients with T2D, GLP-1 secretion in response to an oral glucose tolerance test (OGTT) is defective (Wang et al. 2016). Dusaulcy (2016) demonstrates that within HFD fed mice, those with highest HbA1c exhibit L-cell dysfunction, whereas HFD fed mice with lower HbA1C had molecular adaptations in enteroendocrine L-cells permitting increased GLP-1 biosynthesis and release. Glp-1R$^{-/-}$ mice have elevated

plasma glucagon during an IPGTT (Ali et al. 2011). This indicates that an IPGTT is able to stimulate GLP-1 secretion even when glucose is not delivered orally. This important contribution of GLP-1 in controlling glycaemia during an IPGTT may be altered following HFD, an effect from which αCPT1a-KO mice may be protected at 12 weeks. In order to investigate this, GLP-1 and insulin would need to be reassessed in αCPT1a-KO mice following 12 week HFD. We would not expect substantial GLP-1 secretion following an IPGTT. Rather, an oral glucose tolerance test (OGTT) is used to stimulate GLP-1 secretion by activation of enteroendocrine L-cells (Meier et al. 2007). However, we were trying to investigate the cause of the difference between the HFD fed αCPT1a-KO and CON mice observed during the 12-week IPGTT. In order to fully characterise L-cell function, and stimulate substantial secretion of GLP-1, an OGTT would be most appropriate for interrogation of L-cell function.

6.3.3 Counterregulation of αCPT1a-KO

Pancreatic α cells also express the CPT1β homologue and CPT1c at the RNA level (Benner et al. 2014, DiGruccio et al. 2016). It has been suggested that in the absence of one, expression of the other may be upregulated (Kim et al. 2014). Although this has never been validated in islets, relative expression of CPT1a and CPT1b can shift in heart muscle depending on the metabolic/stress state (He et al. 2012). The αCPT1a-KO model has a loss of CPT1a protein in 85% of α cells, causing a significant (40% at 1 mM glucose) reduction in glucagon secretion relative to controls. In light of this, the model remains a robust model for interrogating α cell fatty acid oxidation in the α cell following HFD. However, further characterisation of

the model is needed to fully assess the role of altered fat metabolism in α cell function.

6.3.4 Etomoxir in the study of α cell $[Ca^{2+}]_i$ dynamics

Although etomoxir has been used to study $[Ca^{2+}]_i$ (Sekirov et al. 2010, Briant et al. 2018) and hormone secretion (Chen et al. 1994, Liu et al. 2003), etomoxir has been shown to induce severe oxidative stress, a process which alters intracellular calcium (O'Connor et al. 2018). Etomoxir can effectively block fatty acid oxidation at 10 µM, however, at 200 µM it has indirect effects on the electron transport chain (Yao et al. 2018). The toxic effects of etomoxir may be dependent upon the tissue in question, with individual cells being differently sensitive than an organ explant such as an islet. However, any effect of etomoxir at 50 µm (the concentration used) on CPT1a/FAO must be separated from other effects on the electron transport chain or effects on oxidative stress.

CPT1a is expressed roughly equally in α, β and δ cells at the RNA level (DiGruccio et al. 2016). Insulin secretion does not seem to be affected by etomoxir (Briant et al. 2018). However, any effect on α cell function may be mediated directly via an effect on α cells, or indirectly via an effect on δ cells and subsequent paracrine signalling. Nevertheless, etomoxir did not have an effect on α cell $[Ca^{2+}]_i$ in either CTL or HFD islets. This indicates that FAO, which should be inhibited at 50 µM etomoxir, is not more or less important for driving $[Ca^{2+}]_i$ oscillation in α cells from either diet.

In the future, incubation of WT and αCPT1-KO islets in elevated FFA could be used to interrogate whether WT islets are more able to switch fuel preference from glucose

following this high fat condition. Subsequent inhibition of fat metabolism by etomoxir may have less of an effect in αCPT1-KO islets compared to WT islets if WT islets have switched to increased fat metabolism following HFD incubation. This would provide an indication as to how easily α cells can alter their fuel preference, and the time frame over which this can occur.

In these *ex vivo* experiments, it was assumed that BSA in the media would provide sufficient FA for metabolism. However, the amount of FA available from the BSA may not be sufficient to maintain FAO in α cells (i.e. intracellular FA concentration is below the K_d for CPT1a). A cell fat storage is poorly characterised and may only be sufficient to fuel the α cell in the short-term. Lack of available FA may explain why inhibiting of CPT1a using etmoxir had a minimal effect. It is worth noting that this set-up (with FA provided in the bound form to BSA) has been used to demonstrate that etomoxir reduces ATP/ADP ratio and glucagon secretion in mouse islets and β oxidation in αTC1-6 cells (Briant et al. 2018) therefore suggesting that provision of BSA is sufficient to drive FAO in α cells. Nevertheless, supplementing the media with elevated FFA (for example at concentrations such as those used in Chapter 3 for the high fat incubation experiments) could be used to interrogate FAO in a setup where the availability of FA for metabolism is guaranteed.

6.3.5 Lipotoxicity in CPT1a KO

It is important to consider the secondary effects of reduced fat metabolism in CPT1a KO mice. The loss of CPT1 function may contribute to accumulation of FA, TAG and DAG in α cells. DAG and TAG accumulation is strongly associated with β cell

dysfunction and reduced insulin secretion (Kelpe et al. 2002, Sawatani et al. 2018). The effect of fat accumulation in α cells is poorly characterised; it is not known whether fat accumulation would result in the elevated glucagon secretion normally associated with the diabetic phenotype, or whether the impact might be similar to that seen in β cells and, in fact, reduce hormone secretion.

In the first instance, fat accumulation in α cells could be compared between CPT1a CTL and KO islets to establish whether reduced FAO increases fat storage. Further to this, fat accumulation can be induced by increasing expression of diacylglycerol acyltransferase (DGAT) using a viral vector (Kelpe et al. 2002). DGAT catalyses the last step of TAG synthesis, increasing TG content. This could be used to investigate the effect of TAG accumulation on α cell function.

6.3.6 Time sensitivity of αCPT1a-KO protection

Our first experimental timepoint in these experiments was 12 weeks. We demonstrate in previous chapters that metabolic changes occur within 6 weeks of HFD and that α cell function is markedly changed by 12 weeks. Furthermore, it is well characterised that islet function is changed within a few days of high fat feeding (Stamateris et al. 2013). Therefore, any protective effect of αCPT1a-KO on α cell function may already be lost by the first 12 week timepoint. Interrogating whole body physiology and α cell function in αCPT1-KO mice and islets at earlier timepoints may provide an indication as to whether αCPT1a-KO is transiently protective against the effect of HFD, and the mechanisms by which this may occur.

At 12 weeks of HFD, mean glucose in CON mice at 30 min of the GTT is 29 mM compared to 20 mM in αCPT1a-KO mice. By 20 weeks, blood glucose had decreased in CON mice (to 27 mM) and increased in HFD mice (to 26 mM). This indicates that it is not simply that αCPT1a-KO mice "caught up" with controls (i.e. a protective effect of αCPT1a-KO was lost at some point between 12 and 20 weeks) nor is it that the effect of the HFD on CON mice was transient, with a recovery from glucose intolerance by 20 weeks. Rather, both groups appear to have moved closer to each other in their averages. Time dependence and transience of metabolic phenotype during HFD have been reported before with the role of α cell plasticity specifically identified as a factor in the progression of the HFD phenotype – at 12 weeks female mice exhibit reduced α cell proliferation, increased apoptosis and reduced cell mass, by 24 weeks these parameters normalise relative to controls but hyperglycaemia developed as a result of β cell dysfunction (Merino et al. 2015). αCPT1a-KO could alter the kinetics of this transition where bye αCPT1a-KO mice take longer to develop metabolic dysfunction.

6.3.7 Future considerations

In order to further assess the role of CPT1a in development of α cell dysfunction, a number of parameters remain to be investigated. Firstly, we would need to confirm the protective effect of αCPT1a-KO during the 12-week HFD and whether this is due to altered GLP-1 levels. In order to thoroughly interrogate GLP-1, the OGTT remains the gold standard for stimulation of GLP-1 secretion. However, we are interested in altered α cell function, rather than altered L-cell function. Ideally, to isolate the effects of αCPT1a-KO on α cells, we would use an αCPT1a-KO line where L-cells are

unaffected (e.g. by using a tamoxifen-inducible Cre induced by tamoxifen injection into the pancreatic duct).

The preceding chapters have described in-depth characterisation of α cell function under normal, and high fat conditions (including high fat incubations and high fat diet). In order to identify pathway alterations that may underlie α cell dysfunction, we assessed RNA expression in α and non-α cells from HFD and CTL mice.

Figure 6.2

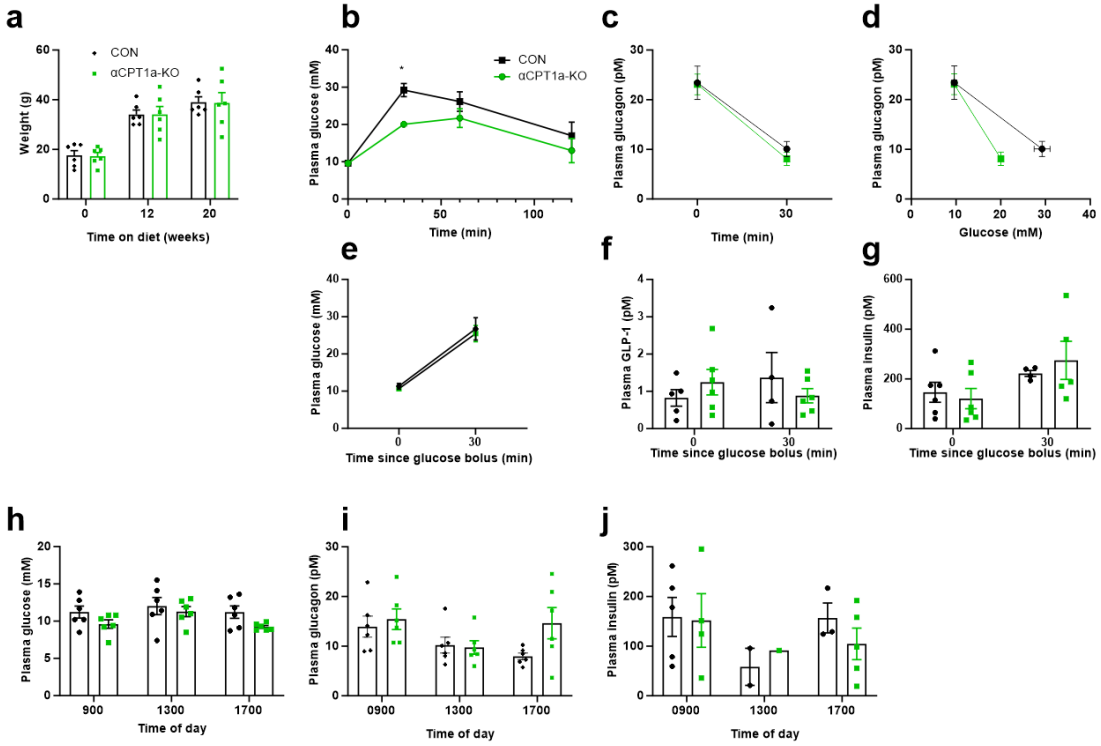

Figure 6.2 *High fat diet in CON (black) and αCPT1a-KO (green) female mice, n=6 mice per group.* ***a,*** *Weight gain following 12 and 20 weeks (two- way ANOVA with Sidak's multiple comparisons test).* ***b,*** *Plasma glucose (mM) during 12 week GTT (p=0.0105 at 30 min, two-way ANOVA followed by Sidak's multiple comparisons test).* ***c,*** *Plasma glucagon (pM) at 0 and 30 min of 12 week GTT (p>0.05 at all time-points, p<0.01 for effect of glucose in both genotypes).* ***d,*** *Linear regression of plasma glucagon:glucose concentration during 12 week GTT. CON vs HFD gradient was different between groups (p=0.0208), y-intercept was not (p=0.22).* ***e,*** *Plasma glucose during 0 and 30 min GTT at 20 weeks (p=0.0003 in CON and p=0.0004 in αCPT1a-KO mice for the effect of glucose, no effect of genotype, two-way ANOVA followed by Sidak's multiple comparisons test).* ***f,*** *GLP-1 at 0 and 30 min of 20 week GTT (p>0.05, for all comparisons, two-way ANOVA followed by Sidak's multiple comparisons test).* ***g,*** *Insulin (pM) at 0 and 30 min of week 20 GTT (p>0.05, for all comparisons, two-way ANOVA followed by Sidak's multiple comparisons test). Plasma glucose (**h**), glucagon (**i**) and insulin (**j**) levels at rest at 12 weeks (p>0.05 for differences between groups at all time points in all hormones, two-way ANOVA followed by Sidak's multiple comparisons test).*

Figure 6.3

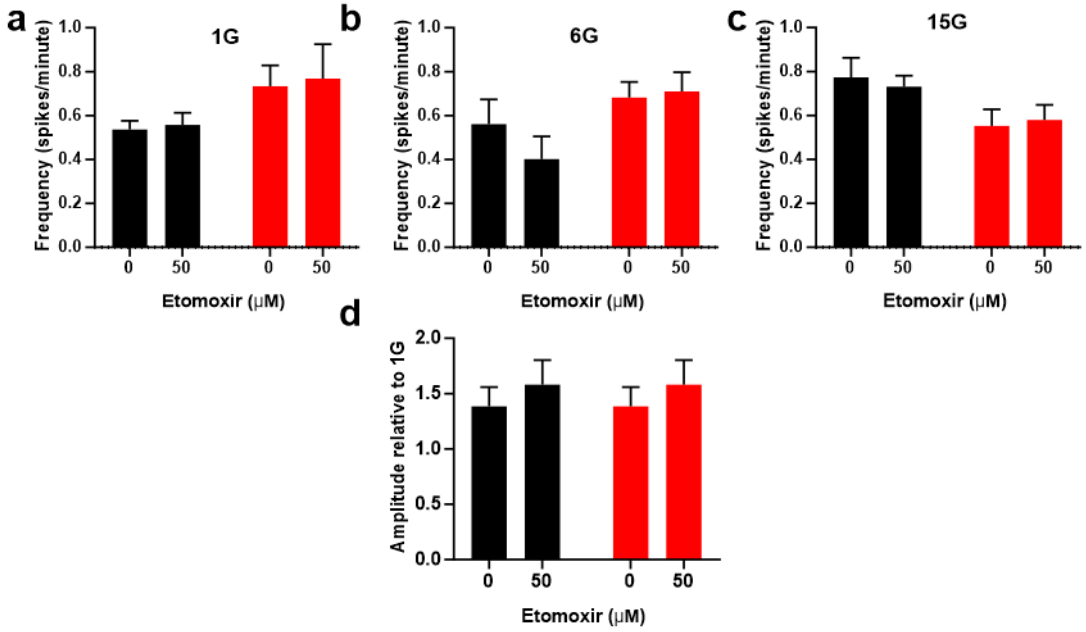

Figure 6.3 *50 μM Etomoxir does not affect α cell $[Ca^{2+}]_i$ oscillation frequency in CTL (black) and HFD (red) islets.* ***a,*** *1 mM glucose (n=38-94 cells).* ***b,*** *6 mM glucose (n=42-47 cells).* ***c,*** *15 mM glucose (n=63-80 cells).* ***d,*** *Spike amplitude at 6 mM glucose (n=20-29 cells). All 3-5 recordings with islets from 2-3 mice. All two-way ANOVA followed by Sidak's multiple comparisons test.*

Chapter 7

7. RNAseq in FACS sorted α and non-α cells

7.1 Introduction

7.1.1 Justification of RNAseq

As demonstrated in the previous chapters, α cell dysfunction occurs in obesity and prediabetes and is thought to contribute to the development of disease. In order to understand why, and by which mechanisms, α cell abnormalities develop, we must understand how gene expression differs and how this may contribute to cell physiology. RNAseq of FACS sorted α and non α cells is a technique to identify genes whose altered expression may be driving changes in cell function. This information can be used for onward interrogation of targets and pathways.

RNAseq has been used to study gene expression in pancreatic cells from human islets. These studies identified some specific changes in α cells including increased expression of RGS4 and CHRM3, which are negative regulators of glucose stimulated insulin secretion (GSIS) (Segerstolpe et al. 2016), and alterations in expression of genes that correlate with Gcg expression (Xin et al. 2016). However, in these single cell sequencing experiments, many of the genes identified were not consistently expressed between individual cells. This highlights the variability of islet cells and a limitation of single sequencing – large n-numbers, at great cost, are needed to identify changes in cell populations given the noise of these samples (3386 and 1492 cells respectively). Carrying out single-cell RNAseq in islets has been extensively reviewed by Mawla et al. (2019). Here we employ bulk RNAseq as it allows for larger

number of cells to be analysed, although this is at the expense of being able to know cell-cell variability. With bulk RNAseq, signal:noise ratio can be improved and broad trends in expression more easily identified.

7.2 Results

There were no significant differences between CTL and HFD islets during FACS in terms of cell number, cell survival, % of cells RFP+, and % of cells RFP- (**Figure 7.1a-d**).

Independent of diet, the α cell fractions were significantly enriched for 2341 genes ($p<0.05$, FDR<0.15) including known mouse α cell genes (*Irx1, Mafb, Gcg, Ppy, Pyy* (DiGruccio et al. 2016, Dusaulcy et al. 2019). The 10 most significantly enriched genes in the α cell fraction are outlined in **Figure 7.3a.** The non α cell fraction (putatively the "β cell" fraction) was significantly enriched for 2190 genes including known β cell genes (*Ins1, Ins2, Prlr, Ucn3, Insm1*). The 10 genes most enriched in the β cell fraction are outlined in **Figure 7.3b.** This demonstrates cell type enrichment in the samples and validates the methodology.

Following HFD, no genes were differentially expressed (DE) between HFD and CTL α cells (430 genes $p<0.05$ however FDR>0.15). In the β cell fraction, 1507 genes had a $p<0.05$ of which 56 had an FDR<0.15 (**Figure 7.4a**). A selection of 10 DE genes (previously shown to be altered following HFD or identified as involved in T2D on http://www.type2diabetesgenetics.org/) are outlined in (**Figure 7.4b**).

Principle component analysis failed to identify any differences distinct clusters of expressed genes that differed between HFD and CTL samples but demonstrated that samples can be separated based in cell type (α or non α, **Figure 7.2f**)

GO enrichment revealed DE of genes involved in toxic substance response, RNA transport, RNA splicing regulation, RNA export and translation between HFD and CTL

non-α cells. When all transcripts were compared between HFD and CTL (regardless of cell type), DE of genes involved in carbohydrate homeostasis, purine ribonucleotide biosynthetic process, peptide hormone secretion and response to glucagon were identified.

7.3 Discussion

7.3.1 Sorting separates α and non α cells

RNAseq data shows good separation between α and putative β cells for known α and non α cell genes, validating the specificity of RFP expression. The data clearly demonstrates enrichment of the α cell fraction for known α cell genes. DiGruccio *et al.* (2016) showed significant enrichment of a number of the same α cell markers (*Ttr, Gcg, Mafb, Irx1, Irx2*). The fold difference in expression is greater in the DiGruccio *et al.* dataset. However, they have used islets from triple transgenic mice expressing three separate genetically encoded markers within each sort to identify the different cell types. This allows for a much "cleaner" sort as each cell is selected on the basis of a) expressing one marker and b) expressing none of the other markers. The authors do not discuss the prevalence of cells positive for more than one marker. Recently, the far-red fluorescent GLP-1R antagonist LUXendin645 has been shown to be highly specific for β cells. In the future, this could be used as an additional label for FACS separation of live non-α cells to generate cleaner separation of cell populations (Ast et al. 2020).

Fold differences can be strongly affected by low read numbers in either group. The authors pooled islets from 12 mice per sequencing run. Our dataset, although more varied, gives an indication of animal to animal variation. The issue of RNAseq in α cells has been reviewed by Gromada et al. (2018). They found that across studies, only 97 genes are reproducibly enriched or unique for any one cell type. The authors suggest that regulation of cell identity by such a small number of genes may permit cell-type plasticity within islets.

7.3.2 RNAseq in HFD islets

HFD caused DE of 56 β cell genes, but no changes in gene expression were identified between HFD and CTL α cells. Specifically, we were interested in a number of genes based on our previous experimental work. Although none of the differences were significant, some changes were somewhat in line with the experimental work (downregulation of SST in all cells, upregulation of glucagon in all cells, downregulation of glucokinase, upregulation of *Cpt1α*, all $p<0.02$ but FDR=0.92 therefore not statistically significant).

HFD did not cause a significant increase in either the expression of β cell genes in GcgRFP α cells, or vice versa, indicating that cell identity and specificity of RFP expression is maintained following HFD. GO enrichment showed overall DE in genes involved in peptide hormone secretion and glucose response indicating islet-wide changes in genes involved in glucose sensitivity and secretion. This is in agreement with changes observed in secretion and glucose sensitivity observed throughout our experiments and in previous studies into islet function following HFD. In the non-α cell fraction, changes in the toxic response pathway may indicate that the altered diet is toxic to β cells.

7.3.3 β cell gene expression is more sensitive to HFD than α cell expression

In line with our observation that very few genes are altered, a review found that less than 0.5% of detectable islet genes are effected by T2D (Gromada et al. 2018). Furthermore, it has been reported that HFD in mice does not induce many changes in gene expression in α cells, with more effects seen in β cells (Dusaulcy et al. 2019).

It is worth noting that the putative β cell fraction consists of all non-α cells, so will include a proportion of transcripts from δ and γ cells. Changes in 11-39 α cell genes were identified, but changes in 99-3192 β cell genes were identified (depending on analysis approach). The DE genes identified by Dusaulcy et al. (2019) failed to validate a number of target genes they had previously identified to be DE (identified using a candidate gene approach and qPCR including *Gcg, Pcsk1/3, Foxa1, Pou3f4, scn3a* and *cMaf* (Dusaulcy et al. 2016)). This highlights the challenges of identifying meaningful changes in α cell gene expression, and reproducing previous results.

Of the 52 genes identified by Dusaulcy *et al.* (2019) as DE between HFD and CTL β cells (EdgeR analysis, $p<0.05$, FDR<0.15), 2 are in common with genes we identified; *Prss2* – Serine protease 2 is associated with pancreatitis, and *Nupr1* – nuclear protein 1 is associated with pancreatic cancer where it protects cancer cells from stress induced death. Of the 56 significantly DE genes we have identified in the β cell fraction, the human homologues of 34 are known to contain polymorphisms with strong evidence for signal association with T2D or associated disorders (e.g. CVD and BMI) according to the T2D knowledge portal (http://www.type2diabetesgenetics.org/). Such genes include; *PRDX2*, most well characterised in erythrocytes, is important in eliminating peroxides generated during oxidative metabolism (Johnson et al. 2010); and *DENND4C* which promotes GDP exchange for GTP and stimulates delivery of GLUT4 to the plasma membrane (Sano et al. 2011); *PRKCSH* whose downregulation has been shown to reduce expression of the nonselective cation channel *TRPP2* (Hofherr et al. 2014); *ALODA,* encodes Aldolase A which acts as a catalytic enzyme in glycolysis (Berg et al. 2002). Increased

cation flux through *TRPP2* as a result of increased *PRKCSH* expression could explain the elevated insulin secretion we see following HFD, as could elevated glycolysis as a result of increased *ALODA* expression.

7.3.4 Future considerations

7.3.4a Sample size and power

In the β cells, amongst the most significantly DE genes, we saw an effect size ranging from roughly 50% to 10%, with a SD of roughly 10% from the mean. In order to detect an effect of 10% (2 tailed) in a sample with SD of 10%, you would need an n of 16 for each group. We expected a larger effect on gene expression – with our sample size of 8, a 20% difference between the groups would be detectable. In the Dusaulcy *et al.* (2019) dataset, RNA from 2-4 mice were pooled to obtain 50ng mRNA (corresponding to 50000 sorted cells). Their analysis was performed on 4 CTL and 4 HFD samples obtained through this mechanism. Although they have analysed RNA from 8-16 mice in total, they have no indication of animal-animal variability. This heterogeneity may be an important feature of altered gene regulation following HFD – the phenotypic effects of HFD are known to be heterogeneous as we have seen in our *in vivo* work (e.g. variations in weight gain and plasma hormone concentrations etc.) and as seen by Dusaulcy et al. (2016). Within HFD mice, those with the highest HbA1c had elevated glucagonaemia, worse glucose tolerance during GTT, and reduced GLP-1 levels compared to HFD littermates with lower HbA1c (Dusaulcy et al. 2016). This highlights the heterogeneity seen in HFD mice, being able to identify the mouse from which individual transcripts originated may be important in identifying changes in gene expression which underlie altered α cell function.

7.3.4b FACS sorting of cells for RNAseq

Although we could identify good separation of α and β cell genes, we do still see *Ins* and *Sst* expression in the RFP^+ fraction of our cells. In single cell RNAseq, *Ins* is the

62nd most abundantly expressed gene in α cells, however when sorted cells are cultured, no insulin protein can be found by staining (Blodgett et al. 2015). We expect to see some *Ins1/2* expression in the α cell fraction, as demonstrated in **Figure 3.4**a, we see that 6% of GCaMP3^{+}ve cells are insulin positive. Furthermore, a well calibrated FACS machine has an error rate of approximately 1%, and if RNA is present outside of cells due to cells breakage or lysis, contamination is inevitable (Mawla et al. 2019).

Due to the high expression of *Gcg* in α cells and *Ins* in β cells (in α cells, approximately 1/3 of all reads are accounted for by *Gcg*), cross-contamination of cell types between samples during FACS could also contribute to a significant increase in "contaminating" reads, as could the inadvertent inclusion of doublets consisting of both α and non α cells into either fraction (Benner et al. 2014, DiGruccio et al. 2016). This indicates that collection of a completely "pure" RNA sample is not possible with current technologies, and highlights how observations from RNAseq data should be used to inform onward experimental work.

7.3.4c RNAseq approach

Here, we employed bulk RNAseq due to its advantages in cost and its ability to identify broad changes in gene expression. A disadvantage of bulk RNAseq is that is reduces the ability to identify changes in expression of RNA transcripts normally present at very low levels (as they may be missed altogether). Using bulk RNAseq reduces incidence of 3' bias seen in single cell RNAseq experiments – during cDNA amplification, reverse transcription begins at the 3' end of each transcript. If DNA polymerase stalls or becomes unattached only a fragment of the transcript will be

amplified. In single cell samples, due to a lower abundance of transcripts, this occurs more often. This can result in highly expressed genes going undetected. For example the well-known β cell transcription factor *MAFA* has been undetectable in 22% of β cells, similarly *ARX* is undetected in 18% of singly sequenced α cells (Mawla et al. 2019). The inability to identify these known cell transcription factors, casts doubt on how rigorous differences identified between cell types can be. Bulk RNAseq is less prone to 3' bias due to the higher availability of transcripts and, resulting, higher TIN number (Mawla et al. 2019). Furthermore, you do not get an indication of cell to cell variation in mRNA levels which can be identified by single cell RNAseq.

In future, "in-drop" techniques may offer an appropriate middle-ground between single-cell and bulk sequencing techniques (Zilionis et al. 2017). In this method, individual cells are suspended in a lipid droplet where reverse transcription of RNA occurs for preparation of the cDNA library. When sequencing is carried out, individual transcripts can be deconvoluted and grouped according to the cell from which they originated. In-drop techniques offer significant advancements in the number of cells that can be analysed in one reaction, but do not limit the level of detail obtained for each individual cell. One disadvantage of in-drop techniques is that as each cDNA transcript is labelled for its individual cell using a unique nucleotide "barcode" the read depth of the analysis is reduced (as reads are "used up" reading the barcode). However, in light of the heterogeneity of islet cells, this may be a worthwhile payoff. This would allow identification of different cell populations (a higher level of detail than current α/non α). This approach has been used in T2D human islets and

identified a subpopulation of β cells with an elevated stress response (Baron et al. 2016).

7.3.5 Conclusions

The data presented demonstrated clear separation of α and non α cell fractions. Following HFD no specific genes demonstrated altered expression in α cells however a number of pathways associated with translation, metabolism, and secretion appear to be altered in β cells. Ideally, this work would be repeated as with increased power, differences between the groups may be identified. Further to these experiments, staining for proteins encoded by the most DE genes (or RNA quantification using qPCR) should be used to follow-up these identified leads.

Figure 7.1

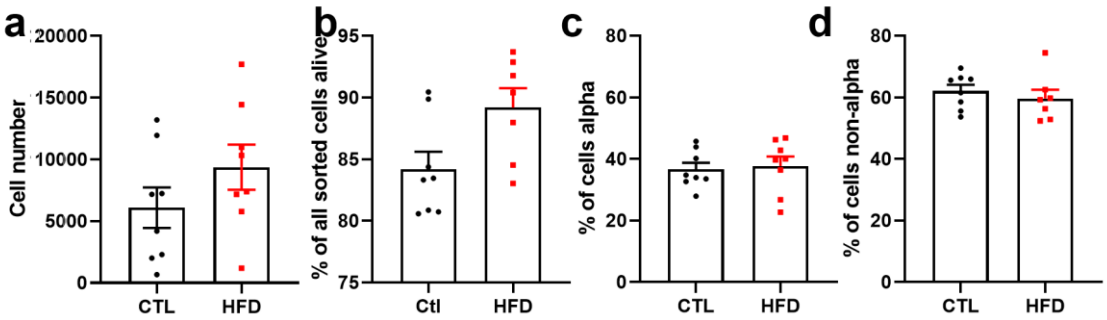

Figure 7.1 *Statistics of FACS sorted α and non-α cells. In all figures CTL (black) and HFD (red).* ***a,*** *cell number for each FACS sort.* ***b,*** *% of cells live/dead in each sort.* ***c,*** *% of cells α (RFP+ve).* ***d,*** *% of cells non α (RFP-ve). (n=8 HFD and 8 CTL mice, all t-tests).*

Figure 7.2

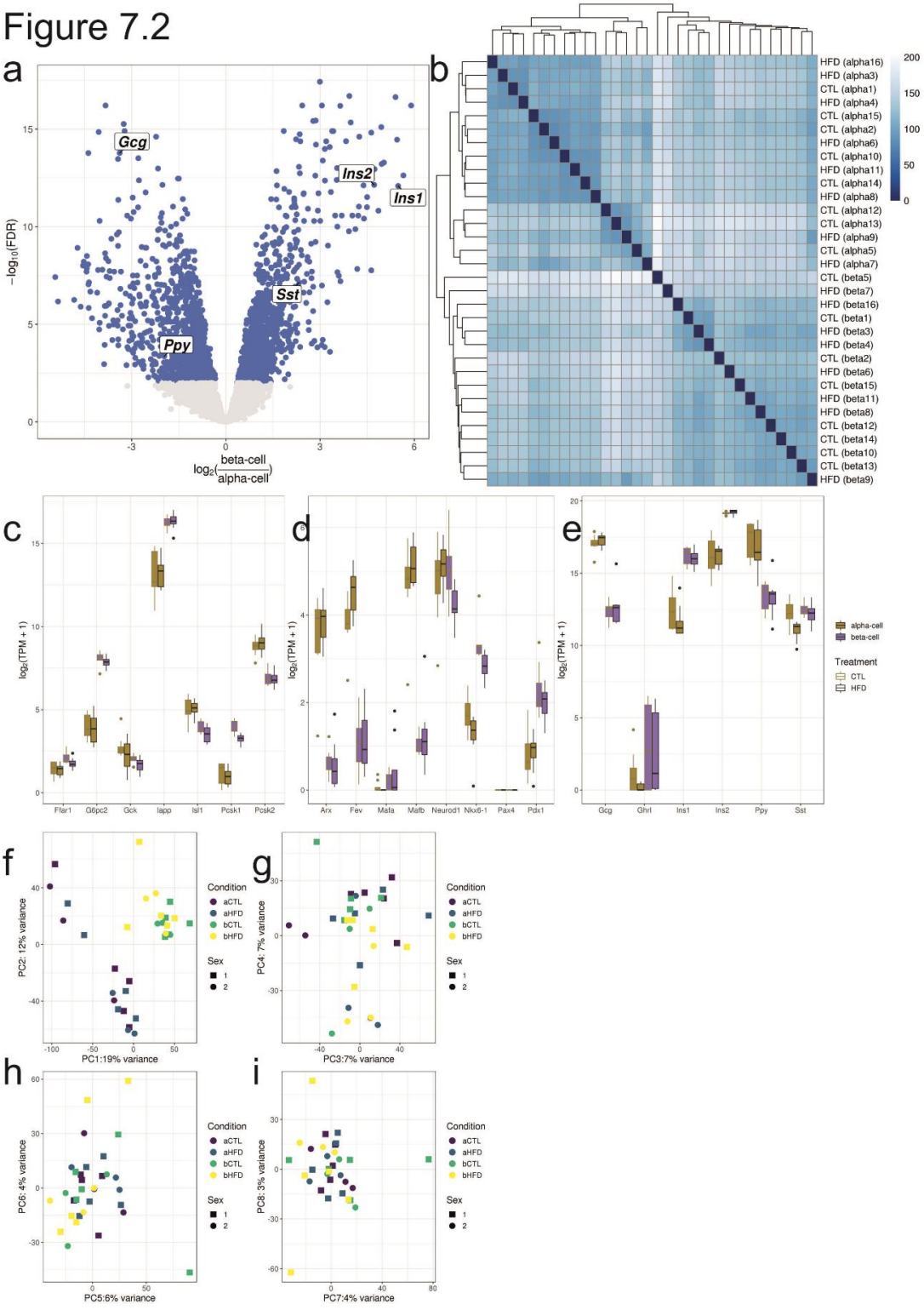

Figure 7.2 a, *Volcano plot showing the ratio of β to α cell expression vs. –log of the false discovery rate.* ***b,*** *relatedness of gene expression profile for individual samples demonstrates clustering of α and β cells but no clear distinction between HFD and CTL samples.* ***c-e,*** *gene expression of major hormone genes in transcripts per million (TPM).* ***f-l,*** *principle component (PC) analysis.*

Figure 7.3

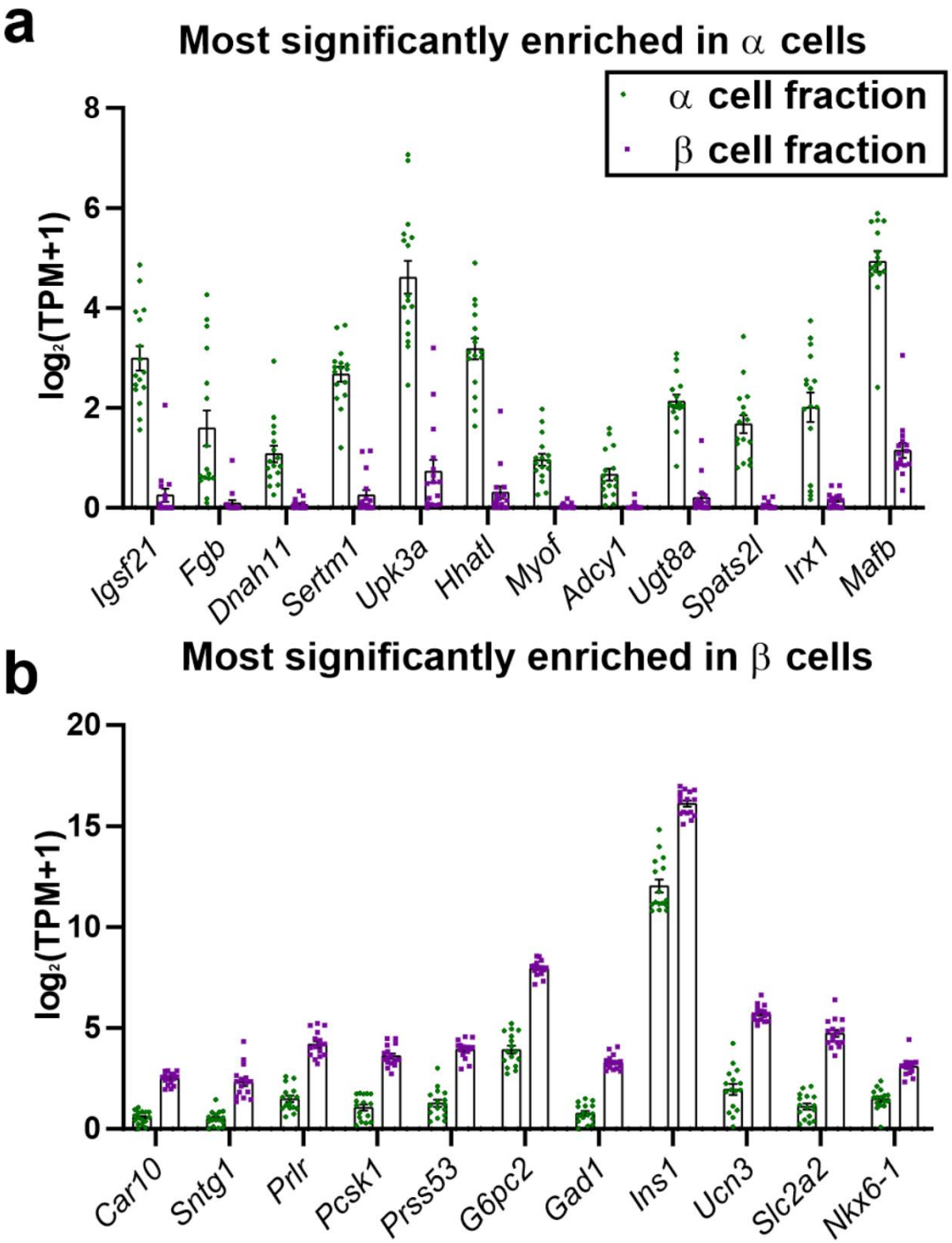

Figure 7.3 *Most significant enriched genes in α (a) and β (b) cell fractions (all genes p<0.05, FDR <0.05, n=16 α and 16 non α cell samples).*

Figure 7.4

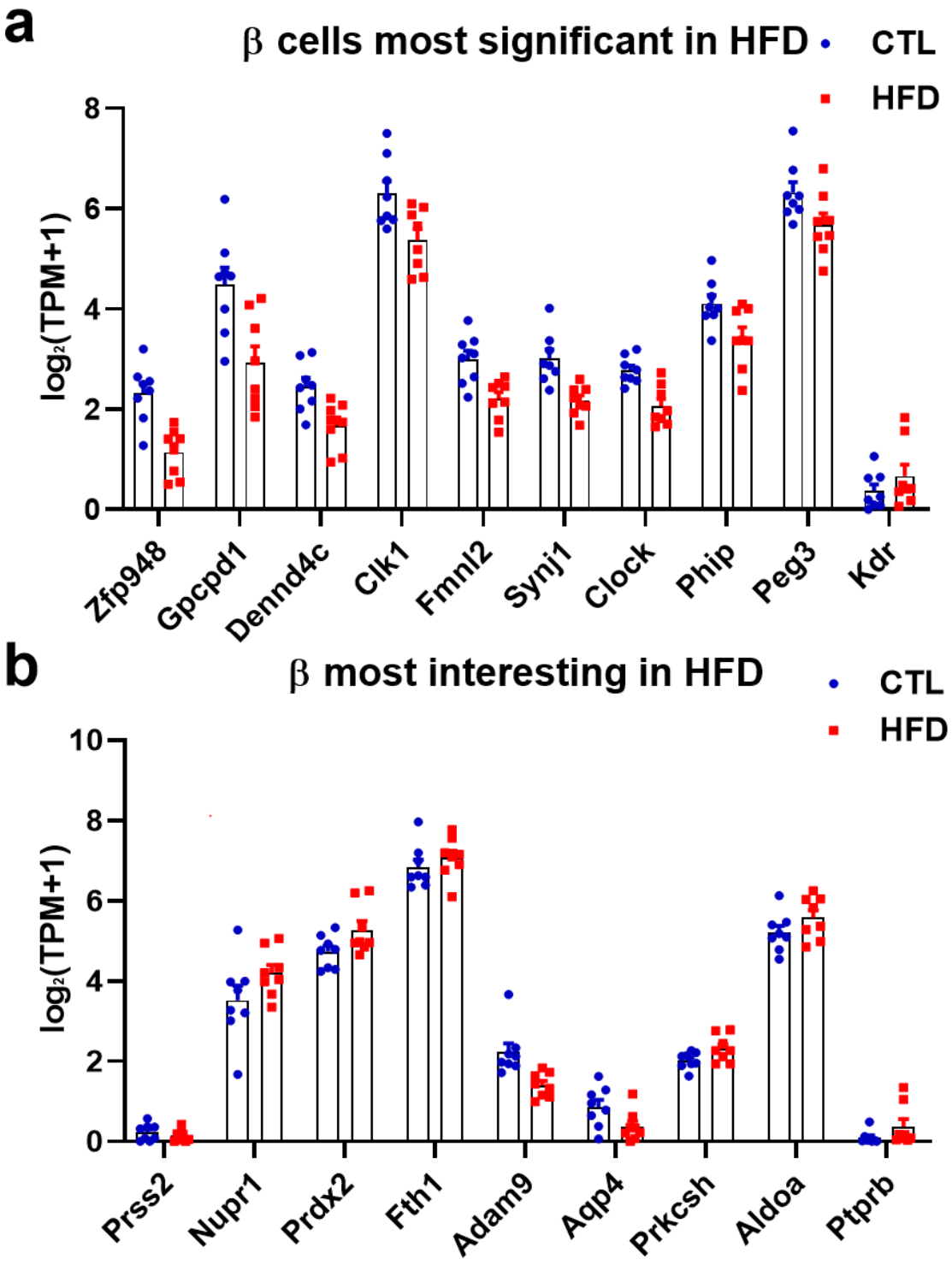

Figure 7.4 *Most significant DE genes between HFD and CTL β cell samples (a) and (b) a selection of DE genes known to be effected by HFD in β cells or identified as associated with T2D using http://www.type2diabetesgenetics.org/ (All genes p<0.05, FDR <0.05, n=8 HFD and 8 CTL mice).*

Chapter 8

8. Discussion

8.1 Summary

The overarching aim of this thesis was to understand the nature of glucose regulation of glucagon secretion under normal and diabetogenic conditions.

In Chapter 3 a model for identifying and studying $[Ca^{2+}]_i$ signalling in α cells (GcgGCaMP3) was developed and validated.

Chapters 4 and 5 addressed the *in vivo* and *ex vivo* aspects of altered α cell function during HFD.

Chapter 6 drew on this with preliminary investigations into the role of α cell fat metabolism in hyperglucagonaemia.

Finally, in Chapter 7, we investigated whether changes in gene expression underlie functional changes in islet cells following HFD.

8.2 Key findings

The $[Ca^{2+}]_i$ data, which contained a sample size of cells 3-fold greater than any existing study, revealed the importance of frequency modulation in α cell responses to changing glucose concentrations. Through thorough *in vivo* phenotyping following HFD, compared to CTL fed mice, we identified a time-of-day-dependent elevation of plasma glucagon, elevated glucagon secretion in response to hypoglycaemia, and inadequate suppression of glucagon in response to hyperglycaemia. Elevated glucagon secretion and increased $[Ca^{2+}]_i$ oscillation frequency underlie the

hyperglucagonaemia observed *in vivo*. We demonstrated that this may result from intrinsic changes in the islet. In particular, from reduced secretion of SST from δ cells and/or reduced α cell sensitivity to SST. We also found that α cell expression of *Cpt1a* in proglucagon-expressing cells contributes to GTT induced hyperglycaemia at 12 weeks HFD. Finally, RNAseq failed to detect any changes in gene expression that may account for the observed changes of α cell function.

Together, these data provide a comprehensive account of α cell behaviour under normal and HFD conditions. These data add to the understanding of α cell contribution to disease development in obesity and prediabetes.

8.3 Regulation of glucagon secretion by glucose

To date, the mechanisms by which glucose regulates glucagon secretion remain poorly understood. $[Ca^{2+}]_i$ is known to drive vesicle fusion at the plasma membrane. However studies have failed to identify a clear and reproducible pattern of $[Ca^{2+}]_i$ response to changing glucose concentrations in α cells. Considering that glucagon secretion is altered in T2D, understanding the regulation of α cell $[Ca^{2+}]_i$ signalling and hormone secretion is key to addressing hyperglucagonaemia therapeutically.

8.3.1 α cell $[Ca^{2+}]_i$ oscillations are frequency modulated in response to glucose

With improved ability to identify $[Ca^{2+}]_i$ oscillations in α cells (due to the expression of GcgGCaMP3), we attained the statistical power to pick apart characteristic features of $[Ca^{2+}]_i$ signalling (221 cells from 12 islets from 9 mice). Measuring $[Ca^{2+}]_i$ in a larger population of cells has many advantages and enabled us to determine, in a statistically robust fashion, that glucose produces a decrease in the frequency of

$[Ca^{2+}]_i$ oscillations. It also made possible the identification of α cell heterogeneity in terms of glucose responsiveness; whereas 73% of the cells responded to a change from 1 to 6 mM glucose with a reduction of $[Ca^{2+}]_i$ oscillation frequency (of 10% or more), 23% responded with an increase. This heterogeneity has 'clouded' the picture in earlier studies but it now appears it is an example of a 'low n fallacy'. For example, there may be different subsets of α cells that are more or less easily identified by pharmacological tools (which have been used previously) and respond differently to changing glucose concentration compared to the larger population of cells identified using genetic markers. We found that increasing glucose concentration from 1 to 6 mM glucose reduced both $[Ca^{2+}]_i$ oscillation frequency and glucagon secretion by 70%. The comparable magnitude of this suppression suggests that glucagon secretion is indeed $[Ca^{2+}]_i$-dependent.

Although we saw an increase in glucagon secretion following HFD, we did not see that this was due to a change in $[Ca^{2+}]_i$ oscillation amplitude. Our observations have implications for the way in which $[Ca^{2+}]_i$ data are interpreted in future – particular attention should be paid to frequency, rather than simply AUC of $[Ca^{2+}]_i$ imaging data.

The question of the relative importance of the amplitude of a $[Ca^{2+}]_i$ signal, relative to their frequency remains of interest. Some substrates *do* cause an increase in $[Ca^{2+}]_i$ oscillation amplitude; examples include adrenaline and glutamate (Santos-Silva et al. 2015, Hamilton et al. 2018). Therefore, amplitude may be of importance depending on the secretagogue used. It also worth pointing out that there might be steep concentration gradients of $[Ca^{2+}]_i$ within the α cell. Measurements of exocytosis

suggest that exocytosis in α cells is regulated by large and localized $[Ca^{2+}]_l$ transients at the inner mouth of the Ca_v channels (Zhang et al. 2013). Therefore, amplitude may be important in determining secretory output via effects on local $[Ca^{2+}]_l$ concentrations, particularly at the plasma membrane. GCaMP3 measurements do not have the spatial or temporal resolution to resolve these within the cell. In the future, total internal reflection (TIRF) microscopy would be a useful tool to thoroughly interrogate local changes in $[Ca^{2+}]_i$ as this technique permits higher spatial resolution and specifically reports measurements in the immediate vicinity of the plasma membrane (Ravier et al. 2010).

In order to definitively link change in Ca^{2+}_i to glucagon secretion, Ca^{2+}_i imaging or patch clamp electrophysiology alongside capacitance recordings could be used to link exocytosis to electrical activity and Ca^{2+}_i signalling. Caged Ca^{2+}_i (which when photolyzed using a laser, release high concentrations of Ca^{2+}_i into the intracellular space) in combination with capacitance recordings could be used to determine the dependence of vesicle fusion on Ca^{2+}_i concentration and oscillation frequency. This has been used in β cells to characterise vesicle pools with differing Ca^{2+}_i dependencies (Ge et al. 2006).

8.3.2 How may frequency modulation of $[Ca^{2+}]_i$ oscillations be achieved in α cells

Our data suggest that glucose regulates glucagon secretion via a change in α cell $[Ca^{2+}]_l$ oscillation frequency. However, it remains unclear how this modulation occurs. As discussed in the Introduction (Chapter 2), there are two main theories for how α cell activity is altered in response to glucose – the K_{ATP} theory (Ravier et al. 2005,

Zhang et al. 2013) and the SOC theory (Liu et al. 2004, Vieira et al. 2007, Watts et al. 2014). However, neither theory explicitly outlines how a change in the frequency of calcium spike might be achieved. Below these two models are considered in greater detail.

8.3.2a Frequency modulation and the K_{ATP} theory

In β cells, glucose produces a concentration-dependent increase in the duration of $[Ca^{2+}]_i$ oscillations (via closure of K_{ATP} channels producing permanent membrane depolarization and uninterrupted action potential firing) (Rorsman et al. 2018). In the K_{ATP} theory, an increase in glucose concentration depolarises V_m, as a result Na_v channels remain inactivated and there is insufficient inward current to activate HVA Ca_v channels. In this model, the duration and/or the amplitude of the $[Ca^{2+}]_i$ oscillations can be expected to increase and decrease, respectively (Zhang et al., 2013). The $[Ca^{2+}]_i$ oscillations observed in α cells at low glucose resemble those seen in β cells exposed to insulin-stimulating glucose concentrations. Although α cells express K_{ATP} channels, glucose does not produce an increase in the duration of the $[Ca^{2+}]_i$ oscillations but rather reduces their frequency.

8.3.2b Frequency modulation and the SOC theory

In the SOC model, depletion of intracellular $[Ca^{2+}]_i$ at low glucose activates SOC channels which provides positive current for activation of depolarising cation channels and $[Ca^{2+}]_i$ entry from outside of cells. This model postulates that electrical activity will cease at high glucose, which is difficult to reconcile with the observation that action potentials are maintained in α cells at glucose concentrations above 6 mM

(albeit with a smaller spike height (Zhang et al. 2013)). Nevertheless, in this model, the ability of α cells to exhibit $[Ca^{2+}]_i$ oscillations during ER filling may rely on the ratio of expression between SOC and STIM1 as documented in mouse oocytes (Takahashi et al. 2013). In these cells, $[Ca^{2+}]_i$ transients during fertilisation rely on ER calcium. In these cells, the rate of ER filling has been shown to depend on expression of the SOC channel STIM1 which determines $[Ca^{2+}]_i$ oscillation frequency (Takahashi et al. 2013).

To date, no α cell SOC current has been identified by electrophysiological measurement but we acknowledge that such a current may be difficult to detect as it is likely to be small and therefore difficult to resolve over background noise. Nevertheless, small currents may have a large effect on electrical activity because α cells have a very high input resistance.

The rate of release of Ca^{2+}_i from intracellular stores and the sensitivity of InsP3 receptors to stimulation is dependent on ER calcium concentration (Missiaen et al. 1992). The ability of α cells to refill calcium stores may determine $[Ca^{2+}]_i$ oscillation frequency (with maximal frequency permitted when Ca^{2+}_i stores are full). However, under the SOC model, the α cell is most able to refill ER Ca^{2+}_i stores at high glucose concentrations where there is enough ATP to drive SERCA. This is difficult to reconcile with the SOC model as at high glucose concentrations we have demonstrated a decrease in α cell $[Ca^{2+}]_i$ oscillation frequency.

With the data we present, we are unable to resolve the differences in the two hypotheses – in order to do so, more thorough interrogation of the factors which may alter $[Ca^{2+}]_i$ oscillation frequency is needed.

8.3.3 $[Ca^{2+}]_i$ independent control of glucagon secretion

We show here that the capacity of glucose to inhibit glucagon secretion is associated with a reduction of $[Ca^{2+}]_i$. This provides circumstantial evidence that the control of glucagon secretion is exerted via changes in $[Ca^{2+}]_i$ dynamics. However, there are alternative theories that instead postulate that glucose regulates glucagon secretion by $[Ca^{2+}]_i$ independent mechanisms.

Le Marchand et al. (2010) found no reduction in α cell $[Ca^{2+}]_i$ as glucose concentration is elevated despite an inhibition of secretion. Although based on a fairly small number of experiments (n=22 cells from 7 islets), the authors hypothesized that inhibition of glucagon secretion at high glucose may be independent of $[Ca^{2+}]_i$. Potential mechanisms could include reduced granule mobilisation to the membrane decreasing glucagon exocytosis.

It also been proposed that glucose may inhibit glucagon secretion by lowering $[cAMP]_i$ in α cells (Yu et al. 2019). Application of SST decreases $[cAMP]_i$ (via SSTR2 $G_{\alpha i}$ inhibition of AC (Schuit et al. 1989, Elliott et al. 2015)). Although antagonism of SST increases $[cAMP]_i$ at 1 mM glucose, $[cAMP]_i$ is still inhibited by high glucose concentrations even during SST antagonism (Tengholm et al. 2017) and the mechanism by which an elevation of glucose might reduce $[cAMP]_i$ remains obscure. A weakness of this hypothesis is that neither inhibition of PKA, nor genetic ablation of Epac2 (PKA and Epac2 are the main downstream effectors of cAMP) interferes with glucagon secretion evoked by low glucose (De Marinis et al. 2010)).

8.4 Impact of HFD on pancreatic islet and α cell function

8.4.1 Summary of HFD observations

At the systemic level, feeding mice a HFD elevated basal plasma glucagon and increased glucagon:glucose ratio. In the perfused pancreas, stimulation of glucagon secretion by low glucose concentration was greater in HFD fed mice than those fed a control diet. A similar pattern was observed in isolated islets. In isolated islets, $[Ca^{2+}]_i$ imaging revealed a higher proportion of active cells following HFD (60% in CTL *vs.* 70% in HFD at 6 mM glucose) and an increase in the $[Ca^{2+}]_i$ oscillation frequency. We consistently see that α cells from CTL mice respond to increasing glucose concentration with a decrease in activity and that HFD consistently results in elevated α cell activity (whether it be $[Ca^{2+}]_i$ oscillation frequency, glucagon secretion, or plasma glucagon level). This indicates that HFD induces an increase in α cell $[Ca^{2+}]_i$ signalling and output that can be demonstrated, and is consistent, across experimental paradigms.

8.4.2 Mechanisms of altered SST signalling

As to the mechanism, we observed reduced sensitivity of glucagon secretion to inhibition by SST following HFD feeding. Paradoxically, the reduced sensitivity correlated with suppression of SST secretion. This is remarkable as reduced secretion of SST would be expected to increased responsiveness to exogenous SST via receptor sensitization. RNAseq analyses did not reveal any changes in gene expression that may account for these changes and expression of SSTRs was unaffected.

It is now important to dissect how this may occur. δ cells express GPR120, a NEFA receptor which when stimulated by fatty acids, reduces SST secretion at high glucose (Stone et al. 2014). We did not identify any changes in GPR120 expression at the mRNA level following HFD, identifying a change in δ cell gene expression within the mixed non α cell fraction sequenced would require a huge change in gene expression. To determine whether increased NEFA signalling inhibits SST secretion during HFD, δ cell GPR120$^{-/-}$ mice could be put on a HFD to see whether they are protected from loss of SST secretion. This would provide evidence that fatty acid signalling in δ cells and the downstream consequences of this contribute to islet dysfunction and disease pathology in T2D.

Adipokines, secreted from the adipose tissue, include leptin and adiponectin. Plasma leptin levels correlate to fat mass, which is increased in obesity (acute fasting decreases leptin levels therefore fat mass is not the only regulator) (Couillard et al. 1997). Leptin has targets throughout the body but a main mechanism of action is via the hypothalamus to induce anorexia (Satoh et al. 1997). In obesity, leptin resistance is thought to contribute to loss of this effect (Munzberg et al. 2004). It is notable that expression of LepR at the mRNA level is low/undetectable in mouse islets (Soedling et al. 2015, DiGruccio et al. 2016). However, human δ cells have been reported to be upregulated for LepR expression (at the mRNA and protein level) compared to other islet cell types (Lawlor et al. 2017). Furthermore, leptin inhibits $[Ca^{2+}]_i$ and glucagon secretion in αTC1-9 cells, mouse islets and human islets (Tuduri et al. 2009, Marroqui et al. 2011). It is therefore tempting to consider whether leptin resistance in α or δ cells contributes to increased glucagon secretion.

8.4.3 HFD and α cell function

Although we have not measured circulating NEFA in our mice, circulating concentrations are elevated following HFD feeding of mice (Pinnick, unpublished), and rats (Liu et al. 2013).

NEFA are elevated within 24 hours and remain elevated at 5 days of fasting (Owen et al. 1990) as is circulating glucagon concentration (Marliss et al. 1970). When this is considered in the context of the SOC model of α cell electrical activity, intermittent elevations in $[ATP]_i$ level may be necessary for refilling of $[Ca^{2+}]_i$ stores. β-oxidation is elevated in α cells at low glucose concentrations (Briant et al. 2018). Therefore, under conditions of prolonged hypoglycaemia, metabolism of FA may be important to maintain glucagon secretion. We did not study the effects of prolonged low glucose on $[Ca^{2+}]_i$ oscillation frequency – in the imaging recordings, each condition was applied for approximately 10 minutes. Prolonged recordings with and without FAs could be used to investigate the ability of α cells to maintain $[Ca^{2+}]_i$ oscillations at low glucose concentrations, and whether the reliance of α cells on FAs is altered following HFD.

Although prolonged incubation in palmitate has been shown to be toxic to β cells (Moffitt et al. 2005), many of the studies that investigate the role of FAs in islet physiology use this approach. Following prolonged incubation in 0.5 mM palmitate or oleate (avoiding the toxicity of palmitate), glucose secretion is elevated. This effect is not as large if islets are incubated in palmitate or oleate at *high* glucose

concentrations (Collins et al. 2008). This highlights the importance of FAs in determining α cell activity under hypoglycaemic conditions.

In addition to the effects on metabolism, acute exposure to palmitate (0.5 mM) increases α cell $[Ca^{2+}]_i$ and glucagon secretion. This effect is lost if L-type Ca_v channels are inhibited using isradipine (Olofsson et al. 2004). Therefore, FAs may modulate glucagon secretion via direct effects on channel activity. In β cells, palmitate can stimulate insulin secretion (Olofsson et al. 2004). As in α cells, this stimulation is sensitive to inhibition by isradipine. The authors demonstrate that in β cells, palmitate stimulation of insulin secretion occurs independently of modulation of K_{ATP} current, suggesting that metabolism of the palmitate (and production of ATP) is not driving secretion. They also demonstrate that palmitate increases the ready releasable pool of insulin granules which elevates vesicle fusion when a depolarisation is induced (using patch clamp electrophysiology). These data clearly demonstrate that FAs can alter islet cell activity (through modulation of L-type Ca_v channels) independently of effects on metabolism. Although the mechanism is not known, arachidonic acid (a polyunsaturated fatty acid) has been shown to increase the mean closed time of Ca_v channels (reviewed by Roberts-Crowley et al. (2009)). *In vivo* high levels of arachidonic acid would not occur in isolation, but this data demonstrates that fatty acids can alter ion channel dynamics. Changes in Ca_v currents, as a result of increased plasma NEFA in HFD may drive altered $[Ca^{2+}]_i$ oscillation frequency, and therefore secretion.

In islets, incubation with differing ratios of oleic acid, palmitic acid, and linoleic acid influence the phospholipid fatty acid composition in the plasma membrane (Moffitt et al. 2005). In β cells, unsaturation and shorter fatty acid length in the phospholipid bilayer facilitates membrane curvature and fluidity, and therefore vesicle fusion (MacDonald et al. 2015). The specific composition of plasma NEFA following HFD may alter incorporation of saturated fatty acids into the lipid bilayer, therefore altering α cell secretory output. Considering that the HFD consists of a large component of dietary saturated fat, it may be that the increased $[Ca^{2+}]_i$ oscillation frequency observed is adaptive to a change in membrane rigidity.

In summary, FAs are known to influence islet cell function via numerous mechanisms. Measurements of β-oxidation at low and high glucose concentrations could be used to assess whether fat metabolism is increased in α cells following HFD. Likewise, our αCPT1a-KO experiments were limited to an *in vivo* assessment of glycaemia and glucagon secretion following HFD. Firstly, it is essential to identify whether the protective effect of αCPT1a-KO is mediated by a change in the α cells (rather than an effect on enteroendocrine L-cells). If this appears to be the case, the role of fat metabolism could be interrogated *ex vivo* by comparing secretion and $[Ca^{2+}]_i$ activity at different glucose concentrations and under conditions with and without FAs.

8.5 Reflections on the whole thesis

8.5.1 The magnitude of secretory response

Throughout this work, we have used various experimental paradigms to investigate α cell physiology. Namely, plasma samples taken *in vivo*, perfusate collected from the *in situ* perfused mouse pancreas, and hormone secretion *ex vivo* from isolated islets.

In isolated islets, the $[Ca^{2+}]_i$ oscillation frequency is 4 times higher at 1 mM glucose compared to 6 mM but secretion is 3 times higher. Importantly, in vivo during an ITT plasma glucagon increases 8-fold when plasma glucose is reduced from 10 to 5 mM (**Figure 4.4**). The stronger stimulation in vivo might reflect the contribution of innervation by sympathetic efferent nerves, circulating amino acids (Boden et al. 1984, Holst et al. 2017), or peripheral endocrine signalling (including the presence of GIP from the gut which stimulates glucagon secretion; (Meier et al. 2003)) to stimulation of glucagon secretion.

8.5.2 The importance of SST sensitivity

In addition to differences in the magnitude of α cell stimulation, we have observed variations in the sensitivity of glucagon secretion to inhibition by SST. In isolated islets, the IC_{50} for inhibition of $[Ca^{2+}]_i$ oscillation frequency was approximately 1nM. However, in the perfused pancreas, the IC_{50} for inhibition of glucagon secretion was 21 pM. The reason for the discrepancy in sensitivity is unknown but one possible explanation is that SST differentially affects $[Ca^{2+}]_i$ signalling and exocytosis. Alternatively, the perfused pancreas preparation may enable more efficient delivery

of SST to the α cells or prevent SSTR desensitization due to accumulation of secreted SST in the islet interstitium.

8.6 Implications for understanding and treatment of T2D

8.6.1 Relevance to human disease

The studies summarised here are based on experiments in mice. To conduct these studies on human islets would not have been feasible; access to human islets is limited and for obvious reasons it is not possible to study the effects of diet using human islets. The quality of human islets is also highly variable. Mice have obvious advantages in all these respects and they are also possible to genetically modify (for example, to express genetically encoded $[Ca^{2+}]_i$ sensors). However, we acknowledge that the use of mouse islets has limitations. Islet architecture differs intrinsically between mouse and human, as does the homeostatic set point for glycaemia, generating the question as to when a mouse becomes diabetic. Nonetheless, many of our observations fit the clinical features of T2D/prediabetes in people including glucose intolerance and hyperglucagonaemia (Dunning et al. 2007, Faerch et al. 2008, Faerch et al. 2016).

Given that T2D is associated with α cell dysregulation manifested as hypersecretion of glucagon, the question arises whether the defect can be therapeutically targeted. GRA1 is a GCGR antagonist administration of which improves glycaemia in HFD mice (Mu et al. 2012). Changes in liver enzymes, and increases in circulating cholesterol have, to date, impeded progress in the development of GCGR antagonism for therapeutic use in people (Sammons et al. 2015, Pearson et al. 2016). The CGGR

antagonist LY2409021 was effective in reducing glycaemia in T2D patients in a phase 2 study (Kazda et al. 2016). However a subsequent hepatic safety study was terminated (Eli Lilly, unpublished, update October 2019). Likewise, the GCGR antagonist IONIS-$GCGR_{RX}$ reduced HbA1C in T2D patients on metformin but increased hepatic lipid content (Morgan et al. 2019). In a phase 1 study with healthy participants, anti GCGR human monoclonal antibody REGN1193 increased plasma alanine aminotransferase (ALT, indicating hepatic dysfunction (Kostic et al. 2018)). In studies in diabetic patients on metformin, antagonists with fewer/more tolerable hepatic side effects have now been tested (Kazierad et al. 2018, Pettus et al. 2020). Despite the hepatic side effects, GCGR antagonists may be appropriate for treatment of acute hyperglycaemia as hepatic function quickly returns once administration ceases (Kelly et al. 2015).

Rather than targeting the GCGR as a means of treating hyperglucagnaemia, it may be possible to develop agents that act at the α cell itself. Our observation that α cells have reduced SST sensitivty is of interest and suggest that taking the detour via the δ cell may represent a means of restoring α cell function.

8.7 Summary, thesis aims

There were five main aims of this thesis, addressed as follows;

1. Generate and validate GCaMP3 model

This was successfully achieved in Chapter 3 allowing us to make novel observations about the nature of glucose regulation of α cell $[Ca^{2+}]_i$ signalling.

2. *In vivo* - Carry out extensive metabolic phenotyping

This was addressed in Chapter 4 where we identified HFD-induced elevations in plasma glucagon during insulin-induced hypoglycaemia, and an increase in the glucagon:glucose ratio – indicating an inability of glucose to inhibit glucagon secretion.

3. *Ex vivo* - Interrogate functional alterations in α cell activity following HFD

This aim was addressed throughout Chapters 5-7. We demonstrate that hyperglucagonaemia is associated with increased glucagon secretion *in situ* in the perfused pancreas, and *ex vivo* in isolated islets. An increase in α cell $[Ca^{2+}]_i$ oscillation frequency accompanied this increase in glucagon secretion and may occur as a result of reduced paracrine inhibition by SST from neighbouring δ cells.

4. Interrogation of the role of fat metabolism in glucagon secretion from α cells

In Chapter 6 we identified a protective effect of loss of CPT1a in proglucagon expressing cells.

5. Investigate changes in α cell gene expression following HFD

Finally, we investigated whether HFD induces changes in mRNA expression in α and non α cells. We demonstrate in Chapter 7 that changes in α cell physiology that result from the HFD occur independently of any statistically significant changes in α cell gene expression.

8.8 Conclusions

We show that α cell dysfunction can occur under conditions similar to that of prediabetes prior to the development of many of the clinical features of T2D. This suggests that α cell dysfunction is a contributing factor to the development of T2D rather than a consequence of it. If this can be confirmed, then normalising α cell function could help to prevent/reverse the progression of T2D. An interesting therapeutic angle to investigate is whether the change in α cell sensitivity to SST occurs in human islets in obesity and T2D, and how this is modulated.

Abdelhalim, S. M., A. Guenifi, S. Efendic and C. G. Ostenson (1993). "Both somatostatin and insulin responses to glucose are impaired in the perfused pancreas of the spontaneously noninsulin-dependent diabetic gk (goto-kakizaki) rats." Acta Physiologica Scandinavica 148(2): 219-226.
Ackermann, A. M., J. Zhang, A. Heller, A. Briker and K. H. Kaestner (2017). "High-fidelity Glucagon-CreER mouse line generated by CRISPR-Cas9 assisted gene targeting." Molecular Metabolism 6(3): 236-244.
Ahren, B., E. Simonsson, A. J. W. Scheurink, H. Mulder, U. Myrsen and F. Sundler (1997). "Dissociated insulinotropic sensitivity to glucose and carbachol in high-fat diet-induced insulin resistance in C57BL/6J mice." Metabolism-Clinical and Experimental 46(1): 97-106.
Albrechtsen, N. J. W., B. G. Challis, I. Damjanov and J. J. Holst (2016). "Do glucagonomas always produce glucagon?" Bosnian Journal of Basic Medical Sciences 16(1): 1-7.
Albrechtsen, N. J. W., K. Faerch, T. M. Jensen, D. R. Witte, J. Pedersen, Y. Mahendran, A. E. Jonsson, K. D. Galsgaard, M. Winther-Sorensen, S. S. Torekov, T. Lauritzen, O. Pedersen, F. K. Knop, T. Hansen, M. E. Jorgensen, D. Vistisen and J. J. Holst (2018). "Evidence of a liver-alpha cell axis in humans: hepatic insulin resistance attenuates relationship between fasting plasma glucagon and glucagonotropic amino acids." Diabetologia 61(3): 671-680.
Albrechtsen, N. J. W., J. Pedersen, K. D. Galsgaard, M. Winther-Sorensen, M. P. Suppli, L. Janah, J. Gromada, H. Vilstrup, F. K. Knop and J. J. Holst (2019). "The Liver-alpha-Cell Axis and Type 2 Diabetes." Endocrine Reviews 40(5): 1353-1366.
Ali, S., B. J. Lamont, M. J. Charron and D. J. Drucker (2011). "Dual elimination of the glucagon and GLP-1 receptors in mice reveals plasticity in the incretin axis." Journal of Clinical Investigation 121(5): 1917-1929.
Alquier, T. and V. Poitout (2018). "Considerations and guidelines for mouse metabolic phenotyping in diabetes research." Diabetologia 61(3): 526-538.
Alsalim, W., A. Tura, G. Pacini, B. Omar, R. Bizzotto, A. Mari and B. Ahren (2016). "Mixed meal ingestion diminishes glucose excursion in comparison with glucose ingestion via several adaptive mechanisms in people with and without type 2 diabetes." Diabetes Obesity & Metabolism 18(1): 24-33.
Andralojc, K. M., A. Mercalli, K. W. Nowak, L. Albarello, R. Calcagno, L. Luzi, E. Bonifacio, C. Doglioni and L. Piemonti (2009). "Ghrelin-producing epsilon cells in the developing and adult human pancreas." Diabetologia 52(3): 486-493.
Anoop, S., A. Misra, S. P. Bhatt, S. Gulati, H. Mahajan and G. Prabakaran (2017). "High Plasma Glucagon Levels Correlate with Waist-to-Hip Ratio, Suprailiac Skinfold Thickness, and Deep Subcutaneous Abdominal and

Intraperitoneal Adipose Tissue Depots in Nonobese Asian Indian Males with Type 2 Diabetes in North India." Journal of Diabetes Research.
Asada, N., I. Shibuya, T. Iwanaga, K. Niwa and T. Kanno (1998). "Identification of alpha- and beta-cells in intact isolated islets of Langerhans by their characteristic cytoplasmic Ca2+ concentration dynamics and immunocytochemical staining." Diabetes 47(5): 751-757.
Ashcroft, F. M. and P. Rorsman (1990). "ATP-SENSITIVE K+ CHANNELS - A LINK BETWEEN B-CELL METABOLISM AND INSULIN-SECRETION." Biochemical Society Transactions 18(1): 109-111.
Ast, J., A. Arvaniti, N. H. F. Fine, D. Nasteska, F. B. Ashford, Z. Stamataki, Z. Koszegi, A. Bacon, B. J. Jones, M. A. Lucey, S. Sasaki, D. I. Brierley, B. Hastoy, A. Tomas, G. D'Agostino, F. Reimann, F. C. Lynn, C. A. Reissaus, A. K. Linnemann, E. D'Este, D. Calebiro, S. Trapp, K. Johnsson, T. Podewin, J. Broichhagen and D. J. Hodson (2020). "Super-resolution microscopy compatible fluorescent probes reveal endogenous glucagon-like peptide-1 receptor distribution and dynamics." Nature communications 11(1): 467-467.
Bailey, S. J., M. A. Ravier and G. A. Rutter (2007). "Glucose-dependent regulation of gamma-aminobutyric acid (GABA(A)) receptor expression in mouse pancreatic islet alpha-cells." Diabetes 56(2): 320-327.
Barg, S., J. Galvanovskis, S. O. Gopel, P. Rorsman and L. Eliasson (2000). "Tight coupling between electrical activity and exocytosis in mouse glucagon-secreting alpha-cells." Diabetes 49(9): 1500-1510.
Baron, M., A. Veres, S. L. Wolock, A. L. Faust, R. Gaujoux, A. Vetere, J. H. Ryu, B. K. Wagner, S. S. Shen-Orr, A. M. Klein, D. A. Melton and I. Yanai (2016). "A Single-Cell Transcriptomic Map of the Human and Mouse Pancreas Reveals Inter- and Intra-cell Population Structure." Cell Systems 3(4): 346-+.
Basnayake, K., D. Mazaud, A. Bemelmans, N. Rouach, E. Korkotian and D. Holcman (2019). "Fast calcium transients in dendritic spines driven by extreme statistics." Plos Biology 17(6).
Bataille, D. (1996). Preproglucagon and Its Processing. Glucagon III. Handbook of Experimental Pharmacology. P. J. Lefèbvre. Berlin, Springer. 123.
Beaudry, J. L., A. M. D'Souza, T. Teich, R. Tsushima and M. C. Riddell (2013). "Exogenous Glucocorticoids and a High-Fat Diet Cause Severe Hyperglycemia and Hyperinsulinemia and Limit Islet Glucose Responsiveness in Young Male Sprague-Dawley Rats." Endocrinology 154(9): 3197-3208.
Bechtold, D. A., T. M. Brown, S. M. Luckman and H. D. Piggins (2008). "Metabolic rhythm abnormalities in mice lacking VIP-VPAC(2) signaling." American Journal of Physiology-Regulatory Integrative and Comparative Physiology 294(2): R344-R351.
Benner, C., T. van der Meulen, E. Caceres, K. Tigyi, C. J. Donaldson and M. O. Huising (2014). "The transcriptional landscape of mouse beta cells compared

to human beta cells reveals notable species differences in long non-coding RNA and protein-coding gene expression." Bmc Genomics 15.
Bennett, M. K., N. Calakos, K. G. Miller and R. H. Scheller (1992). "Syntaxin - a synaptic protein implicated in docking of synaptic vesicles at presynaptic active zones." Molecular Biology of the Cell 3: A3-A3.
Berg, J., J. Tymoczko and L. Stryer (2002). Biochemistry.

Section 16.1 Glycolysis Is an Energy-Conversion Pathway in Many Organisms. New york, W H Freeman.
Berg, J. M., J. L. Tymoczko and L. Stryer (2002). Biochemistry, W.H. Freeman.
Blodgett, D. M., A. Nowosielska, S. Afik, S. Pechhold, A. J. Cura, N. J. Kennedy, S. Kim, A. Kucukural, R. J. Davis, S. C. Kent, D. L. Greiner, M. G. Garber, D. M. Harlan and P. diIorio (2015). "Novel Observations From Next-Generation RNA Sequencing of Highly Purified Human Adult and Fetal Islet Cell Subsets." Diabetes 64(9): 3172-3181.
Bock, T., B. Pakkenberg and K. Buschard (2005). "Genetic background determines the size and structure of the endocrine pancreas." Diabetes 54(1): 133-137.
Boden, G., I. Rezvani and O. E. Owen (1984). "Effects of glucagon on plasma amino-acids." Journal of Clinical Investigation 73(3): 785-793.
Bokhari, S., E. Plummer, P. Emmerson, A. Gupta and C. Meyer (2014). "Glucose Counterregulation in Advanced Type 2 Diabetes: Effect of beta-Adrenergic Blockade." Diabetes Care 37(11): 3040-3046.
Bollheimer, L. C., H. C. Landauer, S. Troll, J. Schweimer, C. E. Wrede, J. Scholmerich and R. Buettner (2004). "Stimulatory short-term effects of free fatty acids on glucagon secretion at low to normal glucose concentrations." Metabolism-Clinical and Experimental 53(11): 1443-1448.
Bonds, D. E., M. E. Miller, R. M. Bergenstal, J. B. Buse, R. P. Byington, J. A. Cutler, R. J. Dudl, F. Ismail-Beigi, A. R. Kimel, B. Hoogwerf, K. R. Horowitz, P. J. Savage, E. R. Seaquist, D. L. Simmons, W. I. Sivitz, J. M. Speril-Hillen and M. E. Sweeney (2010). "The association between symptomatic, severe hypoglycaemia and mortality in type 2 diabetes: retrospective epidemiological analysis of the ACCORD study." Bmj-British Medical Journal 340.
Boron, W. F. and E. Boulpaep, L. (2009). Medical Physiology. Philadelphia, USA, Saunders Elsevier.
Brand, C. L., B. Rolin, P. N. Jorgensen, I. Svendsen, J. S. Kristensen and J. J. Holst (1994). "Immunoneutralization of endogenous glucagon with monoclonal glucagon antibody normalizes hyperglycemia in moderately streptozotocin-diabetic rats." Diabetologia 37(10): 985-993.
Braun, M., R. Ramracheya, M. Bengtsson, A. Clark, J. N. Walker, P. R. Johnson and P. Rorsman (2010). "gamma-Aminobutyric Acid (GABA) Is an Autocrine

Excitatory Transmitter in Human Pancreatic beta-Cells." Diabetes 59(7): 1694-1701.
Braun, M., A. Wendt, K. Buschard, A. Salehi, S. Sewing, J. Gromada and P. Rorsman (2004). "GABA(B) receptor activation inhibits exocytosis in rat pancreatic beta-cells by G-protein-dependent activation of calcineurin." Journal of Physiology-London 559(2): 397-409.
Braun, M., A. Wendt, J. Karanauskaite, J. Galvanovskis, A. Clark, P. E. MacDonald and P. Rorsman (2007). "Corelease and differential exit via the fusion pore of GABA, serotonin, and ATP from LDCV in rat pancreatic beta cells." Journal of General Physiology 129(3): 221-231.
Brereton, M. F., M. Iberl, K. Shimomura, Q. Zhang, P. Proks, A. A. Adriaenssens, I. I. Spiliotis, W. Dace, K. K. Mattis, F. M. Gribble, F. Reimann, A. Clark, P. Rorsman and F. M. Ashcrot (2014). "Reversible changes in pancreatic islet structure and function produced by elevated blood glucose." Diabetologia 57: S93-S93.
Briant, L., A. Salehi, E. Vergari, Q. Zhang and P. Rorsman (2016). "Glucagon secretion from pancreatic alpha-cells." Upsala Journal of Medical Sciences 121(2): 113-119.
Briant, L. J. B., M. S. Dodd, M. V. Chibalina, N. J. G. Rorsman, P. R. V. Johnson, P. Carmeliet, P. Rorsman and J. G. Knudsen (2018). "CPT1a-Dependent Long-Chain Fatty Acid Oxidation Contributes to Maintaining Glucagon Secretion from Pancreatic Islets." Cell Reports 23(11): 3300-3311.
Brissova, M., M. J. Fowler, W. E. Nicholson, A. Chu, B. Hirshberg, D. M. Harlan and A. C. Powers (2005). "Assessment of human pancreatic islet architecture and composition by laser scanning confocal microscopy." Journal of Histochemistry & Cytochemistry 53(9): 1087-1097.
Broder, J., A. Majumder, E. Porter, G. Srinivasamoorthy, C. Keith, J. Lauderdale and A. Sornborger (2007). "Estimating weak ratiometric signals in imaging data. I. Dual-channel data." Journal of the Optical Society of America a-Optics Image Science and Vision 24(9): 2921-2931.
Butler, S. O., I. F. Btaiche and C. Alaniz (2005). "Relationship between hyperglycemia and infection in critically ill patients." Pharmacotherapy 25(7): 963-976.
Cabrera, O., M. C. Jacques-Silva, S. Speier, S.-N. Yang, M. Kohler, A. Fachado, E. Vieira, J. R. Zierath, R. Kibbey, D. M. Berman, N. S. Kenyon, C. Ricordi, A. Caicedo and P.-O. Berggren (2008). "Glutamate is a positive autocrine signal for glucagon release." Cell Metabolism 7(6): 545-554.
Carlsson, P. O., A. Andersson and L. Jansson (1996). "Pancreatic islet blood flow in normal and obese-hyperglycemic (ob/ob) mice." American Journal of Physiology-Endocrinology and Metabolism 271(6): E990-E995.
Carpentier, A. C., F. Frisch, D. Cyr, P. Genereux, B. W. Patterson, R. Giguere and J. P. Baillargeon (2005). "On the suppression of plasma nonesterified fatty

acids by insulin during enhanced intravascular lipolysis in humans." American Journal of Physiology-Endocrinology and Metabolism 289(5): E849-E856.
Carvalho, C. P. F., R. B. Oliveira, A. Britan, J. C. Santos-Silva, A. C. Boschero, P. Meda and C. B. Collares-Buzato (2012). "Impaired beta-cell-beta-cell coupling mediated by Cx36 gap junctions in prediabetic mice." American Journal of Physiology-Endocrinology and Metabolism 303(1): E144-E151.
Charles, A. C., E. T. Piros, C. J. Evans and T. G. Hales (1999). "L-type Ca2+ channels and K+ channels specifically modulate the frequency and amplitude of spontaneous Ca2+ oscillations and have distinct roles in prolactin release in GH(3) cells." Journal of Biological Chemistry 274(11): 7508-7515.
Chen, C., H. Chmelova, C. M. Cohrs, J. A. Chouinard, S. R. Jahn, J. Stertmann, I. Uphues and S. Speier (2016). "Alterations in beta-Cell Calcium Dynamics and Efficacy Outweigh Islet Mass Adaptation in Compensation of Insulin Resistance and Prediabetes Onset." Diabetes 65(9): 2676-2685.
Chen, S. Y., A. Ogawa, M. Ohneda, R. H. Unger, D. W. Foster and J. D. McGarry (1994). "More direct evidence for a malonyl-CoA-carnitine palmitoyltransferase-i interaction as a key event in pancreatic beta-cell signaling." Diabetes 43(7): 878-883.
Cheng, X., S. Y. Kim, H. Okamoto, Y. Xin, G. D. Yancopoulos, A. J. Murphy and J. Gromada (2018). "Glucagon contributes to liver zonation." Proceedings of the National Academy of Sciences of the United States of America 115(17): E4111-E4119.
Cho, J. H., L. Y. Chen, M. H. Kim, R. H. Chow, B. Hille and D. S. Koh (2010). "Characteristics and Functions of alpha-Amino-3-Hydroxy-5-Methyl-4-Isoxazolepropionate Receptors Expressed in Mouse Pancreatic alpha-Cells." Endocrinology 151(4): 1541-1550.
Cho, J. H., C. J. Swanson, J. Chen, A. Li, L. G. Lippert, S. E. Boye, K. Rose, S. Sivaramakrishnan, C. M. Chuong and R. H. Chow (2017). "The GCaMP-R Family of Genetically Encoded Ratiometric Calcium Indicators." Acs Chemical Biology 12(4): 1066-1074.
Collins, S. C., M. B. Hoppa, J. N. Walker, S. Amisten, F. Abdulkader, M. Bengtsson, J. Fearnside, R. Ramracheya, A. A. Toye, Q. Zhang, A. Clark, D. Gauguier and P. Rorsman (2010). "Progression of Diet-Induced Diabetes in C57BL6J Mice Involves Functional Dissociation of Ca(2+) Channels From Secretory Vesicles." Diabetes 59(5): 1192-1201.
Collins, S. C., A. Salehi, L. Eliasson, C. S. Olofsson and P. Rorsman (2008). "Long-term exposure of mouse pancreatic islets to oleate or palmitate results in reduced glucose-induced somatostatin and oversecretion of glucagon." Diabetologia 51(9): 1689-1693.
Conarello, S. L., G. Jiang, J. Mu, Z. Li, J. Woods, E. Zycband, J. Ronan, F. Liu, R. S. Roy, L. Zhu, M. J. Charron and B. B. Zhang (2007). "Glucagon receptor

knockout mice are resistant to diet-induced obesity and streptozotocin-mediated beta cell loss and hyperglycaemia." Diabetologia 50(1): 142-150.
Couillard, C., P. Mauriege, D. Prudhomme, A. Nadeau, A. Tremblay, C. Bouchard and J. P. Despres (1997). "Plasma leptin concentrations: gender differences and associations with metabolic risk factors for cardiovascular disease." Diabetologia 40(10): 1178-1184.
Dadi, P. K., B. Luo, N. C. Vierra and D. A. Jacobson (2015). "TASK-1 Potassium Channels Limit Pancreatic alpha-Cell Calcium Influx and Glucagon Secretion." Molecular Endocrinology 29(5): 777-787.
Dana, H., Y. Sun, B. Mohar, B. K. Hulse, A. M. Kerlin, J. P. Hasseman, G. Tsegaye, A. Tsang, A. Wong, R. Patel, J. J. Macklin, Y. Chen, A. Konnerth, V. Jayaraman, L. L. Looger, E. R. Schreiter, K. Svoboda and D. S. Kim (2019). "High-performance calcium sensors for imaging activity in neuronal populations and microcompartments." Nature Methods 16(7): 649-+.
De Marinis, Y. Z., A. Salehi, C. E. Ward, Q. Zhang, F. Abdulkader, M. Bengtsson, O. Braha, M. Braun, R. Ramracheya, S. Amisten, A. M. Habib, Y. Moritoh, E. Zhang, F. Reimann, A. H. Rosengren, T. Shibasaki, F. Gribble, E. Renstrom, S. Seino, L. Eliasson and P. Rorsman (2010). "GLP-1 Inhibits and Adrenaline Stimulates Glucagon Release by Differential Modulation of N- and L-Type Ca2+ Channel-Dependent Exocytosis." Cell Metabolism 11(6): 543-553.
Deeds, M. C., J. M. Anderson, A. S. Armstrong, D. A. Gastineau, H. J. Hiddinga, A. Jahangir, N. L. Eberhardt and Y. C. Kudva (2011). "Single dose streptozotocin-induced diabetes: considerations for study design in islet transplantation models." Laboratory Animals 45(3): 131-140.
Denwood, G., A. Tarasov, A. Salehi, L. Vergari, R. Ramracheya, H. Takahashi, V. O. Nikolaev, S. Seino, F. Gribble, F. Reimann, P. Rorsman and Q. Zhang (2019). "Glucose stimulates somatostatin secretion in pancreatic delta-cells by cAMP-dependent intracellular Ca-2+ release." Journal of General Physiology 151(9): 1094-1115.
Diabetes UK (2019). Tackling the crisis:

Transforming diabetes care for a better future

England, Diabetes UK.
DiGruccio, M. R., A. M. Mawla, C. J. Donaldson, G. M. Noguchi, J. Vaughan, C. Cowing-Zitron, T. van der Meulen and M. O. Huising (2016). "Comprehensive alpha, beta and delta cell transcriptomes reveal that ghrelin selectively activates delta cells and promotes somatostatin release from pancreatic islets." Molecular Metabolism 5(7): 449-458.
Ding, W. G., E. Renstrom, P. Rorsman, K. Buschard and J. Gromada (1997). "Glucagon-like peptide I and glucose-dependent insulinotropic polypeptide stimulate Ca2+-induced secretion in rat alpha-cells by a protein kinase A-mediated mechanism." Diabetes 46(5): 792-800.

Dobbins, R. L., S. N. Davis, D. W. Neal, C. Cobelli, J. Jaspan and A. D. Cherrington (1995). "Compartmental modeling of glucagon kinetics in the conscious dog." Metabolism-Clinical and Experimental **44**(4): 452-459.
Dobbs, R., H. Sakurai, H. Sasaki, G. Faloona, I. Valverde, D. Baetens, L. Orci and R. Unger (1975). "Glucagon - Role in hyperglycemia of diabetes-mellitus." Science **187**(4176): 544-547.
Drigo, R. A. E., S. Jacob, C. F. Garcia-Prieto, X. F. Zheng, M. Fukuda, H. T. T. Nhu, O. Stelmashenko, F. L. M. Pecanha, R. Rodriguez-Diaz, E. Bushong, T. Deerinck, S. Phan, Y. Ali, I. Leibiger, M. Chua, T. Boudier, S. H. Song, M. Graf, G. J. Augustine, M. H. Ellisman and P. O. Berggren (2019). "Structural basis for delta cell paracrine regulation in pancreatic islets (vol 10, 3700, 2019)." Nature Communications **10**.
Drucker, D. J. and S. Asa (1988). "GLUCAGON GENE-EXPRESSION IN VERTEBRATE BRAIN." Journal of Biological Chemistry **263**(27): 13475-13478.
Dunning, B. E. and J. E. Gerich (2007). "The role of alpha-cell dysregulation in fasting and postprandial hyperglycemia in type 2 diabetes and therapeutic implications." Endocrine Reviews **28**(3): 253-283.
Dusaulcy, R., S. Handgraaf, S. Skarupelova, F. Visentin, C. Vesin, M. Heddad-Masson, F. Reimann, F. Gribble, J. Philippe and Y. Gosmain (2016). "Functional and Molecular Adaptations of Enteroendocrine L-Cells in Male Obese Mice Are Associated With Preservation of Pancreatic alpha-Cell Function and Prevention of Hyperglycemia." Endocrinology **157**(10): 3832-3843.
Dusaulcy, R., S. Handgraaf, S. Skarupelova, F. Visentin, C. Vesin, M. Heddad-Masson, F. Reimann, F. Gribble, J. Philippe and Y. Gosmain (2016). "Functional and Molecular Adaptations of Enteroendocrine L-Cells in Male Obese Mice Are Associated With Preservation of Pancreatic α-Cell Function and Prevention of Hyperglycemia." Endocrinology **157**(10): 3832-3843.
Dusaulcy, R., S. Handgraaf, F. Visentin, C. Howald, E. T. Dermitzakis, J. Philippe and Y. Gosmain (2019). "High-fat diet impacts more changes in beta-cell compared to alpha-cell transcriptome." Plos One **14**(3).
Eisenstein, A. B. and I. Strack (1978). "Amino-acid stimulation of glucagon-secretion by perifused islets of high-protein-fed rats." Diabetes **27**(4): 370-376.
Ellingsgaard, H., J. A. Ehses, E. B. Hammar, L. Van Lommel, R. Quintens, G. Martens, J. Kerr-Conte, F. Pattou, T. Berney, D. Pipeleers, P. A. Halban, F. C. Schuit and M. Y. Donath (2008). "Interleukin-6 regulates pancreatic alpha-cell mass expansion." Proceedings of the National Academy of Sciences of the United States of America **105**(35): 13163-13168.
Elliott, A. D., A. Ustione and D. W. Piston (2015). "Somatostatin and insulin mediate glucose-inhibited glucagon secretion in the pancreatic alpha-cell by lowering cAMP." American Journal of Physiology-Endocrinology and Metabolism **308**(2): E130-E143.

Faerch, K., A. Vaag, J. J. Holst, C. Glumer, O. Pedersen and K. Borch-Johnsen (2008). "Impaired fasting glycaemia vs impaired glucose tolerance: similar impairment of pancreatic alpha and beta cell function but differential roles of incretin hormones and insulin action." Diabetologia 51(5): 853-861.
Faerch, K., D. Vistisen, G. Pacini, S. S. Torekov, N. B. Johansen, D. R. Witte, A. Jonsson, O. Pedersen, T. Hansen, T. Lauritzen, M. E. Jorgensen, B. Ahren and J. J. Holst (2016). "Insulin Resistance Is Accompanied by Increased Fasting Glucagon and Delayed Glucagon Suppression in Individuals With Normal and Impaired Glucose Regulation." Diabetes 65(11): 3473-3481.
Felig, P., E. Marliss and G. F. Cahill (1969). "Plasma amino acid levels and insulin secretion in obesity." New England Journal of Medicine 281(15): 811-+.
Figueroa-Romero, C., M. Sadidi and E. L. Feldman (2008). "Mechanisms of disease: The oxidative stress theory of diabetic neuropathy." Reviews in Endocrine & Metabolic Disorders 9(4): 301-314.
Fisher-Wellman, K. H., T. E. Ryan, C. D. Smith, L. A. A. Gilliam, C. T. Lin, L. R. Reese, M. J. Torres and P. D. Neufer (2016). "A Direct Comparison of Metabolic Responses to High-Fat Diet in C57BL/6J and C57BL/6NJ Mice." Diabetes 65(11): 3249-3261.
Froy, O. and R. Miskin (2010). "Effect of feeding regimens on circadian rhythms: Implications for aging and longevity." Aging-Us 2(1): 7-27.
Ge, Q., Y. M. Dong, Z. T. Hu, Z. X. Wu and T. Xu (2006). "Characteristics of Ca2+-exocytosis coupling in isolated mouse pancreatic beta cells." Acta Pharmacologica Sinica 27(7): 933-938.
Gelling, R. W., X. Q. Du, D. S. Dichmann, J. Romer, H. Huang, L. Cui, S. Obici, B. Tang, J. J. Holst, C. Fledelius, P. B. Johansen, L. Rossetti, L. A. Jelicks, P. Serup, E. Nishimura and M. J. Charron (2003). "Lower blood glucose, hyperglucagonemia, and pancreatic alpha cell hyperplasia in glucagon receptor knockout mice." Proceedings of the National Academy of Sciences of the United States of America 100(3): 1438-1443.
Gerich, J. E. (1993). "Control of glycemia." Baillieres Clinical Endocrinology and Metabolism 7(3): 551-586.
Gerich, J. E., M. Langlois, C. Noacco, J. H. Karam and P. H. Forsham (1973). "Lack of glucagon response to hypoglycemia in diabetes - evidence for an intrinsic pancreatic alpha cell defect." Science 182(4108): 171-173.
Gonzalez, A., B. Merino, L. Marroqui, P. Neco, P. Alonso-Magdalena, E. Caballero-Garrido, E. Vieira, S. Soriano, R. Gomis, A. Nadal and I. Quesada (2013). "Insulin Hypersecretion in Islets From Diet-Induced Hyperinsulinemic Obese Female Mice Is Associated With Several Functional Adaptations in Individual beta-Cells." Endocrinology 154(10): 3515-3524.
Gopel, S. O., T. Kanno, S. Barg, X. G. Weng, J. Gromada and P. Rorsman (2000). "Regulation of glucagon release in mouse alpha-cells by K-ATP channels and

inactivation of TTX-sensitive Na+ channels." Journal of Physiology-London 528(3): 509-520.
Gromada, J., K. Bokvist, W. G. Ding, S. Barg, K. Buschard, E. Renstrom and P. Rorsman (1997). "Adrenaline stimulates glucagon secretion in pancreatic A-cells by increasing the Ca2+ current and the number of granules close to the L-type Ca2+ channels." Journal of General Physiology 110(3): 217-228.
Gromada, J., P. Chabosseau and G. A. Rutter (2018). "The alpha-cell in diabetes mellitus." Nature Reviews Endocrinology 14(12): 694-704.
Gromada, J., X. S. Ma, M. Hoy, K. Bokvist, A. Salehi, P. O. Berggren and P. Rorsman (2004). "ATP-sensitive K+ channel-dependent regulation of glucagon release and electrical actiflty by glucose in wild-type and SUR1(-/-) mouse alpha-cells." Diabetes 53: S181-S189.
Groop, L. C., R. C. Bonadonna, S. Delprato, K. Ratheiser, K. Zyck, E. Ferrannini and R. A. Defronzo (1989). "GLUCOSE AND FREE FATTY-ACID METABOLISM IN NON-INSULIN-DEPENDENT DIABETES-MELLITUS - EVIDENCE FOR MULTIPLE SITES OF INSULIN RESISTANCE." Journal of Clinical Investigation 84(1): 205-213.
Guo, S., C. Dai, M. Guo, B. Taylor, J. S. Harmon, M. Sander, R. P. Robertson, A. C. Powers and R. Stein (2013). "Inactivation of specific beta cell transcription factors in type 2 diabetes." Journal of Clinical Investigation 123(8): 3305-3316.
Gustavsson, N., S.-H. Wei, D. N. Hoang, Y. Lao, Q. Zhang, G. K. Radda, P. Rorsman, T. C. Sudhof and W. Han (2009). "Synaptotagmin-7 is a principal Ca2+ sensor for Ca2+-induced glucagon exocytosis in pancreas." Journal of Physiology-London 587(6): 1169-1178.
Gylfe, E. (2016). "Glucose control of glucagon secretion-'There's a brand-new gimmick every year'." Upsala Journal of Medical Sciences 121(2): 120-132.
Hamilton, A., Q. Zhang, A. Salehi, M. Willems, J. G. Knudsen, A. K. Ringgaard, C. E. Chapman, A. Gonzalez-Alvarez, N. C. Surdo, M. Zaccolo, D. Basco, P. R. V. Johnson, R. Ramracheya, G. A. Rutter, A. Galione, P. Rorsman and A. I. Tarasov (2018). "Adrenaline Stimulates Glucagon Secretion by Tpc2-Dependent Ca2+ Mobilization From Acidic Stores in Pancreatic alpha-Cells." Diabetes 67(6): 1128-1139.
Hauge-Evans, A. C., A. J. King, D. Carmignac, C. C. Richardson, I. C. A. F. Robinson, M. J. Low, M. R. Christie, S. J. Persaud and P. M. Jones (2009). "Somatostatin Secreted by Islet delta-Cells Fulfills Multiple Roles as a Paracrine Regulator of Islet Function." Diabetes 58(2): 403-411.
He, L., T. Kim, Q. Long, J. Liu, P. Wang, Y. Zhou, Y. Ding, J. Prasain, P. A. Wood and Q. Yang (2012). "Carnitine Palmitoyltransferase-1b Deficiency Aggravates Pressure Overload-Induced Cardiac Hypertrophy Caused by Lipotoxicity." Circulation 126(14): 1705-+.

Heller, R. S., T. J. Kieffer and J. F. Habener (1997). "Insulinotropic glucagon-like peptide I receptor expression in glucagon-producing alpha-cells of the rat endocrine pancreas." Diabetes 46(5): 785-791.
Heller, S. R., I. A. Macdonald and R. B. Tattersall (1987). "Counterregulation in type-2 (non-insulin-dependent) diabetes-mellitus - normal endocrine and glycemic responses, up to 10 years after diagnosis." Diabetologia 30(12): 924-929.
Herman, M. A. and B. B. Kahn (2006). "Glucose transport and sensing in the maintenance of glucose homeostasis and metabolic harmony." Journal of Clinical Investigation 116(7): 1767-1775.
Herzig, S., F. X. Long, U. S. Jhala, S. Hedrick, R. Quinn, A. Bauer, D. Rudolph, G. Schutz, C. Yoon, P. Puigserver, B. Spiegelman and M. Montminy (2001). "CREB regulates hepatic gluconeogenesis through the coactivator PGC-1." Nature 413(6852): 179-183.
Hex, N., C. Bartlett, D. Wright, M. Taylor and D. Varley (2012). "Estimating the current and future costs of Type 1 and Type 2 diabetes in the UK, including direct health costs and indirect societal and productivity costs." Diabetic Medicine 29(7): 855-862.
Hmeadi, M. O., P. E. Lund, N. R. Gandasi, A. Tengholm and S. Barg (2019). "Paracrine control of alpha cell glucagon exocytosis is compromised in human type 2 diabetes." Diabetologia 62: S56-S56.
Hodson, D. J., R. K. Mitchell, E. A. Bellomo, G. Sun, L. Vinet, P. Meda, D. Li, W.-H. Li, M. Bugliani, P. Marchetti, D. Bosco, L. Piemonti, P. Johnson, S. J. Hughes and G. A. Rutter (2013). "Lipotoxicity disrupts incretin-regulated human beta cell connectivity." Journal of Clinical Investigation 123(10): 4182-4194.
Hofherr, A., C. Wagner, S. Fedeles, S. Somlo and M. Kottgen (2014). "N-Glycosylation Determines the Abundance of the Transient Receptor Potential Channel TRPP2." Journal of Biological Chemistry 289(21): 14854-14867.
Holst, J. J., N. J. W. Albrechtsen, J. Pedersen and F. K. Knop (2017). "Glucagon and Amino Acids Are Linked in a Mutual Feedback Cycle: The Liver-alpha-Cell Axis." Diabetes 66(2): 235-240.
Hong, J., P. B. Jeppesen, I. Nordentoft and K. Hermansen (2007). "Fatty acid-induced effect on glucagon secretion is mediated via fatty acid oxidation." Diabetes-Metabolism Research and Reviews 23(3): 202-210.
Hsu, P.-F., S.-H. Sung, H.-M. Cheng, J.-S. Yeh, W.-L. Liu, W.-L. Chan, C.-H. Chen, P. Chou and S.-Y. Chuang (2013). "Association of Clinical Symptomatic Hypoglycemia With Cardiovascular Events and Total Mortality in Type 2 Diabetes A nationwide population-based study." Diabetes Care 36(4): 894-900.
Hughes, D. S. and P. Narendran (2014). Alpha cell function in type 1 diabetes, THE BRITISH JOURNAL OF DIABETES AND VASCULAR DISEASE. 14.

Hummel, K. P., P. W. Lane and D. L. Coleman (1972). "INFLUENCE OF GENETIC BACKGROUND ON EXPRESSION OF MUTATIONS AT DIABETES LOCUS IN MOUSE .1. C57BL-KSJ AND C57BL-6J STRAINS." Biochemical Genetics 7(1): 1-&.
Ishihara, H., P. Maechler, A. Gjinovci, P. L. Herrera and C. B. Wollheim (2003). "Islet beta-cell secretion determines glucagon release from neighbouring alpha-cells." Nature Cell Biology 5(4): 330-335.
Johansson, H., E. Gylfe and B. Hellman (1987). "THE ACTIONS OF ARGININE AND GLUCOSE ON GLUCAGON-SECRETION ARE MEDIATED BY OPPOSITE EFFECTS ON CYTOPLASMIC CA-2+." Biochemical and Biophysical Research Communications 147(1): 309-314.
Johnson, R. M., Y.-S. Ho, D.-Y. Yu, F. A. Kuypers, Y. Ravindranath and G. W. Goyette (2010). "The effects of disruption of genes for peroxiredoxin-2, glutathione peroxidase-1, and catalase on erythrocyte oxidative metabolism." Free Radical Biology and Medicine 48(4): 519-525.
Jorgensen, M. S., K. S. Tornqvist and H. Hvid (2017). "Calculation of Glucose Dose for Intraperitoneal Glucose Tolerance Tests in Lean and Obese Mice." Journal of the American Association for Laboratory Animal Science 56(1): 95-97.
Jurgens, C. A., M. N. Toukatly, C. L. Fligner, J. Udayasankar, S. L. Subramanian, S. Zraika, K. Aston-Mourney, D. B. Carr, P. Westermark, G. T. Westermark, S. E. Kahn and R. L. Hull (2011). "beta-Cell Loss and beta-Cell Apoptosis in Human Type 2 Diabetes Are Related to Islet Amyloid Deposition." American Journal of Pathology 178(6): 2632-2640.
Karpe, F., J. R. Dickmann and K. N. Frayn (2011). "Fatty Acids, Obesity, and Insulin Resistance: Time for a Reevaluation." Diabetes 60(10): 2441-2449.
Kazda, C. M., Y. Ding, R. P. Kelly, P. Garhyan, C. Shi, C. N. Lim, H. Fu, D. E. Watson, A. J. Lewin, W. H. Landschulz, M. A. Deeg, D. E. Moller and T. A. Hardy (2016). "Evaluation of Efficacy and Safety of the Glucagon Receptor Antagonist LY2409021 in Patients With Type 2 Diabetes: 12-and 24-Week Phase 2 Studies." Diabetes Care 39(7): 1241-1249.
Kazierad, D. J., K. Chidsey, V. R. Somayaji, A. J. Bergman and R. A. Calle (2018). "Efficacy and safety of the glucagon receptor antagonist PF-06291874: A 12-week, randomized, dose-response study in patients with type 2 diabetes mellitus on background metformin therapy." Diabetes Obesity & Metabolism 20(11): 2608-2616.
Kelly, R. P., P. Garhyan, E. Raddad, H. Fu, C. N. Lim, M. J. Prince, J. A. Pinaire, M. T. Loh and M. A. Deeg (2015). "Short-term administration of the glucagon receptor antagonist LY2409021 lowers blood glucose in healthy people and in those with type 2 diabetes." Diabetes Obesity & Metabolism 17(4): 414-422.
Kelpe, C. L., L. M. Johnson and V. Poitout (2002). "Increasing triglyceride synthesis inhibits glucose-induced insulin secretion in isolated rat islets of

Langerhans: A study using adenoviral expression of diacylglycerol acyltransferase." Endocrinology 143(9): 3326-3332.
Kenty, J. H. R. and D. A. Melton (2015). "Testing Pancreatic Islet Function at the Single Cell Level by Calcium Influx with Associated Marker Expression." Plos One 10(4).
Kim, A., K. Miller, J. Jo, G. Kilimnik, P. Wojcik and M. Hara (2009). "Islet architecture A comparative study." Islets 1(2): 129-136.
Kim, J. Y., R. C. Hickner, R. L. Cortright, G. L. Dohm and J. A. Houmard (2000). "Lipid oxidation is reduced in obese human skeletal muscle." American Journal of Physiology-Endocrinology and Metabolism 279(5): E1039-E1044.
Kim, T., L. He, M. S. Johnson, Y. Li, L. Zeng, Y. Ding, Q. Long, J. F. Moore, J. D. Sharer, T. R. Nagy, M. E. Young, P. A. Wood and Q. Yang (2014). "Carnitine Palmitoyltransferase 1b Deficiency Protects Mice from Diet-Induced Insulin Resistance." Journal of diabetes & metabolism 5(4): 361-361.
Knudsen, L., B. F. Hansen, P. Jensen, T. A. Pedersen, K. Vestergaard, L. Schaffer, B. Blagoev, M. B. Oleksiewicz, V. V. Kiselyov and P. De Meyts (2012). "Agonism and Antagonism at the Insulin Receptor." Plos One 7(12).
Koenig, M., S. Bulik and H.-G. Holzhuetter (2012). "Quantifying the Contribution of the Liver to Glucose Homeostasis: A Detailed Kinetic Model of Human Hepatic Glucose Metabolism." Plos Computational Biology 8(6).
Koo, S. H., L. Flechner, L. Qi, X. M. Zhang, R. A. Screaton, S. Jeffries, S. Hedrick, W. Xu, F. Boussouar, P. Brindle, H. Takemori and M. Montminy (2005). "The CREB coactivator TORC2 is a key regulator of fasting glucose metabolism." Nature 437(7062): 1109-1114.
Koster, J. C., M. A. Permutt and C. G. Nichols (2005). "Diabetes and insulin secretion - The ATP-sensitive K+ channel (K-ATP) connection." Diabetes 54(11): 3065-3072.
Kostic, A., T. A. King, F. Yang, K. C. Chan, G. D. Yancopoulos, J. Gromada and J. B. Harp (2018). "A first-in-human pharmacodynamic and pharmacokinetic study of a fully human anti-glucagon receptor monoclonal antibody in normal healthy volunteers." Diabetes Obesity & Metabolism 20(2): 283-291.
Kristinsson, H., E. Sargsyan, H. Manell, D. M. Smith, S. O. Gopel and P. Bergsten (2017). "Basal hypersecretion of glucagon and insulin from palmitate-exposed human islets depends on FFAR1 but not decreased somatostatin secretion." Scientific Reports 7.
Lai, B. K., H. Chae, A. Gómez-Ruiz, P. Cheng, P. Gallo, N. Antoine, C. Beauloye, J. C. Jonas, V. Seghers, S. Seino and P. Gilon (2018). Somatostatin is Only Partly Required for the Glucagonostatic Effect of Glucose but is Necessary for the Glucagonostatic Effect of K ATP Channel Blockers, Diabetes.
Lai, Y., X. C. Lou, C. Q. Wang, T. Xia and J. S. Tong (2014). "Synaptotagmin 1 and Ca2+ drive trans SNARE zippering." Scientific Reports 4.

Landstedt-Hallin, L., U. Adamson and P. E. Lins (1999). "Oral glibenclamide suppresses glucagon secretion during insulin-induced hypoglycemia in patients with type 2 diabetes." Journal of Clinical Endocrinology & Metabolism 84(9): 3140-3145.
Larger, E., N. J. W. Albrechtsen, L. H. Hansen, R. W. Gelling, J. Capeau, C. F. Deacon, O. D. Madsen, F. Yakushiji, P. De Meyts, J. J. Holst and E. Nishimura (2016). "Pancreatic alpha-cell hyperplasia and hyperglucagonemia due to a glucagon receptor splice mutation." Endocrinology Diabetes and Metabolism Case Reports.
Law, C. W., Y. S. Chen, W. Shi and G. K. Smyth (2014). "voom: precision weights unlock linear model analysis tools for RNA-seq read counts." Genome Biology 15(2).
Lawlor, N., J. George, M. Bolisetty, R. Kursawe, L. Sun, V. Sivakamasundari, I. Kycia, P. Robson and M. L. Stitzel (2017). "Single-cell transcriptomes identify human islet cell signatures and reveal cell-type specific expression changes in type 2 diabetes." Genome Research 27(2): 208-222.
Le Marchand, S. J. and D. W. Piston (2010). "Glucose suppression of glucagon secretion metabolic and calcium responses from alpha-cells in intact mouse pancreatic islets." Journal of Biological Chemistry 285(19): 14389-14398.
Le Marchand, S. J. and D. W. Piston (2012). "Glucose Decouples Intracellular Ca2+ Activity from Glucagon Secretion in Mouse Pancreatic Islet Alpha-Cells." Plos One 7(10).
Lee, H.-K., Y. Yang, Z. Su, C. Hyeon, T.-S. Lee, H.-W. Lee, D.-H. Kweon, Y.-K. Shin and T.-Y. Yoon (2010). "Dynamic Ca2+-Dependent Stimulation of Vesicle Fusion by Membrane-Anchored Synaptotagmin 1." Science 328(5979): 760-763.
Lee, Y., E. D. Berglund, M.-y. Wang, X. Fu, X. Yu, M. J. Charron, S. C. Burgess and R. H. Unger (2012). "Metabolic manifestations of insulin deficiency do not occur without glucagon action." Proceedings of the National Academy of Sciences of the United States of America 109(37): 14972-14976.
Lee, Y., M.-Y. Wang, X. Q. Du, M. J. Charron and R. H. Unger (2011). "Glucagon Receptor Knockout Prevents Insulin-Deficient Type 1 Diabetes in Mice." Diabetes 60(2): 391-397.
Leibiger, B., T. Moede, T. P. Muhandiramlage, D. Kaiser, P. V. Sanchez, I. B. Leibiger and P.-O. Berggren (2012). "Glucagon regulates its own synthesis by autocrine signaling." Proceedings of the National Academy of Sciences of the United States of America 109(51): 20925-20930.
Leiter, E. H. (2009). "Selecting the "Right" Mouse Model for Metabolic Syndrome and Type 2 Diabetes Research." Type 2 Diabetes: Methods and Protocols 560: 1-17.

Li, J., Q. Yu, P. Ahooghalandari, F. M. Gribble, F. Reimann, A. Tengholm and E. Gylfe (2015). "Submembrane ATP and Ca2+ kinetics in alpha-cells: unexpected signaling for glucagon secretion." Faseb Journal 29(8): 3379-3388.
Liu, H. S., M. S. Jan, C. K. Chou, P. H. Chen and N. J. Ke (1999). "Is green fluorescent protein toxic to the living cells?" Biochemical and Biophysical Research Communications 260(3): 712-717.
Liu, L., J. Yang, F. Qian and C. Lu (2017). "Hypothalamic-pituitary-adrenal axis hypersensitivity in female rats on a post-weaning high-fat diet after chronic mild stress." Experimental and Therapeutic Medicine 14(1): 439-446.
Liu, T.-W., T. D. Heden, A. Blandon, E. M. Morris, K. L. Fritsche and J. P. Thyfault (2013). "High-fat diet alters serum fatty acid profiles in obesity prone rats: implications for in-vitro studies." Faseb Journal 27.
Liu, Y. J., H. Y. Cheng, H. Drought, M. J. MacDonald, G. W. G. Sharp and S. G. Straub (2003). "Activation of the K-ATP channel-independent signaling pathway by the nonhydrolyzable analog of leucine, BCH." American Journal of Physiology-Endocrinology and Metabolism 285(2): E380-E389.
Liu, Y. J., E. Vieira and E. Gylfe (2004). "A store-operated mechanism determines the activity of the electrically excitable glucagon-secreting pancreatic alpha-cell." Cell Calcium 35(4): 357-365.
Lund, A., J. I. Bagger, N. J. W. Albrechtsen, M. Christensen, M. Grondahl, B. Hartmann, E. R. Mathiesen, C. P. Hansen, J. H. Storkholm, G. van Hall, J. F. Rehfeld, D. Hornburg, F. Meissner, M. Mann, S. Larsen, J. J. Holst, T. Vilsboll and F. K. Knop (2016). "Evidence of Extrapancreatic Glucagon Secretion in Man." Diabetes 65(3): 585-597.
Lund, A. and F. K. Knop (2019). "Extrapancreatic glucagon: Present status." Diabetes Research and Clinical Practice 147: 19-28.
Ma, X. S., Y. Zhang, J. Gromada, S. Sewing, P. O. Berggren, K. Buschard, A. Salehi, J. Vikman, P. Rorsman and L. Eliasson (2005). "Glucagon stimulates exocytosis in mouse and rat pancreatic alpha-cells by binding to glucagon receptors." Molecular Endocrinology 19(1): 198-212.
MacDonald, M. J., L. Ade, J. M. Ntambi, I. U. Ansari and S. W. Stoker (2015). "Characterization of Phospholipids in Insulin Secretory Granules and Mitochondria in Pancreatic Beta Cells and Their Changes with Glucose Stimulation." Journal of Biological Chemistry 290(17): 11075-11092.
MacDonald, P. E., Y. Z. De Marinis, R. Ramracheya, A. Salehi, X. Ma, P. R. V. Johnson, R. Cox, L. Eliasson and P. Rorsman (2007). "A K-ATP channel-dependent pathway within alpha cells regulates glucagon release from both rodent and human islets of langerhans." Plos Biology 5(6): 1236-1247.
Manell, H., J. Staaf, L. Manukyan, H. Kristinsson, J. Cen, R. Stenlid, I. Ciba, A. Forslund and P. Bergsten (2016). "Altered Plasma Levels of Glucagon, GLP-1 and Glicentin During OGTT in Adolescents With Obesity and Type 2 Diabetes." Journal of Clinical Endocrinology & Metabolism 101(3): 1181-1189.

Marliss, E. B., T. T. Aoki, R. H. Unger, J. S. Soeldner and G. F. Cahill (1970). "GLUCAGON LEVELS AND METABOLIC EFFECTS IN FASTING MAN." Journal of Clinical Investigation 49(12): 2256-&.
Marroqui, L., E. Vieira, A. Gonzalez, A. Nadal and I. Quesada (2011). "Leptin downregulates expression of the gene encoding glucagon in alphaTC1-9 cells and mouse islets." Diabetologia 54(4): 843-851.
Mawla, A. M. and M. O. Huising (2019). "Navigating the Depths and Avoiding the Shallows of Pancreatic Islet Cell Transcriptomes." Diabetes 68(7): 1380-1393.
McDuffie, M., N. A. Maybee, S. R. Keller, B. K. Stevens, J. C. Garmey, M. A. Morris, E. Kropf, C. Rival, K. Ma, J. D. Carter, S. A. Tersey, C. S. Nunemaker and J. L. Nadler (2008). "Nonobese diabetic (NOD) mice Congenic for a targeted deletion of 12/15-lipoxygenase are protected from autoimmune diabetes." Diabetes 57(1): 199-208.
McGuinness, O. P., J. E. Ayala, M. R. Laughlin and D. H. Wasserman (2009). "NIH experiment in centralized mouse phenotyping: the Vanderbilt experience and recommendations for evaluating glucose homeostasis in the mouse." American Journal of Physiology-Endocrinology and Metabolism 297(4): E849-E855.
Meier, J. J., C. F. Deacon, W. E. Schmidt, J. J. Holst and M. A. Nauck (2007). "Suppression of glucagon secretion is lower after oral glucose administration than during intravenous glucose administration in human subjects." Diabetologia 50(4): 806-813.
Meier, J. J., B. Gallwitz, N. Siepmann, J. J. Holst, C. F. Deacon, W. E. Schmidt and M. A. Nauck (2003). "Gastric inhibitory polypeptide (GIP) dose-dependently stimulates glucagon secretion in healthy human subjects at euglycaemia." Diabetologia 46(6): 798-801.
Menegaz, D., D. W. Hagan, J. Almaca, C. Cianciaruso, R. Rodriguez-Diaz, J. Molina, R. M. Dolan, M. W. Becker, P. C. Schwalie, R. Nano, F. Lebreton, C. Kang, R. Sah, H. Y. Gaisano, P. O. Berggren, S. Baekkeskov, A. Caicedo and E. A. Phelps (2019). "Mechanism and effects of pulsatile GABA secretion from cytosolic pools in the human beta cell." Nature Metabolism 1(11): 1110-+.
Menge, B. A., L. Gruber, S. M. Jorgensen, C. F. Deacon, W. E. Schmidt, J. D. Veldhuis, J. J. Holst and J. J. Meier (2011). "Loss of Inverse Relationship Between Pulsatile Insulin and Glucagon Secretion in Patients With Type 2 Diabetes." Diabetes 60(8): 2160-2168.
Merino, B., P. Alonso-Magdalena, M. Lluesma, P. Neco, A. Gonzalez, L. Marroqui, M. Garcia-Arevalo, A. Nadal and I. Quesada (2015). "Pancreatic alpha-cells from female mice undergo morphofunctional changes during compensatory adaptations of the endocrine pancreas to diet-induced obesity." Scientific Reports 5.

Miller, H. C., M. Kidd, I. M. Modlin, P. Cohen, R. Dina, P. Drymousis, P. Vlavianos, G. Kloeppel and A. Frilling (2015). "Glucagon receptor gene mutations with hyperglucagonemia but without the glucagonoma syndrome." World Journal of Gastrointestinal Surgery 7(4): 60-66.
Missiaen, L., H. Desmedt, G. Droogmans and R. Casteels (1992). "CA2+ RELEASE INDUCED BY INOSITOL 1,4,5-TRISPHOSPHATE IS A STEADY-STATE PHENOMENON CONTROLLED BY LUMINAL CA2+ IN PERMEABILIZED CELLS." Nature 357(6379): 599-602.
Moens, K., H. Heimberg, D. Flamez, P. Huypens, E. Quartier, Z. D. Ling, D. Pipeleers, S. Gremlich, B. Thorens and F. Schuit (1996). "Expression and functional activity of glucagon, glucagon-like peptide I, and glucose-dependent insulinotropic peptide receptors in rat pancreatic islet cells." Diabetes 45(2): 257-261.
Moffitt, J. H., B. A. Fielding, R. Evershed, R. Berstan, J. M. Currie and A. Clark (2005). "Adverse physicochemical properties of tripalmitin in beta cells lead to morphological changes and lipotoxicity in vitro." Diabetologia 48(9): 1819-1829.
Montgomery, M. K., N. L. Hallahan, S. H. Brown, M. Liu, T. W. Mitchell, G. J. Cooney and N. Turner (2013). "Mouse strain-dependent variation in obesity and glucose homeostasis in response to high-fat feeding." Diabetologia 56(5): 1129-1139.
Morgan, E. S., L.-J. Tai, N. C. Pham, J. K. Overman, L. M. Watts, A. Smith, S. W. Jung, M. Gajdosik, M. Krssak, M. Krebs, R. S. Geary, B. F. Baker and S. Bhanot (2019). "Antisense Inhibition of Glucagon Receptor by IONIS-GCGR(Rx) Improves Type 2 Diabetes Without Increase in Hepatic Glycogen Content in Patients With Type 2 Diabetes on Stable Metformin Therapy." Diabetes Care 42(4): 585-593.
Mu, J., S. A. Qureshi, E. J. Brady, E. S. Muise, M. R. Candelore, G. Q. Jiang, Z. H. Li, M. S. Wu, X. D. Yang, Q. Dallas-Yang, C. Miller, Y. S. Xiong, R. B. Langdon, E. R. Parmee and B. B. Zhang (2012). "Anti-Diabetic Efficacy and Impact on Amino Acid Metabolism of GRA1, a Novel Small-Molecule Glucagon Receptor Antagonist." Plos One 7(11).
Munzberg, H., J. S. Flier and C. Bjorbaek (2004). "Region-specific leptin resistance within the hypothalamus of diet-induced obese mice." Endocrinology 145(11): 4880-4889.
Nadal, A., I. Quesada and B. Soria (1999). "Homologous and heterologous asynchronicity between identified alpha-, beta- and delta-cells within intact islets of Langerhans in the mouse." Journal of Physiology-London 517(1): 85-93.
Nagel, F. and S. Schulz (2010). "Structural determinants of agonist-selective signaling at the SST2A somatostatin receptor." Naunyn-Schmiedebergs Archives of Pharmacology 381: 11-11.

Nakamura, H., H. Jinzu, K. Nagao, Y. Noguchi, N. Shimba, H. Miyano, T. Watanabe and K. Iseki (2014). "Plasma amino acid profiles are associated with insulin, C-peptide and adiponectin levels in type 2 diabetic patients." Nutrition & Diabetes 4.
Nauck, M. A., M. M. Heimesaat, K. Behle, J. J. Holst, M. S. Nauck, R. Ritzel, M. Hufner and W. H. Schmiegel (2002). "Effects of glucagon-like peptide 1 on counterregulatory hormone responses, cognitive functions, and insulin secretion during hyperinsulinemic, stepped hypoglycemic clamp experiments in healthy volunteers." Journal of Clinical Endocrinology & Metabolism 87(3): 1239-1246.
Nicholson, A., P. C. Reifsnyder, R. D. Malcolm, C. A. Lucas, G. R. MacGregor, W. D. Zhang and E. H. Leiter (2010). "Diet-induced Obesity in Two C57BL/6 Substrains With Intact or Mutant Nicotinamide Nucleotide Transhydrogenase (Nnt) Gene." Obesity 18(10): 1902-1905.
O'Connor, R. S., L. L. Guo, S. Ghassemi, N. W. Snyder, A. J. Worth, L. Weng, Y. Kam, B. Philipson, S. Trefely, S. Nunez-Cruz, I. A. Blair, C. H. June and M. C. Milone (2018). "The CPT1a inhibitor, etomoxir induces severe oxidative stress at commonly used concentrations." Scientific Reports 8.
Oh, Y. S., G. D. Bae, D. J. Baek, E.-Y. Park and H.-S. Jun (2018). "Fatty Acid-Induced Lipotoxicity in Pancreatic Beta-Cells During Development of Type 2 Diabetes." Frontiers in Endocrinology 9.
Olofsson, C. S., A. Salehi, S. O. Gopel, C. Holm and P. Rorsman (2004). "Palmitate stimulation of glucagon secretion in mouse pancreatic alpha-cells results from activation of L-type calcium channels and elevation of cytoplasmic calcium." Diabetes 53(11): 2836-2843.
Olofsson, C. S., A. Salehi, C. Holm and P. Rorsman (2004). "Palmitate increases L-type Ca2+ currents and the size of the readily releasable granule pool in mouse pancreatic beta-cells." Journal of Physiology-London 557(3): 935-948.
Orgaard, A. and J. J. Holst (2017). "The role of somatostatin in GLP-1-induced inhibition of glucagon secretion in mice." Diabetologia 60(9): 1731-1739.
Ostenson, C. G. (1979). "Regulation of glucagon-release - effects of insulin on the pancreatic a2-cell of the guinea-pig." Diabetologia 17(5): 325-330.
Ouhilal, S., P. Vuguin, L. Cui, X.-Q. Du, R. W. Gelling, S. E. Reznik, R. Russell, A. F. Parlow, C. Karpovsky, N. Santoro and M. J. Charron (2012). "Hypoglycemia, hyperglucagonemia, and fetoplacental defects in glucagon receptor knockout mice: a role for glucagon action in pregnancy maintenance." American Journal of Physiology-Endocrinology and Metabolism 302(5): E522-E531.
Owen, O. E., L. Tappy, M. A. Mozzoli and K. j. Smalley (1990). Acute starvation. The metabolic and molecular basis of acquired disease. London, UK., Bailliere Tindall. 1: 550-570.
Pacini, G., B. Omar and B. Ahren (2013). "Methods and Models for Metabolic Assessment in Mice." Journal of Diabetes Research.

Parker, H. E., A. Adriaenssens, G. Rogers, P. Richards, H. Koepsell, F. Reimann and F. M. Gribble (2012). "Predominant role of active versus facilitative glucose transport for glucagon-like peptide-1 secretion." Diabetologia 55(9): 2445-2455.
Patro, R., G. Duggal, M. I. Love, R. A. Irizarry and C. Kingsford (2017). "Salmon provides fast and bias-aware quantification of transcript expression." Nature Methods 14(4): 417-+.
Paulsen, S. K., S. B. Pedersen, S. Fisker and B. Richelsen (2007). "11,beta-HSD type 1 expression in human adipose, tissue: Impact of gender, obesity, and fat localization." Obesity 15(8): 1954-1960.
Pearson, M. J., R. H. Unger and W. L. Holland (2016). "Clinical Trials, Triumphs, and Tribulations of Glucagon Receptor Antagonists." Diabetes Care 39(7): 1075-1077.
Pettus, J. H., D. D'Alessio, J. P. Frias, E. G. Vajda, J. D. Pipkin, J. Rosenstock, G. Williamson, M. A. Zangmeister, L. Zhi and K. B. Marschke (2020). "Efficacy and Safety of the Glucagon Receptor Antagonist RVT-1502 in Type 2 Diabetes Uncontrolled on Metformin Monotherapy: A 12-Week Dose-Ranging Study." Diabetes care 43(1): 161-168.
Peyot, M. L., E. Pepin, J. Lamontagne, M. G. Latour, B. Zarrouki, R. Lussier, M. Pineda, T. L. Jetton, S. R. M. Madiraju, E. Joly and M. Prentki (2010). "beta-Cell Failure in Diet-Induced Obese Mice Stratified According to Body Weight Gain: Secretory Dysfunction and Altered Islet Lipid Metabolism Without Steatosis or Reduced beta-Cell Mass." Diabetes 59(9): 2178-2187.
Pian, M. S., L. G. Dobbs and N. Duzgunes (1988). "Positive correlation between cytosolic free calcium and surfactant secretion in cultured rat alveolar type-ii cells." Biochimica Et Biophysica Acta 960(1): 43-53.
Picelli, S., O. R. Faridani, A. K. Bjorklund, G. Winberg, S. Sagasser and R. Sandberg (2014). "Full-length RNA-seq from single cells using Smart-seq2." Nature Protocols 9(1): 171-181.
Quesada, I., A. Nadal and B. Soria (1999). "Different effects of tolbutamide and diazoxide in alpha-, beta-, and delta-cells within intact islets of Langerhans." Diabetes 48(12): 2390-2397.
Quesada, I., M. G. Todorova, P. Alonso-Magdalena, M. Beltra, E. M. Carneiro, F. Martin, A. Nadal and B. Soria (2006). "Glucose induces opposite intracellular ca(2+) concentration oscillatory patterns in identified alpha- and beta-cells within intact human islets of langerhans." Diabetes 55(9): 2463-2469.
Quoix, N., R. Cheng-Xue, Y. Guiot, P. L. Herrera, J. C. Henquin and P. Gilon (2007). "The GluCre-ROSA26EYFP mouse: A new model for easy identification of living pancreatic alpha-cells." Febs Letters 581(22): 4235-4240.
Rajan, S., L. M. Dickson, E. Mathew, C. M. O. Orr, J. H. Ellenbroek, L. H. Philipson and B. Wicksteed (2015). "Chronic hyperglycemia downregulates

GLP-1 receptor signaling in pancreatic beta-cells via protein kinase A." Molecular Metabolism 4(4): 265-276.
Ramracheya, R., C. Chapman, M. Chibalina, H. Q. Dou, C. Miranda, A. Gonzalez, Y. Moritoh, M. Shigeto, Q. Zhang, M. Braun, A. Clark, P. R. Johnson, P. Rorsman and L. J. B. Briant (2018). "GLP-1 suppresses glucagon secretion in human pancreatic alpha-cells by inhibition of P/Q-type Ca2+ channels." Physiological Reports 6(17).
Ramracheya, R., C. Ward, M. Shigeto, J. N. Walker, S. Amisten, Q. A. Zhang, P. R. Johnson, P. Rorsman and M. Braun (2010). "Membrane Potential-Dependent Inactivation of Voltage-Gated Ion Channels in alpha-Cells Inhibits Glucagon Secretion From Human Islets." Diabetes 59(9): 2198-2208.
Raskin, P., Y. Fujita and R. H. Unger (1975). "Effect of insulin-glucose infusions on plasma glucagon levels in fasting diabetics and nondiabetics." Journal of Clinical Investigation 56(5): 1132-1138.
Ratzki-Leewing, A., S. B. Harris, S. Mequanint, S. M. Reichert, J. B. Brown, J. E. Black and B. L. Ryan (2018). "Real-world crude incidence of hypoglycemia in adults with diabetes: Results of the InHypo-DM Study, Canada." Bmj Open Diabetes Research & Care 6(1).
Ravazzola, M., R. H. Unger and L. Orci (1981). "Demonstration of glucagon in the stomach of human fetuses." Diabetes 30(10): 879-882.
Ravier, M. A., R. Cheng-Xue, A. E. Palmer, J. C. Henquin and P. Gilon (2010). "Subplasmalemmal Ca2+ measurements in mouse pancreatic beta cells support the existence of an amplifying effect of glucose on insulin secretion." Diabetologia 53(9): 1947-1957.
Ravier, M. A. and G. A. Rutter (2005). "Glucose or insulin, but not zinc ions, inhibit glucagon secretion from mouse pancreatic alpha-cells." Diabetes 54(6): 1789-1797.
Reaven, G. M., C. Hollenbeck, C. Y. Jeng, M. S. Wu and Y. D. I. Chen (1988). "Measurement of plasma-glucose, free fatty-acid, lactate, and insulin for 24-h in patients with NIDDM." Diabetes 37(8): 1020-1024.
Reetz, A., M. Solimena, M. Matteoli, F. Folli, K. Takei and P. Decamilli (1991). "GABA AND PANCREATIC BETA-CELLS - COLOCALIZATION OF GLUTAMIC-ACID DECARBOXYLASE (GAD) AND GABA WITH SYNAPTIC-LIKE MICROVESICLES SUGGESTS THEIR ROLE IN GABA STORAGE AND SECRETION." Embo Journal 10(5): 1275-1284.
Ritchie, M. E., B. Phipson, D. Wu, Y. F. Hu, C. W. Law, W. Shi and G. K. Smyth (2015). "limma powers differential expression analyses for RNA-sequencing and microarray studies." Nucleic Acids Research 43(7).
Roberts-Crowley, M. L., T. Mitra-Ganguli, L. W. Liu and A. R. Rittenhouse (2009). "Regulation of voltage-gated Ca2+ channels by lipids." Cell Calcium 45(6): 589-601.

Rocha, D. M., R. H. Unger and G. R. Faloona (1972). "Glucagon-stimulating activity of 20 amino-acids in dogs." Journal of Clinical Investigation 51(9): 2346-&.
Rorsman, P. and F. M. Ashcroft (2018). "PANCREATIC beta-CELL ELECTRICAL ACTIVITY AND INSULIN SECRETION: OF MICE AND MEN." Physiological Reviews 98(1): 117-214.
Rorsman, P. and F. M. Ashcroft (2018). "Pancreatic β-cell electrical activity and insulin secretion: of mice and men." Physiological Reviews 98(1): 117-214.
Rorsman, P., P. O. Berggren, K. Bokvist, H. Ericson, H. Mohler, C. G. Ostenson and P. A. Smith (1989). "Glucose-inhibition of glucagon-secretion involves activation of GABAa-receptor chloride channels." Nature 341(6239): 233-236.
Rorsman, P., M. Braun and Q. Zhang (2012). "Regulation of calcium in pancreatic alpha- and beta-cells in health and disease." Cell Calcium 51(3-4): 300-308.
Rufer, A. C., R. Thoma and M. Hennig (2009). "Structural insight into function and regulation of carnitine palmitoyltransferase." Cellular and Molecular Life Sciences 66(15): 2489-2501.
Ruiter, M., S. E. La Fleur, C. van Heijningen, J. van der Vliet, A. Kalsbeek and R. M. Buijs (2003). "The daily rhythm in plasma glucagon concentrations in the rat is modulated by the biological clock and by feeding behavior." Diabetes 52(7): 1709-1715.
Salehi, A., E. Vieira and E. Gylfe (2006). "Paradoxical stimulation of glucagon secretion by high glucose concentrations." Diabetes 55(8): 2318-2323.
Sammons, M. F. and E. C. Y. Lee (2015). "Recent progress in the development of small-molecule glucagon receptor antagonists." Bioorganic & Medicinal Chemistry Letters 25(19): 4057-4064.
Samols, E. and G. C. Weir (1979). "ADRENERGIC MODULATION OF PANCREATIC A, B, AND D-CELLS - ALPHA-ADRENERGIC SUPPRESSION AND BETA-ADRENERGIC STIMULATION OF SOMATOSTATIN SECRETION, ALPHA-ADRENERGIC STIMULATION OF GLUCAGON-SECRETION IN THE PERFUSED DOG PANCREAS." Journal of Clinical Investigation 63(2): 230-238.
Sano, H., G. R. Peck, A. N. Kettenbach, S. A. Gerber and G. E. Lienhard (2011). "Insulin-stimulated GLUT4 Protein Translocation in Adipocytes Requires the Rab10 Guanine Nucleotide Exchange Factor Dennd4C." Journal of Biological Chemistry 286(19): 16541-16545.
Santos-Silva, J. C., R. A. Ribeiro, J. F. Vettorazzi, E. Irles, S. Rickli, P. C. Borck, P. M. Porciuncula, I. Quesada, A. Nadal, A. C. Boschero and E. M. Carneiro (2015). "Taurine supplementation ameliorates glucose homeostasis, prevents insulin and glucagon hypersecretion, and controls beta, alpha, and delta-cell masses in genetic obese mice." Amino Acids 47(8): 1533-1548.
Satoh, N., Y. Ogawa, G. Katsuura, M. Hayase, T. Tsuji, K. Imagawa, Y. Yoshimasa, S. Nishi, K. Hosoda and K. Nakao (1997). "The arcuate nucleus as a

primary site of satiety effect of leptin in rats." Neuroscience Letters 224(3): 149-152.
Sawatani, T., Y. K. Kaneko and T. Ishikawa (2018). "DAG Accumulation due to Type 1 DGK Inhibition Has Contradictory Dual Effect on Ca2(+) Signaling in Pancreatic beta Cells." Diabetes 67.
Schade, D. S. and R. P. Eaton (1974). "ROLE OF INSULIN AND GLUCAGON IN OBESITY." Diabetes 23(8): 657-661.
Schaub, J. R., X. Lu, B. Doneske, Y.-K. Shin and J. A. McNew (2006). "Hemifusion arrest by complexin is relieved by Ca2+-synaptotagmin I." Nature Structural & Molecular Biology 13(8): 748-750.
Schmittgen, T. D. and K. J. Livak (2008). "Analyzing real-time PCR data by the comparative C-T method." Nature Protocols 3(6): 1101-1108.
Schnedl, W. J., S. Ferber, J. H. Johnson and C. B. Newgard (1994). "STZ TRANSPORT AND CYTOTOXICITY - SPECIFIC ENHANCEMENT IN GLUT2-EXPRESSING CELLS." Diabetes 43(11): 1326-1333.
Schoors, S., U. Bruning, R. Missiaen, K. C. S. Queiroz, G. Borgers, I. Elia, A. Zecchin, A. R. Cantelmo, S. Christen, J. Goveia, W. Heggermont, L. Godde, S. Vinckier, P. P. Van Veldhoven, G. Eelen, L. Schoonjans, H. Gerhardt, M. Dewerchin, M. Baes, K. De Bock, B. Ghesquiere, S. Y. Lunt, S. M. Fendt and P. Carmeliet (2015). "Fatty acid carbon is essential for dNTP synthesis in endothelial cells (vol 520, pg 192, 2015)." Nature 526(7571): 144-144.
Schuit, F. C., M. P. Derde and D. G. Pipeleers (1989). "SENSITIVITY OF RAT PANCREATIC A-CELLS AND B-CELLS TO SOMATOSTATIN." Diabetologia 32(3): 207-212.
Segerstolpe, A., A. Palasantza, P. Eliasson, E.-M. Andersson, A.-C. Andreasson, X. Sun, S. Picelli, A. Sabirsh, M. Clausen, M. K. Bjursell, D. M. Smith, M. Kasper, C. Ammala and R. Sandberg (2016). "Single-Cell Transcriptome Profiling of Human Pancreatic Islets in Health and Type 2 Diabetes." Cell Metabolism 24(4): 593-607.
Sekirov, I., S. L. Russell, L. C. M. Antunes and B. B. Finlay (2010). "Gut Microbiota in Health and Disease." Physiological Reviews 90(3): 859-904.
Shuai, H., Y. Xu, Q. Yu, E. Gylfe and A. Tengholm (2016). "Fluorescent protein vectors for pancreatic islet cell identification in live-cell imaging." Pflugers Archiv-European Journal of Physiology 468(10): 1765-1777.
Soedling, H., D. J. Hodson, A. E. Adrianssens, F. M. Gribble, F. Reimann, S. Trapp and G. A. Rutter (2015). "Limited impact on glucose homeostasis of leptin receptor deletion from insulin- or proglucagon-expressing cells." Molecular Metabolism 4(9): 619-630.
Sollner, T., S. W. Whitehart, M. Brunner, H. Erdjumentbromage, S. Geromanos, P. Tempst and J. E. Rothman (1993). "Snap receptors implicated in vesicle targeting and fusion." Nature 362(6418): 318-324.

Solomou, A., G. Meur, E. Bellomo, D. J. Hodson, A. Tomas, S. M. Li, E. Philippe, P. L. Herrera, C. Magnan and G. A. Rutter (2015). "The Zinc Transporter Slc30a8/ZnT8 Is Required in a Subpopulation of Pancreatic alpha-Cells for Hypoglycemia-induced Glucagon Secretion." Journal of Biological Chemistry 290(35): 21432-21442.
Solomou, A., E. Philippe, P. Chabosseau, S. Migrenne-Li, J. Gaitan, J. Lang, C. Magnan and G. A. Rutter (2016). "Over-expression of Slc30a8/ZnT8 selectively in the mouse a cell impairs glucagon release and responses to hypoglycemia." Nutrition & Metabolism 13.
Srinivasan, K., B. Viswanad, L. Asrat, C. L. Kaul and P. Ramarao (2005). "Combination of high-fat diet-fed and low-dose streptozotocin-treated rat: A model for type 2 diabetes and pharmacological screening." Pharmacological Research 52(4): 313-320.
Stamateris, R. E., R. B. Sharma, D. A. Hollern and L. C. Alonso (2013). "Adaptive beta-cell proliferation increases early in high-fat feeding in mice, concurrent with metabolic changes, with induction of islet cyclin D2 expression." American Journal of Physiology-Endocrinology and Metabolism 305(1): E149-E159.
Starke, A., T. Imamura and R. H. Unger (1987). "Relationship of glucagon suppression by insulin and somatostatin to the ambient glucose-concentration." Journal of Clinical Investigation 79(1): 20-24.
Starke, A. A. R., G. Erhardt, M. Berger and H. Zimmermann (1984). "Elevated pancreatic glucagon in obesity." Diabetes 33(3): 277-280.
Stephens, F. B., D. Constantin-Teodosiu and P. L. Greenhaff (2007). "New insights concerning the role of carnitine in the regulation of fuel metabolism in skeletal muscle." Journal of Physiology-London 581(2): 431-444.
Stern, J. H., G. I. Smith, S. W. Chen, R. H. Unger, S. Klein and P. E. Scherer (2019). "Obesity dysregulates fasting-induced changes in glucagon secretion." Journal of Endocrinology 243(2): 149-160.
Stokkan, K. A., S. Yamazaki, H. Tei, Y. Sakaki and M. Menaker (2001). "Entrainment of the circadian clock in the liver by feeding." Science 291(5503): 490-493.
Stone, V. M., S. Dhayal, K. J. Brocklehurst, C. Lenaghan, M. S. Winzell, M. Hammar, X. Xu, D. M. Smith and N. G. Morgan (2014). "GPR120 (FFAR4) is preferentially expressed in pancreatic delta cells and regulates somatostatin secretion from murine islets of Langerhans." Diabetologia 57(6): 1182-1191.
Stripecke, R., M. D. Villacres, D. C. Skelton, N. Satake, S. Halene and D. B. Kohn (1999). "Immune response to green fluorescent protein: implications for gene therapy." Gene Therapy 6(7): 1305-1312.
Strowski, M. Z., R. M. Parmar, A. D. Blake and J. M. Schaeffer (2000). "Somatostatin inhibits insulin and glucagon secretion via two receptor

subtypes: An in vitro study of pancreatic islets from somatostatin receptor 2 knockout mice." Endocrinology 141(1): 111-117.
Takahashi, T., T. Kikuchi, Y. Kidokoro and H. Shirakawa (2013). "Ca2+ influx-dependent refilling of intracellular Ca2+ stores determines the frequency of Ca2+ oscillations in fertilized mouse eggs." Biochemical and Biophysical Research Communications 430(1): 60-65.
Tassava, T. M., T. Okuda and D. R. Romsos (1992). "Insulin-secretion from Ob/Ob mouse pancreatic-islets - effects of neurotransmitters." American Journal of Physiology 262(3): E338-E343.
Tengholm, A. and E. Gylfe (2017). "cAMP signalling in insulin and glucagon secretion." Diabetes Obesity & Metabolism 19: 42-53.
Tian, L., S. A. Hires, T. Mao, D. Huber, M. E. Chiappe, S. H. Chalasani, L. Petreanu, J. Akerboom, S. A. McKinney, E. R. Schreiter, C. I. Bargmann, V. Jayaraman, K. Svoboda and L. L. Looger (2009). "Imaging neural activity in worms, flies and mice with improved GCaMP calcium indicators." Nature Methods 6(12): 875-U113.
Tornehave, D., P. Kristensen, J. Romer, L. B. Knudsen and R. S. Heller (2008). "Expression of the GLP-1 Receptor in Mouse, Rat, and Human Pancreas." Journal of Histochemistry & Cytochemistry 56(9): 841-851.
Tran, H. V., J. M. Gore, C. E. Darling, A. S. Ash, C. I. Kiefe and R. J. Goldberg (2018). "Hyperglycemia and risk of ventricular tachycardia among patients hospitalized with acute myocardial infarction." Cardiovascular Diabetology 17.
Tuduri, E., L. Marroqui, S. Soriano, A. B. Ropero, T. M. Batista, S. Piquer, M. A. Lopez-Boado, E. M. Carneiro, R. Gomis, A. Nadal and I. Quesada (2009). "Inhibitory Effects of Leptin on Pancreatic alpha-Cell Function." Diabetes 58(7): 1616-1624.
Uhlen, M., L. Fagerberg, B. M. Hallstrom, C. Lindskog, P. Oksvold, A. Mardinoglu, A. Sivertsson, C. Kampf, E. Sjostedt, A. Asplund, I. Olsson, K. Edlund, E. Lundberg, S. Navani, C. A. Szigyarto, J. Odeberg, D. Djureinovic, J. O. Takanen, S. Hober, T. Alm, P. H. Edqvist, H. Berling, H. Tegel, J. Mulder, J. Rockberg, P. Nilsson, J. M. Schwenk, M. Hamsten, K. von Feilitzen, M. Forsberg, L. Persson, F. Johansson, M. Zwahlen, G. von Heijne, J. Nielsen and F. Ponten (2015). "Tissue-based map of the human proteome." Science 347(6220).
Unger, R. H., Aguilarp.E, W. A. Muller and A. M. Eisentraut (1970). "STUDIES OF PANCREATIC ALPHA CELL FUNCTION IN NORMAL AND DIABETIC SUBJECTS." Journal of Clinical Investigation 49(4): 837-+.
Unger, R. H., A. Ohneda, Aguilarp.E and A. M. Eisentraut (1969). "Role of aminogenic glucagon secretion in blood glucose homeostasis." Journal of Clinical Investigation 48(5): 810-+.
Unger, R. H. and L. Orci (1975). "Essential role of glucagon in pathogenesis of diabetes-mellitus." Lancet 1(7897): 14-16.

VanCauter, E., K. S. Polonsky and A. J. Scheen (1997). "Roles of circadian rhythmicity and sleep in human glucose regulation." Endocrine Reviews 18(5): 716-738.
Vergari, E., J. G. Knudsen, R. Ramracheya, A. Salehi, Q. Zhang, J. Adam, I. W. Asterholm, A. Benrick, L. J. B. Briant, M. V. Chibalina, F. M. Gribble, A. Hamilton, B. Hastoy, F. Reimann, N. J. G. Rorsman, I. I. Spiliotis, A. Tarasov, Y. Wu, F. M. Ashcroft and P. Rorsman (2019). "Insulin inhibits glucagon release by SGLT2-induced stimulation of somatostatin secretion." Nature Communications 10.
Vieira, E., A. Salehi and E. Gylfe (2007). "Glucose inhibits glucagon secretion by a direct effect on mouse pancreatic alpha cells." Diabetologia 50(2): 370-379.
Walker, J. N., R. Ramracheya, Q. Zhang, P. R. V. Johnson, M. Braun and P. Rorsman (2011). "Regulation of glucagon secretion by glucose: paracrine, intrinsic or both?" Diabetes Obesity & Metabolism 13: 95-105.
Wang, B., P. C. Chandrasekera and J. J. Pippin (2014). "Leptin- and leptin receptor-deficient rodent models: relevance for human type 2 diabetes." Current diabetes reviews 10(2): 131-145.
Wang, X.-L., F. Ye, J. Li, L.-Y. Zhu, G. Feng, X.-Y. Chang and K. Sun (2016). "Impaired secretion of glucagon-like peptide 1 during oral glucose tolerance test in patients with newly diagnosed type 2 diabetes mellitus." Saudi Medical Journal 37(1): 48-54.
Watts, M. and A. Sherman (2014). "Modeling the Pancreatic alpha-Cell: Dual Mechanisms of Glucose Suppression of Glucagon Secretion." Biophysical Journal 106(3): 741-751.
Wei, J., X. Song, X. Liu, Z. Ji, N. Ranasinha, J. Wu and Y. Miao (2018). "Glucagonoma and Glucagonoma Syndrome: One Center's Experience of Six Cases." Journal of Pancreatic Cancer 4(1): 11-16.
Wendt, A., B. Birnir, K. Buschard, J. Gromada, A. Salehi, S. Sewing, P. Rorsman and M. Braun (2004). "Glucose inhibition of glucagon secretion from rat alpha-cells is mediated by GABA released from neighboring beta-cells." Diabetes 53(4): 1038-1045.
Whitaker, M. (2010). "Calcium in Living Cells." Calcium in Living Cells 99: 1-316.
Winzell, M. S. and B. Ahren (2004). "The high-fat diet-fed mouse - A model for studying mechanisms and treatment of impaired glucose tolerance and type 2 diabetes." Diabetes 53: S215-S219.
Winzell, M. S., C. L. Brand, N. Wierup, U. G. Sidelmann, F. Sundler, E. Nishimura and B. Ahren (2007). "Glucagon receptor antagonism improves islet function in mice with insulin resistance induced by a high-fat diet." Diabetologia 50(7): 1453-1462.

Wise, J. K., R. Hendler and P. Felig (1973). "Influence of glucocorticoids on glucagon secretion and plasma amino-acid concentrations in man." Journal of Clinical Investigation 52(11): 2774-2782.
Wu, Y. L., Y. P. Ding, Y. Tanaka and W. Zhang (2014). "Risk Factors Contributing to Type 2 Diabetes and Recent Advances in the Treatment and Prevention." International Journal of Medical Sciences 11(11): 1185-1200.
Xin, Y. and J. Gromada (2016). GSE81608: RNA Sequencing of Single Human Islet Cells Reveals Type 2 Diabetes Genes, Gene Expression Omnibus.
Yao, C.-H., G.-Y. Liu, R. Wang, S. H. Moon, R. W. Gross and G. J. Patti (2018). "Identifying off-target effects of etomoxir reveals that carnitine palmitoyltransferase I is essential for cancer cell proliferation independent of beta-oxidation." Figshare.
Yu, Q., H. Y. Shuai, P. Ahooghalandari, E. Gylfe and A. Tengholm (2019). "Glucose controls glucagon secretion by directly modulating cAMP in alpha cells." Diabetologia 62(7): 1212-1224.
Zariwala, H. A., B. G. Borghuis, T. M. Hoogland, L. Madisen, L. Tian, C. I. De Zeeuw, H. K. Zeng, L. L. Looger, K. Svoboda and T. W. Chen (2012). "A Cre-Dependent GCaMP3 Reporter Mouse for Neuronal Imaging In Vivo." Journal of Neuroscience 32(9): 3131-3141.
Zhang, C. Y. (2006). "Uncoupling protein-2 negatively regulates insulin secretion and is a major link between obesity, beta cell dysfunction, and type 2 diabetes." Neurosignals 15(1): 52-52.
Zhang, H., A. Qiao, L. Yang, N. Van Eps, K. S. Frederiksen, D. Yang, A. Dai, X. Cai, H. Zhang, C. Yi, C. Cao, L. He, H. Yang, J. Lau, O. P. Ernst, M. A. Hanson, R. C. Stevens, M.-W. Wang, S. Reedtz-Runge, H. Jiang, Q. Zhao and B. Wu (2018). "Structure of the glucagon receptor in complex with a glucagon analogue." Nature 553(7686): 106-+.
Zhang, Q., M. V. Chibalina, M. Bengtsson, L. N. Groschner, R. Ramracheya, N. J. G. Rorsman, V. Leiss, M. A. Nassar, A. Welling, F. M. Gribble, F. Reimann, F. Hofmann, J. N. Wood, F. M. Ashcroft and P. Rorsman (2014). "Na + current properties in islet α- and β-cells reflect cell-specific Scn3a and Scn9a expression." Journal of Physiology-London 592(21): 4677-4696.
Zhang, Q., M. V. Chibalina, M. Bengtsson, L. N. Groschner, R. Ramracheya, N. J. G. Rorsman, V. Leiss, M. A. Nassar, A. Welling, F. M. Gribble, F. Reimann, F. Hofmann, J. N. Wood, F. M. Ashcroft and P. Rorsman (2014). "Na+ current properties in islet alpha- and beta-cells reflect cell-specific Scn3a and Scn9a expression." Journal of Physiology-London 592(21): 4677-4696.
Zhang, Q., R. Ramracheya, C. Lahmann, A. Tarasov, M. Bengtsson, O. Braha, M. Braun, M. Brereton, S. Collins, J. Galvanovskis, A. Gonzalez, L. N. Groschner, N. J. G. Rorsman, A. Salehi, M. E. Travers, J. N. Walker, A. L. Gloyn, F. Gribble, P. R. V. Johnson, F. Reimann, F. M. Ashcroft and P. Rorsman (2013). "Role of K-ATP

Channels in Glucose-Regulated Glucagon Secretion and Impaired Counterregulation in Type 2 Diabetes." Cell Metabolism 18(6): 871-882.
Zhang, Y., K. R. Parajuli, G. E. Fava, R. Gupta, W. Xu, L. U. Nguyen, A. F. Zakaria, V. A. Fonseca, H. Wang, F. Mauvais-Jarvis, K. W. Sloop and H. Wu (2019). "GLP-1 Receptor in Pancreatic alpha-Cells Regulates Glucagon Secretion in a Glucose-Dependent Bidirectional Manner." Diabetes 68(1): 34-44.
Zhang, Y., Y. Zhang, R. N. Bone, W. Cui, J.-B. Peng, G. P. Siegal, H. Wang and H. Wu (2012). "Regeneration of Pancreatic Non-beta Endocrine Cells in Adult Mice following a Single Diabetes-Inducing Dose of Streptozotocin." Plos One 7(5).
Zhou, C., D. Dhall, N. N. Nissen, C.-R. Chen and R. Yu (2009). "Homozygous P86S Mutation of the Human Glucagon Receptor Is Associated With Hyperglucagonemia, alpha Cell Hyperplasia, and Islet Cell Tumor." Pancreas 38(8): 941-946.
Zhou, H. R., T. Zhang, J. S. Harmon, J. Bryan and R. P. Robertson (2007). "Zinc, not insulin, regulates the rat alpha-cell response to hypoglycemia in vivo." Diabetes 56(4): 1107-1112.
Zilionis, R., J. Nainys, A. Veres, V. Savova, D. Zemmour, A. M. Klein and L. Mazutis (2017). "Single-cell barcoding and sequencing using droplet microfluidics." Nature Protocols 12(1).